UNIVERSITY OF VALENCIA
FACULTY OF MEDICINE AND ODONTOLOGY
DEPARTMENT OF PHYSIOLOGY
PhD Program in Physiology

ACUTE INFLAMMATORY AND FIBROGENIC RESPONSES INDUCED IN LIVER CELLS BY EFAVIRENZ

Doctoral Thesis

FERNANDO ALEGRE GUERRA

Directors:

Dr. Juan Vicente Esplugues Mota

Dr. Nadezda Apostolova Atanasovska

Dr. Ana Blas García

PhD program tutor:

Dr. José Viña Ribes

Valencia, 2017

UNIVERSITY OF VALENCIA
FACULTY OF MEDICINE AND ODONTOLOGY
DEPARTMENT OF PHYSIOLOGY

Dr. JUAN VICENTE ESPLUGUES MOTA, Catedrático de Universidad en el Departamento de Farmacología de la Universitat de València.

Dra. NADEZDA APOSTOLOVA ATANASOVSKA, Profesor Ayudante Doctor del Departamento de Farmacología de la Universitat de València.

Dra. ANA BLAS GARCÍA, Investigadora postdoctoral del CIBERehd en el Departamento de Farmacología de la Universitat de València.

CERTIFICAN:

Que la presente memoria, titulada "Acute inflammatory and fibrogenic responses induced in liver cells by efavirenz", presentada por el Licenciado en Veterinaria **D. Fernando Alegre Guerra,** ha sido realizada bajo nuestra dirección y asesoramiento en el Departamento de Farmacología de la Facultad de Medicina y Odontología de la Universitat de València.

Concluido el trabajo experimental y bibliográfico, autorizamos la presentación y defensa de esta Tesis Doctoral en el Programa de Doctorado en Fisiología de la Universitat de València.

Para que así conste a los efectos oportunos, se expide el presente certificado en Valencia, a 7 de Marzo de 2017.

Fdo. Dr. Juan Vicente Esplugues Mota **Fdo. Dra. Nadezda Apostolova**

Fdo. Dra. Ana Blas García

This doctoral thesis has been supported by the Instituto de Salud Carlos III, Ministerio de Economía y Competitividad [grants PI11/00327, PI14/00312 and CIBER06/04/0071], the Conselleria d'Educació, Formació I Ocupació, Generalitat Valenciana [grants PROMETEO/2010/060, PROMETEOII/2014/035, ACOMP/2013/236 and GVA/2014/118], and the University of Valencia [grant UV-INV-PRECOMP12-80613]. I have been recipient of predoctoral trainee research grant PFIS (FI12/00198) and mobility of research staff (MV16/00004), both from Instituto de Salud Carlos III, Ministerio de Economía y Competitividad; and a scholarship from Fundación Juan Esplugues.

"IF YOU CAN

DREAM IT,

YOU CAN

DO IT"

- WALT DISNEY -

A mi madre, a mi hermano, a mi abuela,
y por siempre a Sonia

ACKNOWLEDGEMENTS

Pues bueno…aquí estoy ya, escribiendo los agradecimientos de mi tesis doctoral, lo cual significa que estoy al final de otra etapa de mi vida. Decidí no hacerla en la tierra en la que crecí, y aunque al principio me dio cierto miedo, a día de hoy puedo decir que ha sido uno de mis mejores aciertos, y que volvería a hacerlo de la misma forma, ya que me ha ayudado a encontrarme a mí mismo y terminar de definir mi propia personalidad, apartado de las mismas influencias que conocía desde niño. Llegar hasta este punto no ha sido fácil, he tenido que recorrer todo el Levante español: Alicante, Murcia, Barcelona…hasta llegar por fin a Valencia, donde se me dio una buena oportunidad después de tantos años de trabajo durante mis estudios universitarios, pero bueno, como dijo Antoine de Saint-Exupéry en El principito, uno de los libros que marcó mi niñez **"Caminando en línea recta no puede uno llegar muy lejos"**, y en mi caso se ha cumplido completamente, ya que he hecho hasta "trompos" para llegar aquí.

Me gustaría empezar dedicando mis primeras palabras de agradecimiento a los que han sido mis directores de tesis. **Juan Vicente**, muchas gracias por toda la confianza depositada en mí desde el minuto 1, creo que incluso más de la que me merezco, ya que no sé si he estado a la altura de las expectativas. No tengo suficientes palabras de agradecimiento por todo lo que has hecho por Sonia (mi novia,☺) y por mí, puedo decir sin duda alguna que te has comportado como un padre con nosotros. Siempre me llevaré conmigo todas las conversaciones sobre la vida, el esfuerzo, política (aunque yo haya votado a Podemos☺), historia, etc. **Nade**, quiero que sepas que aparte de ser una científica de pura cepa y tener una mente brillante - eso no es ningún misterio y todo el mundo conoce - me gustaría destacar que en ti he conocido a una persona fantástica y con un gran corazón. Me ha encantado trabajar contigo, pero sobre todo de conocerte como persona. Muchas gracias por todos tus consejos durante la tesis, muchas gracias por exigirme cuando debías porque sabías que podía hacerlo cuando yo pensaba que no, cada empujón tuyo me ha servido para ser mejor investigador. **Ana**, contigo creo que me sentiré siempre en deuda, sé que no te lo hice pasar bien al principio debido a mi exigencia extrema. NO FUI JUSTO, LO SIENTO. Quiero que sepas que sin tu dirección y consejos gran parte de mi tesis no habrían existido, pero además quiero decirte que trabajar a tu lado me ha hecho conocer a una persona buena, con un gran corazón, y una sonrisa fantástica que te anima

cuando estás de bajón, pero que además ama la ciencia, y que eres un ejemplo de constancia y superación.

Además de a mis directores de tesis, también quisiera agradecer los consejos y palabras de ánimos del profesorado e investigadores integrantes de nuestro grupo. Muchas gracias **Loles**, por siempre derrochar alegría positiva a los predoctorales cuando lo vemos todo negro; **Ángeles**, por tus palabras de ánimo, cercanía, simpatía y preocuparte por mí; **Sara**, por orientarme cuando necesitaba algún consejo; **Carlos**, por ser siempre tan servicial cuando he necesitado tu ayuda; a **Mª Ángeles**, por siempre transmitir buenas vibraciones en el departamento; y a **Víctor** y **Miguel Martí**, por ser siempre tan cercanos.

Por supuesto una tesis doctoral y cualquier trabajo de investigación no puede llegar a buen puerto sin la ayuda, colaboración y consejos de tus compañeros, y además sin su compañía y amistad, que hacen más llevadero los problemas surgidos durante los experimentos o las críticas de tus resultados por parte de tus directores o profesorado del departamento. Por ello, quisiera dedicar unas palabras al *Liver Team* original, al genuino. **Haryes**, sólo hemos estado juntos durante la mitad de mi tesis, pero quiero que sepas que has sido una pieza fundamental para mi adaptación al laboratorio y además agradecerte tu buen humor constante. **Miriam**, que más que ser una compañera de trabajo eres una amiga por todos los momentos buenos vividos juntos estos años, pero también estresantes; muchas gracias por siempre ofrecerme tu ayuda cuando la he necesitado, ha sido un placer estar estos años contigo en el laboratorio. Muchas gracias por todo. **Alberto**, primero pedirte disculpas si alguna vez te has llevado una mala contestación de mi parte, no te la merecías seguro, eres un buen compañero, un buen amigo, y una persona con un buen corazón. Muchas gracias por toda la ayuda prestada estos años cuando la he necesitado y por estar siempre dispuesto a ayudar con una sonrisa en la cara, siempre te lo agradeceré.

Por suerte, nuestro grupo de investigación ha ido creciendo y creciendo, cuando otros grupos han ido menguando, lo cual dice mucho de la calidad científica y humana de los componentes que forman nuestro grupo, del cual me siento muy orgulloso. Aunque seamos tantos y hayan pasado otros tantos por el laboratorio durante mi estancia en el mismo, quiero dedicaros unas palabras. **Dolo**, para mí ha sido un verdadero placer haberte conocido, me he reído mucho contigo, muchas gracias por tu sinceridad y amistad, eres un buen ejemplo de trabajo duro y constancia a un nivel altísimo, sin dejar de lado en ningún momento tu

vida personal, totalmente un ejemplo a seguir. **María**, aunque tú y yo coincidimos poco tiempo en el labo porque estuve en San Diego, decirte que has sido un verdadero descubrimiento como persona, eres muy trabajadora y tu alegría hacía que los días en el laboratorio fueran mucho más interesantes. **Dulce**, que decirte a ti que no sepas a estas alturas, que eres como una hermana, muchas gracias por tu positividad, alegría incansable, por ser un ejemplo de superación y lucha, muchas gracias por enseñarme a relativizar los malos momentos vividos. **Isa**, hemos coincidido en el último tramo de mi tesis, pero sin duda mi estancia por aquí hubiera sido mucho más aburrida sin ti, me has aportado amistad, buenos consejos y mucha alegría, nunca se me olvidará todas las veces que te he hecho ruborizar jajajaja. **Ainhoa**, mushasha nos conocemos desde hace relativamente poco, pero desde casi el principio congeniamos, muchas gracias por tu amistad, cercanía, dulzura, alegría y también por ser un bicho!!!, haciendo que el buen rollo y las risas desbordaran el departamento. Bueno no me puedo olvidar de las tres mosqueteras de la nueva generación del *Liver Team*. Muchas gracias, **Ángela**, por tu reggaetón y buenas formas; **Olga**, por tu alegría y locura; y **Laia**, por tu sinceridad aplastante y risas. Habéis hecho que estos últimos meses por el laboratorio sean sin duda mucho más divertidos.

También quiero agradecer a **Victor**, **Patri**, **Pedro**, **Laura**, **Fer**, o el sector parejitas, por tener siempre alguna anécdota graciosa que contar y por enseñarnos que en el labo además de fluir la ciencia, también fluye el LOVE ☺. Tampoco me quiero olvidar de **Jorge**, con nuestras charlas políticas y de ¡Homeland!, ni de **Lara**, **Mariam**, **Pablo**, **Antonio**, **Antonio Hernández**, **Rosa**, **Raquel**, **Arantxa**, **Susana**, **Irene**, **Sandra**, **Noelia**, **Amelia**, **Dora**, **Raúl**, **Nicole**, **César**, por hacer que el trabajo diario en el laboratorio fuera más fácil, interesante y divertido. Por supuesto, no me puedo olvidar de las personas que han pasado por nuestro laboratorio de visita. **Edu**, eres el "puto amo", contigo me he reído hasta que me dolían los abdominales, has sido un verdadero descubrimiento, me lo he pasado genial durante tu estancia por nuestro laboratorio, muchas gracias por tu amistad, tus historias desternillantes y buena actitud. **Bibi**, I'm glad that our paths have crossed, thank you so much for your warmth and kindness. I hope to see you again someday.

Without the slightest doubt, my months in San Diego have been one of the best experiences of my life. I want to thank Dr. Ariel Feldstein for giving me the opportunity to spend time in his lab and for placing his trust in me from the

beginning. **Ariel**, it has been a great pleasure to have met such a great scientist and human being. My stay in San Diego allowed me to meet some wonderful people. **Casey**, "yankee", thanks for your help and happiness in the lab. **Aki**, thanks for your assistance with my experiments. **David**, thank you for your kind-heartedness, I know that you will be an awesome MD wherever you are. **Davide**, thank you for your friendship and for helping me throughout my months in San Diego. Without you everything would have been different. **Susi** and **Flo**, the best German couple in the world, thanks for your sincere friendship and joy, you are a fantastic couple, don't ever change!. **Lucy** and **Ale**, my favourite Italian girls, thanks for your happiness, your laughs and your closeness. **Roberto**, muchas gracias por tu increíble simpatía y muchas gracias por aportar tantas risas, con tus bailes y voz melódica jajaja. **Milos**, **Gwena**, **Marc**, **Hilde**, **Luis Sebastian**, thanks for all the dinners and parties!. And I must not forget **Monse**, **Maurizio**, **Lia**, **Rabia** and **Eileen**; thanks for your friendliness and for making my stay there so memorable.

Brian, muchas gracias por todo, soy de los que piensa que es bueno tener pocos amigos y buenos, que muchos y poco interesantes, prácticamente formas parte de mi familia. Has sido un apoyo fundamental todos estos años, no sólo para mí, también has ayudado mucho a Sonia mientras yo estaba fuera, algo que siempre te agradeceré. Muchas gracias por escucharme en los momentos de bajón porque las cosas no me salían como quería, y aconsejarme siempre cómo actuar, y por ayudarme con mil cosas que son imposible enumerar en unos simples agradecimientos.

Muchas gracias **mamá** y **hermano**, sin vuestro apoyo incondicional y amor no habría terminado esta tesis. Hemos pasado muy malos momentos estos años, pero siempre habéis estado ahí para que no me rindiera. Muchas gracias *family*. **Abuela**, esta tesis también te la dedico, gracias por todas tus oraciones y cariño.

Por último, mis palabras van dedicadas a ti, el amor de mi vida. **Sonia**, desde hace poco mi mujer, la que me cambió profundamente, la culpable de que sea como soy ahora. Muchas gracias por todo, esta tesis es tan tuya como mía. Sin duda, tu apoyo, confianza, cariño, amor y consejos me han hecho terminar esta tesis. Tan sólo me bastaba mirarte para relajarme en los momentos de más estrés, o un abrazo tuyo para consolarme en los días en que los experimentos no me salían. Gracias por hacerme sentir cada día especial. **Te amo mi amore**.

ABBREVIATIONS & ACRONYMS

/c	Drug boosted with cobicistat
/r	Drug boosted with ritovanir
1,3-DCP	1,3-dichloro-2-propanol
3MA	3-Methyladenine
3TC	Lamivudine
6-OHDA	6-hydroxydopamine, also known as oxidopamine
ABC	Abacavir
ABC	Avidin-Biotinylated peroxidase complexes
ActD	Actinomycin D
AIDS	Acquired immunodeficiency syndrome
AIM2	Absent in melanoma 2
ALP	Alkaline phosphatase
ALT	Alanine aminotransaminase
AMP. SIZE	Amplicon size
AP-1	Activator protein 1
APC	Antigen presenting cells
aPKC	Atypical protein kinases C
APS	Ammonium persulfate
ARE	Antioxidant response element
ASC	Apoptosis-associated speck-like protein containing a CARD domain
ASH	Alcoholic steatohepatitis
ASK1	Apoptosis signal-regulating kinase 1
ATF6	Activating transcription factor 6
ATG	Autophagy-related
ATP	Adenosine triphosphate
ATV	Atazanavir
AZT	Zidovudine
BAPTA	1,2-bis(o-aminophenoxy)ethane-N,N,N′,N′-tetraacetic acid
BCA	Bicinchoninic acid
BimEL	Bim extra long
bp	Base pair

BSA	**Bovine serum albumin**
bZIP	**Basic-leucine zipper domain**
cART	**Combination antiretroviral therapy**
CCCP	**Carbonyl cyanide m-chlorophenyl hydrazine**
CCL	**C-C motif chemokine ligand**
CCR	**C-C motif chemokine receptor**
CD	**Cluster of differentiation**
CDAA	**Choline-deficient L-amino acid- defined diet**
cDNA	**Complementary DNA**
CHOP	**C/EBP homologous protein**
CI-ND1	**Complex I-NADH dehydrogenase subunit 1**
CIV-II	**Complex IV- subunit II**
CM	**Conditioned medium**
CNS	**Central nervous system**
CONC.	**Concentration**
Ctrol	**Control**
CV-β	**Complex V (ATP synthase)-subunit beta**
CXCL	**C-X-C motif chemokine ligand**
CXCR	**C-X-C motif chemokine receptors**
CYP	**Cytochrome P450**
DAB	**3,3'-diaminobenzidine tetrahydrochloride**
DAMP	**Damage-associated molecular pattern**
ddI	**Didanosine**
DHHS	**Department of Health and Human Services**
DILI	**Drug-induced liver injury**
DMEM	**Dulbecco's Modified Eagle's Medium**
DMSO	**Dimethyl sulfoxide**
DNA	**Deoxyribonucleic acid**
DRV	**Darunavir**
dsDNA	**Double stranded DNA**
DSS	**Dextran sulfate sodium**
DTG	**Dolutegravir**

DTT	**Dithiothreitol**
E. coli	***Escherichia coli***
EBSS	**Earle's Balanced Salt Solution**
ECACC	**European Collection of Authenticated Cell Cultures**
ECM	**Extracellular matrix**
EDTA	**Ethylenediaminetetraacetic acid**
EFV	**Efavirenz**
EGTA	**Ethylene glycol-bis (2-aminoethylether)-N,N,N′,N′-tetraacetic acid**
ELISA	**Enzyme-linked immunosorbent assay**
ER	**Endoplasmic reticulum**
ERK	**Extracellular Signal-regulated Kinase**
ETC	**Electron transport chain**
EthBr	**Ethidium bromide**
EVG	**Elvitegravir**
FADD	**Fas-associated protein with death domain**
FDA	**US Food and Drug Administration**
FI	**Fusin inhibitors**
FTC	**Emtricitabine**
GAPDH	**Glyceraldehyde 3-phosphate dehydrogenase**
GCL	**Glutamate-cysteine ligase**
$GdCl_3$	**Gadolinium chloride**
gDNA	**Genomic DNA**
GeSIDA	**Grupo de Estudio del SIDA de la Sociedad Española de Enfermedades Infecciosas y Microbiología Clínica**
gp	**Glycoprotein**
GRP78	**78 kDa glucose-regulated protein**
GST	**Glutathione S transferase**
h	**Human**
HAART	**Highly active antiretroviral therapy**
HBSS	**Hanks' Balanced Salt Solution**
HBV	**Hepatitis B virus**

HCC	**Hepatocellular carcinoma**
HCV	**Hepatitis C virus**
HEPES	**4-(2-hydroxyethyl)-1-piperazineethanesulfonic acid**
hHSC	**Human hepatic stellate cells**
HIF-1α	**Hypoxia-inducible factor 1-alpha**
HIV	**Human immunodeficiency virus**
HMGB-1	**High mobility group box 1**
HMOX1	**Heme oxygenase 1**
HR	**Heptad repeat**
HRP	**Horseradish peroxidase**
HS	**Horse serum**
HSC	**Hepatic stellate cells**
HSC70	**Heat shock cognate 70 kDa protein**
HSP	**Heat shock protein**
HTAB	**Hexadecyltrimethylammonium bromide**
I.V.	**Intravenous**
ICAM-1	**Intercellular adhesion molecule 1**
iFBS	**Heat-inactivated fetal bovine serum**
IFN-γ	**Interferon gamma**
IgG	**Immunoglobulin G**
IHC	**Immunohistochemistry**
II	**Integrase inhibitor**
IL	**Interleukin**
IL-1R	**Interleukin-1 receptor**
IL-1Ra	**Interleukin-1 receptor antagonist**
IRAK1	**Interleukin 1 Receptor Associated Kinase 1**
IRE1α	**Inositol-requiring enzyme 1 alpha**
IRF	**Interferon regulatory factor**
JNK	**c-Jun N-terminal kinase**
KC	**Kupffer cells**
kDa	**Kilodalton**
Keap1	**Kelch-like ECH-associated protein 1**

KIR	Keap1-interacting region
KO	Knockout
LAMP-2A	Lysosome-associated membrane protein 2A
LC3	Microtubule-associated protein 1 light chain 3
LIR	LC3-interacting region
LPS	Lipopolysaccharide
LPSc	LPS cocktail
mAb	Monoclonal antibody
MAPK	Microtubule associated protein kinase
MAVS	Mitochondrial antiviral signaling
MCP	Monocyte chemoattractant protein
MEM	Minimum essential medium
MMP	Matrix metalloproteinase
MPO	Myeloperoxidase
MPP+	1-methyl-4-phenylpyridinium
mRNA	Messenger ribonucleic acid
MSU	Monosodium urate crystals
mtDNA	Mitochondrial DNA
mTORC1	Mammalian target of rapamycin complex 1
MTT	3-(4,5-dimethylthiazol-2-yl)-2,5-diphenyl tetrazolium bromide
MTXR	Methotrexate
MVC	Maraviroc
MW	Molecular weight
n	Number of independent experiments
NAO	Nonyl acridine orange
NASH	Non-alcoholic steatohepatitis
NBR1	Neighbor of BRCA1 gene 1
NDP52	Nuclear dot protein 52 kDa
NEAA	Non-Essential Amino Acid
NES	Nuclear export signal
NF-κB	Nuclear factor-kappa B
NIH	US National Institutes of Health

NK cells	**Natural killer cells**
NLR	**NOD-like receptor**
NLRP3	**NLR family pyrin domain containing 3**
NLS	**Nuclear localization signal**
NNRTI	**Non-nucleoside reverse transcriptase inhibitors**
NO	**Nitric oxide**
NOD	**Nucleotide-binding domain**
NQO1	**NAD(P)H quinone oxidoreductase 1**
Nrf2	**Nuclear factor erythroid 2-related factor 2**
NRTI	**Nucleoside reverse transcriptase inhibitors**
OxPhos	**Oxidative phosphorylation**
P.O.	**Per os**
PAGE	**Polyacrylamide gel electrophoresis**
PAMP	**Pathogen-associated molecular pattern**
PB1	**Phox1 and Bem1p domain**
PBS	**Phosphate-buffered saline**
PBS-T	**Phosphate-buffered saline-Tween**
PCR	**Polymerase chain reaction**
PDGF-β	**Platelet-derived growth factor subunit beta**
PE	**Phosphatidylethanolamine**
PERK	**PKR-related ER kinase**
PI	**Protease inhibitor**
PI3K	**Phosphoinositide 3-kinase**
PI3P	**Phosphatidylinositol 3-phosphate**
PMA	**Phorbol myristate acetate**
***p*NA**	***p*-nitroanilide**
pol-γ	**DNA polymerase gamma**
PPAR-γ	**Peroxisome proliferator-activated receptor gamma**
PRR	**Pattern recognition receptor**
qRT-PCR	**Quantitative RT-PCR**
RagC	**Ras-related GTP-binding protein C**
RAGE	**Receptor for advanced glycation end-product**

RAL	Raltegravir
RANKL	Receptor activator of NF-κB ligand
Raptor	Regulatory-associated protein of mTOR
RIP1	Receptor-interacting serine/threonine-protein kinase 1
RNA	Ribonucleic acid
ROS	Reactive oxygen species
Rot	Rotenone
RPMI	Roswell Park Memorial Institute
RPV	Rilpivirine
RQ	RNA quality
RT	Reverse transcription
RT	Room temperature
Sal.	Saline
SDS	Sodium dodecyl sulfate
SEM	Standard error of the mean
SERCA	Sarco/endoplasmic reticulum Ca2+-ATPase
SI	Sterile inflammation
SQSTM1	Sequestosome 1
ssRNA	Single-stranded RNA
STAT	Signal transducer and activator of transcription
T-20	Enfuvirtide
TAA	Thioacetamide
TAF	Tenofovir alafenamide
TAX1BP1	Tax1-binding protein 1
TB	TRAF6 binding motif
TBS-T	Tris-buffered saline-Tween
TDF	Tenofovir disoproxil fumarate
TE	Tris-EDTA
TEMED	N,N,N′,N′-tetramethylethylenediamine
TG	Thapsigargin
TGF-β1	Transforming growth factor beta 1
Th1/2	Type 1/2 T helper

TIMP	**Tissue inhibitors of metalloproteinase**
TLR	**Toll-like receptor**
TMB	**3,3',5,5'-tetramethylbenzidine**
TMRM	**Tetramethylrhodamine, methyl ester**
TNFR1	**Tumor necrosis factor receptor 1**
TNF-α	**Tumor necrosis factor alpha**
TRAF6	**Tumor necrosis factor receptor-associated factor 6**
TRAIL	**TNF-related apoptosis-inducing ligand**
TRX	**Thioredoxin**
TXNIP	**Thioredoxin (TRX)-interacting protein**
Ub	**Ubiquitin**
UBA	**Ubiquitin-associated domain**
ULK	**UNC51-like kinase**
UPR	**Unfolded protein response**
UPS	**Ubiquitin proteasome system**
US	**United Stated (of America)**
VCAM-1	**Vascular cell adhesion protein 1**
Veh	**Vehicle**
VPS	**Vacuolar protein sorting**
WB	**Western Blotting**
XBP1	**X-box binding protein 1**
α-SMA	**Alpha-smooth muscle actin**
$\Delta\Psi_m$	**Mitochondrial membrane potential**
ρ^o	**Rho^o**

LIST OF FIGURES

LIST OF TABLES

RESUMEN

INTRODUCCIÓN

Diversos agentes hepatotóxicos y enfermedades hepáticas pueden conducir al desarrollo de fibrosis hepática debido a la presencia de respuestas inflamatorias desreguladas (Kubes and Mehal 2012). Tanto la inflamación hepática como la fibrogénesis son procesos mediados por conocidas vías reguladas por el factor de transcripción NF-κB y por los inflamasomas, complejos multiproteicos intracelulares que reconocen patrones moleculares asociados a patógenos y a daño (*PAMPs* y *DAMPs*) (Martinon et al. 2009; Gurung et al. 2015). NLRP3 es el inflamasoma más ampliamente estudiado, habiéndose involucrado en el inicio y progresión de varios procesos hepáticos, como son el daño hepático inducido por fármacos, el hígado graso no alcohólico y la fibrosis hepática (Friedman et al. 2013; Mehal 2014; Szabo and Iracheta-Vellve 2015; Tilg et al. 2016). El inflamasoma NLRP3 está compuesto por varios dominios, concretamente el receptor NLRP3 (*NOD-like receptor protein 3*), el adaptador proteico ASC (*apoptosis-associated speck-like protein containing CARD*, codificado por el gen *PYCARD*) y la serina proteasa caspasa-1 (Latz et al. 2013; Netea et al. 2015). Tras la detección de patrones moleculares nocivos para la célula, la pro-caspasa-1 es procesada y activada dando lugar a caspasa-1 induciendo así la maduración de interleucina (IL)-1β e IL-18, que son liberadas de las células mediante vías no convencionales, incluidas el transporte en micropartículas o a través de la muerte celular por piroptosis (Lopez-Castejon and Brough 2011; Brydges et al. 2013; Dinarello et al. 2013; Sollberger et al. 2014). El inflamasoma NLRP3 es activado en repuesta a una amplia variedad de estímulos que frecuentemente están relacionados con la producción de especies reactivas de oxígeno (ERO), la liberación de proteínas mitocondriales al citosol, la homeostasis del Ca^{2+} y el estrés de retículo endoplásmico (RE) (Gurung et al. 2015). A este respecto, estudios *in vitro* han descrito que efavirenz (EFV), uno de los fármacos antirretrovirales más ampliamente utilizados en el tratamiento de la infección por el virus de la inmunodeficiencia humana (VIH), modifica la expresión de ciertos genes relacionados con la inflamación (Gomez-Sucerquia et al. 2012) y ejerce una serie de acciones en los hepatocitos que pueden desencadenar la inducción del inflamasoma NLRP3 y la subsiguiente inflamación hepática. Entre estas acciones se encuentra el incremento de la producción de ERO, la perturbación de la homeostasis del Ca^{2+}, la disfunción mitocondrial, la activación

de la autofagia para promover la supervivencia celular y el estrés de RE (Apostolova et al. 2010, 2011, 2013; Blas-García et al. 2010).

La fibrogénesis es una respuesta multicelular estrechamente relacionada con la activación de rutas inflamatorias, durante la cual las células estrelladas hepáticas (CEHs) interaccionan con células residentes en el hígado y células inmunitarias (Seki and Schwabe 2015) desencadenando varios procesos, como cambios en la producción de proteínas de la matriz extracelular (MEC) y citoquinas, que exacerban la inflamación (Friedman 2008). Después de la iniciación y perpetuación del daño hepático, la regresión y/o resolución del mismo son mediadas por diferentes mecanismos, incluyendo la desactivación de las CEHs y la activación del sistema inmune. Concretamente, los macrófagos hepáticos son piezas fundamentales en la homeostasis y patogénesis hepática, llevando a cabo un complejo papel tanto en la inflamación hepática como en la resolución del daño (Tacke and Zimmermann 2014). En el contexto de nuestro estudio, es importante destacar que algunos de los procesos fisiopatológicos involucrados en la activación de las CEHs han sido atribuidos al tratamiento con EFV (Hernández-Gea et al. 2012, 2013), y que se ha demostrado que el VIH induce directamente la secreción de citoquinas y producción de colágeno en CEHs (Tuyama et al. 2010).

La proteína *sequestosome* 1 (SQSTM1) /p62 /A170 o ZIP3 (a partir de aquí p62), es una proteína de 62 kDa expresada en la mayoría de los tejidos e inducida por estrés celular. Está codificada por un gen de respuesta rápida (*SQSTM1*) que se activa por una amplia variedad de señales extracelulares relacionadas con la proliferación celular, diferenciación y, particularmente, estrés oxidativo (Ishii et al. 2013). En los últimos años, múltiples evidencias han mostrado su implicación en patologías humanas causadas por defectos en la homeostasis proteica, como en las enfermedades neurodegenerativas de Alzheimer y Parkinson (Kuusisto et al. 2001; Geetha et al. 2012), así como por mutaciones en *SQSTM1*, como ocurre en enfermedades óseas (Laurin et al. 2002) y enfermedades neuronales (Rea et al. 2014). Además, un aumento de la actividad de p62 ha sido relacionado con carcinogénesis, bien debido a una potenciación de la expresión de la proteína (Puissant et al. 2012; Moscat et al. 2016) o por su anormal acumulación debido a defectos en la autofagia (Mathew et al. 2009). Sin embargo, el papel de p62 en los efectos adversos de los fármacos utilizados en clínica no ha sido estudiado en profundidad.

p62 es una proteína multifuncional, ya que contiene una serie de dominios que le permiten interaccionar con una amplia variedad de rutas de transducción involucradas en la proliferación, supervivencia y muerte celular. Esta proteína está involucrada en la activación de la ruta de señalización de Keap1-Nrf2 a través de un mecanismo de retroalimentación positiva en el que la transcripción de *SQSTM1* es incrementada por Nrf2 (Jain et al. 2010; Puissant et al. 2012). Un segundo papel de p62 es coordinar los procesos reguladores mediados por la ubiquitina (Nezis and Stenmark 2012; Puissant et al. 2012), facilitando la degradación dependiente del proteasoma de proteínas ubiquitinadas (Harper and Schulman 2006). p62 también participa en el proceso autofágico a distintos niveles, ya que permite la activación de mTORC1 en los lisosomas y puede actuar como receptor para la autofagia de proteínas ubiquitinadas que se encuentran agregadas en los llamados "cuerpos de p62" (Pankiv et al. 2010). Además, p62 es en sí mismo un substrato para la autofagia selectiva y es frecuentemente utilizado como marcador del flujo autofágico (Manley et al. 2013; Katsuragi et al. 2015). Numerosas evidencias han asociado p62 con vías de señalización que controlan la inflamación. De esta forma, la implicación de p62 en la función de los inflamasomas es variada; por ejemplo, se ha mostrado que p62 es esencial para controlar la activación del inflamasoma NLRP3, actuando en la inhibición de la actividad del inflamasoma a través de su participación en la autofagia, permitiendo así la degradación de los inflamasomas activos (Zhong et al. 2016). Por otra parte, esta proteína multifuncional también se ha descrito como un actor fundamental en la fisiología normal de la mitocondria, ya que su depleción produce un aumento de la fisión mitocondrial, caída del potencial de membrana ($\Delta\Psi_m$) y pérdida de la integridad del ADN mitocondrial (Seibenhener et al. 2013).

OBJETIVOS

El objetivo general de este estudio fue explorar las respuestas inflamatoria y fibrogénica agudas inducidas por el fármaco antirretroviral EFV en células hepáticas, así como profundizar en los mecanismos moleculares y celulares implicados en su regulación, empleando modelos *in vitro* e *in vivo*.

Los objetivos específicos abordados para alcanzar el objetivo general fueron:

1. Evaluar si la disfunción mitocondrial y estrés de RE inducido por EFV en hepatocitos están asociados con una activación de la respuesta inflamatoria a través de las vías dependientes de NF-κB y del inflamasoma NLRP3.
2. Caracterizar los efectos de EFV en CEHs, con respecto a la función mitocondrial, el estrés de RE, y la autofagia, con especial énfasis en la lipofagia.
3. Analizar el papel de EFV en la activación del inflamasoma NLRP3, y en la inducción de respuestas inflamatorias y fibrogénicas en CEHs.
4. Determinar el papel de los macrófagos hepáticos en la inducción y/o progresión del daño hepático inducido por EFV.
5. Evaluar la expresión y localización sub-celular de p62 en células hepáticas tratadas con EFV, que constituye un modelo de flujo autofágico activado y disfunción mitocondrial/estrés de RE.
6. Analizar la función de p62 en la disfunción mitocondrial y respuesta inflamatoria inducida en hepatocitos por EFV.

RESULTADOS

Salvo que se indique lo contrario, los tratamientos fueron realizados con concentraciones clínicamente relevantes de EFV durante 24 h.

Efectos de efavirenz en las rutas inflamatorias en células Hep3B

Activación de la ruta de señalización de NF-κB

EFV indujo la translocación nuclear de NF-κB en la línea celular de hepatoma humano Hep3B, tal y como demuestran la reducción de los niveles proteicos de su inhibidor IκB-α, y el incremento de la expresión proteica de la subunidad p65 de este factor de transcripción en los extractos nucleares, acciones que ocurren de forma dependiente de la concentración del fármaco. Además, EFV aumentó la expresión de diferentes genes relacionados con la inflamación y comúnmente relacionados con este factor de transcripción, tales como *IL6*, *SERPINE1* y *TNF*.

Activación del inflamasoma NLRP3

EFV potenció significativamente la transcripción de *NLRP3* y de su citoquina efectora *IL1B,* mientras que la expresión de *IL18* fue reducida con la

concentración más baja evaluada de EFV (10 μM). La activación del inflamasoma NLRP3 fue confirmada por una profunda reducción de la expresión proteica de la pro-caspasa-1 y un aumento de la actividad de la caspasa-1 en las células tratadas con EFV.

Efectos de efavirenz en las rutas inflamatorias y activación de las células LX-2

Inducción de estrés celular: mitocondria y retículo endoplásmico

EFV produjo disfunción mitocondrial de forma dependiente de la concentración en células LX-2 (línea celular humana de CEHs), reduciendo el $\Delta\Psi_m$ e induciendo la producción de ERO de origen mitocondrial. Las células tratadas con EFV también mostraron una masa mitocondrial aumentada, aunque tan solo con la mayor concentración (50 μM). Además, la expresión proteica de dos importantes mediadores de estrés de RE, GRP78 y CHOP, fue aumentada de manera significativa y concentración-dependiente, si bien ensayos de microscopía de fluorescencia solo mostraron alteraciones en la apariencia del RE en las células tratadas con EFV 50 μM. Estos resultados muestran que EFV induce en esta línea celular un perfil de alteraciones similar al previamente descrito en hepatocitos (Apostolova et al. 2010, 2013), aunque las células LX-2 parecen menos vulnerables al daño celular inducido por EFV.

Degradación de *lipid droplets* intracelulares por autofagia

La autofagia es un proceso celular involucrado en la activación de las CEHs para proporcionar energía a través de la hidrólisis de lípidos neutros (*lipid droplets*). La evaluación del contenido lipídico intracelular reveló una respuesta diferencial entre las concentraciones de EFV, ya que 10 y 25 μM disminuyeron la intensidad de señal del marcador de lípidos Rojo Nilo, mientras que 50 μM indujo un ligero incremento en este parámetro. La incubación con el inhibidor autofágico 3MA, revertió esta disminución en las células tratadas con EFV 25 μM, sugiriendo, por tanto, un papel de la autofagia. El análisis de la intensidad de fluorescencia del marcador lisosomal, *Lysotracker Green,* que actúa como un indicador del flujo autofágico, mostró un incremento significativo sólo con 50 μM. Además, EFV indujo un aumento en la expresión del marcador de autofagia LC3-II, sugiriendo una inducción de la autofagia en las CEHs tratadas con este fármaco. Con el objetivo de valorar si EFV estaba activando la lipofagia en CEHs, analizamos el

índice de correlación entre el marcador autofágico LC3 y la señal Rojo Nilo, mediante experimentos de microscopía confocal que revelaron un solapamiento significativo y concentración-dependiente de ambas señales, confirmando de esta forma la inducción de la degradación autofágica de *lipid droplets*.

Modulación de la respuesta inflamatoria en células LX-2

Tras determinar los efectos perjudiciales de este fármaco antirretroviral en la función celular, evaluamos si estas acciones podrían llevar a la activación del inflamasoma NLRP3 y producción de citoquinas en CEHs, que potenciarían la repuesta inflamatoria de los hepatocitos. EFV aumentó la transcripción de *NLRP3* en estas células e indujo la expresión de citoquinas pro-inflamatorias, concretamente *IL1B, IL6 y TNF* y, al igual que en células Hep3B, no se observaron cambios en los niveles de expresión de *IL18*. El perfil pro-inflamatorio sugerido por los análisis de RT-PCR cuantitativa, fue confirmado realizando un *array* en el que EFV potenció la expresión de estos genes analizados por RT-PCR cuantitativa, y de otros genes implicados en la inflamación y estrés celular, tales como *CASP1, IL33, PYCARD* y *PANX1*. Como se esperaba, el análisis por Western Blot (WB) de extractos proteicos totales de células LX-2 tratadas con EFV, reveló una expresión significativamente incrementada del receptor NLRP3. Experimentos adicionales corroboraron la activación del inflamasoma NLRP3, ya que células LX-2 incubadas con 25 o 50 μM de EFV mostraron un incremento en la actividad de la caspasa-1 y un aumento de la secreción de IL-1β.

Activación de rutas fibrogénicas

Los resultados obtenidos muestran que EFV potencia significativamente la transcripción de mediadores relacionados con CEHs activadas, tales como los marcadores de fibrogénesis (*TGFB1*) y de degradación alterada de la MEC (*TIMP1, MMP2* y *MMP9*), aunque no se observaron cambios significativos en la expresión de *COL1A1*.

Efectos de efavirenz en la función y fenotipo de los macrófagos derivados de células U937

Los resultados obtenidos en un *array* similar al realizado en células LX-2 demostraron una reducción en la expresión de algunos componentes del inflamasoma, tales como *NLRP3* y *CASP1* en macrófagos, mientras que otros

fueron ligeramente sobre-expresados, concretamente *PYCARD* e *IL1B*. En lo que respecta a la ruta purinérgica, observamos una expresión aumentada de *P2XR7,* que codifica el receptor P2X7, aunque los niveles de expresión de *PANX1* fueron similares a los encontrados en las células tratadas con vehículo. EFV también indujo un incremento significativo, y dependiente de la concentración, de varios mediadores que pueden tener una acción anti-inflamatoria en los macrófagos, tales como *NLRP12* y *RIPK2*. Por otra parte, el análisis de las proteínas NLRP3 y caspasa-1 por WB no reveló cambios significativos, mientras que la expresión proteica del factor de transcripción anti-inflamatorio PPAR-γ se vio incrementada significativamente en los macrófagos tratados con EFV. La influencia del tratamiento con este fármaco en la polarización de los macrófagos hacia los fenotipos M1 o M2 fue evaluada mediante el análisis de la expresión génica de marcadores específicos. Nuestros resultados sugieren que en macrófagos derivados de la línea celular de monocitos U937, EFV incrementa la expresión tanto de marcadores del fenotipo M1 (*NOS2* y *CD86*) como del M2 (*ARG1* y *MRC1*) promoviendo la resolución de la respuesta inflamatoria inicial.

Efavirenz induce efectos similares en células primarias hepáticas

El tratamiento con EFV en hepatocitos y CEHs primarias humanas reprodujo los mismos patrones de expresión génica que los previamente detectados en las líneas celulares humanas. De hecho, las alteraciones observadas fueron substancialmente más intensas en las células primarias que en las líneas celulares. Además, los resultados obtenidos en las células de Kupffer confirmaron la polarización inducida por EFV hacia el fenotipo anti-inflamatorio M2, tal y como demuestran la reducción de los marcadores del fenotipo M1 y el incremento de marcadores de M2. Los resultados obtenidos en células primarias validan los modelos celulares empleados y sugieren un papel dual de EFV en la progresión del daño hepático.

La depleción de las células de Kupffer modula los efectos hepáticos de efavirenz en un modelo *in vivo*

La expresión de genes pro-inflamatorios y fibrogénicos en tejido hepático completo de ratones C57BL/6 tratados con EFV difiere de la obtenida *in vitro* en hepatocitos y CEHs, ya que ninguno de los genes evaluados fue

significativamente incrementado en las muestras hepáticas. Con el objetivo de evaluar si esta discrepancia entre los resultados obtenidos *in vitro* e *in vivo* era resultado de una neutralización *in vivo* de los diferentes efectos inducidos por EFV en hepatocitos, CEHs y macrófagos, se realizaron experimentos co-administrándoles EFV y $GdCl_3$ a los ratones. La inyección intravenosa de este último compuesto indujo la depleción selectiva de los macrófagos en el hígado, como fue demostrado por la reducción de la expresión del marcador macrofágico F4/80 (evaluado mediante RT-PCR cuantitativa, inmunohistoquímica y WB). Las respuestas obtenidas en el tejido hepático de los ratones tratados con EFV estuvieron en línea con aquellas observadas en las células LX-2 y Hep3B. Concretamente, los ratones tratados con EFV y $GdCl_3$ mostraron un aumento de marcadores fibrogénicos (*Col1a1, Acta2, Vim, Timp1* y *Mmp2*), e inflamatorios y de daño (*Tnf, Il33* y *Nos2*). Sin embargo, no se observaron cambios significativos en la expresión de los componentes del inflamasoma NLRP3 y de *Tgfb1*, descartando así la participación de estas vías en el papel resolutivo de los macrófagos en los ratones tratados con EFV. Además, la expresión de la citoquina anti-inflamatoria IL-10 fue significativamente reducida por EFV solo en los animales con descenso en los niveles de macrófagos. Finalmente, el ensayo de actividad de la mieloperoxidasa confirmó una potenciación de la respuesta inflamatoria en los ratones tratados con EFV y $GdCl_3$, y demostró que la administración de este fármaco antirretroviral a dosis superiores aumenta la actividad de esta enzima, incluso sin la depleción de los macrófagos.

Efectos de efavirenz en la expresión de p62 en hepatocitos

El análisis de la expresión proteica de p62 por WB en extractos de proteínas totales obtenidos de células Hep3B tratadas con EFV indicó un incremento concentración-dependiente. Con el objetivo de explorar el marco temporal de este efecto, estudiamos la expresión de p62 en células Hep3B tratadas durante 4, 8, 24 y 48 h. Observamos que los niveles proteicos de p62 son ya incrementados de forma significativa a las 4 h, alcanzando el valor máximo a las 24 h de exposición y que continuaron elevados a las 48 h. Cabe destacar que en células Hep3B carentes de mitocondrias funcionales (fenotipo rho^0), el incremento en la expresión de p62 fue significativamente menor, apuntando al hecho de que la mitocondria juega un papel importante en la activación de p62.

Finalmente, el análisis de la expresión génica mediante RT-PCR cuantitativa reveló que EFV produce un incremento significativo en los niveles de ARN mensajero de p62 en células Hep3B. Este hallazgo fue reproducido en hepatocitos humanos, descartando así la posibilidad de que este incremento estuviera relacionado con la naturaleza tumoral de las células Hep3B y confirmando nuestros resultados previos que indican que estas células son un modelo fiable para estudios farmacológicos. Las células Hep3B co-tratadas con EFV y actinomicina D, un inhibidor de la transcripción génica, no mostraron aumentos en la expresión de la proteína p62, sugiriendo que esta potenciación en los niveles de p62 tiene lugar a nivel transcripcional.

Regulación de la localización sub-celular de p62 en células Hep3B tratadas con efavirenz

Una vez analizada la expresión proteica de p62 en extractos celulares totales, se exploró la presencia de esta proteína en los diferentes compartimentos sub-celulares, mediante el análisis de los niveles de expresión proteica de p62 en extractos proteicos de fracciones enriquecidas en mitocondrias y comparados con los de la fracción citosólica. La pureza de estas fracciones fue corroborada con la expresión de los marcadores proteicos: porina (proteína mitocondrial) y actina (proteína del citoesqueleto). EFV indujo un incremento significativo de p62 en ambas fracciones, aunque este incremento fue significativamente mayor en la fracción mitocondrial, señalando de nuevo el importante papel de la mitocondria en la regulación de la expresión de esta proteína ante la exposición con EFV.

Regulación de la expresión de p62

Nuestro siguiente objetivo fue analizar el mecanismo a través del cual se realiza la inducción de p62. EFV provoca un incremento en la concentración del Ca^{2+} citosólico en células Hep3B debido en gran medida a su papel como inductor de estrés de RE (Apostolova et al. 2013), por lo que decidimos analizar la participación de este ion en el aumento de la expresión de p62. Con la intención de explorar esta posibilidad, las células fueron tratadas con EFV en presencia o ausencia del quelante de Ca^{2+} intracelular, BAPTA. Los resultados obtenidos muestran que el Ca^{2+} juega un papel parcial en el incremento de la expresión

génica y proteica de p62 producida por EFV, ya que este aumento fue parcialmente revertido en presencia de BAPTA.

Varios factores de transcripción se han vinculado con la regulación de la expresión génica de p62, como son Nrf2 y NF-κB (Puissant et al. 2012). Teniendo en cuenta el efecto específico de inducción dual de estrés de RE y disfunción mitocondrial en nuestro modelo, decidimos investigar si la potenciación en la expresión de p62 fue mediada por el factor de transcripción CHOP, conocido por ser activado tanto por estrés de RE como por agentes oxidantes. Para ello, silenciamos de forma transitoria *DDTI3* (gen codificante de CHOP) mediante ARN de interferencia (ARNi) y evaluamos los efectos de EFV en estas células. Conviene resaltar que en las células control (no tratadas con EFV o vehículo) el silenciamiento de *DDIT3* redujo significativamente la expresión de p62, un efecto que se reprodujo en las células tratadas con EFV, sugiriendo de esta forma que el incremento de la expresión de p62 fue en gran parte mediado por CHOP. La implicación de CHOP en la regulación de la transcripción de *SQSTM1* por EFV fue confirmada mediante la realización de un ensayo ChIP, demostrando la interacción de CHOP con el promotor de *SQSTM1*. Mediante esta técnica además descartamos la participación de Nrf2 y NF-κB en la regulación de p62 en nuestro modelo.

Implicación de p62 en la autofagia, función mitocondrial y activación de la respuesta inflamatoria

Como se ha mencionado previamente, EFV (10 y 25 μM) induce autofagia en el modelo de células hepáticas empleado en este trabajo de investigación (Apostolova et al. 2011). Teniendo en cuenta que p62 es degradado por autofagia, y que es comúnmente empleado como un marcador de este mecanismo, analizamos la participación de p62 en el proceso autofágico inducido por EFV. Para ello, evaluamos los niveles de LC3-II en células Hep3B silenciadas transitoriamente para *SQSTM1* mediante ARNi. El análisis proteico de LC3-II reveló que el silenciamiento de *SQSTM1* no afectó a la expresión de LC3-II en células tratadas con EFV ni a los niveles basales de la misma. La ausencia de correlación entre la autofagia y p62 también fue demostrada con otra aproximación, mediante el uso del inhibidor farmacológico de la autofagia 3MA,

cuyo co-tratamiento con EFV no tuvo efectos significativos en la expresión génica de p62.

Además, decidimos explorar los efectos del silenciamiento de *SQSTM1* en la función mitocondrial de células tratadas con EFV. El análisis de dicha función mediante microscopía de fluorescencia, mostró que p62 no está involucrado en la caída en el $\Delta\Psi_m$ inducido por EFV; sin embargo, la deficiencia de p62 supuso una potenciación en la producción de ERO de origen mitocondrial en las células tratadas con EFV. Dado que el silenciamiento de *SQSTM1* supone un incremento en los niveles de ERO en las células expuestas a EFV, hipotetizamos que p62 podría estar cumpliendo un importante papel en la regulación de la respuesta inflamatoria inducida por EFV en hepatocitos. El análisis de la expresión génica de varios marcadores pro-inflamatorios mostró que el silenciamiento de *SQSTM1* potenció significativamente el incremento de la expresión de estos marcadores, concretamente *NLRP3, IL1B, IL6* y *TNF*. Todos estos resultados sugieren que p62 cumple una importante función protectora frente el estrés oxidativo mitocondrial y la activación del inflamasoma en este complejo modelo de toxicidad farmacológica.

CONCLUSIONES

1. La disfunción mitocondrial y estrés de RE inducidos por concentraciones clínicamente relevantes de EFV en hepatocitos están asociados con la translocación nuclear de NF-κB, promoviendo la transcripción de citoquinas pro-inflamatorias y componentes del inflamasoma NLRP3. Además, la actividad del inflamasoma NLRP3 está potenciada, incrementado de esta forma la actividad de la caspasa-1.
2. EFV induce disfunción mitocondrial, estrés de RE, y autofagia de lípidos neutros intracelulares en las CEHs, los cuales son importantes eventos celulares implicados en la transdiferenciación fenotípica de las CEHs a miofibroblastos.
3. EFV incrementa la expresión génica de clásicos mediadores fibrogénicos y pro-inflamatorios en las CEHs; además, este fármaco induce la activación del inflamasoma NLRP3 y la secreción de IL-1β.
4. Los efectos pro-inflamatorios y fibrogénicos hallados *in vitro* en hepatocitos y CEHs, no fueron reproducidos en un modelo murino de exposición aguda a EFV, el cual no mostró daño hepático evidente.

5. Los hallazgos *in vivo* pueden ser debidos a que EFV promueve la polarización de los macrófagos hacia el fenotipo anti-inflamatorio M2, que puede estar mediado por una expresión incrementada de PPAR-γ. Asimismo, la depleción de los macrófagos hepáticos *in vivo* resulta en la aparición de los efectos encontrados en hepatocitos y CEHs, enfatizando de esta forma el importante papel de los macrófagos en la mediación del daño hepático inducido por EFV.
6. La expresión de p62 es aumentada en hepatocitos tratados con EFV, y esto ocurre a través del factor de transcripción CHOP, mientras que otros reguladores conocidos de esta proteína, tales como Nrf2 y NF-κB no están involucrados.
7. Los niveles incrementados de p62 ejercen un papel protector frente a los efectos producidos por EFV, tales como la producción de ERO mitocondriales y citoquinas pro-inflamatorias, así como la activación del inflamasoma NLRP3, un papel que parece ser independiente de la autofagia.

ABSTRACT

Efavirenz (EFV) is among the antiretroviral drugs most widely employed against the human immunodeficiency virus (HIV) infection. Despite being considered a safe, highly efficient and well-tolerated drug, there is growing concern about EFV-induced adverse events. It has been associated with hepatotoxic effects, and although the mechanisms involved are yet to be clarified, evidence has shown that in cultured cells, it induces a pattern of actions in hepatocytes, including endoplasmic reticulum (ER) stress and mitochondrial dysfunction, which could underlie induction of hepatic inflammation. The NLRP3 inflammasome is an important regulator of inflammatory and fibrogenic responses in several liver disorders such as drug-induced liver injury, non-specific hepatitis and non-alcoholic steatohepatitis.

In the present work, we explore the inflammatory and fibrogenic responses produced by short-term exposure to the antiretroviral drug EFV in major liver cell types -hepatocytes, hepatic stellate cells (HSCs) and macrophages-, by performing *in vitro* (human hepatic cell lines and primary cells) and *in vivo* experiments (liver tissue samples from C57BL/6 mice). EFV triggered a pro-inflammatory response in hepatocytes, that involved NF-κB and the NLRP3 inflammasome, and it also activated HSCs, thereby enhancing expression of pro-inflammatory cytokines (such as IL-1β, TNF-α, IL-6), components of the NLRP3 inflammasome and purinergic signaling, and fibrogenic (TGF-β1, TIMP-1, MMP-2, MMP-9 and collagen 1α1) mediators in the latter cell type. NLRP3 inflammasome was not altered in EFV-treated macrophages, but these cells polarized towards the anti-inflammatory and pro-resolving M2 phenotype and displayed upregulated anti-inflammatory markers (PPAR-γ, NLRP12 and IL-10). Unexpectedly, no evidence of liver injury was observed in EFV-treated mice, which did not display increases in inflammatory and fibrogenic markers. However, when macrophages were depleted, it resulted in the *in vivo* manifestation of the deleterious effects detected in hepatocytes and HSCs.

Additionally, we explored the role of p62 in EFV-induced hepatocyte damage. SQSTM1/p62 is a stress-induced scaffold protein involved in multiple cellular processes including autophagic clearance, regulation of inflammatory responses and redox homeostasis. Our results show that, despite activation of autophagy, p62 protein content is increased due to enhanced *SQSTM1* transcription in hepatocytes. This EFV-induced increase in p62 levels is mediated through the transcription factor CHOP, and not through its traditional regulators, NF-κB and

Nrf2. Our data also suggest that p62 exerts a protective function against several EFV-induced actions such as mitochondrial reactive oxygen species production and expression of pro-inflammatory cytokines and components of the NLRP3 inflammasome.

In conclusion, EFV elicits a cell-specific activation of pro-inflammatory (including the NLRP3 inflammasome) and pro-fibrogenic pathways in hepatocytes and HSCs. Macrophages appear to counteract these EFV-induced deleterious actions in the liver, by their polarization towards the anti-inflammatory M2 phenotype. In hepatocytes, EFV specifically up-regulates p62, which alleviates the mitochondrial dysfunction and inflammatory response. Considering the previously reported EFV-induced toxic effects on hepatocytes, our findings highlight the dynamic nature of the interaction that takes place among liver cell populations, and may help to understand the variability in adverse hepatic events observed in EFV-treated patients. Convergence with other liver-injury-promoting factors in the HIV-infected population, such as other antiretroviral drugs, co-infections (hepatitis B and/or C) or metabolic co-morbidities, could enhance the deleterious actions of this compound and contribute to the pathogenesis of liver disease.

INDEX

Chapter I. INTRODUCTION

I.1. HUMAN IMMUNODEFICIENCY VIRUS (HIV) AND ANTIRETROVIRAL THERAPY

I.1.1. HIV life cycle and infection

HIV is a retrovirus which includes two subtypes, HIV-1 and HIV-2. HIV-1 is more pathogenic and more prevalent than HIV-2, and is the main responsible for the well-known global pandemic, the acquired immunodeficiency syndrome (AIDS) (Barré-Sinoussi et al. 2013; Deeks et al. 2015). HIV has infected >78 million people since the beginning of the epidemic in 1981 and is one of the main causes of morbidity and mortality worldwide. Sub-Saharan Africa carries the highest burden of HIV, accounting for more than 70,8% of the global burden of infection, especially Southern Africa (Maartens et al. 2014; GBD 2013 Mortality and Causes of Death Collaborators 2015; UNAIDS 2016a). According to the last official statistics, in 2015 there were 36.7 million people living with HIV, of which approximately 2.1 million were newly infected, and 1.1 million died of the infection (UNAIDS 2016b; Yoshimura 2017).

Activated $CD4^+$ T lymphocytes are the main target of HIV, and its entry into cells is mediated by means of the binding of the viral *Env* glycoprotein to cell surface proteins CD4 and the chemokine co-receptors, CXCR4 and CCR5. Other cells holding these receptors are also infected, such as resting $CD4^+$ T cells, macrophages, monocytes and dendritic cells (Maartens et al. 2014). Moreover, HIV infection can happen independently of the CD4 receptor, as occurs in astrocytes (Liu et al. 2004) and renal tubular epithelial cells (Chen et al. 2011). Like all retroviruses, the genome of HIV is composed of two copies of ssRNA, which is transcribed to dsDNA by the viral reverse transcriptase and is then integrated into the genome of the host cell by the viral integrase to produce new viral particles. Concomitant with or soon after budding of the new virions from the cell, they are matured by the HIV protease which cleaves the viral polyproteins into active subunits to produce infectious proteins (Figure I.1) (Arts and Hazuda 2012; Laskey and Siliciano 2014; Freed 2015). The different steps of the viral life cycle inside the host cells (entry, reverse transcription, genome integration and proteolytic maturation) can be inhibited by several available inhibitors, which constitute the current pharmacological treatment of HIV infection.

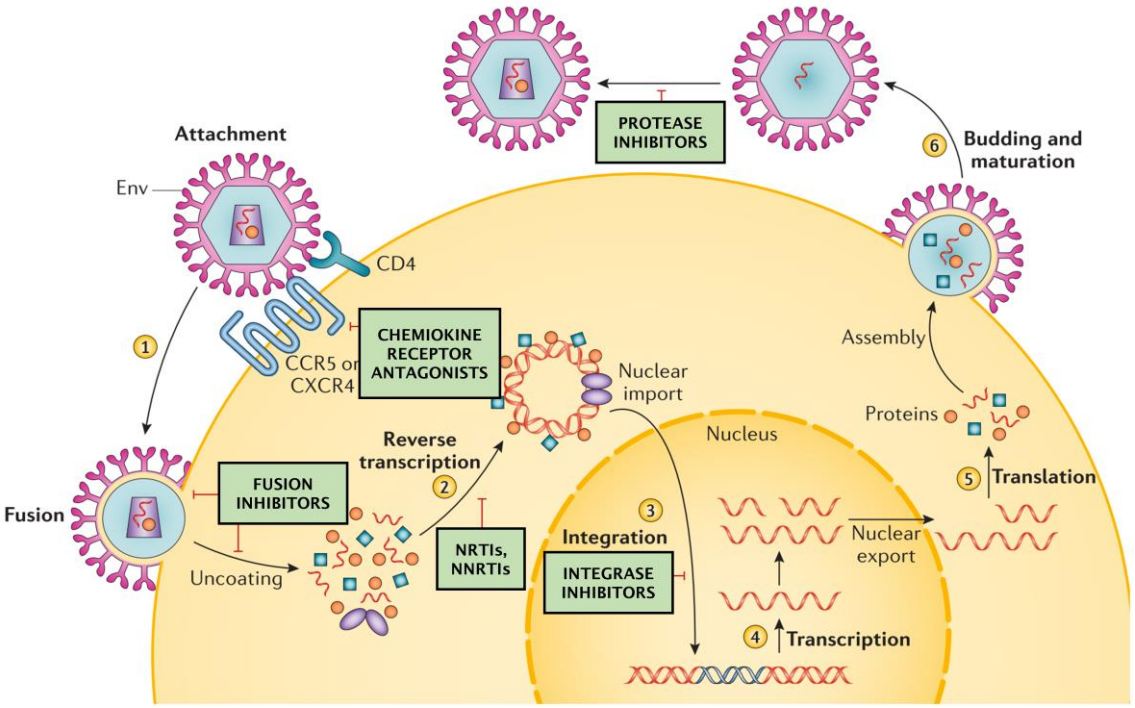

Figure I.1. Schematic overview of the HIV life cycle showing the stages that are targeted by antiretroviral drugs (green boxes). Adapted from Deeks et al., 2015.

Infection with HIV typically occurs by sexual transmission following exposure to cell-associate or cell-free infectious virus in semen or mucosal surfaces. Less common routes include exposure during blood transfusion, injection of drugs of abuse, and exposure of neonates to HIV from infected mother (Moir et al. 2011; Maartens et al. 2014). It is estimated that 50-90 % of patients experience an acute HIV syndrome after two or four weeks following infection, a period during which HIV replicates aggressively, reaching the highest plasma levels of HIV RNA (1-10 million copies/mL) (Stevenson 2003; Moir et al. 2011). The acute HIV syndrome is characterized by flu-like symptoms associated with high viral load, fever and lymphadenopathy (Gurunathan et al. 2009). Once the immune system develops a HIV-specific response, the viremia declines markedly for several months reaching the viral set point and most of patients exhibit a period of clinical latency that lasts for years (Pantaleo et al. 1993; Moir et al. 2011). During this period, patients suffer a progressive depletion of the $CD4^+$ T cells with a deterioration of the immune system, which leads to the development of an immunodeficiency status (or AIDS) where the individuals may be more susceptible to other opportunistic infections, such as *Mycobacterium tuberculosis*, toxoplasmosis or candidiasis (Pantaleo et al. 1993; Deeks et al. 2013, 2015; Naif 2013). Nowadays, the availability and

efficacy of antiretroviral drugs frequently avoid the development of AIDS in HIV-infected patients because of their high efficiency to attenuate HIV replication.

I.1.2. Antiretroviral drugs

Before the development of antiretroviral drugs, the clinical management of patients consisted in the treatment of opportunistic infections and AIDS-related illness with limited success (Arts and Hazuda 2012; Barré-Sinoussi et al. 2013). The first step in anti-HIV therapy was made in 1987, when the FDA (US Food and Drug Administration) approved zidovudine (AZT) to treat HIV infection, a drug that had been originally developed for cancer treatment. Its use decreased opportunistic infections and mortality in patients with AIDS, but nevertheless AZT monotherapy quickly developed viral resistance, and the ineffectiveness of long-term therapy forced the development of HIV specific antiviral drugs in order to suppress the viral replication (Larder et al.; Fischl et al. 1987; Broder 2010). Subsequently, the first nucleoside analogue reverse transcriptase inhibitors (NRTIs), protease inhibitors (PIs) and non-nucleoside analogue reverse transcriptase inhibitors (NNRTIs) were developed in early 1990s, and although they were individually active and produced a rapid decay in viremia, the success was limited due to the appearance of viral resistances and toxic effects (Ho et al. 1995; Wei et al. 1995; Hammer et al. 1996; Thompson et al. 2012; Laskey and Siliciano 2014). The modern era of antiretroviral therapy began in 1997, with the introduction of three drug combinations, known as combined antiretroviral therapy (cART) or highly active antiretroviral therapy (HAART). cART effectively suppresses the HIV replication cycle, which reduces HIV viral load and increases circulating levels of $CD4^+$ T lymphocytes, resulting in a restoration of immune system (Autran et al. 1997; Lederman et al. 1998; Barré-Sinoussi et al. 2013; Maartens et al. 2014). The success of cART results in part from the election of drugs that are directed against at least two different stages of the viral cycle, decreasing the probability of selecting virus clones and thus preventing the evolution of drug resistance. Although cART cannot completely eliminate the virus, this treatment regimen has transformed AIDS from a progressive and fatal disease to a chronic manageable infection, markedly reducing the morbidity and mortality associated with HIV infection (e.g., in South Africa, life expectancy

increased 11 years over the period 2003-2011) (Palella et al. 1998; Arts and Hazuda 2012; Thompson et al. 2012; Maartens et al. 2014; Deeks et al. 2015).

The range of available drugs has continued to expand and, currently, 26 antiviral drugs are approved for use in adults by European and US agencies (Table I.1). They are classified in six families, each targeting a specific stage in the HIV replication cycle (Figure I.1): CCR5 co-receptor antagonist, fusion inhibitor (FI), NRTIs, NNRTIs, integrase inhibitors (IIs) and PIs (AIDSinfo 2016; UNAIDS 2016a).

I.1.2.1. CCR5 co-receptor antagonist

The pharmacological action of this drug class consists in binding to the hydrophobic transmembrane pocket of CCR5 co-receptor in the plasma membrane of the host cell, which modifies the co-receptor conformation, hence preventing its interaction with the HIV envelope glycoprotein (gp) 120, required for CCR5-dependent viral entry. Maraviroc (MVC), the only approved CCR5 antagonist, has exclusive tropism for this receptor, being ineffective against viral strains with tropism to CXCR4, another co-receptor that may be used by HIV to interact with host cell (De Clercq 2007; Wilkin and Gulick 2012; Van Der Ryst 2015).

I.1.2.2. Fusion inhibitor

Currently, enfuvirtide (T-20) is the only drug available in this class, which was derived from a motif found in the viral transmembrane glycoprotein gp41. T-20 binds competitively to heptad repeat (HR) 1 region and mimics the HR2 activity of gp41, thereby preventing the conformational change necessary for gp41 to initiate fusion between the viral envelope and the membrane of the host cell, and consequently the HIV entry (Chan et al. 1997; Fung HB 2004; Hardy and Skolnik 2004).

DRUG CLASS	GENERIC NAME	FDA APPROVAL DATE
CCR5 Antagonist	Maraviroc (MVC)	August 6, 2007
FI	Enfuvirtide (T-20)	March 13, 2003
NRTIs	Abacavir (ABC)	December 17, 1998
	Didanosine (ddI)	October 9, 1991
	Emtricitabine (FTC)	July 2, 2003
	Lamivudine (3TC)	November 17, 1995
	Stavudine (d4T)	June 24, 1994
	Tenofovir disoproxil fumarate (TDF)	October 26, 2001
	Tenofovir alafenamide (TAF)	November 5, 2015
	Zidovudine (AZT)	March 19, 1987
NNRTIs	Efavirenz (EFV)	September 17, 1998
	Etravirine (ETR)	January 18, 2008
	Neviparine (NPV)	June 21, 1996
	Rilpivirine (RPV)	May 20, 2011
IIs	Dolutegravir (DTG)	August 13, 2013
	Elvitegravir (EVG)	September 24, 2014
	Raltegravir (RAL)	October 12, 2007
PIs	Atazanavir (ATV)	June 20, 2003
	Darunavir (DRV)	June 23, 2006
	Fosamprenavir (FPV)	October 20, 2003
	Indivanir (IDV)	March 13, 1996
	Nelfinavir (NFV)	March 14, 1997
	Ritonavir (RTV)	March 1, 1996
	Saquinavir (SQV)	December 6, 1995
	Tripanavir (TPV)	June 22, 2005
	Lopinavir (LPV)	September 15, 2000

Table I.1. Anti-HIV drugs approved by FDA (AIDSinfo 2016).

I.1.2.3. Nucleoside reverse transcriptase inhibitors

NRTIs were the first agents approved by FDA for the treatment of HIV infection (Young 1988). These drugs are analogues of the natural nucleoside substrates and are integrated preferentially into viral DNA (Deeks et al. 2013). NRTIs are prodrugs, thus they need to be incorporated into the host cell and phosphorylated by cellular kinases in order to gain an antiviral effect (Hart et al. 1992). NRTIs inhibit HIV replication by substituting the endogenous nucleotides, which prevents the formation of a 3'-5'-phosphodiester bond between the drug and incoming 5'-nucleoside triphosphates during the reverse transcription of viral RNA, leading to the termination of the elongation of the new viral DNA chain (Nurutdinova and Overton 2009; Arts and Hazuda 2012; De Clercq 2013). Unluckily, they also act as substrates for DNA polymerase gamma (pol-γ) of host cells, and their interference with mitochondrial DNA (mtDNA) synthesis leads to a reduction in the mtDNA content, thus inducing mitochondrial toxicity (Feng et al. 2001; Nurutdinova and Overton 2009; Apostolova et al. 2011b, 2011c).

I.1.2.4. Non-nucleoside reverse transcriptase inhibitors

These drugs are non-competitive inhibitors of HIV-1 reverse transcriptase by binding close to the active site and inducing the formation of a hydrophobic pocket which causes a conformational change of the enzyme and reduces its activity (Usach et al. 2013). NNRTIs are characterized by long plasma half-lives which allows a unique daily dose (de Béthune 2010). NNRTIs exhibit a substantial interindividual variability in their pharmacokinetic; therefore, their plasma levels can differ greatly among different patients. These drugs are biotransformed through cytochrome P450 (CYP) system and exert variable effects on specific isoenzymes of CYP: inhibition, induction or mixed (e.g. EFV acts as a CYP2C9 and 2C19 inhibitor, and a 2B6 inducer); thus, they can trigger variable effects on other drugs whose metabolism occurs through the same pathway (Ma et al. 2005; Blas-Garcia et al. 2011; Usach et al. 2013).

I.1.2.5. Integrase inhibitors

Drugs belonging to this pharmacological group bind to the active site of HIV-1 integrase, and this only happens when the integrase forms a complex with the

reversely transcribed viral DNA. Currently, there are three drugs available in this drug class, DTG, EVG and RAL, which seem to be safe, potent and well tolerated (Koelsch and Cooper 2009; Wong et al. 2016).

I.1.2.6. Protease inhibitors

HIV-1 protease cleaves Gag and Gag-Pol polyproteins into their functional proteins (protease, reverse transcriptase and integrase), thereby enabling the maturation of HIV-1 virions, which happens during the final stages of the HIV replication cycle. PIs are designed as competitive inhibitors that tightly bind to and inhibit the viral protease promoting the release of noninfectious and immature virions (Hughes et al. 2011; Zhengtong et al. 2015). These drugs are quickly metabolized by the liver and are commonly co-administered with low-dose RTV, employed as a boosting agent because of its capacity to inhibit the CYP metabolic pathway, in order to increase their half-lives (Deeks SG 1997).

I.1.3. Guidelines of antiretroviral therapy

Nowadays, almost 50% of HIV-infected people worldwide have access to cART, (Deeks et al. 2015; UNAIDS 2016a, 2016b). This combined therapy has been considered for 20 years the standard treatment for HIV-infected patients, both anti-HIV drug-naïve and drug-experienced (De Clercq 2010; Kanters et al. 2016). It was designed to decrease the probability of developing drug resistance, to reduce specific drug side effects by diminishing their individual dosages, and to obtain a synergic effect between different drugs which exert their pharmacological action at different molecular targets (De Clercq 2009).

HIV-infected patients can be exposed to antiretroviral compounds for decades, considering extended virologic suppression, improved clinical results and longer life expectancy in cART-treated patients. Hence, it is a priority to improve the tolerability and safety of cART regimens without lessening their clinical efficacy (Cihlar and Fordyce 2016). The choice of a cART regimen is based on the antiviral potency, drug tolerability, convenience of the drug regimen (dose frequency), clinical status of the patients, drug interactions, risk of resistance and cost (Günthard et al. 2016). According to the current guidelines, first-line cART in adults consists of two NRTIs combined with a third agent that can be a NNRTI, an II or a boosted PI (Table I.2) (Badowski et al. 2016; Cihlar and Fordyce 2016; Kanters et al. 2016).

Recommended antiretroviral regimens for treatment-naïve patients			
Regimen	**Components**		
	NRTI	**NRTI**	**Third agent**
II-based	ABC[a]	3TC	DTG
	TDF or TAF[b]	FTC	DTG
	TDF or TAF	FTC	EVG/c[c]
	TDF or TAF	FTC	RAL
PI-based	TDF or TAF	FTC	DRV/r[d]
Alternative antiretroviral regimens for treatment-naïve patients			
Regimen	**Components**		
	NRTI	**NRTI**	**Third agent**
NNRTI-based	TDF or TAF	FTC	EFV
	TDF or TAF	FTC	RPV[e]
PI-based	TDF or TAF	FTC	ATV/c or ATV/r
	ABC	3TC	DRV/c or DRV/r
	TDF or TAF	FTC	DRV/c

Table I.2. Antiretroviral regimens based on guidelines developed by the US DHHS Panel on antiretroviral guidelines for adults and adolescents (AIDSinfo 2016). [a] only for patients who are HLA-B*5701 negative; [b] TAF is a modified TDF, which has alafenamide instead of difumarate in its structure; [c] /c, drug boosted with cobicistat, a pharmacokinetic enhancer; [d] /r, drug boosted with RTV; [e] if HIV RNA <100000 copies/mL and CD4 >200 cells/mm^3, otherwise may cause virologic failure.

cART has been successful in increasing life expectancy of HIV patients and therefore, modern HIV epidemic manifests a demographic aging shift. As a consequence, HIV patients are now also treated for several age-related non-AIDS disorders, such as cardiovascular diseases, liver diseases, neurocognitive diseases or cancer (Carr 2003; Deeks et al. 2013; Guaraldi et al. 2014a, 2014b; Badowski et al. 2016; Slim and Saling 2016; Yoshimura 2017). Due to the fact that cART only suppresses HIV replication and does not eradicate it, this therapy is administered for life. Hence, and considering that even small toxic effects might contribute to increase the severity of non-AIDS-related comorbidities, treatment guidelines should recommend regimens based not only on their antiviral potency but also on their long-term toxicity. Although knowledge about antiretroviral drugs toxicities is increasing, there are still not

enough evidence as to firmly establish which antiretroviral drug class or combinations are safer (Carr 2003; Flexner 2007; Franchi et al. 2009; Blas-Garcia et al. 2011; Deeks et al. 2013; Margolis et al. 2014; Slim and Saling 2016).

I.1.4. Side effects of antiretroviral therapy

Antiretroviral resistance, adherence and toxicity are the main problems of cART, which must be overcome in order to obtain the benefits of this therapy. cART-related toxicity and adverse effects have been described with all antiretroviral drugs, and have been considered the most common reason for discontinuing or refusing cART. The majority of cART-induced adverse effects arise from the therapeutic doses of antiretroviral drugs and drug-drug interactions, whereas overdosing, either intentional or unintentional, is a rare event (Carr 2003; Domingo and Lozano 2011; Margolis et al. 2014). Most side effects are associated with the long-term administration, although adverse events upon acute exposure have also been reported. Overall, gastrointestinal disturbances, hypersensitivity and skin reactions, central nervous system (CNS)/neuropsychiatric conditions and liver toxicity tend to appear early after initiation of treatment. Other side effects, such as lipid and glucose metabolism (hyperlipidemia, lipodystrophy, and impaired glucose tolerance), kidney abnormalities, bone metabolic disorders and mitochondrial toxicity, generally develop after chronic exposure to the drugs. Although each antiretroviral agent has its own toxicological profile several adverse events tend to be shared by compounds within the same drug class (Table I.3) (Hofman and Nelson 2006; Blas-García et al. 2010; Fernandez-Montero et al. 2013; Kalapila and Marrazzo 2016).

Different factors may influence the appearance of side effects, including gender, the presence of underlying diseases, concomitant medications, diet, drug interactions and genetic factors. Regarding the latter, it has been reported that the administration of standard doses of most anti-HIV drugs results in significant variations in their plasma concentrations among different individuals due to differences in their metabolism of drugs, an effect which influences the incidence of drug-induced side effects, or even the presence of certain toxicities (e.g. ABC and the presence of HLA-B*5701 allele) (Rodríguez-Nóvoa et al. 2006; Domingo and Lozano 2011; AIDSinfo 2016).

Mounting evidence shows that second-generation antiretroviral drugs have a safer profile than earlier agents/compounds, but drug-related adverse effects continue to occur, including drug interactions, though to a lesser extent than with the first generation of drugs. On the other hand, it is important to emphasize that the vast majority of HIV-infected people live in areas where the older antiretroviral agents with worse side effects are still often prescribed as major treatments (Fernandez-Montero et al. 2013; UNAIDS 2016a).

DRUG CLASS	ADVERSE EFFECTS	COMMENTS
NRTIs	Nephrotoxicity	TDF
	Hypersensitivity reactions	Seen with ABC in human leukocyte antigen B*57:01-positive individuals
	Lactic acidosis	Rare. Common with AZT
	Lipoatrophy	AZT
	Loss of bone mineral density	Prolonged TDF use
	Bone marrow suppression, macrocytic anemia	AZT
	Fanconi syndrome	Rare condition associated with TDF
	Myopathy	AZT
	Increased risk of cardiovascular events	ABC, ddI
	Diarrhea, pancreatitis, neuropathy	ddI
	Non-cirrhotic portal hypertension, hepatic steatosis	Can occur months to years after starting ddI and d4T
	Hyperpigmentation	FTC
NNRTIs	Several drug interactions	Mostly noted with EFV
	Rash	All NNRTIs
	Neuropsychiatric side effects	Mostly associated with EFV. RPV has also been related to psychiatric effects
	Hepatic effects	NVP > other NNRTIs
	Dyslipidemia	Mostly associated with EFV
	Stevens-Johnson syndrome	NVP > other NNRTIs
	Teratogenicity	EFV
	Cardiovascular diseases	RPV: QTc prolongation

DRUG CLASS	ADVERSE EFFECTS	COMMENTS
PIs	Several drug interactions	PIs are potent inhibitors of the cytochrome CYP450
	Gastrointestinal symptoms	GI intolerance (e.g. nausea, vomiting, diarrhea)
	Diabetes, insulin resistance	Less with newer PIs (ATV, DRV)
	Dyslipidemia	Less with newer PIs (ATV, DRV)
	Hepatotoxicity	All PIs
	Lipohypertrophy	Mostly with older PIs
	Nephrolithiasis, cholelithiasis	ATV
	Rash/Stevens-Johnson syndrome	ATV, DRV, LPV/r, FPV, TPV
	Cardiovascular disease	Mostly with ATV, SQV, LPV, RTV
FI	Elevated serum transaminases	T-20
CCR5 antagonist	Hepatotoxicity	MVC
IIs	Gastrointestinal symptoms	EVG/c
	Hypersensitivity reaction	Mostly with RAL and DTG
	Neuropsychiatric side effects	Mostly DTG and RAL
	Myopathy	RAL

Table I.3. Common antiretroviral drug-associated adverse effects (AIDSinfo 2016).

I.1.4.1. Antiretroviral therapy-associated hepatotoxicity

Hepatotoxicity or drug-induced liver injury (DILI) has become one of the most common disadvantages of cART, responsible for morbidity, mortality and treatment discontinuation in HIV-infected patients (Calmy et al. 2009; Núñez 2010; Jones and Núñez 2012; Casado 2013; Fernandez-Montero et al. 2013). Although a universally accepted definition for DILI has not been agreed yet, elevated liver enzyme levels have been employed as a marker of liver toxicity in different clinical trials and cohort studies. AIDS Clinical Trials Group defined severe liver toxicity as presence of an increase in plasma alanine aminotransferase (ALT) and alkaline phosphatase (ALP) levels greater than five- and two-fold above the upper normal limit, respectively (Jones and Núñez 2012; Medina-Caliz et al. 2016; Neukam et al. 2016). Following this criterion,

most of studies have shown that the incidence of increased liver transaminases levels is around 2-18% after one or more months on cART, or even up to 30% in some reports (Hernandez et al. 2001; Sulkowski et al. 2002; Casado 2013). To ascertain the liver toxicity associated to each antiretroviral compound is complicated because of the use of a combined therapy, co-exposure to other liver toxins or the presence of preexisting hepatic conditions (Spengler et al. 2002; Abrescia et al. 2005). Nevertheless, extensive use of these drugs has contributed to elucidate which drugs are more potentially hepatotoxic, namely NVP, EFV, LPV, RTV, AZT, d4T or ddI (Domingo and Lozano 2011; Jones and Núñez 2012).

Besides the toxicity associated with a specific antiretroviral drug or class, other risk factors have been associated with cART-induced liver injury in HIV-infected patients. One of the main non-drug related factors is chronic hepatitis with either HCV or HBV, considering that co-infected patients experience up to 6 times greater increases in plasma levels of liver enzymes compared to HIV mono-infected patients. Moreover, severe alcohol consumption, drug abuse, drug interactions, age, gender, ethnicity, hepatic steatosis and genetic markers (e.g. CYP2B6 and HLA-DRB1*01 alleles) may cause major susceptibility to cART-induce liver damage (Abrescia et al. 2005; Soriano et al. 2008; Barve et al. 2010; Kovari and Weber 2011; Jones and Núñez 2012).

cART-related DILI can be mediated by several mechanisms including direct cell stress, lactic acidosis/mitochondrial inhibition, disturbances of glucose/lipid metabolism, fatty acid infiltration, hypersensitivity reactions and immune reconstitution (Núñez 2010; Fernandez-Montero et al. 2013). The severity of cART-induced liver toxicity may range from asymptomatic with transient liver enzyme elevations to several hepatotoxicity clinical syndromes, such as hepatitis, non-alcoholic steatohepatitis (NASH), non-cirrhotic portal hypertension or even acute liver failure followed, although rarely, by death (Clark et al. 2002; Núñez 2010; Casado 2013; Fernandez-Montero et al. 2013).

Importantly, newer antiretroviral drugs are safer for the liver (Neukam et al. 2011; Blas-García et al. 2014), but due to the aging of the HIV-infected patients and their longer life expectancy, cART-associated liver toxicity will probably continue to be a major challenge in the treatment of HIV.

I.1.5. Efavirenz

EFV, chemically described as (4S)-6-chloro-4-(2-cyclopropylethynyl)-1,4-dihydro-4-(trifluoromethyl)-2H-3,1-benzoxazin-2-one (Figure I.2), is a benzoxazinone derivate discovered by Merck in 1995 and approved by FDA in 1998 (Huff et al. 1995; Waters et al. 2007; de Béthune 2010). Due to availability of new antiretroviral drugs (e.g. IIs) with a safer toxicological profile, EFV is part of alternative cART regimens in western countries, but this NNRTI is one of the most widely used anti-HIV drugs in developing countries because of its high efficacy and low cost (Kanters et al. 2016; Neukam et al. 2016; Sonderup et al. 2016). Time-to-peak plasma concentration is 3-5 h and steady-state plasma concentrations are reached in 6-10 days (Maggiolo 2009; Blas-Garcia et al. 2011; Usach et al. 2013). The long half-life of EFV (45-52 h) has allowed its one-daily dosing, with a recommended dose of 600 mg in adults, exhibiting a prolonged effect on the suppression of viral replication. To avoid the emergence of resistance to this NNRTI, it is prescribed with two other antiretroviral drugs, traditionally NRTIs. A daily standard dose of EFV usually results in plasma levels of 5.6±3.2 μM – 12.9±3.7 μM (Starr et al. 1999; Staszewski et al. 1999; Maggiolo 2009). Nevertheless, EFV plasma levels vary substantially as a result of interindividual variability in its pharmacokinetics, with levels as high as 30-50±3.2 μM in up to 40% of EFV-treated patients (Marzolini et al. 2001; Taylor et al. 2001; Burger et al. 2006; Stöhr et al. 2008; Carr et al. 2010), and even concentrations of 80 μM have been reported (Hasse et al. 2005; Kwara et al. 2009a; van Luin et al. 2009; Gounden et al. 2010).

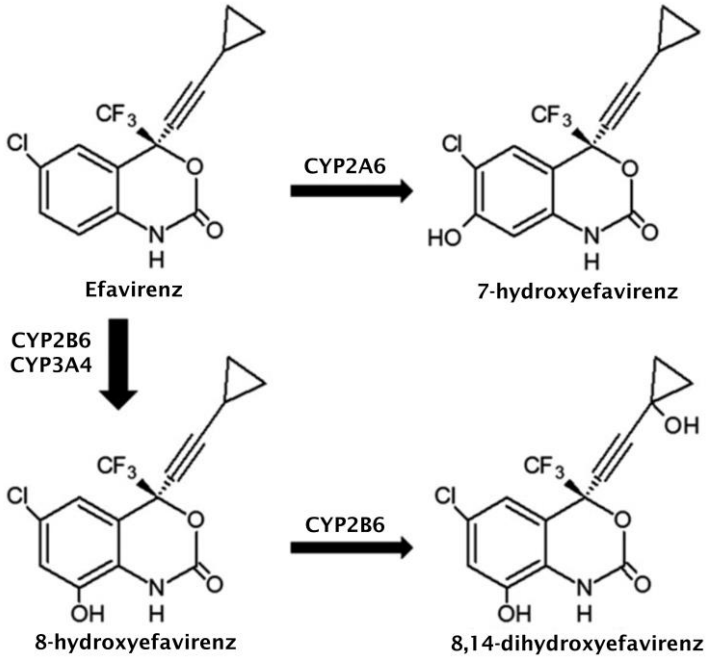

Figure I.2. Chemical structure of EFV and its metabolic pathways. This NNRTI is mostly metabolized to biologically inactive 8-hydroxyefavirenz, but is also biotransformed to 8,14-dihydroxyefavirenz and 7-hydroxyefavirenz, in reactions catalyzed by CYP2B6, CYP2A6 and CPY3A4 (Apostolova et al. 2015b).

Most of EFV (90%) is biotransformed in the liver into pharmacological inactive hydroxylated metabolites through the CYP system, where its isoform CYP2B6 plays a crucial role. Several studies have shown that CYP2B6 is implicated in the hydroxylation of EFV to 8-hydroxyefavirenz (its most important metabolite); in addition, the isoforms CYP3A4 and CYP2A6 are also involved (see Figure I.2) (Marzolini et al. 2001; Ward et al. 2003; Apostolova et al. 2015b). Abundant evidence has shown that polymorphisms in CYP2B6 may be to responsible for the interindividual variations in EFV plasma concentrations and the development of toxicity , being the 516G > T polymorphism in exon 4 of the CYP2B6 gene the allelic variant most widely associated with increased plasma EFV concentrations (Haas et al. 2004; Lowenhaupt et al. 2007; Stöhr et al. 2008; Kwara et al. 2009; Leger et al. 2009; Mathiesen et al. 2009; Ramachandran et al. 2009; Wyen et al. 2011; Elsharkawy et al. 2013).

EFV is commonly considered an efficacious and safe drug (Kryst et al. 2015; Kanters et al. 2016); nevertheless, there is a concern about the adverse effects induced by EFV-containing cART, including rash (Manosuthi et al. 2006), neuropsychiatric disorders (Gutiérrez et al. 2005; Lowenhaupt et al. 2007;

Mathiesen et al. 2009; Decloedt et al. 2013), lipid and metabolic disturbances (Tashima et al. 2003; Aberg 2009; Loko et al. 2011), and liver toxicity (Mugusi et al. 2012; Echenique and Rich 2013). EFV-induced DILI is an uncommon event, however it has been associated with significant morbidity and mortality upon the beginning of the therapy in cART naïve-patients without prior AIDS-defining illness (Sonderup et al. 2016). Moreover, severe liver injury has been reported in 1-8% of EFV-treated patients (Martín-Carbonero et al. 2003; Manfredi et al. 2004) and it has been correlated with acute liver failure, sub-massive necrosis, mixed cholestasis-hepatitis and non-specific hepatitis (Clark et al. 2002; Hoffmann et al. 2007; Macías et al. 2012; Elsharkawy et al. 2013; Fink and Bloch 2013; Sonderup et al. 2015, 2016).

The molecular mechanisms underlying EFV-induced liver injury remains unclear. Mitochondrial toxicity has been involved in the liver toxicity related to cART, but it has been usually attributed to NRTIs, because of their ability to inhibit pol-γ which is responsible for mtDNA replication (Feng et al. 2001; Walker et al. 2002; Nurutdinova and Overton 2009). However, the mechanism behind EFV-induced liver toxicity is different to that exerted by NRTIs, considering that EFV does not inhibit pol-γ. Experiments performed *in vitro* have shown that EFV provokes deleterious effects in hepatocytes involving mitochondrial dysfunction due to specific inhibition of complex I of the electron transport chain (ETC), decreased ATP production and mitochondrial membrane potential ($\Delta\Psi_m$), bioenergetic stress and elevated reactive oxygen species (ROS), which leads to a rapid intracellular increased of lipid droplets, and subsequently triggers autophagy activation to promote cell survival (Apostolova et al. 2010, 2011d, 2011e; Blas-García et al. 2010; Imaizumi et al. 2015; Polo et al. 2015). Other studies in hepatocytes uncovered that EFV-induced oxidative stress and mitochondrial dysfunction lead to apoptotic cell death (Apostolova et al. 2010; Bumpus 2011) through the activation of the ASK1-JNK-BimEL pathway (Bumpus 2011). Simultaneously, EFV induces endoplasmic reticulum (ER) stress and activates the unfolded protein response (UPR), where mitochondria play a relevant role (Gomez-Sucerquia et al. 2012; Apostolova et al. 2013; Hu et al. 2015; Polo et al. 2015). In this line, studies with neurons and glia cells have revealed that EFV induces acute mitochondrial dysfunction, oxidative stress and autophagy similar to those described in hepatocytes, and promotes nitric oxide (NO) production, further undermining

their mitochondrial function (Funes et al. 2014; Purnell and Fox 2014; Apostolova et al. 2015a).

I.2. MECHANISMS OF DRUG-INDUCED LIVER INJURY

Damage and cellular death of hepatocytes are essential processes in the development of drug-induced liver injury, which can be induced by the drug itself or by its metabolites. Damaged hepatocytes release danger signals, also known as damage-associated molecular patterns (DAMPs), which favor the progression and/or perpetuation of liver injury because of the activation of pro-inflammatory and fibrogenic responses. Factors contributing to initial cellular injury by drugs include mitochondrial dysfunction, oxidative stress and ER stress, all of them described in cART-related liver toxicity and with EFV, as mentioned above (Pessayre et al. 2012; Yuan and Kaplowitz 2013; Fontana 2014; Chen et al. 2015). DILI can be manifested clinically as cholestasis, hepatocellular injury or a mixture of both, such as hepatitis, steatohepatitis, fibrosis or cholestatic hepatitis (Fisher et al. 2014; Fontana 2014; Leise et al. 2014). Considering that the mechanisms of liver injury induced by drugs are diverse, we will focus on those that can be associated with EFV-induced cellular stress, such as liver inflammatory and fibrogenic responses.

I.2.1. Hepatic inflammation and fibrogenesis

Hepatic inflammation is a complex process that originates as a response to diverse stress conditions and usually serves as a mechanism to protect hepatocytes from damage, to remove cellular debris, to favor the re-establishment of homeostasis, and to promote the repair and regeneration of liver damage. Nevertheless, dysregulated inflammatory responses lead to hepatocyte damage, augmented leukocyte infiltration, and secretion of pro-fibrogenic mediators such as platelet-derived growth factor subunit beta (PDGF-β) and transforming growth factor beta 1 (TGF-β1). This condition has been associated with almost all liver insults, including pathogens, alcohol overconsumption, ischemia/reperfusion injury, xenobiotics (e.g. drugs), and metabolic conditions such as alcoholic steatohepatitis (ASH), NASH, and diabetes (Navad et al. 2008; Bieghs and Trautwein 2013; Brenner et al. 2013; Woolbright and Jaeschke 2015).

The inflammation in absence of infection, also known as sterile inflammation (SI), is a genuine inflammatory response with all its cellular components, including macrophage activation, neutrophilic infiltration, and chemokine and cytokine production, where diverse endogenous factors, or DAMPs, released from dying cells, play a crucial role in the development of the response. SI is especially relevant in a wide range of liver diseases, such as NASH and DILI (Chen and Núñez 2010; Kubes and Mehal 2012; Hoque et al. 2013).

As previously mentioned, liver inflammation also induces a fibrogenic response. Fibrogenesis is a reversible wound-healing response to either acute or chronic cellular injury characterized by the accumulation of extracellular matrix (ECM) in order to mitigate tissue damage, but it can also lead to scar formation. Although this process is a multicellular response, activated hepatic stellate cells (HSCs) are the main cell type responsible for ECM deposition (approximately 90%). The fibrogenic response observed during acute liver injury promotes the survival of hepatocytes by downregulating pro-apoptotic pathways (Hernandez-Gea and Friedman 2011; Czaja 2014; Seki and Schwabe 2015; Trautwein et al. 2015).

I.2.2. Key cellular players

During inflammatory and fibrogenic responses, liver resident cells [hepatocytes, HSCs, Kupffer cells (KCs), cholangiocytes and liver sinusoidal cells] and infiltrating immune cells (e.g. neutrophils, macrophages and lymphocytes) interact dynamically, either to promote or to resolve inflammation and fibrogenesis (Heymann and Tacke 2016). Each cell type plays an important role in the development of these processes but the description of all their functions is beyond the objective of this dissertation; we will only focus on the fundamental actions exerted by hepatocytes, HSCs and KCs.

I.2.2.1. Hepatocytes

Liver injury can result from multiple etiologies, but in many cases, it occurs due to direct damage of hepatocytes. This cell type, the major parenchymal population in the liver, plays a pivotal role in metabolism, protein synthesis and detoxification. During damage, hepatocytes interact with surrounding cells (including HSCs, KCs, infiltrating immune cells and endothelial cells), resulting in the release of pro-inflammatory signals, ROS, proliferation-associated

cytokines, and activation of repair pathways (Tu et al. 2015; Zhou et al. 2015; Crispe 2016; Woolbright and Jaeschke 2016). Hepatocyte death has been considered the main driver of liver inflammation and fibrogenic response, and it has been widely categorized as inflammatory (necrosis, necroptosis and pyroptosis) and non-inflammatory (apoptosis), depending on its capacity to induce disruption of cellular integrity with a subsequent release of the cellular contents to extracellular medium and promotion of inflammatory response (McDonald and Kubes 2016). However, mounting evidence has revealed that tumor necrosis factor (TNF)-induced apoptosis promotes the secretion of pro-inflammatory cytokines and chemokines, including interleukin (IL)-6, IL-8, chemokine (C-X-C motif) ligand 1 (CXCL1) and monocyte chemoattractant protein 1 (MCP-1), by dying cells (Cullen et al. 2013; Kearney et al. 2013). In this line, engulfment of apoptotic bodies originated in hepatocytes enhances the secretion of fibrogenic and pro-inflammatory cytokines [TNF-α, TGF-β1, and TNF-related apoptosis-inducing ligand (TRAIL)] from macrophages (Canbay et al. 2003a), and directly induces the activation of HSCs (Canbay et al. 2003b; Zhan et al. 2006).

As mentioned before, damaged and dying hepatocytes are capable of releasing DAMPs, which act on neighboring hepatocytes as well as on non-parenchymal cells (Luedde et al. 2014; Wree et al. 2016), promoting, directly or indirectly, SI and exacerbation of injury in acute liver diseases, including acetaminophen-induced liver injury (Woolbright and Jaeschke 2016) and hepatic ischemia-reperfusion injury (Tsung et al. 2005). DAMPs, also termed alarmins because of their capability to alert the immune system, constitute a group of chemically heterogeneous molecules, which provide several signals, such as “activation” (immunostimulatory mediators), “eat-me” (phagocytosis mediators), “find-me” (chemotactic mediators) “tolerogenic” (immunosuppressive mediators) and ‘tissue repair’ (regeneration mediators) (Zitvogel et al. 2010; Krysko et al. 2011; Galluzzi et al. 2012a; Brenner et al. 2013). They can be originated from different subcellular compartments, including nucleus, ER, cytosol and plasma membrane, and they are usually modified by oxidation and proteolysis (Garg et al. 2010). Moreover, DAMPs can be originated as end-stage degradation products (e.g. uric acid). Mitochondria have emerged as an important source of alarmins (including cytochrome *c*, ATP, and mtDNA), which is not surprising keeping in mind the “endosymbiont hypothesis” of their origin (Gray et al.

2008; Krysko et al. 2011; Galluzzi et al. 2012a). Importantly, DAMPs may not always induce the activation of pro-inflammatory pathways, for example IL-33 is released during liver injury from stressed cells in order to promote activation of HSCs and subsequent fibrogenic response (Erhardt and Tiegs 2012; Mchedlidze et al. 2013). A large number of DAMPs have been identified so far and the number is continuously growing (Table I.4). These danger signals are recognized by pattern recognition receptors (PRRs), that include Toll-like receptors (TLRs) and NOD-like receptors (NLRs), and non-PRRs, such as purinergic receptors, located on both non-immune and immune cells (Feldman et al. 2015).

DAMP	RECEPTOR
ATP	Various P2X and P2Y
Cytochrome c	Unknown
mtDNA	TLR9, NLRP3
Nuclear DNA	TLR9, AIM2
ROS	NLRP3
Histones	NLRP3, TLRs
HMGB-1	RAGE, TLR4/2, CD24, NLRP3
Uric acid	NLRP3
IL-1α	IL-1R
IL-33	IL-1RL1
HSPs	TLR4/2, CD24, CD14, CD91
S100 proteins	RAGE

Table I.4. Most widely studied DAMPs and their main receptors. Information obtained from (Krysko et al. 2011; Kubes and Mehal 2012; Brenner et al. 2013; McDonald and Kubes 2016; Wree et al. 2016). Abbreviations: AIM2: absent in melanoma 2; ATP: adenosine triphosphate; CD: cluster of differentiation; DNA: deoxyribonucleic acid; HMGB-1: high mobility group box 1; HSPs: heat shock proteins; IL: interleukin; IL-1RL1: interleukin 1 receptor like 1; NLRP3: NOD-like receptors, family pyrin domain containing 3; RAGE: receptor for advanced glycation end-product; ROS: reactive oxygen species; TLR: Toll-like receptors.

Among the diverse insults that can provoke hepatocyte injury, and subsequent cellular death, are:

- **Pro-inflammatory cytokines:** Members of the TNF protein superfamily, such as TNF-α, Fas ligand and TRAIL are among the major signals of

hepatocyte cell death. Fas ligand and TRAIL signaling typically activates cell death through FADD/caspase-8 pathway. TNF-α activates the versatile protein RIP1 (receptor-Interacting serine/threonine-protein kinase 1), which can activate the pro-apoptotic caspase cascade and/or the anti-apoptotic/pro-inflammatory pathway leading to nuclear factor-kappa-B (NF-κB) activation, thus TNF-dependent signaling is crucial in regulation of cellular homeostasis (Han et al. 2009; Duprez et al. 2011; Liedtke and Trautwein 2012; Luedde et al. 2014). Another relevant mediator of the inflammatory response is IL-1β, which has potent pro-inflammatory actions through its binding to the IL-1 receptor (IL-1R) and activation of the NF-κB; in addition, its caspase-1-mediated proteolysis is associated with pyroptotic cell death (Bieghs and Trautwein 2013; Davidovich et al. 2014). The processing and functions of this cytokine will be discussed in depth in *I.2.3.2. Inflammasomes* section.

- **Oxidative stress:** Mitochondria are the main generators of ROS as a normal by-product of the mitochondrial respiratory chain (mainly produced by ETC complex I and III). ROS is a collective term for several free radical and non-radical molecules such as superoxide anion and hydrogen peroxide. In physiological settings, the cytotoxic potential of ROS is counteracted by a diverse battery of antioxidant systems, which include catalases, superoxide dismutases, thioredoxin and glutathione. However, in response to multiple stimuli or organelle disorders (e.g. mitochondrial dysfunction), ROS production exceeds the buffer capacity of the antioxidant systems, resulting in oxidative stress. This effect leads to the activation of a cellular response in order to re-establish the redox homeostasis and this can be coupled to an inflammatory response, followed by cellular damage, progressive mitochondrial dysfunction and cell death (apoptosis or necrosis) (Kroemer et al. 2007; Apostolova et al. 2011a; Jaeschke 2011; Galluzzi et al. 2012b; Brenner et al. 2013; Li et al. 2015).

- **ER stress:** The ER is the organelle responsible for regulation of Ca^{2+} homeostasis and synthesis, post-translational modification and folding of proteins. Its function is disrupted by challenges such as mutant protein expression, energy/nutrient deprivation, altered redox, or Ca^{2+}

homeostasis. These conditions lead to ER stress and the activation of an adaptive mechanism known as UPR, which is characterized by (1) attenuation of protein translation, (2) upregulation of factors that promote protein folding and degradation (chaperones and proteases), and (3) degradation of misfolded proteins by autophagy. Under stress conditions, unfolded proteins competitively displace the ER-resident chaperone glucose-regulated protein, 78 kDa (GRP78) from the ER stress sensors inositol-requiring enzyme 1 alpha (IRE1α), activating transcription factor 6 (ATF6) and PKR-related ER kinase (PERK), resulting in activation of UPR in order to re-establish the homeostasis. However, prolonged signaling via ER stress sensors can promote the initiation of non-mitochondria and/or mitochondria-dependent apoptosis that involves, among other proteins, the transcription factor C/EPB homologous protein (CHOP), and caspase-12 and JNK (c-Jun N-terminal kinase) signaling pathways (Malhi and Kaufman 2011; Hetz 2012; Apostolova et al. 2013; Brenner et al. 2013).

I.2.2.2. Hepatic stellate cells

HSCs are non-parenchymal cells within the perisinusoidal space of Disse, interposed between sinusoidal endothelium and hepatocytes. This privileged localization, besides their dendritic cytoplasmic processes, facilitates their contact with other HSCs, hepatocytes, endothelial cells and KCs (Friedman 2008; Puche et al. 2013). HSCs contribute to key homeostatic functions of the liver such as development and regeneration (e.g. quiescent HSCs can produce hepatocyte and vascular endothelial-growth factors), retinoid metabolism (they are the main depot of vitamin A in the liver), ECM homeostasis, lipid metabolism, immunoregulation and drug detoxification (Hernandez-Gea and Friedman 2011; Wallace et al. 2015). Besides these important functions, when the liver is injured, HSCs coordinate a tightly regulated cellular network, which results in net deposition of fibril-forming collagen-rich ECM at sites where liver has been damaged. To develop the scar, following the liver injury, activated HSCs undergo trans-differentiation of quiescent vitamin A-rich cells to myofibroblast-like cells, which are characterized by augmented proliferation and migration, loss of lipid droplets, abundant secretion of ECM proteins, and enhanced contractility, and by the release of pro-fibrogenic and pro-inflammatory factors (Iredale et al. 2013; Pellicoro et al. 2014). Activated HSCs

are characterized by an enhanced expression of alpha-smooth muscle actin (α-SMA), desmin and vimentin, and therefore, they are usually employed as markers of HSC activation. In addition, they secrete massive amounts of scar-forming type I and III collagens (among others ECM proteins), express a wide range of matrix metalloproteinases (MMPs, such as MMP-2 and MMP-9), and specific tissue inhibitors of metalloproteinases (TIMPs, such as TIMP-1), proteins that prevent matrix metalloproteinase-directed degradation of collagen, thus allowing the scar formation (Figure I.3) (Benyon and Arthur 2001; Hemmann et al. 2007; Mann and Mann 2009; Puche et al. 2013).

HSC activation involves two well-established stages: initiation (or pre-inflammatory stage) and perpetuation. Initiation refers to a series of gene expression and phenotype alterations in HSCs initiated by paracrine signals from neighboring cells. The signals involved in the activation of HSCs include ROS, lipopolysaccharide (LPS), lipid peroxides, nucleotides, apoptotic bodies and other death cell signals, activation of latent TGF-β1, osteopontin, PDGF-β, and inflammatory cytokines (Kojima et al. 2000; Nieto et al. 2002; Canbay et al. 2003b; Smedsrød et al. 2009; Urtasun et al. 2012; Brenner et al. 2013; Novo et al. 2014; Vaughn et al. 2014). Viral agents have been also reported to directly activate HSCs, including HCV (Schuppan et al. 2003), HBV (Iser and Lewin 2009) and HIV (Tuyama et al. 2010). Sustained release of these stimuli from surrounding cells, plus several paracrine and autocrine loops, results in the perpetuation of stellate activation, which includes different changes in HSC behavior, including chemotaxis, proliferation, fibrogenesis, matrix degradation, contractility and retinoid loss (Hernandez-Gea and Friedman 2011; Wallace et al. 2015).

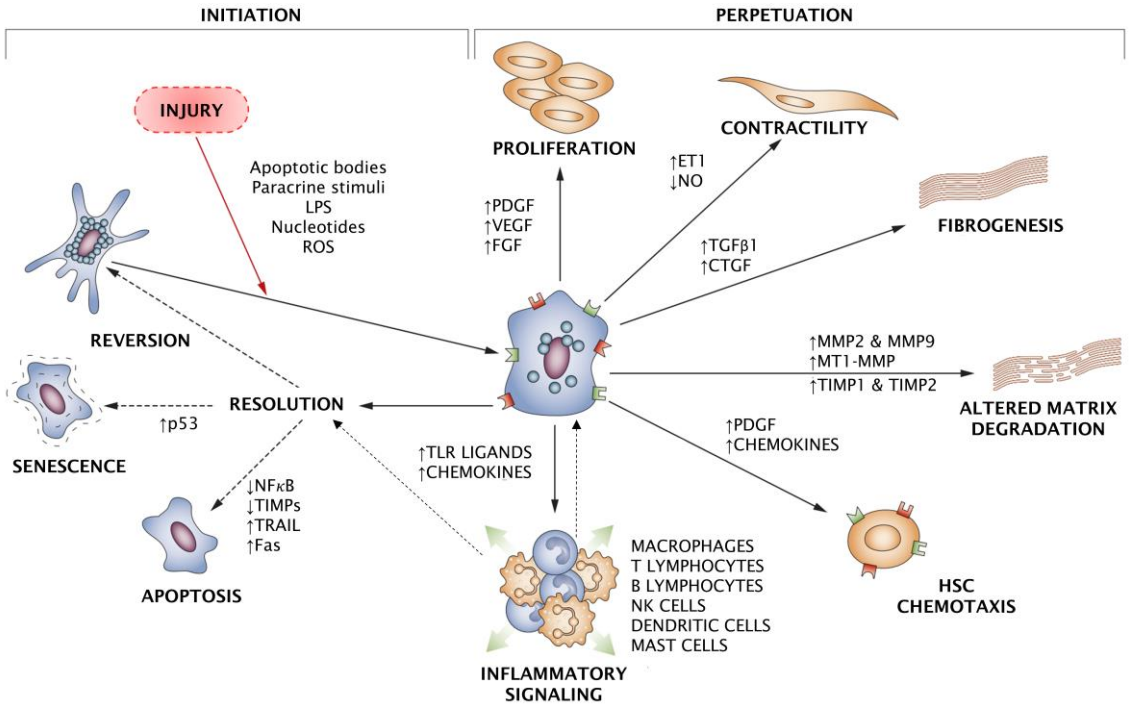

Figure I.3. HSC activation pathways. Initiation is triggered by diverse stimuli such as oxidative stress, ER stress, apoptotic bodies, LPS, nucleotides and paracrine stimuli from surrounding cell types including hepatocytes, hepatic macrophages and sinusoidal endothelium. Initiation is followed by perpetuation; characteristic changes of this process are increased contractility, proliferation, enhanced ECM turnover, fibrogenesis, chemotaxis and inflammatory signaling. Resolution of hepatic fibrosis, which occurs once the primary liver injury has been resolved, leads to loss of activated HSCs, either through senescence, apoptosis, or reversion of activated HSCs to a more quiescent phenotype, where immune cells may play a relevant role. Abbreviations: CTGF: connective tissue growth factor; ET1: endothelin 1; FGF: fibroblast growth factor; LPS: lipopolysaccharide; MMP: matrix metalloproteinase; MT1-MMP: membrane type matrix metalloproteinase; NF-κB: nuclear factor kappa B; NK: natural killer; NO: nitric oxide; PDGF: platelet-derived growth factor; TGF-β1: transforming growth factor beta 1; TIMP: tissue inhibitor of metalloproteinase; TLR: Toll-like receptor; TRAIL: tumor-necrosis-factor-related apoptosis-inducing ligand; VEGF: vascular endothelial growth factor. Adapted from Friedman, SL. Nat. Rev. Gastroenterol. Hepatol. 7(8), 425-436 (2010) (Friedman 2010).

Autophagy, a highly regulated pathway that maintains energy homeostasis, is critical for HSC activation, primarily via lipophagy, providing essential energy substrates through the hydrolysis of retinyl esters, stored within cytoplasmic droplets (Hernández-Gea et al. 2012; Czaja et al. 2013; He et al. 2014). These

findings somewhat explain why HSCs lose their retinoids as they are activated; however, the necessity of stored retinoids for activation is a matter of debate due to the fact that HSCs from mice with lack of retinoid droplets through genetic knockout of the storage protein Lecithin:retinol acyltransferase (LRAT) are able to become activated (Lee et al. 2015). This autophagic response has been linked to the activation of UPR and ER stress, which have been viewed as pro-fibrotic events. Oxidative stress, an established component of HSC activation pathway, interferes with ER homeostasis in the liver and activates the UPR, thereby promoting autophagy via the IRE1α-XBP1 and PERK pathways; blockade of these pathways attenuates autophagic activity and stellate cell activation (Hernández-Gea et al. 2013; Tanjore et al. 2013). In addition, a significant correlation has been found between ER stress and HSC activation in patients (Koo et al. 2016).

As pointed out above, HSC functions are much more diverse; for example, they also play a crucial role in the inflammatory and immune responses. HSCs express PRRs, whereby these cells are highly responsive to DAMPs and PAMPs (as is LPS), resulting in the activation of pro-inflammatory pathways, such as activator protein 1 (AP-1) and NF-κB, and subsequent production of pro-inflammatory cytokines and chemokines. Interestingly, AP-1 and NF-κB are important factors in the activation of HSCs, promoting an increased cytokine production in activated HSCs. These enhanced inflammatory responses can induce hepatocyte cell death, and thereby empower and perpetuate fibrogenic stimuli (Hellerbrand et al. 1998; Paik et al. 2003, 2006; Schwabe et al. 2003; Cohen-Naftaly and Friedman 2011; Czaja 2014; Weiskirchen and Tacke 2014). Nevertheless, HSCs produce lower cytokine levels when compared to immune cells, thus contributing minimally to overall liver inflammation. In this regard, HSCs probably behave as recipients of inflammatory signals, to regulate their activation and subsequently ensure their survival (Seki and Schwabe 2015). During liver injury, HSCs can also act as non-professional antigen presenting cells (APCs), mainly when they are activated, thereby modulating the adaptive immunity (Viñas et al. 2003). In addition, HSCs can regulate the immune response through several mechanisms, including the expression and delivery of chemokines (e.g. CCL2, CXCL10, CCL5) and integrins (e.g. VCAM-1, ICAM-1) (Weiskirchen and Tacke 2014), thus driving the adhesion and migration of immune cells, but can also directly interact with these cells. Several types of

immune cells can modulate the progression and resolution of the fibrogenic response (Puche et al. 2013), including natural killer (NK) cells (anti-fibrotic function by killing and/or inhibiting activated HSCs) (Gao et al. 2009), B lymphocytes (promote fibrosis in an antibody-independent manner) (Novobrantseva et al. 2005), T lymphocytes (responsible for initiating/maintaining the adaptive immunity) (Szabo et al. 2012) and macrophages (play a pivotal role due to their potential for exerting both anti- and pro-fibrotic properties by secreting/regulating TGF-β1, PDGF-β, MMPs, and TIMPs) (Ramachandran and Iredale 2012).

I.2.2.3. Hepatic macrophages

The liver shelters roughly 80% of all macrophages of the body, and they are divided in two types depending on their origin: (1) resident liver macrophages or KCs, which are positioned in liver sinusoids, originated from fetal yolk-sac precursors, and whose homeostatic self-renewal depends on macrophage colony-stimulating factor (M-CSF); and (2) macrophages derived from infiltrating blood monocytes (Naito et al. 1997; Davies et al. 2013; Possamai et al. 2014; Ju and Tacke 2016). Liver macrophages are key players in the liver inflammation and also hold remarkable functional diversity, being implicated in hepatic homeostasis, progression and regression of acute and chronic inflammation and fibrosis (Heymann and Tacke 2016). Their pleiotropic actions and diverse roles in liver diseases are due to their high plasticity, as a response to environmental signals arising from parenchymal and immune cells. Macrophages have been traditionally categorized either into “pro-inflammatory” M1 or “immunoregulatory” M2, but now it is known that the complex biology of macrophages subsets is not reflected by this simple dichotomous nomenclature (Martinez et al. 2009; Tacke and Zimmermann 2014). M2 macrophages are classified into several subtypes (M2a, M2b y M2c) which pursue wound healing or anti-inflammatory resolution (Martinez and Gordon 2014; Rőszer 2015), but an in-depth overview of these differences is beyond the aim of this thesis. During liver injury, macrophages can develop multiple actions (e.g. phagocytosis, cytokine and chemokine secretion, ECM remodeling and cellular crosstalk), and furthermore, these macrophages isolated from injured tissues often show M1 and M2 markers simultaneously, corroborating

that macrophage polarization is more complex than the M1:M2 concept (Ramachandran et al. 2012).

The microenvironment is a critical determinant in macrophage polarization (Figure I.4), which is regulated by different mechanisms, including transcription factors, epigenetic mechanisms, signaling pathways and post-transcriptional regulators (Sica and Mantovani 2012). M1 macrophages activation is normally controlled by NF-κB, signal transducer and activator of transcription 1 (STAT1) and interferon regulatory factor 5 (IRF5) signaling pathways, which are induced by lipoproteins, phagocytosis of necrotic cells, bacterial cell wall constituents (e.g. LPS), and cytokines such as interferon (IFN)-γ, TNF-α and IL-12 in response to deleterious insults. The M1-like phenotype macrophages are characterized by high production of NO and ROS, expression of high levels of the co-stimulatory molecule CD86, and secretion of pro-inflammatory cytokines and chemokines, including IL-1β, IL-12, TNF-α, IL-6, CCL2 and CCL5, promoting the Th1 response, and strong tumoricidal and microbicidal activity (Benoit et al. 2008; Lawrence and Natoli 2011; Murray and Wynn 2011; Martinez and Gordon 2014). On the other hand, a predominance of STAT6, STAT3 and peroxisome proliferator-activated receptor (PPAR)-γ activation promotes M2 macrophage polarization, which can be activated by parasites, immune complexes, apoptotic cells and cytokines such as IL-4, IL-13, IL-10 and TGF-β1. M2-like phenotype is widely considered as wound-healing and pro-resolving, and these macrophages are characterized by efficient phagocytosis activity, high expression of scavenging, mannose and galactose receptors, production of ornithine through the arginase pathway and secretion of immune-modulatory mediators, including interleukin-1 receptor antagonist (IL-1Ra), IL-4, IL-10, IL-13 and TGF-β1 (Zimmermann et al. 2012; Murray et al. 2014; Sica et al. 2014; Rőszer 2015).

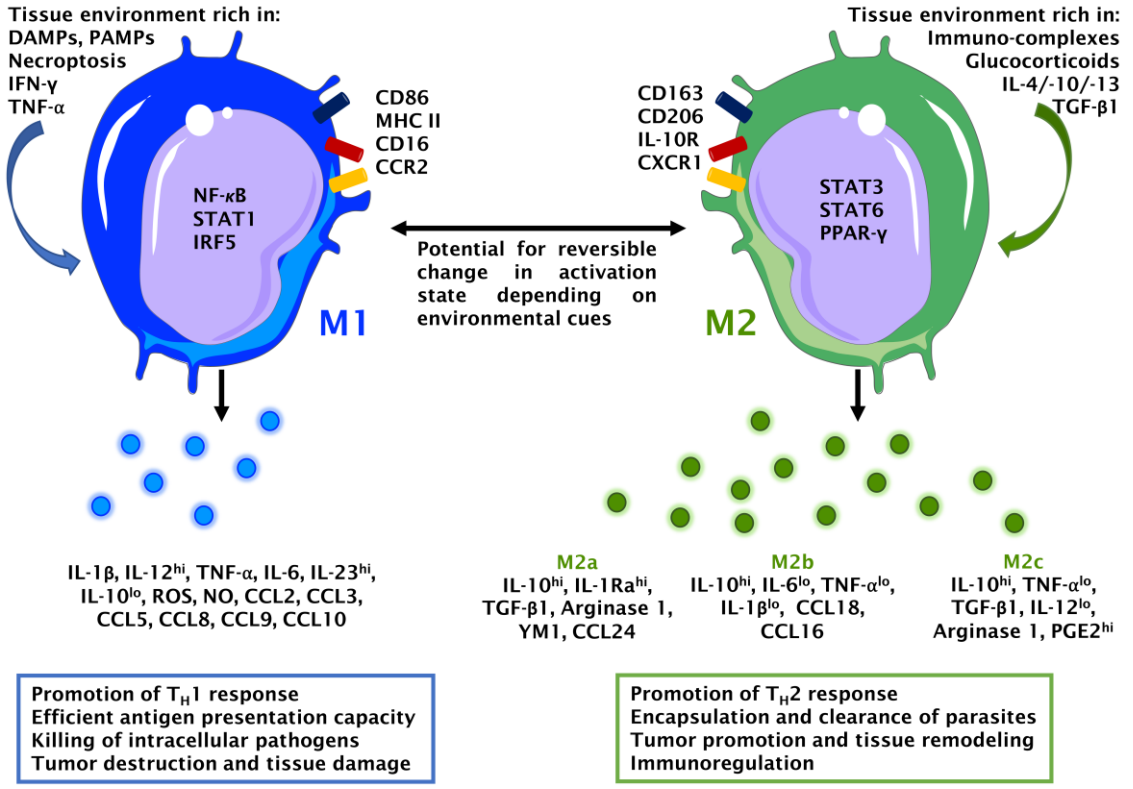

Figure I.4. Macrophage polarization is influenced by environmental mediators. This simplified scheme shows the main markers, transcription factors and effectors related to the pro-inflammatory M1-like and the anti-inflammatory/pro-resolving M2-like phenotypes (Biswas and Mantovani 2010; Duque and Descoteaux 2014; Possamai et al. 2014; Wynn and Vannella 2016). Abbreviations: CCL: C-C chemokine ligand; CCR: C-C chemokine receptor; CD: cluster of differentiation; CXCR: C-X-C chemokine receptor; DAMPs: damage-associated molecular patterns; IFN: interferon; IL: Interleukin; IL-1Ra: interleukin-1 receptor antagonist; IRF: interferon regulatory factor; MHC II: major histocompatibility complex class II; NF-κB: nuclear factor kappa B; NO: nitric oxide; PAMPs: pathogen-associated molecular patterns; PGE2: prostaglandin E2; PPAR: peroxisome proliferator-activated receptor; ROS: reactive oxygen species; STAT: signal transducer and activator of transcription; TGF: transforming growth factor; TNF: tumor necrosis factor.

During liver damage, hepatocyte injury and/or death leads to the release of DAMPs, which induce the activation of innate immune and tissue destructive responses by means of production of NF-κB-dependent pro-inflammatory cytokines (e.g. IL-1β, IL-6 and TNF-α) and ROS. This results in a dramatic expansion of hepatic macrophages population with their subsequent polarization towards M1-like phenotype and release of additional inflammatory

mediators strengthening the inflammatory response, which may directly (ROS, TNF-α) or indirectly (through neutrophil recruitment via IL-1β and CXCL2) induce hepatocyte cell death (Figure I.5) (Zimmermann et al. 2012; Brempelis and Crispe 2016; Ju and Tacke 2016). Importantly, at the later stages of inflammation or once the liver insult has been eliminated, and due to changes in the environmental conditions, macrophages may undergo a functional switch towards pro-resolving or anti-inflammatory M2-like phenotype in order to repair damaged tissue (Sica and Mantovani 2012; Possamai et al. 2014).

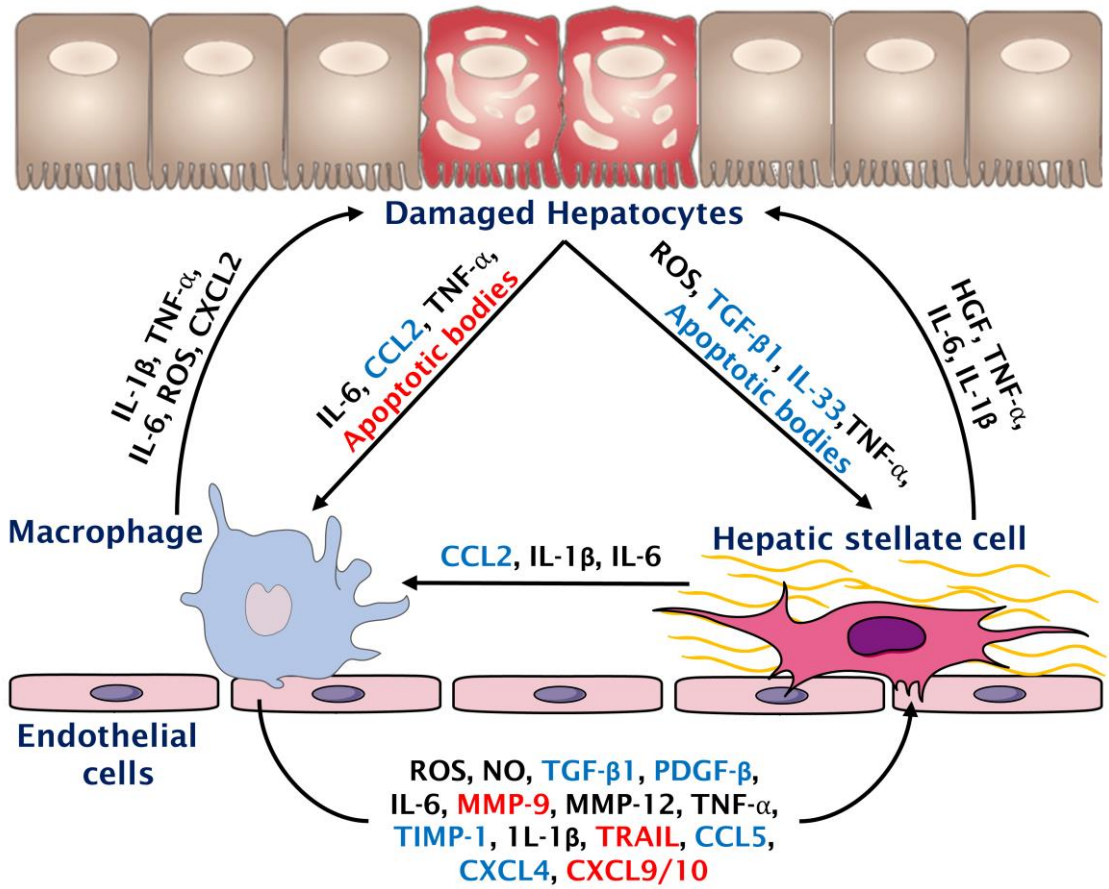

Figure I.5. Intercellular crosstalk in inflammatory and fibrogenic responses following liver injury. Pro-fibrogenic mediators are depicted in blue, in contrast to anti-fibrotic-inducing mediators that are shown in red. Abbreviations: CCL: CC chemokine ligand; CXCL: CXC chemokine ligand; HGF: hepatocyte growth factor; IL: interleukin; MMP: matrix metalloproteinase; NO: nitric oxide; PDGF-β: platelet-derived growth factor beta; ROS: reactive oxygen species; TNF-α: tumor necrosis factor a; TGF-β1: transforming growth factor beta 1; TIMP: tissue inhibitor of metalloproteinases; TRAIL: TNF-related apoptosis-inducing ligand. Modify from (Schuppan and Kim 2013; Trautwein et al. 2015).

Furthermore, mounting evidence has revealed that liver macrophages also play a pivotal role in the fibrogenic response, exerting a dual function on HSCs and matrix deposition. Macrophages can directly activate HSCs through the secretion of pro-fibrotic cytokines such as TGF-β1 (to enhance myofibroblast ECM and TIMP-1 production) and PDGF-β (a potent stimulator of HSC proliferation). Additionally, pro-inflammatory cytokines such as IL-1β and TNF-α not only activate HSCs via NF-κB signaling, but also promote their survival (Ramachandran and Iredale 2012; Sica and Mantovani 2012; Tacke and Zimmermann 2014). However, macrophages can also promote fibrosis resolution, due to the anti-fibrotic effects of IL-10 (Thomas et al. 2011) through secretion of several metalloproteinases (MMP-9, MMP-12 and MMP-13), which favor ECM degradation and thereby promote the resolution of liver injury and fibrosis (Pellicoro et al. 2012; Pradere et al. 2013; Ju and Tacke 2016). Macrophages are also capable of producing factors which can induce HSC apoptosis, including TRAIL and MMP-9 (Figure I.5) (Ramachandran and Iredale 2012). The pro- and anti-fibrotic roles of liver macrophages depend on their capability of polarization and the different subsets of infiltrated macrophages. Although currently there is a controversy about which phenotype is involved in fibrogenesis, M1, M2a-like and M2c-like macrophages seem to be more implicated in this response (Friedman et al. 2013).

I.2.3. Signaling pathways involved in inflammation and fibrosis

I.2.3.1. NF-κB

NF-κB family of transcription factors are considered master regulators of pro-inflammatory signaling pathways in response to both infection and injury, because they control many pro-inflammatory genes including chemokines, cytokines, and adhesion molecules. Moreover, these factors modulate the expression of genes involved in cell cycle, cell growth, apoptosis, wound-healing, immune responses, development and acute phase responses (Pahl 1999; Muriel 2009).

NF-κB is a dimer of members of the Rel family of DNA-binding proteins. This family consists of five cellular DNA-binding subunits: NF-κB1 (p50), NF-κB2 (p52), Rel (c-Rel), RelA (p65) and RelB (Napetschnig and Wu 2013). RelA (p65) contains two potent transactivation domains, which probably makes it the

strongest activator of genes with κB sites, being the classic NF-κB complex the one formed as p50:p65 (Mann and Mann 2009). As uncontrolled inflammation is deleterious, NF-κB pathway is tightly regulated. In unstimulated cells, NF-κB is held in the cytoplasm in an inactive state due to it being bound to an inhibitory protein of the IκB family (such as IκB-α), which masks its nuclear localization site (Christer Baeck 2014). NF-κB signaling is activated by a large number of extracellular stimuli, such as LPS, inflammatory cytokines (e.g. IL-1, TNF-α), pathogens and stress conditions (e.g. oxidative stress, ER dysfunction), which are recognized by different receptors, including TLR, IL-1R and TNFR1. The signaling cascades culminate in the phosphorylation of IκB by a complex consisting of two different catalytic IκB kinase (IKK) subunits and the protein NF-κB essential modulator (NEMO). This phosphorylation marks IκB for subsequent degradation through the proteasome in ubiquitin-dependent pathway, and releases NF-κB from the inhibitory complex, allowing nuclear entry, where it binds to their target sequences and activates gene transcription (Ghosh et al. 1998; Pahl 1999; Lawrence 2009; Napetschnig and Wu 2013). NF-κB actions can be regulated by other transcription factors including PPAR-γ, a regulator of lipid metabolism and a well-known inhibitor of pro-inflammatory gene expression by various mechanisms, such as the trans-repression of NF-κB (Lawrence and Natoli 2011). On the other hand, important players involved in the UPR/ER stress, such as CHOP and ATF6 can induce the activation of NF-κB (Willy et al. 2015; Grootjans et al. 2016).

In the liver, NF-κB is a pivotal regulator involved in virtually every hepatic disease, including non-alcoholic fatty liver disease, viral hepatitis and DILI (Muriel 2009), due to its implication in a wide range of functions in hepatocytes, KCs and HSCs. In response to stimuli, NF-κB mediates both pro-inflammatory and anti-apoptotic activities in hepatocytes, in order to protect them from cell death while inflammatory responses are initiated. This dual role of NF-κB requires a delicate balance, since a dysregulated activation may lead to increased inflammation and subsequent enhanced liver injury and fibrogenesis (Luedde and Schwabe 2011). Furthermore, several studies have involved NF-κB in three key aspects of HSCs biology, including activation, survival and inflammatory responses. NF-κB is dramatically upregulated during HSC activation and, in addition, several NF-κB-dependent pro-inflammatory and pro-fibrotic cytokines (e.g. MCP-1, IL-6, IL-8, and ICAM-1) as well as

macrophage-recruiting chemokines (e.g. CCL2, CXCL5) are highly expressed in activated HSCs (Hellerbrand et al. 1998; Elsharkawy et al. 2005; Anan et al. 2006; Mann and Mann 2009). However, NF-κB also exerts anti-fibrotic effects by attenuating the gene expression of the ECM protein, collagen type 1 (Rippe et al. 1999). As mentioned above, KCs may be key contributors to progression of liver diseases, and NF-κB is essential for the production of inflammatory and fibrogenic cytokines, which enhance the inflammation at the site of liver injury and promote the survival of activated HSCs. In fact, inhibition of NF-κB in hepatic macrophages has been reported to result in reduced liver fibrosis (Son et al. 2007; Luedde and Schwabe 2011).

I.2.3.2. Inflammasomes

Inflammasomes are cytosolic multiprotein complexes that assemble after sensing intracellular danger signals (DAMPs and PAMPs), and they serve as scaffolds to recruit and activate the pro-inflammatory caspase-1 (Guo et al. 2015). These multimeric protein complexes include (Henao-Mejia et al. 2012; Rathinam et al. 2012; Latz et al. 2013; Lamkanfi and Dixit 2014; Vanaja et al. 2015):

- A **sensor protein** belonging to RIG (retinoic acid-inducible gene I)-like receptor (RLR), AIM2 (absent in melanoma-2)-like receptor (ALR), NOD-like receptor [NLRs; nucleotide-binding domain (NOD) and leucine-rich repeat (LRR) containing] family or interferon-γ-inducible protein 16 (IFI16). Most of the inflammasomes described so far contain a NLR sensor molecule, such as NLRP1 [NOD-, LRR- and Pyrin domain (PYD)-containing 1], NLRP3, NLRP6, NLRP7, NLRP12 and NLRC4 (NOD-, LRR- and CARD domain-containing 4).
- An **adaptor protein** ASC (apoptosis-associated speck-like protein containing a CARD domain), necessary to form the inflammasome scaffold for most sensor proteins that lack CARD domains and those that contain PYDs (e.g. AIM2, NLRP3).
- An inactive zymogen, the **pro-caspase-1**. This protease is formed by two domains: the CARD domain, which is removed by cleavage, and two heterodimers formed by p20 and p10 effector domains.

NLRP3 inflammasome is the most fully characterized member of the inflammasome family in liver diseases (Wree et al. 2014a; Szabo and Petrasek

2015; Tilg et al. 2016), and it is considered as a general sensor of tissue damage and infection (Strowig et al. 2012). Following activation, NLRP3 oligomerize through their NOD domain, which serves as a scaffold to recruit and to nucleate ASC monomers through PYD-PYD interactions, converting them in a prion-like form and creating ASC filaments, which are essential for inflammasome activation. Lastly, the inactive pro-caspase-1 is recruited through CARD-CARD interactions with ASC, forming its own prion-like filaments, and subsequently the nearby proximity of pro-caspase-1 induces its auto-proteolytic maturation into active caspase-1 (Bryant and Fitzgerald 2009; Schroder and Tschopp 2010; Lu et al. 2014; Artlett and Thacker 2015; Guo et al. 2015; Matusiak et al. 2015). Inflammasome activation is a "two-hit" process, which represents a key regulatory checkpoint to avoid unnecessary immune responses capable of damaging the host (Sutterwala et al. 2014; Elliott and Sutterwala 2015). In this model, the first hit, known as "priming", requires a non-activating stimulus to trigger the transcription of the components of the inflammasome through the activation of NF-κB signaling, including its downstream effector, pro-IL-1β; whereas pro-IL-18 is constitutively expressed in cells, and its expression may be enhanced just after sustained inflammasome activation (Latz 2010; Latz et al. 2013). Priming stimuli involve any ligand whose receptor signaling leads to the activation of NF-κB, such as TNFRs, TLRs and IL-1R1. Once primed, a second hit or "activation" of NLRP3 occurs in response to either the same and/or additional stimuli, usually a DAMP derived from damaged cells, that promote the activation and the assembly of the NRLP3 inflammasome components (Figure I.6) (Franchi et al. 2009; Creagh 2014; Elliott and Sutterwala 2015; Patel et al. 2017).

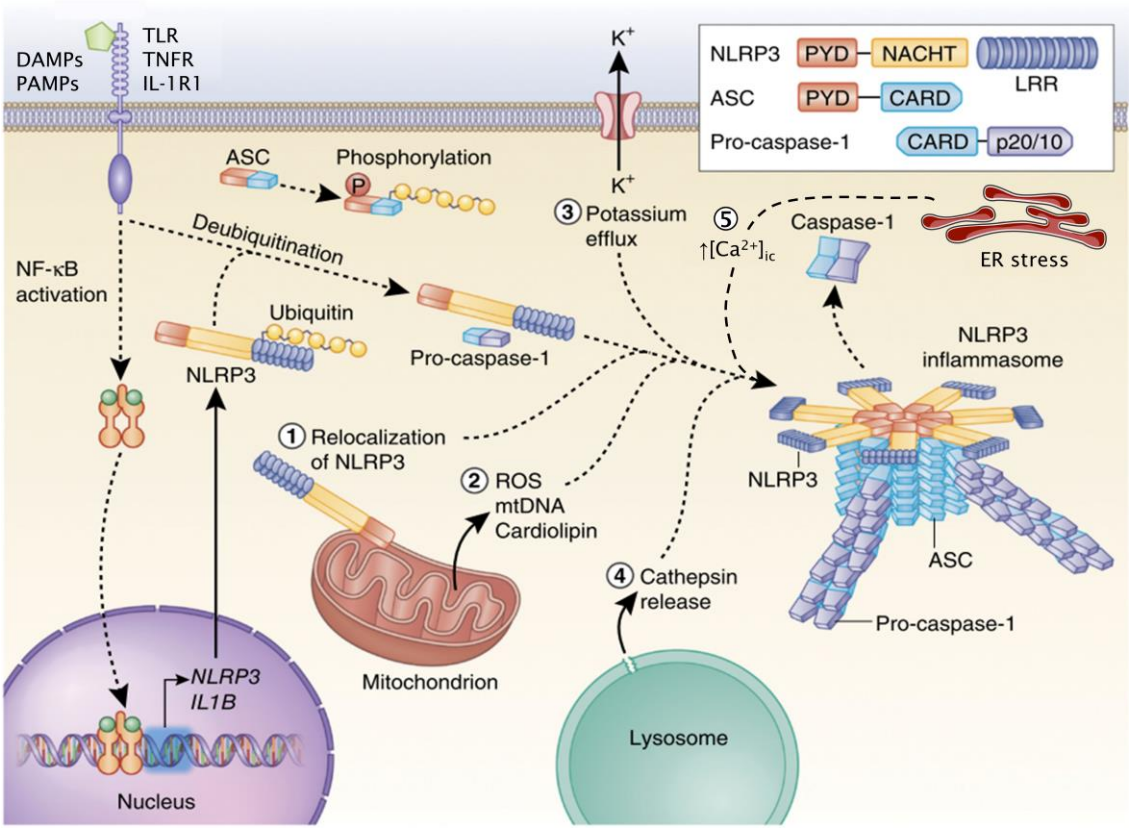

Figure I.6. Mechanisms of NLRP3 inflammasome activation. The inflammasome must be primed before its activation, a process that consists of upregulated gene expression of inflammasome-related proteins, such as *NLRP3* and *IL1B*, through NF-κB-activating stimuli. Additionally, priming immediately licenses NLRP3 by inducing its deubiquitination, allowing its oligomerization, while ASC is ubiquitinated and phosphorylated for inflammasome assembly to occur. After priming, NLRP3 inflammasome activation requires a second signal to activate NLRP3 and lead to the assembly of the NLRP3 inflammasome complex. The most commonly accepted activating stimuli include the release of mitochondrial factors, such as mtDNA or cardiolipin, the relocation of NLRP3 to the mitochondria, K^+ efflux, cathepsin release and rise of the cytosolic Ca^{2+}. Abbreviations: DAMPs: damage-associated molecular patterns; IL-1R: interleukin 1 receptor; mtDNA: mitochondrial DNA; PAMPs: pathogen-associated molecular patterns; ROS: reactive oxygen species; TLR: toll-like receptor; TNFR: tumor necrosis factor receptor. Adapted from Guo et al. 2015.

Several pathways have been implicated in NLRP3 inflammasome activation, and mitochondria seem to play an important role in this process. Mounting evidence has suggested that these organelles supply an ideal platform for NLRP3 inflammasome assembly through the mitochondrial antiviral signaling (MAVS) adaptor protein, which is associated with NLRP3. Additionally, NLRP3

can be directly activated by effectors derived by damaged and/or dysfunctional mitochondria, including mtDNA, phospholipid cardiolipin and mitochondrial ROS (Zhou et al. 2011; Subramanian et al. 2013; Wen et al. 2013; Abais et al. 2015; Gurung et al. 2015). Regarding the latter, the thioredoxin (TRX)-interacting protein (TXNIP), whose main function is to inhibit TRX (an important redox protein and promoter of cell growth), detaches from TRX in a ROS-dependent manner and binds to NLRP3, contributing to NLRP3 inflammasome activation (Zhou et al. 2009, 2011; Lane et al. 2013). Another important event in the activation of this inflammasome is the rise of cytosolic Ca^{2+}. As a major intracellular reservoir, the ER is crucial in this process considering that the loss of ER homeostasis (either by accumulation of unfolded proteins or by disruption of Ca^{2+} storage) leads to ER stress, which is characterized, among other events, by an increase of cytosolic Ca^{2+}; however, the mechanism involved in NLRP3 activation through Ca^{2+} is unclear. Alternatively, Ca^{2+} mobilization may cause mitochondrial dysfunction due to mitochondrial Ca^{2+} overload, promoting inflammasome activation (Lee et al. 2012; Murakami et al. 2012; Rossol et al. 2012; He et al. 2016). Another relevant mechanism involves lysosomal leakage due to the endocytosis of uric acid, amyloid or crystalized cholesterol, which provokes a lysosomal disruption and subsequent release of their content, activating NLRP3 and modifying intracellular pH (Szabo and Csak 2012; Ioannou et al. 2015; Szabo and Petrasek 2015; He et al. 2016). K^+ efflux has also emerged as a common factor in this activation, and it is induced in response to diverse stimuli, such as ATP (through activation of P2X7 receptor), nigericin, microbial-pore-forming toxin, decrease of extracellular osmolarity and metabolic lipids (Figure I.6) (Mariathasan et al. 2006; Ogura et al. 2006; Compan et al. 2012; Luheshi et al. 2012).

Once pro-caspase-1 has been enzymatically activated, this protease can cleave the cytokine precursors of IL-1β and IL-18 into mature, biologically active forms. Active caspase-1 (as well as human caspase-4/-5 and murine caspase-11) is also capable of provoking a pro-inflammatory form of cell death known as pyroptosis, which is characterized by cytoplasmic swelling, hyper-permeabilization and subsequent rupture of the plasma membrane, and release of the cellular content. These features are also common to necrosis, while it shares others with apoptosis, such as DNA fragmentation. (Lamkanfi et al. 2011; Lamkanfi and Dixit 2014; Arrese et al. 2016; Liu et al. 2016). Mature

IL-1β is one of the most potent pro-inflammatory cytokines, and may be a major driver of the pathogenesis of many autoimmune, autoinflammatory and infectious diseases, as well as of SI. Its multiple functions include recruitment of innate immune cells, modulation of adaptive immune cells, enhancement of T cell activation and induction of the expression of cyclooxygenase-2 and prostaglandin E2 (Arend et al. 2008; Tsutsui et al. 2015; Tilg et al. 2016). Mature IL-18 is important for the production of IFN-γ, induction of Th1 responses and potentiation of cytolytic activity of NK cells (Dinarello 2009; Netea et al. 2015). Due to the fact that pro-IL-1β and pro-IL-18 lack a signal peptide for protein release from the cell, their release occurs independently of the classical ER/Golgi pathway. Thus, these cytokines require caspase-1 post-translational processing to release the mature form from the cell, which occurs by unconventional protein secretion that includes micro-particle shedding or through pyroptotic cell death (Lopez-Castejon and Brough 2011; Brydges et al. 2013; Dinarello et al. 2013; Sollberger et al. 2014). Both IL-1β and IL-18 activate NF-κB signaling through binding to their receptors, IL-1R1 and IL-18R respectively, triggering the transcription of pro-inflammatory genes and hence enhancing the inflammatory response to injury (Dinarello 2009). Elegant papers have described the release of inflammasome particles (mainly oligomers formed by ASC or NLRP3) following pyroptotic cell death, spreading the inflammasome signaling to neighbor cells. These inflammasome particles can activate pro-caspase-1 that is released into the extracellular medium or located in the cells as a result of internalization (Baroja-Mazo et al. 2014; Broderick and Hoffman 2014; Franklin et al. 2014).

Although inflammasomes are generally considered pro-inflammatory complexes, recent evidence has shown that NLRP12 inflammasome plays a crucial role attenuating the inflammatory responses in several diseases, such as autoimmune encephalitis and dextran sulfate sodium (DSS)-induced colonic inflammation (Tuncer et al. 2014; Gharagozloo et al. 2015; Shi et al. 2016; Zaki 2016).

Inflammasome activation needs to be tightly regulated to avoid evident cell death or excessive production of cytokines, preventing a potentially harmful reaction in the host. Firstly, as mentioned above, the expression of the inflammasome components, in particular NLRP3, is relatively low and requires a priming signal to be increased (Martinon et al. 2009; Strowig et al. 2012).

Furthermore, cells express proteins that regulate the inflammasome activity by sequestering inflammasome components or directly inhibiting caspase-1 function, such as aryl hydrocarbon receptor and G protein signaling modulator-3 (Stutz et al. 2009; Pedraza-Alva et al. 2015). Autophagy, a catabolic process able to degrade organelles and other structures that has diverse functions in cellular homeostasis and defense, has been identified as a key negative regulator of NLRP3 inflammasome activation. This occurs through various mechanisms, including the removal of endogenous NLRP3 inducers, such as damaged mitochondria and mtDNA, selective degradation of inflammasome components and lysosomal degradation of pro-IL-1β (Henao-Mejia et al. 2012; Jo et al. 2016).

NLRP3 inflammasome has emerged as a crucial player in the onset and progression of several liver diseases, including ischemia/reperfusion injury, DILI, ASH, NASH, liver fibrosis and chronic HCV infection (Friedman 2013; Mehal 2014; Szabo and Iracheta-Vellve 2015; Szabo and Petrasek 2015; Heymann and Tacke 2016; Tilg et al. 2016). During progression of DILI, such as in acetaminophen intoxication, dying hepatocytes release DAMPs (e.g. nuclear DNA, HMGB1, HSPs, etc.) that induce the activation of the NLRP3 inflammasome and consequently promote liver inflammation. Several works have shown that genetic deficiencies in *IL1R1, NLRP3* or *CASP1* provide protection from liver inflammation and injury provoked by drugs (Chen et al. 2007; Imaeda et al. 2009; Sander and Blander 2009; Hoque et al. 2012). *In vivo* studies using IL-1β or IL-1R1 KO mice have revealed that the IL-1 pathway is essential against progression of steatosis to steatohepatitis and liver fibrosis in both murine models of NASH and ASH (Kamari et al. 2011), as well as in murine models of liver fibrosis including exposure to thioacetamide (TAA) and bile duct ligation (Salguero Palacios et al. 2008; Gieling et al. 2009). In this line, experimental models of NASH have shown that NLRP3 inflammasome is required for the fibrotic response (Wree et al. 2014b). Moreover, the persistent activation of the NLRP3 inflammasome in mice leads to a severe liver inflammation, hepatocyte pyroptotic cell death and fibrosis (Wree et al. 2014a); otherwise NLRP3 deficiency protected from choline-deficient L-amino acid-defined diet (CDAA)-induced NASH and fibrosis (Wree et al. 2014b). Other studies with global caspase-1 KO mice fed with high fat diet showed an attenuated hepatic inflammation and fibrogenesis (Dixon et al. 2013), while in

a model associated with fibrotic NASH, caspase-1 deficiency also protects from fibrosis development (Dixon et al. 2012). Furthermore, *in vitro* studies have shown IL-1β promotes HSC activation, with a significant increase in their fibrotic markers, including MMPs, TIMP-1, collagen 1α1 and TGF-β1 (Yan et al. 2008; Miura et al. 2010; Tang et al. 2013; Yaping et al. 2014; Reiter et al. 2016). In this regard, an elegant work showed that NLRP3 inflammasome activation in HSCs in response to monosodium urate crystals (MSU) results in a phenotypic change from quiescent to myofibroblast-like cells, and HSC activation was abrogated in ASC KO cells, suggesting that the inflammasome activation might be enough to produce a fibrogenic response (Watanabe et al. 2009). This association between NLRP3 inflammasome and liver injury has also been explored in human studies, showing that NLRP3 inflammasome components and IL-1β levels in liver tissue are enhanced in both HCV-infected and NASH patients (Negash et al. 2013; Wree et al. 2014b).

I.3. MECHANISMS TO ALLEVIATE THE CELLULAR DAMAGE: ROLE OF SEQUESTOME 1/p62

I.3.1. Structure and functions of p62

Sequestome 1 (SQSTM1), also known as p62, zeta-interacting protein (ZIP) and A170 (hereafter referred to as p62), is a multifunctional signaling hub, an autophagy substrate and stress-inducible protein encoded by an immediate-early response gene *SQSTM1*. First identified as a 62 kDa protein which binds to lymphocyte-specific protein tyrosine kinase, it has been associated with diverse cellular events including cell survival, cell proliferation, differentiation, cell death, inflammation and particularly with oxidative stress response (Ishii et al. 1996; Lee et al. 1998; Moscat and Diaz-Meco 2012; Nezis and Stenmark 2012; Manley et al. 2013; Katsuragi et al. 2015). This protein is expressed in most tissues, and it is mainly distributed in the cytosol, but it is also present in nucleus, lysosomes and autophagosomes (Seibenhener et al. 2007; Pankiv et al. 2010). It has also been reported that p62 is localized in mitochondria in non-stressful conditions, both at the outer and the inner mitochondrial membrane, and that its deficiency provokes mitochondrial dysfunction due to disturbances in $\Delta\Psi_m$, ATP production, and mitochondrial morphology. In

addition, p62 is essential for the maintenance of mitochondrial stability and mtDNA biogenesis (Du et al. 2009; Seibenhener et al. 2013).

In the past years, growing studies have implicated p62 in many human pathologies. High levels of p62, induced by abnormal accumulation via impaired autophagy or by its overexpression, have been found in a wide range of human tumors including hepatocellular carcinoma, lung cancer, gastric cancer and colon cancer, (Moscat et al. 2007, 2016; Mathew et al. 2009; Geetha et al. 2012a). Furthermore, a recent work has revealed that ectopic p62 levels induce tumorigeneses by activating p62-regulated pathways in an autophagy-competent liver (Umemura et al. 2016). It has also been shown that p62 is a major component of protein aggregates in diseases in which proteostasis is defective, such as neurofibrillary tangles in Alzheimer's disease and Lewy bodies in Parkinson's disease (Kuusisto et al. 2001; Zatloukal et al. 2002), while *SQSTM1* mutations have been implicated in human Paget's disease, a chronic bone and metabolic disorder due to increased bone turnover (Laurin et al. 2002; Rea et al. 2014). Regarding liver diseases, p62 has been found as a major component of Mallory-Denk bodies, which are usually related to ASH and NASH, as well as in α1-antitrypsin deficiency aggregates in hepatocytes (Zatloukal et al. 2002, 2007). Additionally, experiments performed in p62 KO mice have suggested that this protein plays a pivotal role in obesity and metabolic syndrome development by regulating HIF-1α, JNK, Akt and ERK signaling pathways, as these mice displayed enhanced adipogenesis, fatty liver, impaired glucose metabolism, insulin resistance and leptin intolerance (Rodriguez et al. 2006; Lee et al. 2010; Geetha et al. 2012b; Seki et al. 2012; Manley et al. 2013; Chen et al. 2016).

The multiple functionality of p62 lies in its structure, which holds six motifs including an N-terminal Phox1 and Bem1p (PB1) domain, a microtubule-associated protein 1 light chain 3 (LC3)-interacting region (LIR), a tumor necrosis factor receptor-associated factor (TRAF) 6 binding (TB) motif, a zinc finger (ZZ), a kelch-like ECH-associated protein 1 (Keap1)-interacting region (KIR), and a C-terminal ubiquitin-associated (UBA) domain. p62 has two nuclear localization signal (NLS) sequences and a nuclear export signal (NES) sequence (Figure I.7) (Komatsu et al. 2012; Moscat and Diaz-Meco 2012; Katsuragi et al. 2015; Taniguchi et al. 2016). These different domains indicate that p62 plays multiple roles, such as signaling suppression and amplification, organelle and

protein quality control and redox homeostasis (Ishii et al. 2013). In response to several insults, p62 is transferred to autophagy substrates, including damaged mitochondria and protein aggregates. p62 acts as a signaling hub for mTORC1 [mammalian target of rapamycin (mTOR) complex 1] activation, the Keap1–Nrf2 (nuclear factor erythroid 2-related factor 2) pathway on autophagic cargoes, and as adaptor for selective autophagy (Moscat and Diaz-Meco 2011; Rogov et al. 2014; Filomeni et al. 2015; Katsuragi et al. 2015). The role of p62 in different cellular events and signaling pathways is discussed in more detail further in the text.

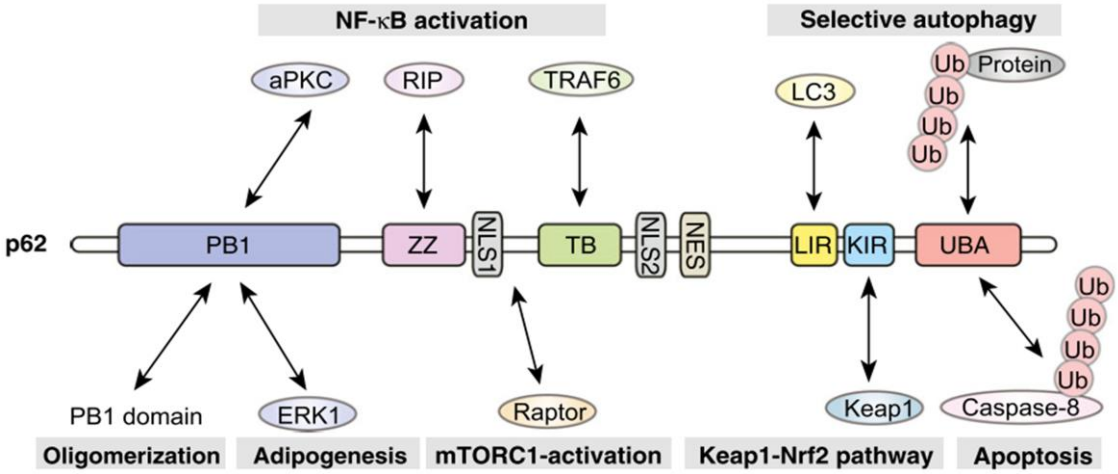

Figure I.7. Domain structure of p62 and its binding partners. Abbreviations: aPKC: atypical protein kinases C; ERK: extracellular signal-regulated kinases; mTORC1: mammalian target of rapamycin complex 1; NF-κB: nuclear factor kappa B; Raptor: regulatory-associated protein of mTOR; RIP: receptor-interacting protein; Ub: ubiquitin. Obtained from Katsuragi et al. 2015.

I.3.2. Regulation of p62 expression

p62 expression is regulated transcriptionally and post-transcriptionally (Moscat and Diaz-Meco 2011; Taniguchi et al. 2016). *SQSTM1* transcription is mediated by the transcription factors NF-κB and Nrf2, which are activated by pro-inflammatory and oxidative stressors, respectively. Moreover, p62 is also involved in the activation of these two transcription factors, hence establishing two positive feedback loops with these proteins (Vadlamudi and Shin 1998; Jain et al. 2010; Kwon et al. 2012; Chen et al. 2014; Won et al. 2016). It has also been demonstrated that p62 expression is regulated by the nuclear hormone receptor farnesoid X receptor (FXR), as well as by JNK signaling

(Puissant and Auberger 2010; Williams et al. 2012). In addition to these transcription factors, *SQSTM1* is also overexpressed by the UPR and ER stress; in fact, ChIP-seq and mRNA-seq assays demonstrated that CHOP directly interacts with *SQSTM1* promoter (Liu et al. 2012; Han et al. 2013). p62 protein levels can be post-transcriptionally regulated by autophagy and ubiquitin proteasome system (UPS). Autophagy quickly degrades p62, due to the interaction of p62 LIR domain with LC3; thus, elevated p62 levels in absence of significant modifications in its mRNA levels are employed as a marker of inefficient or blocked autophagy (Bjørkøy et al. 2009; Jiang and Mizushima 2015; Taniguchi et al. 2016). Moreover, p62 recruits ubiquitinated proteins, due to its ability to non-covalently bind with ubiquitin through its UBA domain, and targets these proteins for degradation via proteasome (also via autophagosomes), being p62 itself also degraded in this process (Figure I.8) (Seibenhener and Babu 2004; Harper and Schulman 2006; Shaid et al. 2012).

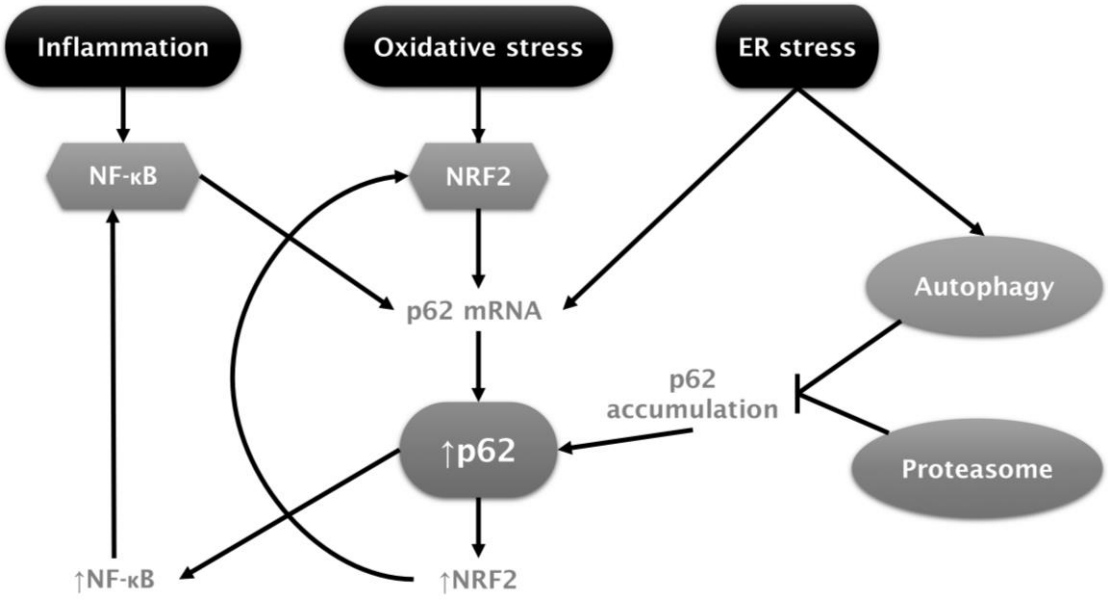

Figure I.8. Pathways through which p62 expression is regulated. Abbreviations: ER: endoplasmic reticulum; NF-κB: nuclear factor kappa B; Nrf2: nuclear factor erythroid 2-related factor 2.

I.3.3. p62-mediated signaling pathways

I.3.3.1. p62 and autophagy

Autophagy refers to a group of tightly regulated stress-responsive catabolic processes by which lysosome enzymes degrade cytoplasmic components

(Morel et al. 2016). This process plays a crucial role in tissue and cellular homeostasis as well as in immune responses, pathogen clearance, regulation of inflammatory responses, development, metabolism, quality control of protein and removal of damaged organelles (e.g. dysfunctional mitochondria) (Glick et al. 2010).

Autophagy is widely classified in three types: macroautophagy (hereafter referred to as autophagy), by which cytoplasmic proteins and organelles are sequestered into double membrane-bound vesicles named autophagosomes; microautophagy, which consists in the degradation of cytosolic proteins by lysosomal proteases after their direct engulfment by endosomal or lysosomal membrane; and chaperone-mediated autophagy, in which cytosolic proteins are selectively recognized by heat shock cognate protein chaperones (e.g. HSC70) and driven to lysosomes through lysosome-associated membrane protein (LAMP)-2A (Figure I.9) (Mizushima and Komatsu 2011; Li et al. 2012; Cuervo and Wong 2014). Although autophagy has initially been considered a non-selective degradation process, it is now known that it can be highly selective, with selective autophagy usually termed according to the cellular material degraded, such as ER (reticulophagy), lipid droplets (lipophagy), mitochondria (mitophagy) and peroxisomes (pexophagy) (Feng et al. 2014).

Autophagy is initiated by autophagosome biogenesis, which is coordinated by membrane complexes containing autophagy-related (ATG) proteins, and comprises four main stages: initiation, nucleation, expansion of the isolation membrane and maturation. The process begins with the formation of the phagophore from the omegasome, a site emanating from the ER where proteins of the ULK (UNC51-like kinase) complex, which contains ULK1 or ULK2, ATG13, FIP200, and ATG101, assemble to initiate autophagosome biogenesis. Then, during nucleation the activated ULK complex targets a class III PI3K complex, including beclin 1, vacuolar protein sorting (VPS) 15, VPS34 and ATG14, to induce the local production of a pool of phosphatidylinositol 3-phosphate (PI3P) that is specific to autophagosomes. Subsequently, in the expansion or elongation stage, the ATG5-ATG12-ATG16 complex is recruited to the autophagosome membrane where it facilitates the lipidation of LC3 with phosphatidylethanolamine (PE). Finally, once the autophagosome has been formed, it fuses with a lysosome in the maturation stage to create an autophagolysosome, in which its engulfed components are degraded by

lysosomal enzymes and recycled (Figure I.9) (Mizushima and Komatsu 2011; Rubinsztein et al. 2012; Kaur and Debnath 2015; Morel et al. 2016).

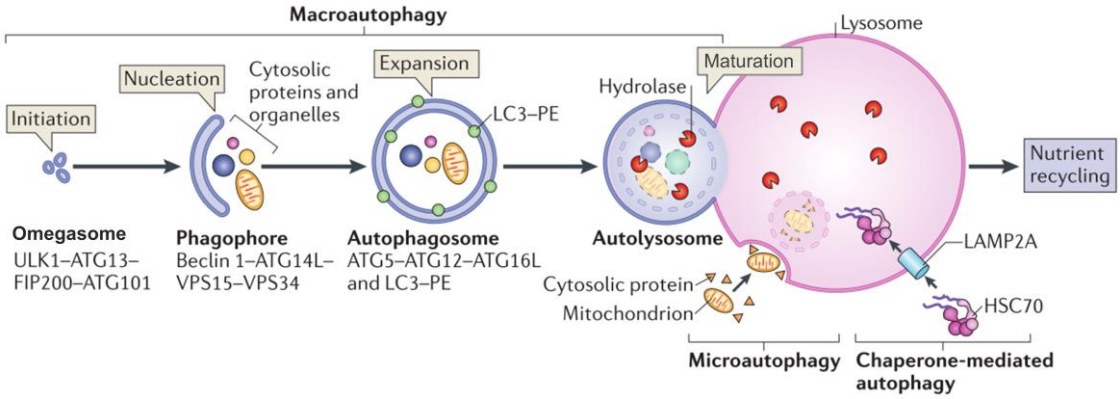

Figure I.9. Overview of mammalian autophagy. Three autophagic pathways deliver cytoplasmic components to lysosomes for their degradation: Chaperone-mediated autophagy translocates cargoes by the HSC70 chaperone to the lysosome through interaction with a protein on its surface, LAMP-2A. Microautophagy engulfs substrates by direct invagination into the lysosome. Macroautophagy is a multi-step process that includes the formation of double-membrane organelles named autophagosomes where cytosolic cargoes are sequestered (initiation, nucleation and expansion steps). Finally, autophagosome fuses with lysosomes, where the cargo is degraded and nutrients are recycled (maturation step). Abbreviations: ATG: autophagy-related; HSC70: heat shock cognate 70; LAMP-2A: lysosome-associated membrane protein 2A; LC3: microtubule-associated protein 1 light chain 3; PE: phosphatidylethanolamine; ULK: UNC51-like kinase; VPS: vacuolar protein sorting. Image adapted from Kaur and Debnath 2015.

mTORC1 is a crucial regulator of the initiation of autophagosome biogenesis. it plays a pivotal role in several cellular events that use or generate large amounts of nutrients and energy, such as cell growth, lipid metabolism (e.g. fatty acid synthesis, lipid oxidation) and protein synthesis (Katsuragi et al. 2015; Taniguchi et al. 2016). Its activation by diverse stimuli, including growth factors and nutrients, blocks the autophagy pathway by phosphorylation of ULK complex, avoiding the onset of autophagosome biogenesis (Morel et al. 2016).

As explained above, p62 is a well-known autophagy substrate usually degraded by this process. However, p62 can also regulate negatively the autophagy pathway, due to its ability to interact with the mTORC1 components Raptor and RagC on the lysosomal membrane in an amino acid-dependent manner,

promoting mTORC1 activation (Duran et al. 2011; Rubinsztein et al. 2012). Furthermore, p62 serves as a docking site and is necessary for mTORC1 localization to the lysosomal membrane in response to inducers, such as amino acids (Manley et al. 2013). The PB1 domain of p62 plays an important role in its self- and hetero-oligomerization with other proteins, including the neighbor of BRCA gene 1 (NBR1) protein, which also contain PB1 domains, to promote packaging of ubiquitinated cargoes and their delivery to the autophagosome. p62 may bind mono- and poly-ubiquitinated organelles and protein aggregates via its C-terminal UBA domain (Johansen and Lamark 2011; Shaid et al. 2012), and moreover its LIR domain enables the direct binding to LC3 (Figures I.7 and I.10), which is responsible for p62 degradation by autophagy (Ichimura et al. 2008). Therefore, p62 plays a crucial role in ubiquitin-selective autophagy. However, p62 deficiency does not result in any autophagy defects (Antonucci et al. 2015; Umemura et al. 2016), suggesting this function of p62 is redundant with that of other autophagy receptors, including NBR1, optineurin and nuclear dot protein 52 kDa (NDP52) (Shaid et al. 2012; Katsuragi et al. 2015), being NBR1 the receptor with greater structural similarity to p62 (Figure I.10) (Lippai and Low 2014; Xu et al. 2015).

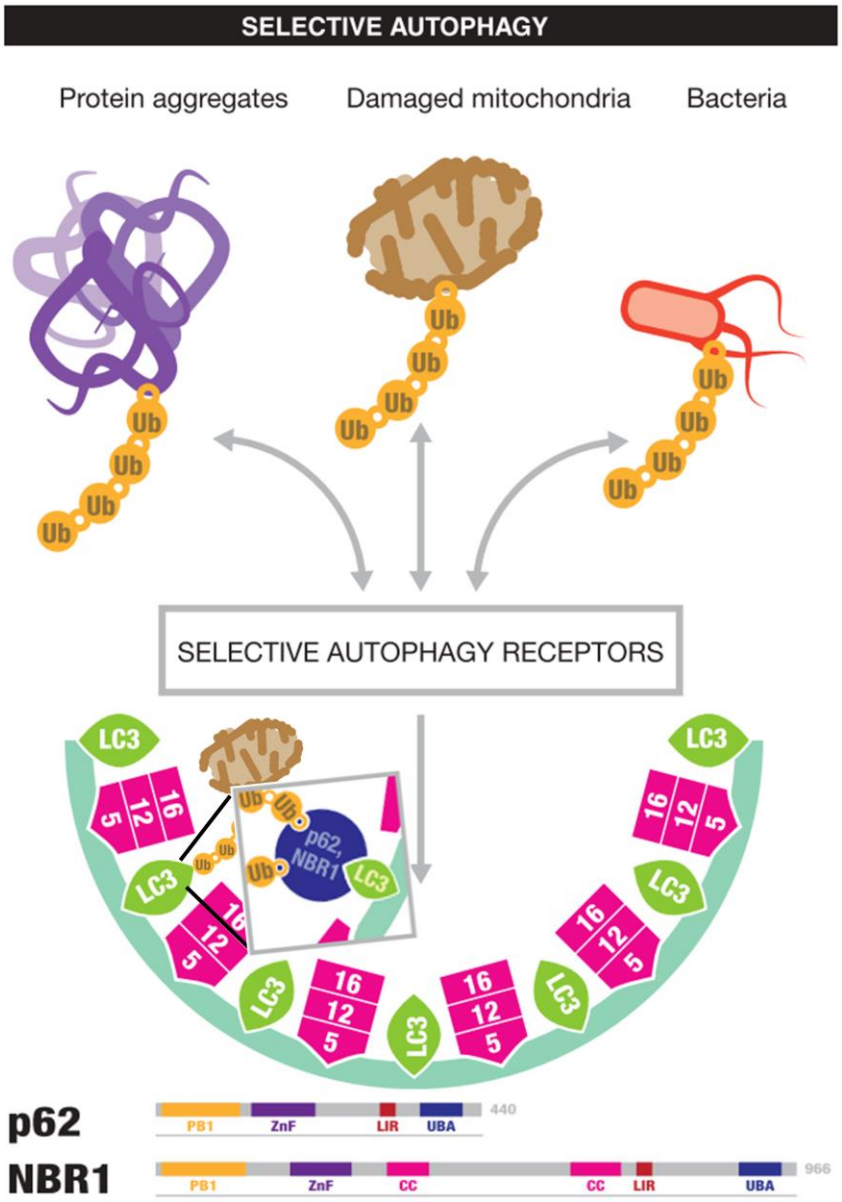

Figure I.10. Role of p62 and NBR1 in autophagy. In selective autophagy, particular substrates such as protein aggregates, mitochondria and pathogens are targeted to the autophagosome by selective autophagy receptors, such as p62 and NBR1. Abbreviation: LC3: microtubule-associated protein 1 light chain 3; NBR1: neighbor of BRCA1 gene 1; Ub: ubiquitin. Image adapted from Shaid et al. 2012.

I.3.3.2. p62 and Nrf2 signaling

The induction of many cytoprotective proteins in response to endogenous and exogenous electrophilic/oxidative stressors, as well as drug detoxification, is mainly regulated by Nrf2 at the transcriptional level (Nguyen et al. 2009; Taguchi et al. 2011). Nrf2, a bZIP transcription factor, heterodimerizes with small Maf proteins and these heterodimers recognize antioxidant response

element (ARE) in the promoter regions of target genes, which encode antioxidant proteins, phase-II drug-metabolizing enzymes, and anti-inflammatory proteins, such as heme oxygenase 1 (HMOX1), glutamate-cysteine ligase (GCL) glutathione S transferases (GSTs) and NAD(P)H quinone oxidoreductase 1 (NQO1) (Jain et al. 2010; Kansanen et al. 2013; Zhang et al. 2015).

Under non-stressful conditions, Nrf2 is constitutively degraded by UPS as its binding partner Keap1 is an adaptor for the cullin-3-type ubiquitin ligase, inducing the Nrf2 ubiquitination and its subsequent proteasome-mediated degradation (Jaramillo and Zhang 2013; Manley et al. 2013). Upon exposure to oxidative stressors, Keap1 undergoes conformational modification, thereby Nrf2 is released from Keap1 binding and translocates into nucleus to enhance the gene expression encoding antioxidant enzymes (Kwon et al. 2012; Katsuragi et al. 2015). In addition, Nrf2 may be activated through a non-canonical pathway where p62 plays a key role. As stated above, p62 can interact with Keap1 by means of its KIR domain, and functions as an oxidant-independent inducer of Nrf2. The phosphorylated KIR motif of p62 markedly increases its affinity to bind to Keap1, interfering in its function and facilitating its degradation through autophagy, hence allowing Nrf2 nuclear translocation (Taguchi et al. 2011; Kwon et al. 2012; Ichimura et al. 2013; Jiang et al. 2015). Additionally, an ARE has been found in the promoter region of *SQSTM1*, which is responsible for p62 upregulation as a response to oxidative stress, resulting in a positive-feedback loop in which *SQSTM1* itself is transcriptionally regulated by Nrf2 (Figure I.11) (Jain et al. 2010; Puissant et al. 2012).

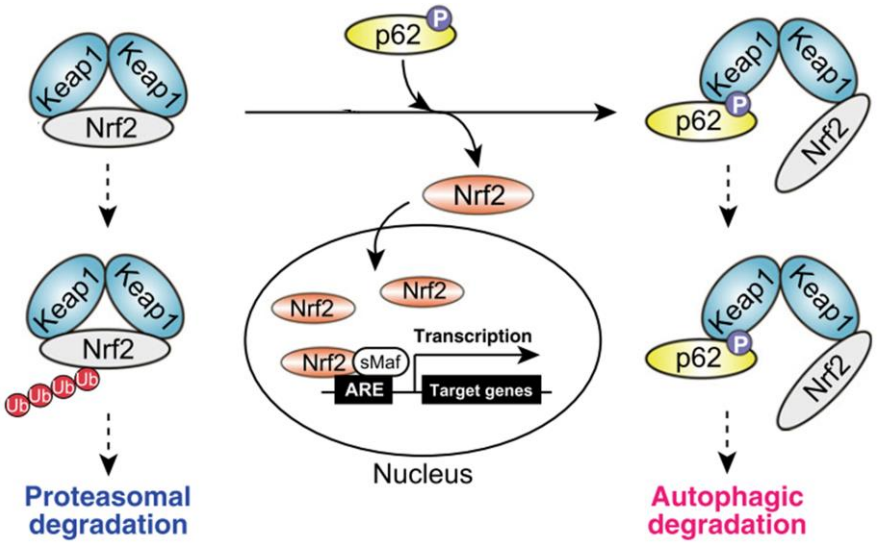

Figure I.11. Involvement of p62 in the regulation of Nrf2 activation. Abbreviations: ARE: antioxidant response element; Keap1: kelch-like ECH-associated protein 1; Nrf2: nuclear factor erythroid 2-related factor 2; sMaf: small Maf proteins. Adapted from Katsuragi et al. 2015.

p62-mediated Nrf2 activation has a controversial role in the progression of liver diseases, such as hepatocellular carcinoma (HCC) and DILI. Results obtained with autophagy-deficient mice showed an increased p62 accumulation leading to persistent Nrf2 activation and favoring the development of liver cancer, that is explained by the capacity of Nrf2 signaling to promote tumor cell survival by augmenting the activity/expression of antioxidant enzymes (Hayes and McMahon 2009; Inami et al. 2011; Moscat and Diaz-Meco 2012; Moscat et al. 2016). In this line, other studies have revealed that Nrf2 activation confers chemoresistance to tumor cells (Hayes and McMahon 2009). Conversely, Nrf2 activation alleviates lipogenic or drug-induced liver injury that involves oxidative stress (Manley et al. 2013); in this way autophagy-deficient mice administered an overdose of acetaminophen, a well-known oxidative stressor of hepatocytes, were more resistant to liver injury due to a persistent p62-mediated Nrf2 activation (Ni et al. 2012).

I.3.3.3. p62 and inflammatory pathways

As pointed out above, NF-κB is one the master regulators of inflammation in response to diverse pro-inflammatory insults, including TNF-α and IL-1β. p62 modulates multiple pathways to tightly regulate activation of NF-κB. The ZZ motif of p62 binds to RIP1, a kinase that regulates TNF-α receptor-mediated

activation of NF-κB through is interaction with TRADD (TNF-α receptor-associated death domain) (Sanz et al. 1999; Moscat et al. 2007; Manley et al. 2013). In addition, p62 interacts with TRAF6 through its TB domain to induce TRAF6 poly-ubiquitination, which regulates NF-κB activation via IKK complex (Wooten et al. 2005). p62 self-oligomerizes through its PB1 domain and binds to aPKC in response to several stimuli, including IL-1 and receptor activator of NF-κB ligand (RANKL), which leads to the activation of NF-κB. Conversely, the PB1 domain of p62 also interacts with deubiquitinases, which abrogates TRAF6 polyubiquitination and acts as a negative regulator of NF-κB activation (Jin et al. 2008; Kim and Ozato 2009; Manley et al. 2013; Taniguchi et al. 2016). In addition, experiments performed in keratinocytes have shown that TLR signaling activates simultaneously both inflammatory and autophagy pathways, including NF-κB activation and inflammatory cytokine production, through autophagy via p62 (Lee et al. 2011). Nevertheless, it is also reported that p62 promotes NF-κB activation and its downstream effectors, including IL-1β and TNF-α, because it captures A20 protein which acts as an important NF-κB suppressor under TLR and TNFR receptors, to sequester it into autophagosomes (Kanayama et al. 2015), and regulates positively NOD2 signaling cascades (Park et al. 2013).

Mounting evidence has addressed the connection between p62 and inflammasomes, and its implication in inflammasome regulation is also multifaceted. It has been revealed that increased p62 protein levels as a result of UPS impairment, enhances IL-1β expression through activation of extracellular ERK and JNK of the MAPK pathway, and induces caspase-1 activation (Choe et al. 2014; Harijith et al. 2014), promoting neutrophil recruitment (Amaral et al. 2012). However, it has been also found that NLRP3 agonists can damage mitochondria in macrophages, causing release of additional mitochondrial inducers such as mtDNA and ROS, enhancing p62 expression in a NF-κB-dependent manner. This increased p62 expression inhibits inflammasome-dependent SI and IL-1β production by promoting p62-mediated mitophagy. Therefore, NF-κB may restrain its own inflammation-promoting activity (Zhong et al. 2016).

Chapter II. AIMS

The general aim of this study was to explore the acute inflammatory and fibrogenic responses induced by the antiretroviral drug efavirenz in liver cells, and to characterize the cellular and molecular mechanisms implicated, employing *in vitro* and *in vivo* models.

The specific aims established to achieve the general aim were:

1. **To evaluate whether the mitochondrial dysfunction and endoplasmic reticulum stress induced in hepatocytes by efavirenz contribute to the activation of inflammatory responses through NF-κB- and NLRP3 inflammasome-dependent pathways.**

2. **To characterize the effects of efavirenz on hepatic stellate cells regarding mitochondrial function, endoplasmic reticulum stress and autophagy, with special emphasis on lipophagy.**

3. **To analyze the role of efavirenz in the activation of the NLRP3 inflammasome, and in the triggering of inflammatory and fibrogenic responses in hepatic stellate cells.**

4. **To determine the role of liver macrophages in the induction and/or progression of efavirenz-induced liver injury.**

5. **To assess the expression and subcellular location of p62 in efavirenz–treated hepatic cells, a model of activated autophagic flux and mitochondrial dysfunction/endoplasmic reticulum stress.**

6. **To analyze the function of p62 in the mitochondrial dysfunction and inflammatory response induced in hepatocytes by efavirenz.**

Chapter III. MATERIALS AND METHODS

III.1. REAGENTS

III.1.1. Antiretroviral drugs

The antiretroviral drugs employed in this thesis were acquired from Sequoia Research Products (Pangbourne, UK) and were dissolved in their respective vehicles (Table III.1). No significant impact was found on any of the analyzed parameters with these concentrations of the vehicles.

DRUG	BRAND NAME	VEHICLE
Efavirenz (EFV)	Sustiva™	Methanol (*in vitro*)/ DMSO (*in vivo*)
Raltegravir (RAL)	Isentress®	DMSO
Darunavir (DRV)	Prezista®	DMSO
Rilpivirine (RPV)	Edurant®	DMSO
Abacavir (ABC)	Ziagen®	Distilled water
Didanosine (ddI)	Videx®	Distilled water

Table III.1. Antiretroviral drugs employed in this thesis. List of active principles with their respective brand names and vehicles. Abbreviation: DMSO: dimethyl sulfoxide.

III.1.2. General chemical reagents

All general chemical reagents were of analytical grade and were purchased from Sigma-Aldrich Chemicals (Stenheim, Germany), Panreac Química S.L.U. (Barcelona, Spain), Merck (Darmstadt, Germany) and Roche Life Science (Penzberg, Germany).

III.1.3. Cell culture reagents

Media and supplements for cell culture (Table III.2) were obtained from Gibco™ (Thermo Fisher Scientific, Waltham, MA, USA), Sigma-Aldrich Chemicals and Lonza (Basel, Switzerland).

REAGENT	COMPANY
Amphotericin B	Gibco
Collagen type I	Sigma-Aldrich
Cytosine arabinose	Sigma-Aldrich
D-glucose	Sigma-Aldrich
Dimethyl sulfoxide (DMSO)	Sigma-Aldrich
Dulbecco's modified Eagle's medium (DMEM) with low glucose concentration (1 g/L)	Sigma-Aldrich
DMEM with high glucose concentration (4.5 g/L)	Gibco
Foetal bovine serum (FBS)	Lonza
Hank's balanced salt solution (HBSS)	Sigma-Aldrich
Horse serum (HS)	Lonza
Hydrocortisone hemisuccinate	Sigma-Aldrich
Insulin from bovine pancreas	Sigma-Aldrich
L-glutamine	Gibco
Minimum essential medium (MEM)	Gibco
MEM non-essential amino acids solution (NEAA)	Gibco
Penicillin/streptomycin	Gibco
Phosphate-buffered saline (PBS, pH 7.4)	Gibco
Poly-D-lysine solution	Sigma-Aldrich
Primary hepatocyte maintenance supplement: A cocktail solution of 0.8 mg/mL dexamethasone, 6.25 µg/mL human recombinant insulin, 6.25 µg/mL human transferrin, 6.25 ng/mL selenium complex, and 5.35 µg/mL linoleic acid, GlutaMAX™ and HEPES	Gibco
Roswell Park Memorial Institute (RPMI) 1640 medium with GlutaMAX™-I supplement and HEPES	Gibco
RPMI 1640	Lonza
Sodium pyruvate	Gibco
Trypsin-EDTA 0.25%	Gibco
Uridine	Sigma-Aldrich
William's medium E	Sigma-Aldrich
William's medium E without phenol red	Gibco

Table III.2. Reagents used in cell culture with their respective supplier company.

III.2. EXPERIMENTAL MODELS

III.2.1. Human cell lines

The human hepatoblastoma cell line Hep3B (86062703, ECACC, Salisbury, UK) was used as a human hepatocyte model because they display a certain degree of cytochrome CYP2B6 activity capable of metabolizing EFV (Zhu et al. 2007; Lin et al. 2012). These cells were cultured in MEM supplemented with 10% heat-inactivated FBS (iFBS), 1 mM NEAA, 2 mM L-glutamine and 1 mM sodium pyruvate.

LX-2 cells, a human immortalized HSC line, were routinely cultured in DMEM with high glucose concentration (4.5 g/L) supplemented with 10% iFBS. These cells were kindly gifted by Dr. Scott L. Friedman (Icahn School of Medicine at Mount Sinai, New York, NY, USA).

The human monocyte cell line U937 (85011440, ECACC) was maintained in suspension (2-9 x 10^5 cells/mL) in RPMI 1640 supplemented with 10% iFBS and 2 mM L-glutamine. Monocytes were differentiated into macrophages by culturing them in presence of 10 ng/mL phorbol-12-myristate-13-acetate (PMA, Sigma-Aldrich) for 48 h when they were used for experiments.

HepaRG™ cells (HPRGC10, Gibco) are bipotent progenitors isolated from a human hepatoma. They differentiate into hepatocyte-like and biliary epithelial-like cells. Cells were initially maintained at a density of 2.7 x 10^4 cells/cm^2 in William's medium E supplemented with 10% iFBS, 5 µg/mL insulin from bovine pancreas, 2 mM L-glutamine, and 50 µM hydrocortisone hemisuccinate. After 2 weeks, undifferentiated HepaRG™ were cultured in presence of 2% DMSO in the medium for a further 2-week period to induce cell differentiation (Gripon et al. 2002; Anthérieu et al. 2010). Thereafter, hepatocyte-like cells were selectively harvested from differentiated HepaRG through mild tripsinization (0.125% trypsin-EDTA) (Freshney 2011) and reseeded at a density of 8 x 10^4 cells/cm^2 in medium containing 2% DMSO. For treatment, cells were maintained in DMSO-free medium with the drug concentration under assay.

All cell culture media were supplemented with 50 U/mL penicillin and 50 µg/mL streptomycin. Cell cultures were maintained in a cell culture incubator (MCO-19AICUV-PE, Panasonic Healthcare Co. Ltd., Gunma, Japan) at 37º C, with humidified atmosphere of 5% CO_2 and 95% air (AirLiquide Medical, Valencia,

Spain). All cell lines were subcultured when they reached 90-95% confluence, using 0.25% Trypsin-EDTA to detach them, except for U937 cells, which were cultured in suspension. Subconfluent cell cultures of passage number lower than 30 were used for all the experiments.

III.2.2. Primary human cells

Confirmatory experiments were reproduced in primary human hepatocytes (HMCPMS, Gibco), HSCs (hHSCs) (HP-F-S, Zenbio, Durham, NC, USA) and KCs (hKCs) (HUKCCS, Gibco).

Human hepatocytes were seeded in collagen type I coated plates and cultured in William's medium E without phenol red, supplemented with 5% iFBS, 100 U/mL penicillin, 100 µg/mL streptomycin and primary hepatocyte maintenance supplement.

hHSCs were cultured in DMEM with glucose supplemented with 10% iFBS, 100 U/mL penicillin, 100 µg/mL streptomycin and 2.5 µg/mL amphotericin B. Cells were subcultured once they reached 90-95% confluence. The experiments were performed with subconfluent cell cultures of passage number lower than five.

hKCs were seeded in collagen type I coated plates and were maintained in RPMI 1640 medium with GlutaMAX™-I and HEPES, supplemented with 10% iFBS, 100 U/mL penicillin and 100 µg/mL streptomycin.

Collagen type I coating of cultures plates was performed by adding type-I collagen from rat tail diluted 1:120 in PBS for 3 h followed by two washing steps with PBS and, finally, drying and sterilizing under UV light for 1 h in laminar flow cabinet (Telstar Bio-II-A, Telstar Life Science Solutions, Terrasa, Spain).

Primary cell cultures were maintained in a cell culture incubator at 37º C, with humidified atmosphere of 5% CO2 and 95% air (AirLiquide Medical).

III.2.3. Generation and maintenance of rhoº Hep3B cells

To produce rhoº (ρº) cells, Hep3B cells were cultured in the presence of 50 ng/mL ethidium bromide (EthBr) in the medium (which inhibits replication and transcription of mitochondrial DNA without substantially affecting nuclear

DNA) supplemented with 50 μg/mL uridine (Hashiguchi and Zhang-Akiyama 2009) over 8 weeks, refreshing the culture medium every 2 days. To verify the reduction of functional mitochondria, several markers of this phenotype were assessed including mitochondrial oxygen consumption and expression of mitochondrial ETC proteins.

III.2.4. Mice

C57BL/6JRj female mice were supplied by Janvier Labs (Le Genest-Saint-Isle, France). Animals (20±3 g of body weight and 10 weeks of age) were given *ad libitum* access to water and chow diet (Envigo, Huntingdon, UK) and were kept at 21±1º C under a standard light/dark regimen (12 h/12 h). All animal procedures were performed in accordance with the guidelines for the care and use of laboratory animals of the University of Valencia (Valencia, Spain), and were approved by the local ethics committee.

III.2.5. Primary rat neurons

Primary cultures of neurons were obtained from rat cerebral cortex (Almeida and Medina 1997). Neurons were isolated from Wistar rat (purchased from Harlan Laboratories, Barcelona, Spain) fetuses at gestation day 15-16. Prosencephalon was pulled out from the cranium and was cut into small pieces with a scalpel in Solution A, which contained Earle's balanced salt solution (EBSS) (Gibco), 20 μg/mL DNase (Roche Life Science) and 0.3% bovine serum albumin (BSA) (Sigma Aldrich Chemicals), and fragments were then centrifuged at 500×g for 2 min. The supernatant was discarded and the pellet was incubated in Solution B, which contained EBSS, 0.025% trypsin, 60 μg/mL DNase and 0.3% BSA, at 37º C for 15 min. The enzymatic digestion of the tissue was stopped by adding 10% iFBS, and tissue suspension was centrifuged at 500×g for 5 min. After resuspending the pellet in Solution A, it was homogenized by several passages through a glass Pasteur pipette; tissue homogenate was allowed to precipitate for 4 min and the supernatant was collected in a new tube. This step was repeated twice. Total supernatant was centrifuged at 500×g for 5 min. The cellular pellet was resuspended in DMEM low glucose supplemented with 10% iFBS, and cells were plated on multiwell cell culture plates previously coated with 15 μg/mL poly-D-lysine at 2.5 x 10^5 cells/cm^2. After 48 h, culture medium was replaced by DMEM supplemented

with 5% HS, 20 mM D-glucose and 10 μM cytosine arabinose (to prevent non-neuronal proliferation). Neurons were used for assays on day 7, when the presence of axons and dendrites was evident in 99% of the cells. The protocol employed was approved by the institutional ethics committee (University of Valencia, Valencia, Spain).

III.3. TREATMENTS

III.3.1. *In vitro* treatments

Unless stated otherwise, cells were treated for 24 h with clinically relevant concentrations of drugs, chosen considering the interindividual pharmacokinetics variability reported in several clinical studies. Treatments were performed using subconfluent cell cultures in medium supplemented with 10% iFBS. Several concentrations of each drug were tested in order to analyze the concentration-dependence of the studied effect.

Additionally, a negative control (untreated cells) and a vehicle control were used in every experiment. The effects of antiretroviral drugs were compared to those triggered by pharmacological modulators of different cellular pathophysiologic processes (Table III.3).

NAME	CONC.	ACTION	COMPANY
3-Methyladenine (3MA)	2.5 mM	Inhibits autophagosome formation by interfering with class III PI3K (Seglen and Gordon 1982)	Sigma-Aldrich
Actinomycin D (ActD)	2 μg/mL	Inhibits gene transcription (Bensaude 2011)	Sigma-Aldrich
BAPTA-AM	10 μM	Intracellular Ca^{2+} chelator (Dieter et al. 1993)	Abcam
CCCP	10 μM	Protonophore used as chemical uncoupler of OxPhos (Lou et al. 2007)	Sigma-Aldrich
Human IL-4	20 ng/mL	Pleiotropic cytokine used to polarize macrophages to M2 (Cosín-Roger et al. 2013)	MACS Miltenyi Biotec
Rotenone (Rot)	25 μM	Inhibitor of complex I of the ETC (Ishiguro et al. 2001)	Sigma-Aldrich

NAME	CONC.	ACTION	COMPANY
Thapsigargin (TG)	2 µM	Highly selective inhibitor of the SERCA that triggers ER-stress (Thastrup et al. 1990)	Sigma-Aldrich
Human TNF-α	25 ng/mL	Potent pro-inflammatory inducers (Medzhitov and Horng 2009; Rauch et al. 2013; Zelová and Hošek 2013) "LPS cocktail" (LPSc), a mixture composed of LPS, IFN-γ and TNF-α, was used as pro-inflammatory positive control, and polarize macrophage to M1 phenotype	MACS Miltenyi Biotec
Human IFN-γ	500 U/mL		Peprotech EC Ltd.
LPS from *E.coli O26:B6* (LPS)	100 ng-1 µg/mL		Sigma-Aldrich

Table III.3. List of pharmacological modulators used, including the specific concentration employed, description of their pharmacological actions and brand names.

Some experiments in Hep3B cells were carried out with conditioned medium from M2 macrophages. In order to generate M2 conditioned medium (CM), macrophages were differentiated from U937 monocytes, and then polarized towards a M2 phenotype by culturing in the presence of 20 ng/mL IL-4 for 72 h (Cosín-Roger et al. 2013). M2 macrophages were washed twice with PBS and were cultured for further 48 h in complete RPMI 1640 medium. M2 CM was then collected and centrifuged at 500×g for 5 min to remove cell debris before its addition to Hep3B cells. As a negative control, M0 CM was generated from undifferentiated U937-derived macrophages (Huang et al. 2013; Hedbrant et al. 2015).

III.3.2. *In vivo* treatments

Animal dosages were estimated using the normalization method based on extrapolation of animal dose to human dose through normalization to body surface area, employed by the Center for Drug Evaluation and Research (a part of the FDA) (Center for Drug Evaluation and Research 2005; Reagan-Shaw et al. 2007). The dosage of EFV was calculated according to the maximum daily therapeutics dose of EFV in humans (600 mg). Thereby, the dosages administered (P.O.) to mice were 2.47 mg, 6.18 mg and 12.36 mg, which approximately reproduce the clinically relevant plasmatic concentrations found

in humans that we employed in our *in vitro* studies (10, 25 and 50 μM, respectively). Mice were sacrificed 24 h after administration of EFV by cervical dislocation, and liver samples were collected.

Key experiments were performed with gadolinium chloride ($GdCl_3$, Fisher Scientific Acros, OTT, Canada), a macrophage selective inhibitor, which was administered (20 mg/kg in saline solution, I.V.) 24 h before the addition of EFV (2.47 mg) (Huang et al. 2010; Kim et al. 2015).

For each experimental condition, groups of five specimens were used, including a negative control (untreated mice) and a vehicle control. All animal procedures were performed in accordance with the guidelines for the care and use of laboratory animals of the University of Valencia, and were approved by the local ethics committee.

III.4. TRANSFECTION OF MAMMALIAN CELLS: TRANSIENT GENE SILENCING

Hep3B cells were transiently transfected using Lipofectamine™ 2000 (Invitrogen, Thermo Fisher Scientific), according to the manufacturer's instructions. Cells were seeded the day before the transfection in t-75 flasks and maintained at 37º C in a CO_2 incubator overnight. For the transfection, 750 pmol of *CHOP/GADD153/DDIT3* siRNA (h) or *SQSTM1/p62* siRNA (h) (both from Santa Cruz Biotechnology, Heidelberg, Germany) and 37.5 μL Lipofectamine™ 2000 were diluted gently in 900 μL of serum-free Opti-MEM® (Invitrogen, Thermo Fisher Scientific) in two separate tubes. As a control, SignalSilence® control siRNA (Cell Signaling) was employed.

Diluted siRNA and diluted Lipofectamine™ 2000 were combined (total volume of 1800 μL), mixed gently and incubated for 20 min at room temperature (RT). The transfection mixture was added to Hep3B cells (80-90% confluence) in t-75 flask containing 13.2 mL of supplemented MEM without antibiotics and mixed gently before incubation for 6 h at 37º C in a cell culture incubator. After 6 h, the medium was replaced by fresh supplemented MEM. The following day, cells were reseeded in the final culture multi-well plates or flasks to perform the experiments.

III.5. PROTEIN EXPRESSION ANALYSIS

III.5.1. Protein extracts

III.5.1.1. Samples collection and preparation

Cells were collected following this procedure: cell culture medium was removed, cells were washed once with a suitable volume of warm PBS and detached by adding trypsin-EDTA (at 37º C for 1 min). The resulting cellular suspension was centrifuged at 800×g for 3 min, at RT (Universal 320 Centrifuge, Heittich; Tuttlingen, Germany), supernatant was then discarded and cell pellet was resuspended in 1 mL ice-cold PBS. The resulting suspension was centrifuged at 500×g for 5 min, at 4º C (5415R, Eppendorf, Eppendorf Ibérica S.L.U., Madrid, Spain). Finally, the supernatant was discarded and cell pellets stored.

III.5.1.2. Whole-cell protein extraction

Cells pellets were resuspended in 40-90 µL complete lysis buffer, whose composition was 20 mM HEPES pH 7.4, 400 mM NaCl, 20% (v/v) glycerol, 0.1 mM EDTA, 10 µM Na_2MoO_4 and 10 mM NaF. Immediately prior to use, 1 mM DTT, 5 mM broad-spectrum serine and cysteine protease inhibitors (cOmplete Mini™ and Pefabloc®, both from Roche Life Science, Barcelona, Spain) and 0.05% detergent solution (NP-40 Surfact-Amps™, Thermo Fisher Scientific) were added. Samples were then vortexed twice at maximum speed for 10 sec, incubated on ice for 15 min, vortexed again at maximum speed for 30 sec and subsequently centrifuged at 16,000×g for 15 min at 4º C. Pellets were discarded, and supernatants (whole-cell protein extracts) were collected in new ice-chilled tubes and stored at -20º C until future use.

III.5.1.3. Mitochondria-enriched extracts

Cell pellets obtained using t-75 flask cell cultures were resuspended in 500 µL fractionation buffer (10 mM Tris-HCl pH 7.5, 1 mM EDTA and 0.25 M sucrose) and immediately homogenized on ice by passage through a 21-gauge needle. Following centrifugation at 500×g for 10 min at 4º C, supernatants were collected and centrifuged at 4º C for 30 min at 16000×g. This new supernatant representing the cytosolic fraction was stored, whereas the pellet

(mitochondrial fraction) was washed by adding 1 mL fractionation buffer. After a new centrifugation step at 11000×g for 10 min at 4º C, the pellet was resuspended in 50 µL mitochondrial buffer (10 mM Tris-acetate pH 8.0, 5 mM $CaCl_2$, 1 mM DTT, 0.5% NP-40 Surfact-Amps™ and 5 mM protease inhibitor cocktail cOmplete Mini™), obtaining a mitochondria-enriched cellular fraction. Both fractions were stored at -20º C.

III.5.1.4. Nuclear and cytosolic protein extraction

In order to obtain nuclear and cytosolic extracts, cell pellets obtained from confluent t-75 flask cell cultures were resuspended in 100 µL of lysis buffer [10 mM HEPES pH 7.5, 2 mM $MgCl_2$, 1 mM DTT, 10 mM NaCl 1 mM EDTA, 1 mM EGTA, 10 mM NaF, 0.1 mM Na_3VO_4, supplemented with 0.2% NP-40 Surfact-Amps™ and 5 mM broad-spectrum serine and cysteine protease inhibitors (cOmplete Mini™ and "Pefabloc®)]. Samples were vortexed at maximum speed for 15 sec and incubated on ice for 15 min. Next, samples were vortexed again at maximum speed for 10 sec and then centrifuged at 16000×g for 10 min, at 4º C. Supernatants (cytosolic fraction) were collected and immediately stored at -20º C until future use. Then, pellets were resuspended in 50 µL nuclear extraction buffer [25 mM HEPES pH7.5, 500 mM NaCl, 1 mM DTT, 10 mM NaF, 10% glycerol, supplemented with 0.2% NP-40 Surfact-Amps™, 5 mM $MgCl_2$, and 5 mM broad-spectrum serine and cysteine protease inhibitors (cOmplete Mini™ and Pefabloc®)], vortexed at maximum speed for 15 sec and sonicated (Branson Digital Sonifier, Emerson Electric Co., MO, USA) for 10 min at 15º C. Subsequently, samples were homogenized by passage through a 25-gauge needle, and were sonicated again for 5 min at 15º C. Finally, samples were centrifuged at 16000×g for 10 min at 4º C and the supernatant (nuclear fraction) was collected and stored at -20º C until use.

III.5.1.5. Total protein extracts from liver tissue

Liver samples (20-35 mg) were homogenized in 900 µL of extraction buffer (0.66 M Tris-HCl pH 7.5, 1 mM EGTA, 1 mM Na_3VO_4, 1 mM NaF and the protease inhibitor cOmplete Mini™) using a MACS™ Dissociator (MACS Miltenyi Biotec, Bergisch Gladbach, Germany). After addition 10 µL of 10% NP-40 Surfact-Amps™ the homogenized samples were sonicated for 5 min at 15º C,

and then centrifuged at 16000×g for 40 min at 4º C. The resulting supernatants (total protein extracts) were collected and stored at -20º C.

III.5.2. Bicinchoninic acid (BCA) assay

The BCA assay was used to quantify protein content in the extracts. This method combines the reduction of Cu^{2+} ions from Cu_2SO_4 to Cu^{1+} by protein in an alkaline medium (the well-known Biuret reaction) with the highly sensitive colorimetric detection of Cu^{1+}, based in the chelation of two molecules of BCA with one Cu^{1+} ion. The purple-colored reaction product of this assay exhibits a strong absorbance at 562 nm, which is approximately linear with increasing protein concentrations over a broad working range (0.02-2 mg/mL) (Smith et al. 1985).

This assay was performed following the manufacturer's instructions (Pierce™ BCA Protein Assay Kit, Thermo Fisher Scientific). A standard protein curve was prepared by serial dilutions of BSA (1-0.03125 mg/mL) in the same extraction buffer as the samples to minimize the background absorbance. 20 µL of diluted sample (1:20) or standard were used per well in a 96-well plate placed on ice, and immediately after 200 µL/well of working mixture reagent was added to each well. This working mixture was always prepared fresh before use, mixing 50 parts of Pierce™ BCA reagent A with 1 part of reagent B. Both the samples and standard curve were assayed in duplicate. Next, the plate was incubated (protected from light) at 37º C for 30 min with gentle rocking. Finally, absorbance was measured at 570 nm employing a Multiskan™ Ascent 354 microplate spectrophotometer (Thermo Labsystems, Thermo Fisher Scientific).

III.5.3. Sodium dodecyl sulfate (SDS)-polyacrylamide gel electrophoresis (PAGE) and Western Blotting (WB)

Both protocols were performed following standard methods.

III.5.3.1. SDS-PAGE

SDS-PAGE was performed using the Mini-PROTEAN® Tetra Cell System (Bio-Rad Laboratories, Hercules, CA, USA). Polyacrylamide gels were made using a mixture of acrylamide/bis-acrylamide solution (37.5:1) (Ultrapure ProtoGel®

supplied by National Diagnostics, Hessle, UK). Resolving gels were prepared with different percentage of polyacrylamide (6-15%) in 0.375 M Tris-HCl pH 8.8 and 0.1% SDS, whereas stacking gels were always prepared with 3.75% polyacrylamide in 0.125 M Tris-HCl pH 6.8 and 0.1% SDS. The polymerization reaction was catalyzed by 0.1% ammonium persulfate (APS) (SERVA, Heidelberg, Germany) and N,N,N′,N′-tetramethylethylenediamine (TEMED, Sigma-Aldrich Chemicals). Extracts with equal total protein amounts were loaded; previously prepared by adding Laemmli sample buffer (0.5 mM Tris-HCl pH6.8, 25% glycerol v/v, 10% SDS, 0.5% β-mercaptoethanol and 0.5% bromophenol blue) and boiled at 100º C for 5 min in order to achieve protein denaturation. To determine the molecular weight of the polypeptides, a molecular weight marker (EZ-Run™ Pre-Stained Rec Protein Ladder, Fisher Bioreagents™, Thermo Fisher Scientific) was also loaded. Electrophoresis was performed in a buffer tank with running buffer (25 mM Tris pH 8.3, 0.1% SDS and 192 mM glycine) at constant voltage of 120 V.

III.5.3.2. Protein transfer to nitrocellulose membrane

SDS-PAGE-resolved proteins were transferred from the resolving polyacrylamide gel to a 0.45 µm nitrocellulose blotting membrane (Amersham™ Protran™ NC, GE Healhcare Life Science, Little Chalfont, UK), using a Mini Trans-Blot® Cell (Bio-Rad Laboratories). The transfer was performed at 4º C for 1 h (proteins with molecular weight up to 100 kDa) or 1.5 h (proteins over 100 kDa) at a constant amperage of 0.4 A, in transfer buffer (25 mM Tris pH 8.3, 192 mM glycine and 20% methanol).

III.5.3.3. Ponceau and antibodies staining

In order to verify the transfer efficiency and quality, the nitrocellulose membrane was soaked in a 0.1% Ponceau/5% acetic acid solution (Sigma-Aldrich Chemicals) for 1 min, which stains proteins. Ponceau staining was removed with Tris-buffered saline-Tween (TBS-T, 20 mM Tris-HCl pH 7.2, 150 mM NaCl and 0.1% Tween-20 v/v) before incubating the membrane in fresh blocking solution (5% fat-free milk powder or BSA, diluted in TBS-T) with continuous gentle shaking, for 1 h, at RT. Once the membrane was blocked, it was incubated with the primary antibody, prepared in blocking solution supplemented with 0.02% sodium azide (Sigma-Aldrich Chemicals) for 3 h, at

RT or overnight at 4º C with continuous gentle shaking. Subsequently, the membrane was washed four times in TBS-T for 10 min, at RT and with vigorous shaking, incubated with a secondary antibody in fresh blocking solution at RT, for 1 h, and washed again. The antibodies used are listed in Table III.4.

PRIMARY ANTIBODIES				
PROTEIN	**SOURCE/CLASS**	**MW (kDa)**	**DILUTION**	**COMPANY**
β-actin	Rabbit polyclonal	40	1:1000	Sigma-Aldrich
α-SMA	Rabbit polyclonal	42	1:1000	Santa Cruz Biotechnology
α-Tubulin	Mouse monoclonal	50	1:1200	Sigma-Aldrich
Caspase-1	Rabbit polyclonal	20-45	1:1000	Cell Signaling Technology
CHOP	Mouse monoclonal	31	1:1000	Abcam
CI subunit NDI	Rabbit polyclonal	36	1:600	Abcam
CIV subunit II	Mouse monoclonal	26	1:1000	Thermo Fisher Scientific
CV subunit β	Mouse monoclonal	57	1:1000	Thermo Fisher Scientific
F4/80	Mouse monoclonal	160	1:500	Santa Cruz Biotechnology
GAPDH	Rabbit polyclonal	36	1:15000	Sigma-Aldrich
GRP78	Rabbit polyclonal	75	1:1000	Abcam
IκB-α	Rabbit polyclonal	35	1:1000	Santa Cruz Biotechnology
Keap1	Rabbit polyclonal	70	1:1000	Proteintech
LC3	Rabbit polyclonal	16-18	1:1000	Sigma-Aldrich
NBR1	Rabbit polyclonal	140	1:1000	Proteintech
NF-κB	Mouse monoclonal	65	1:500	Thermo Fisher Scientific
NLRP3	Rabbit polyclonal	110	1:1000	Cell Signaling
Nrf2	Rabbit polyclonal	57	1:1000	San Cruz Biotechnology
Nucleolin	Rabbit polyclonal	105	1:2500	Sigma-Aldrich

Porin	Rabbit polyclonal	30	1:1000	Abcam
PPAR-γ	Mouse monoclonal	58	1:1000	Thermo Fisher Scientific
SQSTM1	Mouse monoclonal	65	1:1000	Santa Cruz Biotechnology
SECONDARY ANTIBODIES				
ANTIBODY		**LABELING**	**DILUTION**	**COMPANY**
Goat Anti-Mouse IgG (H+L) Antibody		HRP	1:2000	Thermo Fisher Scientific
Goat Anti-Rabbit IgG Antibody		HRP	1:5000	Vector Laboratories

Table III.4. List of primary and secondary antibodies employed in WB assays.

III.5.3.4. Chemiluminescence detection

Immunolabeling was detected by enhanced chemiluminescence, employing Luminata™ Crescendo Western HRP substrate (Merck Millipore, Billerica, MA, USA), Amersham™ ECL™ Start Western Blotting Detection Reagent (GE Healthcare Life Science) or SuperSignal™ West Femto Maximum Sensitivity Substrate (Thermo Fisher Scientific), following manufacturer's instructions. This detection method is based in an oxidation reaction of luminol catalyzed by the enzyme horseradish peroxidase (HRP)-conjugated to the secondary antibody, in the presence of hydrogen peroxide, and giving rise to 3-aminophthalate that emits light at 425 nm (Whitehead et al. 1979). Immunolabeling was visualized with a digital luminescent image analyzer, Fujifilm LAS-3000 Imager (Fujifilm, Tokio, Japan). Densitometric analyses were performed using Multi Gauge V3.0 software (Fujifilm, Tokio, Japan). The protein expression was normalized versus that of expression of the β-actin, α-Tubulin, GAPDH, porin or nucleolin (employed as loading controls).

III.5.3.5. Stripping for reprobing

Stripping, a method that removes antibodies from a nitrocellulose membrane, enables reutilization of the membrane and its incubation with other antibodies. The stripping process was performed in two different ways:

1) Incubation with a stripping solution (62.5 mM Tris-HCl pH 6.7, 100 mM β-mercaptoethanol and 2% SDS), at 56º C for 30 min with vigorous shaking. After that, the membrane was washed with TBS-T three times, for 10 min at RT.
2) Incubation with 0.5 M glycine pH 2.5 for 10 min at RT, and with vigorous shaking. Subsequently, the membrane was washed twice with TBS-T for 10 min, at RT.

Regardless of the protocol used, the membrane was blocked with the blocking solution again before incubating it with the antibodies, following the protocol described in *III.5.3.3. Ponceau and antibodies staining.*

III.5.4. Enzyme-linked immunosorbent assay (ELISA)

IL-1β secretion in the cell culture media was measured by ELISA, using a Human IL-β ELISA Set (Diaclone, Besançon Cedex, France). Following the manufacturer's instructions, 96-well high bind microplates (Corning Inc., Corning, NY, USA) were coated with Capture Antibody in PBS pH 7.4 at 4º C overnight. Wells were washed twice with washing solution (PBS pH 7.4, 0.05% Tween-20), and then non-specific binding sites were blocked with PBS containing 1% BSA for 2 h and washed again three times with washing solution. The standard (serial dilutions of a recombinant human IL-1β) and undiluted supernatants were added to wells in duplicate, besides the diluted biotinylated anti-IL-1β (which was added to all wells), and incubated at RT for 4 h. After washing twice with a washing solution, streptavidin-HRP was added and incubated for 30 min (1:6000 in HRP dilution buffer PBS, 1% BSA and 0.1% Tween-20); this molecule binds to biotin and the conjugated HRP provides enzyme activity for detection using an appropriate chromogen. Following a washing step to remove the excess HRP conjugate, ELISA was developed by the addition of 3,3',5,5'-tetramethylbenzidine solution (TMB, a chromogenic substrate) in each well for 20 min, and the reaction was stopped with 1 M H_2SO_4. Absorbance was measured at 450 nm immediately after adding 1 M H_2SO_4 with an Infinite® 200 PRO series spectrophotometer (TECAN Trading AG, Männendorf, Switzerland). In order to obtain accurate values of IL-1β, the presence of the colored product was also detected at 620 nm and this background absorbance was subtracted from that obtained at 450 nm.

III.6. GENE EXPRESSION ANALYSIS

III.6.1. RNA expression

III.6.1.1. RNA extraction from cell cultures

RNA isolation and purification from cell cultures was performed using the RNeasy® Mini Kit supplied by Qiagen (Hilden, Germany), according to manufacturer's instructions. Briefly, cell pellet was resuspended in 350 µL lysis buffer and was homogenized by passage through a 25-gauge needle. Next, 350 µL of 70% ethanol were added and the solution was transferred to a column which retains RNA. After washing three times, RNA was eluted in 30 µL RNase-free water. The purity and concentration of the RNA were determined spectrophotometrically, using a NanoDrop™ ND-1000 spectrophotometer (Thermo Scientific).

III.6.1.2. RNA extraction from liver tissues

RNA extraction from liver tissues was performed using TriPure Isolation Reagent (Roche Life Science). Liver samples (30-40 mg) were homogenized by MACS™ Dissociator (MACS Miltenyi Biotec) in 750 µL TriPure and samples were then centrifuged at 16000×g for 15 min, at 4º C. Afterwards, 150 µL chloroform was added to the supernatant, in order to separate the different phases (aqueous, interphase and organic), and subsequently the samples were vigorously vortexed, incubated on ice for 15 min and centrifuged at 16000xg for 15 min, at 4º C. The colorless aqueous upper phase, which contains RNA, was transferred to new tubes and RNA was precipitated by incubation with 500 µL isopropanol for 1 h or overnight at -20º C. Precipitated RNA was pelleted by centrifugation at 16000×g for 20 min at 4º C, washed with 1 mL 70% ethanol and pelleted again at 16000×g for 15 min at 4º C. Finally, RNA pellet was air-dried at RT and was resuspended in 50 µL RNase-free water. The purity and concentration of the RNA was determined using a NanoDrop™ ND-1000 spectrophotometer (Thermo Scientific).

III.6.1.3. Complementary DNA (cDNA) synthesis by reverse transcription

cDNA was synthetized by reverse transcription (RT), employing the PrimeScript™ RT Reagent Kit (Perfect Real Time) (TaKaRa Bio Inc., Otsu, Japan). In accordance with the manufacturer's protocol, the reaction was performed using 2 µg RNA and 1X PrimeScript Buffer, 1 µL PrimeScript RT Enzyme Mix I, 50 pmol Random 6-mers and 25 pmol Oligo dT Primer (20 µL final volume). The reaction was carried out in a GeneAmp® PCR System 2400 (PerkinElmer Inc, Waltham, MA, USA) under the following conditions: 37º C for 15 min, 85º C for 5 sec and 4º C for infinity.

III.6.1.4. Quantitative RT-PCR (qRT-PCR)

qRT-PCR was performed with SYBR® Premix Ex Taq™ (Tli RNaseH Plus) (TaKaRa Bio Inc.), containing TaKaRa Ex Taq HS, dNTP mixture, Mg^{2+}, Tli RNase H and SYBR Green I (DNA intercalator that emits fluorescence only when bound to dsDNA, and thus, detection of its fluorescent signal allows quantification of the amplification products). The reaction was performed mixing 1 µL cDNA, 5 µL SYBR® Premix Ex Taq™, 2 µM primers (forward and reverse) and RNase-free water (10 µL final volume). qRT-PCR were carried out in a Lightcycler® 96 Real-Time PCR System (Roche Life Science), following this protocol: 95º C for 30 sec; 95º C for 5 sec, 60º C for 20 sec (50 cycles); 95º C for 1 sec; 65º C for 15 sec; 95º C for 1 sec and 40º C for 30 sec. All experiments were performed in duplicate, together with a negative control (RNase-free water instead of cDNA).

The primer pairs for human or mouse genes used were synthetized by IDT® (Integrated DNA Technologies, Coralville, IA, USA) or Metabion (Planegg, Germany). Their sequences are shown in Table III.5 y III.6 (full gene names are shown in annex I). Before their use in qRT-PCR, primers were tested by performing melting curve analysis and standard electrophoresis on 2% agarose gel containing Goldview™ DNA Safe Stain (UVAT Bio C.B., Valencia, Spain) and using buffer TAE 1x (20 mM Tris pH 7.8, 0.5 mM EDTA and 10 mM sodium acetate).

HUMAN PCR PRIMER PAIRS		
GENE	FORWARD PRIMER (5'→3')	REVERSE PRIMER (5'→3')
ACTB	GGACTTCGAGCAAGAGATGG	CTGTACGCCAACACAGTGCT
ARG1	AGGGACAGCCACGAGGAGGG	AGTTTCTCAAGCAGACCAGCCTTT
CASP1	AGAAAGCCCACATAGAGAAGG	CTCCACATCACAGGAACAGG
CD86	GCACGGACTTGAACAACCAG	CCTTTGTAAATGGGCACGGC
COL1A1	AAGCTGGAAAACCTGGTCGT	AGCACCATCATTTCCACGAG
DDIT3	AGAACCAGGAAACGGAAACAGA	TCTCCTTCATGCGCTGCTTT
GRP78	CTGGGTACATTTGATCTGACTGG	GCATCTTGGTGGCTTTCCAGCCAT
IL10	CCTGCCTAACATGCTTCGAGA	CACATGCGCCTTGATGTCTG
IL18	ATCGCTTCCTCTCGCAAC	CCAGGTTTTCATCATCTTCAGC
IL1B	TTCGACACATGGGATAACGAGG	TTTTTGCTGTGAGTCCCGGAG
IL33	GTGGAAGAACACAGCAAGCA	TCATAAGGCCAGAGCGGAG
IL6	CTCAATATTAGAGTCTCAACCCCCA	GAGAAGGCAACTGGACCGAA
MMP2	CAAGTTCCCCGGCGATGTC	TTCTGGTCAAGGTCACCTGTC
MMP9	GGGCCGCTCCTACTCTGCCT	TCGAGTCAGCTCGGGTCGGG
MRC1	CTTTGGACGGATGGACGAGG	CAAGGAAGGGTCGGATCGTG
NBR1	AGTAGATCCTTTCCCCTCCG	TGCTCAGTCACTTCACCAAG
NLRP3	CTTCTCTGATGAGGCCCAAG	GCAGCAAACTGGAAAGGAAG
NOS2	ATAATGGACCCCAGGCAAG	TCAGCAAGCAGCAGAATGAG
PDGFRB	CCATCAGCAGCAAGGACACCA	CCCGAGCAGGTCAGAACGAA
SERPINE1	CGCTGTCAAGAAGACCCACA	ACCTGCTGAAACACCCTCAC
SQSTM1	GGTTGCCTTTTCCAGTGACG	TCGCAGACGCTACACAAGTC
TGFB1	CTTCAGCTCCACAGAGAAGAACTG	CACGATCATGTTGGACAACTGCTC
TIMP1	AATTCCGACCTCGTCATCAGG	ATCCCCTAAGGCTTGGAACC
TNF	AGCCGCATCGCCGTCTCCTA	CAGCGCTGAGTCGGTCACCC
XBP1	CTGAGTCCGCAGCAGGTG	AACAGGATATCAGACTCTGAATCT

Table III.5. Human primer pairs used in qRT-PCR.

MURINE PCR PRIMER PAIRS		
GENE	FORWARD PRIMER (5'→3')	REVERSE PRIMER (5'→3')
Acta2	GTCCCAGACATCAGGGAGTAA	TCGGATACTTCAGCGTCAGGA
Actb	GCCAACCGTGAAAAGATGACC	GAGGCATACAGGGACAGCAC
Adgre1	TGACTCACCTTGTGGTCCTAA	CTTCCCAGAATCCAGTCTTTCC
Arg1	GTGGGGAAAGCCAATGAAGAG	TCAGGAGAAAGGACACAGGTTG
Casp1	ACAAGGCACGGGACCTATG	TCCCAGTCAGTCCTGGAAATG
Cd163	GACACACGGAGCCATCAAAATC	TCACAGCCACAACAAAGAAACCT
Cd86	GCACGGACTTGAACAACCAG	CCTTTGTAAATGGGCACGGC
Col1a1	GCTCCTCTTAGGGGCCACT	CCACGTCTCACCATTGGGG
Il10	TGGACAACATACTGCTAACCGA	CTGGGGCATCACTTCTACCA
Il1b	GAAATGCCACCTTTTGACAGTG	CTGGATGCTCTCATCAGGACA
Il33	TGCAGGAAAGTACAGCATTCA	CGGGGAAATCTTGGAGTTGG
Mmp2	CAAGTTCCCCGGCGATGTC	TTCTGGTCAAGGTCACCTGTC
Mrc1	TGTGGAGCAGATGGAAGGTC	TGTCGTAGTCAGTGGTGGTTC
Nlrp3	ATTACCCGCCCGAGAAAGG	CATGAGTGTGGCTAGATCCAAG
Nos2	CGCTTGGGTCTTGTTCACTC	GGTCATCTTGTATTGTTGGGCTG
Pparg	GCCCTTTGGTGACTTTATGG	CAGCAGGTTGTCTTGGATGT
Tgfb1	GCGGACTACTATGCTAAAGAGGG	TCAAAAGACAGCCACTCAGG
Timp1	CTTGGTTCCCTGGCGTACTC	ACCTGATCCGTCCACAAACAG
Tnf	CCCTCACACTCAGATCATCTTCT	GCTACGACGTGGGCTACA
Vim	GCTCCTACGATTCACAGCCA	CGTGTGGACGTGGTCACATA

Table III.6. Murine primer pairs used in qRT-PCR.

qRT-PCR data were analyzed using the *comparative C_T method* (Valasek and Repa 2005; Schmittgen et al. 2008) obtaining the relative gene expression of the gene of interest. This method of presenting quantitative gene expression consists in this equation: Fold Change= $2^{-\Delta(\Delta CT)}$, where ΔCT=CT (target gene) - CT (housekeeping gene), and Δ(ΔCT) = ΔCT (treated) - ΔCT (control). *ACTB/Actb* (β-actin) was used as a housekeeping gene.

III.6.1.5. PrimePCR™ assay

With the purpose of analyzing extensively the complex pathway regulated by inflammasomes, we decided to use a PrimePCR™ Pathways Assay (Bio-Rad Laboratories), specifically the *Human Inflammasomes (SAB Target List) H96 plate,* which was customized to our needs. This PrimePCR™ plate is a set of pre-validated and optimized qRT-PCR primers directly dried in wells for using with SYBR® Green. The *Human Inflammasomes plate* is useful to monitor the expression of 84 genes involved in the inflammasome function, protein complexes related to immunity and NOD-like receptor signaling, as well as genes implicated in downstream signaling and inhibition of inflammasomes function. After preliminary tests, the number of genes analyzed was reduced to 25 (those showing relevant changes in their expression) (Figure III.1).

Gene expression in LX-2 cells and U937-derived macrophages treated with EFV or vehicle for 24 h was assessed by this method. RNA extraction was performed according to the protocol detailed in *III.6.1.1. RNA extraction from mammalian cell cultures*. cDNA was synthetized using iScript™ cDNA Synthesis Kit (Bio-Rad Laboratories), and following its instructions 2 µg RNA, 4 µL 5x iScript reaction mix, 1 µL iScript reverse transcriptase, and RNase-free water up to 20 µL of final volume were mixed. Afterwards, cDNA was diluted with RNase-free water up to 100 µL just before preparing the reaction mix, which contains 2x SsOAdvanced™ universal SYBR® Green Supermix (Bio-Rad Laboratories), diluted cDNA and RNase-free water, and subsequently 20 µL of this mixture were added to each well.

All the reactions were performed in a CFX96 Touch™ Real-Time PCR Detection System (Bio-Rad Laboratories). The thermal cycling protocol was 95º C for 2 min, 95º C for 5 sec, 60º C for 30 sec (40 cycles) and 65-95º C (0.5º C increments) for 5 sec/step. Data were analyzed with Bio-rad CFX Manager 3.1 software (Bio-Rad Laboratories).

These PrimePCR™ assays were performed in Prof. Andrea Cossarizza's laboratory, at University of Modena and Reggio Emilia (Modena, Italy), under the supervision of Prof. Marcello Pinti and Dr. Milena Nasi.

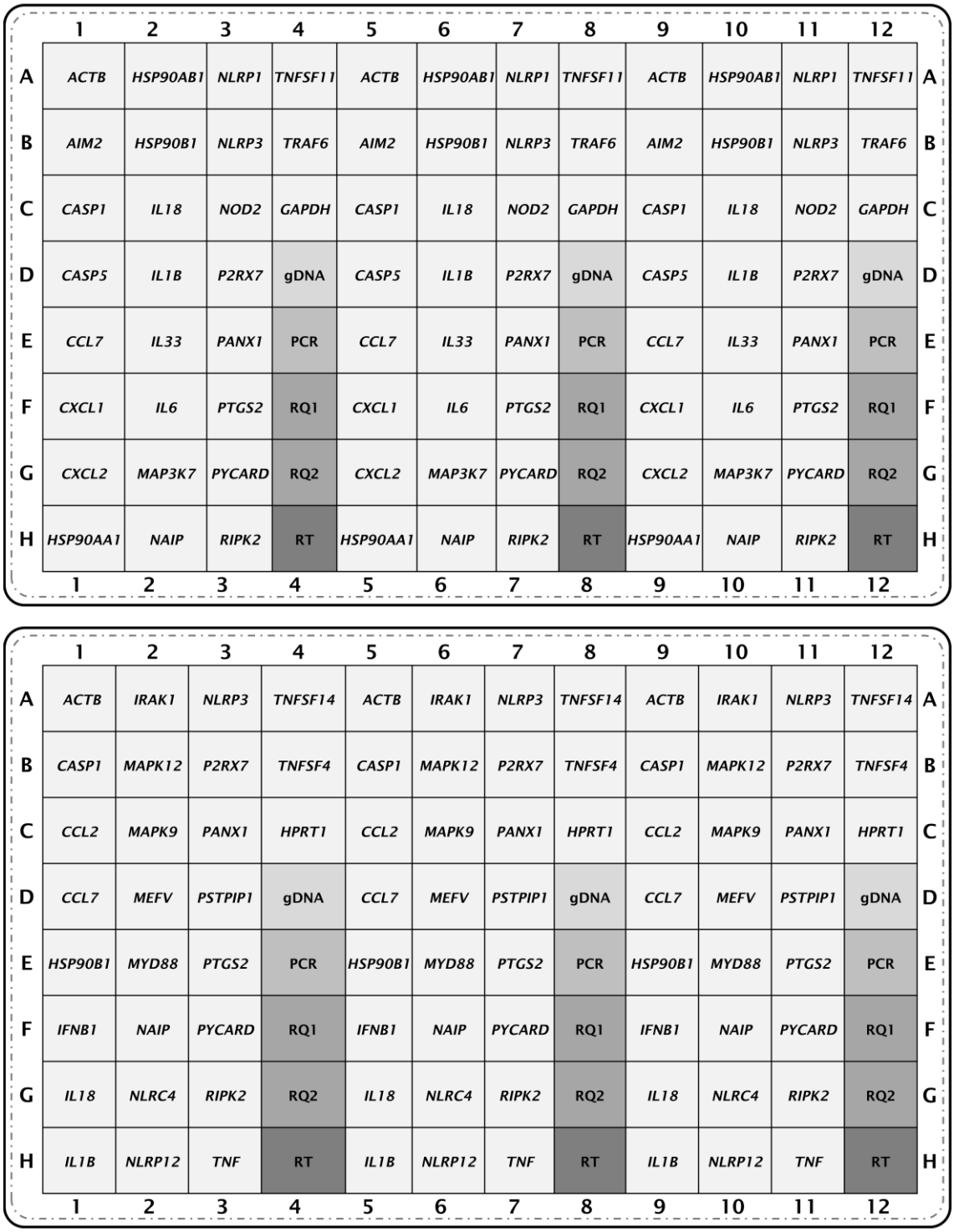

	1	2	3	4	5	6	7	8	9	10	11	12	
A	*ACTB*	*HSP90AB1*	*NLRP1*	*TNFSF11*	*ACTB*	*HSP90AB1*	*NLRP1*	*TNFSF11*	*ACTB*	*HSP90AB1*	*NLRP1*	*TNFSF11*	A
B	*AIM2*	*HSP90B1*	*NLRP3*	*TRAF6*	*AIM2*	*HSP90B1*	*NLRP3*	*TRAF6*	*AIM2*	*HSP90B1*	*NLRP3*	*TRAF6*	B
C	*CASP1*	*IL18*	*NOD2*	*GAPDH*	*CASP1*	*IL18*	*NOD2*	*GAPDH*	*CASP1*	*IL18*	*NOD2*	*GAPDH*	C
D	*CASP5*	*IL1B*	*P2RX7*	gDNA	*CASP5*	*IL1B*	*P2RX7*	gDNA	*CASP5*	*IL1B*	*P2RX7*	gDNA	D
E	*CCL7*	*IL33*	*PANX1*	PCR	*CCL7*	*IL33*	*PANX1*	PCR	*CCL7*	*IL33*	*PANX1*	PCR	E
F	*CXCL1*	*IL6*	*PTGS2*	RQ1	*CXCL1*	*IL6*	*PTGS2*	RQ1	*CXCL1*	*IL6*	*PTGS2*	RQ1	F
G	*CXCL2*	*MAP3K7*	*PYCARD*	RQ2	*CXCL2*	*MAP3K7*	*PYCARD*	RQ2	*CXCL2*	*MAP3K7*	*PYCARD*	RQ2	G
H	*HSP90AA1*	*NAIP*	*RIPK2*	RT	*HSP90AA1*	*NAIP*	*RIPK2*	RT	*HSP90AA1*	*NAIP*	*RIPK2*	RT	H
	1	2	3	4	5	6	7	8	9	10	11	12	

	1	2	3	4	5	6	7	8	9	10	11	12	
A	*ACTB*	*IRAK1*	*NLRP3*	*TNFSF14*	*ACTB*	*IRAK1*	*NLRP3*	*TNFSF14*	*ACTB*	*IRAK1*	*NLRP3*	*TNFSF14*	A
B	*CASP1*	*MAPK12*	*P2RX7*	*TNFSF4*	*CASP1*	*MAPK12*	*P2RX7*	*TNFSF4*	*CASP1*	*MAPK12*	*P2RX7*	*TNFSF4*	B
C	*CCL2*	*MAPK9*	*PANX1*	*HPRT1*	*CCL2*	*MAPK9*	*PANX1*	*HPRT1*	*CCL2*	*MAPK9*	*PANX1*	*HPRT1*	C
D	*CCL7*	*MEFV*	*PSTPIP1*	gDNA	*CCL7*	*MEFV*	*PSTPIP1*	gDNA	*CCL7*	*MEFV*	*PSTPIP1*	gDNA	D
E	*HSP90B1*	*MYD88*	*PTGS2*	PCR	*HSP90B1*	*MYD88*	*PTGS2*	PCR	*HSP90B1*	*MYD88*	*PTGS2*	PCR	E
F	*IFNB1*	*NAIP*	*PYCARD*	RQ1	*IFNB1*	*NAIP*	*PYCARD*	RQ1	*IFNB1*	*NAIP*	*PYCARD*	RQ1	F
G	*IL18*	*NLRC4*	*RIPK2*	RQ2	*IL18*	*NLRC4*	*RIPK2*	RQ2	*IL18*	*NLRC4*	*RIPK2*	RQ2	G
H	*IL1B*	*NLRP12*	*TNF*	RT	*IL1B*	*NLRP12*	*TNF*	RT	*IL1B*	*NLRP12*	*TNF*	RT	H
	1	2	3	4	5	6	7	8	9	10	11	12	

Figure III.1. Layout of the customized Human Inflammasomes (SAB Target List) H96 plate for LX-2 cells (upper panel) and U937-derived macrophages (lower panel). Two housekeeping genes (*ACTB* and *GAPDH* in LX-2 cells; *ACTB* and *HPRT1* in macrophages) and five control assays (gDNA: genomic DNA contamination; PCR: general PCR performance; RQ1 and RQ2: RNA Quality; and RT: reverse transcription) were also included in each plate. The full names of the genes are shown in annex I.

III.6.2. Chromatin immunoprecipitation (ChIP) assay

Hep3B cells treated with EFV or vehicle for 24 h were cross-linked with 1% formaldehyde at RT for 10 min followed by 0.125% glycine for 2 min. Subsequently, cells were washed three times with ice-cold PBS, and centrifuged for 5 min at 5000×g. Cells were then resuspended in 300 µL of SDS sonication buffer [1% SDS, 5 mM EDTA, 50 mM Tris-HCl pH 8.0 and 5mM broad-spectrum protease inhibitors (cOmplete Mini™)] and sonicated three times for 20 sec, followed by a centrifugation at 16000×g for 10 min at 4° C. Supernatants were collected and the immunoprecipitation was performed overnight at 4° C with anti-Nrf2 (Santa Cruz Biotechnology), anti-NF-κB (p65) (Thermo Fisher Scientific), anti-DDIT3 (Abcam) antibodies, or with a control IgG antibody (Thermo Fisher Scientific). After immunoprecipitation, 60 µL protein A-Sepharose beads (GE Healthcare Life Science) were added to the supernatants and incubated overnight at 4° C. Precipitates were washed sequentially, once with low-salt wash buffer (1% Triton™ X-100, 2 mM EDTA, 20 mM Tris-HCl pH 8.0, 150 mM NaCl), twice with high-salt wash buffer (1% Triton™ X-100, 2 mM EDTA, 20 mM Tris-HCl pH 8.0, 500 mM NaCl) and once with LiCl wash buffer (0.25 mM LiCl, 1% NP-40, 0.1% Tween®-20, 1 mM EDTA, 10 mM Tris-HCl pH 8.0) for 5 min each. Precipitates were then washed twice with TE buffer (10 mM Tris-HCl pH 8.0, 1 mM EDTA) and extracted twice with elution buffer (1% SDS, 0.1 M $NaHCO_3$). Eluates were pooled and heated at 65° C for 16 h to reverse the formaldehyde cross-linking in the presence of 0.25 M NaCl. DNA fragments were purified with a PureLink™ Quick PCR purification kit (Thermo Fisher Scientific). PCR was performed using TaKaRa Taq™ (Takara) with specific primers to amplify (35 cycles) the binding site of Nrf2 (Jain et al. 2010), NF-κB or CHOP/DDIT3 (Table III.7) on the SQSTM1 promoter. PCR products were separated by electrophoresis in 2% agarose gel.

TRANSCRIPTION FACTOR	SEQUENCE DIRECTION	SEQUENCES (5'→3')	AMP.SIZE (bp)
NF-κB	sense	ATTACGACAGCGGTCATGGG'	116
	antisense	CTCCCGGAGGGTAAACAAGG	
Nrf2	sense	CTCTCAGGCGCCTGGGCTGCTGAG	152
	antisense	CGGCGGTGGAGAGTGGAAAATGCC	
CHOP	sense	5'-CACCCACACATCACCTTCGC-3'	238
	antisense	5'-ACCAGAGTAACCTGTCCGCC-3'	

Table III.7. Sequences of primers pairs employed for PCR and their respective amplicon sizes.

III.7. CELL VIABILITY ASSAY

Cell viability and proliferation was detected using a MTT based-colorimetric assay (Cell Proliferation Kit I –MTT–, Roche Life Sciences). This assay is based on the reduction of the yellow tetrazolium salt MTT [3-(4,5-dimethylthiazol-2-yl)-2,5-diphenyl tetrazolium bromide] to purple formazan (Mosmann 1983), which takes place only by active mitochondrial reductases, such as NADH and NADPH (Figure III.2), and hence, MTT reduction is related to the number of viable and metabolically active cells. The purple formazan crystals are solubilized, usually with an organic solvent or a SDS solution, and the absorbance of the resulting colored solution is finally quantified spectrophotometrically at 570 nm.

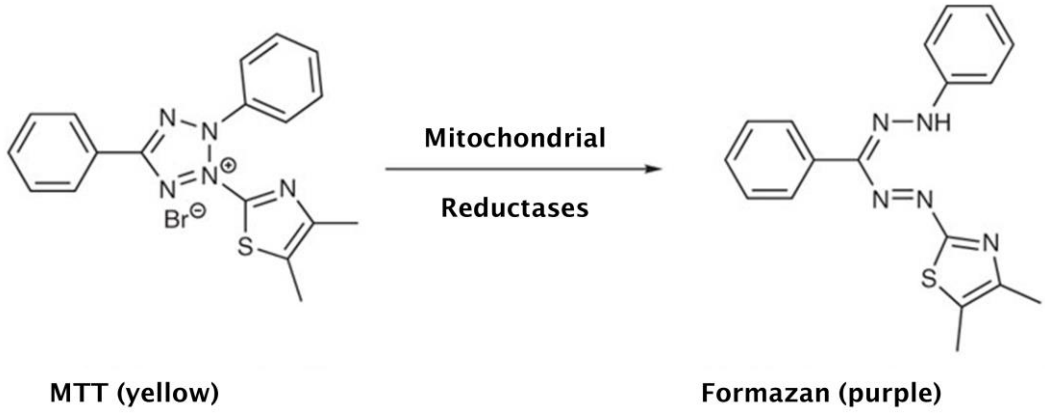

Figure III.2. Metabolization of MTT to a formazan salt by viable cells.

To perform the MTT assay, cells were seeded in 96-well cell culture microplates. MTT reagent was added (20 µL/well) to the cells for the last 4 h of the treatment. Medium was then discarded and 100 µL/well DMSO were added to each well, and the plate was incubated at 37º C for 5 min, in darkness. Following incubation, absorbance was measured at 570 nm and 690 nm employing a Multiskan™ Ascent 354 microplate spectrophotometer. To achieve accurate results, the absorbance measured at 690 nm (background absorbance) was subtracted from the 570 nm absorbance value.

III.8. MITOCHONDRIAL RESPIRATION MEASUREMENT

Cellular O_2 consumption was measured to verify the proper generation of rho^0 Hep3B cells, employing a Clark-type electrode (Oxytherm System, Hansatech Instruments, Norfolk, UK). The Clark electrode, developed by Prof. Lewis C. Clark (Clark et al. 1953), consists of a silver anode, a platinum cathode, and an electrolyte (3 M KCl), where both anode and cathode are immersed. In addition, a thin teflon membrane is placed onto both electrodes, which is permeable to O_2 and allows this molecule to reach the platinum cathode, where it is electrolytically reduced (Figure III.3). The reduction of O_2 generates a current of electrons between both electrodes, producing a potential difference, which is simultaneously recorded by the software connected to the electrode. The Oxytherm System is connected to an integral thermoelectric temperature control that provides measurements at constant temperature.

$$O_2 + 2e^- + 2H_2O \longrightarrow H_2O_2 + 2OH^-$$

Figure III.3. Chemical reaction taking place in Clark-type electrode: oxidation of atmospheric O_2.

The electrode was calibrated in air-saturated respiration buffer (HBSS) before performing each measurement: the atmospheric O_2 concentration was considered as maximal (200 µM O_2), and the electrode zero setting was achieved by adding excess of sodium dithionite (Panreac Química S.L.U.) to the respiration chamber.

The measurement of the O_2 consumption was performed in intact cells, for which cells were detached by trypsinization and counted using a hemocytometer (Neubauer Improved, Laboroptik Ltd., Lancing, UK)

immediately prior to the measurement. For each experiment, 3 million cells were resuspended in 1 mL respiration buffer (HBSS) and taken into the respiration chamber, where the cellular suspension was constantly stirred and maintained at 37º C. The mitochondrial origin of O_2 consumption was confirmed by addition of 1 mM KCN, which is an OxPhos specific inhibitor, acting on mitochondrial cytochrome *c* oxidase. Hep3B cells with functional mitochondrial were used as a control.

Data obtained with the Clark-type electrode were obtained and analyzed with the program O_2 View (Hansatech Instruments, Norfolk, UK).

III.9. CASPASE-1 ACTIVITY ASSAY

Caspase-1 activity was determined by a commercial colorimetric assay kit (Biovision Inc., Milpitas, CA, USA), in accordance with the manufacturer's instructions, with slight modifications. This assay is based on the ability of the active caspase-1 to cleave the labeled substrate YVAD-*p*NA, releasing the chromophore *p*-nitroanilide (*p*NA), which can be detected by spectrophotometry. Briefly, cell pellets were resuspended in chilled cell lysis buffer, in order to obtain protein lysates, whose concentration was determined with the BCA protein assay kit (see *III.5.2.*). Equal amounts of protein (400 µg) diluted in reaction buffer were added in a 96-well plate, in duplicate. Next, 200 µM YVAD-*p*NA were added to each sample and the plate was incubated protected from light, at 37º C for 3 h. Absorbance was measured at 405 nm in an Infinite® 200 PRO series spectrophotometer. Fold-increase in caspase-1 activity was determined by comparison with untreated control cells.

III.10. MYELOPEROXIDASE (MPO) ACTIVITY ASSAY

MPO is a pro-inflammatory enzyme mostly stored in the azurophilic granules of neutrophilic granulocytes, which plays a crucial role in intracellular pathogen killing, but that can provoke inflammatory damage when extracellularly released. MPO catalyzes generation of hypochlorous acid (HOCl) from hydrogen peroxide (H_2O_2) and Cl^- (Figure III.4), a reaction employed as an indirect estimation of neutrophil infiltration and intensity of the inflammatory response in tissues (Suzuki et al. 1983; Young et al. 1989; Pulli et al. 2013).

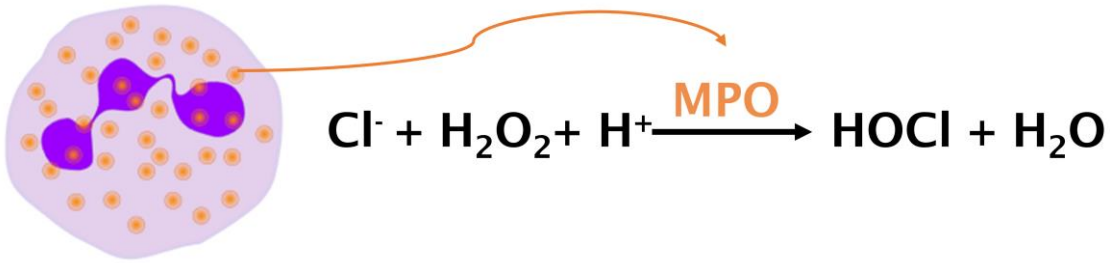

Figure III.4. Generation of hypochlorous acid from hydrogen peroxide by MPO.

Liver samples from C57BL/6 mice treated with EFV or vehicle for 24 h were prepared according to Souza et al. 2001. Upon thawing, samples (≈65 mg) were homogenized in disodium diphosphate buffer (0.02 M Na_2HPO_4, 0.1 M NaCl, 0.015 M Na_4EDTA, pH 4.7; 19 mL of buffer were added per 1 g of sample) using an UltraTurrax® T-45 Homogenizer (IKA®-Werke GmbH & Co. KG, Staufen, Germany), and centrifuged at 300×g for 10 min. Then, the supernatant was discarded and the pellet was subjected to hypotonic lysis in 0.2% NaCl buffer, followed (30 sec later) by addition of an equal volume of 1.6% NaCl and 5% glucose buffer, and vortexed. Both buffers were used in 1 g tissue: 150 mL buffer proportion. After a further centrifugation step, the pellet was resuspended in 1 mL hexadecyltrimethylammonium bromide (HTAB) buffer (0.05 M Na_2HPO_4, 0.5% HTAB, pH 5.4), followed by three free-thaw cycles using liquid nitrogen and a water bath at 37º C. Finally, samples were sonicated at 15º C for 10 min and kept on ice until their use.

MPO activity was assessed by a colorimetric assay. For this, 100 µL of the samples were added in a 96-well plate followed by 50 µL H_2O_2 and 50 µL TMB per well, and the plate was incubated at 37º C for 15 min. TMB is oxidized by the HOCl thus generating a blue product. The reaction was stopped by addition of 50 µL 1 M H_2SO_4 (color of reaction solution changes to yellow) and the absorbance was measured at 450 nm in an Infinite® 200 PRO series spectrophotometer. All activity assays were performed in duplicate. Fold-increase in MPO activity was determined by comparing the results obtained of the liver samples of treated mice with those treated with vehicle.

III.11. FLUORESCENCE MISCROSCOPE: STATIC CYTOMETRY

Static cytometry software connected to a fluorescence microscope is a useful tool for analyzing automatically a broad range of cellular parameters in living adherent cells. Unlike in flow cytometry, cells remain adherent, avoiding appearance of artefacts such as those generated by trypsin-induced cell damage or aggregate formation.

These experiments were performed using an Olympus IX81 fluorescence inverted microscope (Olympus, Hamburg, Germany) connected to the static cytometry software ScanR® v.2.03.2 (Olympus). In addition, the Cell^R software v.2.8 was employed to take images manually.

All treatments were performed in duplicate in 48- or 24-well plates, and 15-25 live-cell images per well were recorded and analyzed. For the last 30 min of treatments, cells were incubated with specific fluorescent probes at 37º C in darkness, and subsequently washed with HBSS; cells were maintained in this buffer during the process of life cell imaging. For all experiments, nuclei were stained with the fluorescent dye Hoechst 33342 (2.5 µM), with the purpose of focusing the cells and perform cell count. All fluorescent probes were purchased from Molecular Probes™ (Thermo Fisher Scientific), except for Hoechst® 33342, which was supplied by Sigma Aldrich Chemicals.

III.11.1. Cell survival/proliferation analysis

Cells were treated and allowed to proliferate exponentially for 24 h, and then counted according to Hoechst® 33342 fluorescence, which emits blue fluorescence when bound to dsDNA (Loken 1980). 25 images per well were analyzed. Detection filters used were 348/496 nm (excitation/emission).

III.11.2. Mitochondrial superoxide production

To assess mitochondrial superoxide production, cells were incubated with 5 µM MitoSOX™, which permeates selectively mitochondria (due to its positive charge) and is immediately oxidized by superoxide, but not by other ROS, producing a red fluorescence. Rotenone was used as positive control. Detection filters used were 510/590 nm (excitation/emission).

III.11.3. Mitochondrial membrane potential

Tetramethylrhodamine methyl ester, (TMRM 5 μM) was employed to assess $\Delta\Psi_m$, given it is only sequestered within active mitochondria. As a positive control, an uncoupler of OxPhos, carbonyl cyanide m-chlorophenyl hydrazine (CCCP, 10 μM) was employed. Detection filters used were 510/590 nm (excitation/emission).

III.11.4. Mitochondrial mass

Mitochondrial mass was analyzed by nonyl acridine orange (NAO, 1 μM) staining. Mitochondrial uptake of this probe is independent of fluctuations on $\Delta\Psi_m$, and it binds specifically to the cardiolipin of the inner mitochondrial membrane in viable mitochondria (Maftah et al. 1989). Detection filters used were 495/519 nm (excitation/emission).

III.11.5. Endoplasmic reticulum signal

To assess the ER signal, 2.5 μM ER-Tracker™ Red (BODIPY® TR Glibenclamide) were added to the cells. This fluorescent dye binds to the sulfonylurea receptors of ATP-sensitive K^+ channels, which are very numerous on ER. Thapsigargin was used as positive control. Detection filter employed were 510/590 nm (excitation/emission).

III.11.6. Lysosomal signal

Lysotracker® Red DND-99 (100 nM) was used to analyze the lysosomal status in the cells. This fluorochrome permeates selectively in acidic organelles (as lysosomes) in live cells. Detection filters employed were 510/590 nm (excitation/emission).

III.11.7. Intracellular lipid accumulation

The quantification of intracellular lipids was assessed by the hyprophobic probe Nile Red, which particularly binds to neutral lipid droplets (Greenspan and Fowler 1985). Following treatment, cells were washed with PBS, incubated with 0.5 μM Nile Red in HBSS for 10 min at RT, and then washed again. Detection filters used were 495/519 nm (excitation/emission).

III.12. CONFOCAL MICROSCOPY: IMMUNOCYTOCHEMISTRY

We used a Leica TCS SP8 X confocal laser-scanning unit with helium-neon and argon gas laser and connected to a Leica DMi8 inverted microscope (Leica Microsystems CMS GmbH, Mannheim, Germany), an equipment belonging to Unidad Central de Investigación en Medicina (UCIM, Universidad de Valencia, Valencia, Spain). Images were recorded at 40X magnification with a HC PL APO 40x/1.30 Oil PH3 CS2 objective, and were analyzed by the Colocalization Colormap script, a plugin in Fiji (an open source software for image analysis; Schindelin et al. 2012), in order to estimate the correlation index between the different dyes.

Cells were cultured on chambered borosilicate coverglasses (Nunc™ Lab-Tek™ Chambered Coverglass, Thermo Fisher Scientific), treated and stained by means of immunocytochemistry whose specifications are detailed below.

III.12.1. Lipophagy

LX-2 cells were fixed for 15 min with 100% methanol (VWR International, Radnor, PA, USA) at -20º C, and were washed with PBS twice for 5 min. Cells were then blocked for 1 h at RT with PBS containing 5% goat serum and 0.3% Triton™ X-100 (Sigma Aldrich Chemicals), and were incubated overnight at 4º C in PBS with 1% BSA and 0.3% Triton™ X-100 containing LC3 XP® Rabbit mAb antibody (1:400, Cell Signaling Technology®). After another washing step, samples were incubated for 1 h with a secondary antibody conjugated with Alexa Fluor® 488 Goat anti-rabbit (1:500, Molecular Probes™) at RT, protected from light, and 5 µM Hoechst® 33342 was added for the last 30 min. Finally, cells were incubated for 10 min in HBSS containing 0.5 µM Nile Red and, after washing them with PBS three times for 5 min each, cells were maintained in HBSS and images were recorded.

III.12.2. NLRP3 inflammasome expression

Hep3B cells were fixed with 4% formaldehyde at RT for 15 min, and were then washed three times with PBS. To block non-specific binding sites, cells were incubated with blocking buffer (1x PBS pH 7.4, 5% normal rabbit serum and 0.3% Triton™ X-100) at RT for 1 h, followed by an incubation overnight at 4º C with NLRP3 goat polyclonal antibody (1:200, Abcam) in antibody dilution buffer

(1x PBS pH 7.4, 1% BSA and 0.3% Triton™ X-100). Afterwards, cells were incubated with the secondary antibody Rabbit anti-goat IgG H&L Alexa Fluor® 488 (1:400, Molecular Probes™) at RT for 1 h in darkness, just after washing them with PBS three times. Nuclei were stained by adding 5 µM Hoechst® 33342 in the last 30 min. Finally, cells were washed three times with PBS and maintained in HBSS before taking the images.

III.12.3. p62 expression

p62 protein expression was analyzed by confocal microscope, following the fixation, blocking and staining instructions detailed in *III.12.2. NLRP3 inflammasome analysis*. The antibodies employed in this experiment were: SQSTM1 mouse monoclonal antibody (1:150, Santa Cruz Biotechnology) and Rabbit anti-mouse IgG H+L Alexa Fluor® 647 (1:400, Molecular Probes™).

III.13. IMMUNOHISTOCHEMISTRY (IHC)

IHC is a powerful method broadly employed in clinical anatomopathological diagnosis and research to detect the presence and localization of proteins in tissue sections (Coons and Kaplan 1950). Immunohistochemical staining is performed with antibodies that bind to the target protein. The antigen-antibody complex can be detected using a secondary antibody conjugated to an enzyme, which cleaves a chromogenic substrate to give rise to a colored precipitate at the location of the protein (Abcam-IHC Protocols 2015).

Fresh mouse liver samples were washed in saline solution and fixed using 10% neutral-buffered formalin solution (Histofix® Preservative, PanReac AppliChem GmbH, Darmstadt, Germany) for 48 h, in order to avoid enzymatic degradation of proteins and preserve tissue structure. After fixation, the tissue block was dehydrated (in graded alcohols and xylene), embedded in paraffin and subsequently samples were cut in a microtome at 5 µm of thickness.

III.13.1. Deparaffinization

Prior to staining, samples must be deparaffinized and rehydrated. To that end, slides were heated at 65º C for 30 min followed by rehydration steps (immersion in xylene for 30 min and in decreasing graded alcohols for 5 min each) and rinsed with PBS for 5 min.

III.13.2. Heat induced epitope retrieval (HIER)

In formalin-fixed tissue, a previous antigen retrieval step is required to perform immunohistochemical staining, due to the formation of methylene bonds during fixation that can cross-link proteins and mask the antigens. The antigen retrieval step breaks the aforementioned bonds, exposing the antigenic sites, and therefore allowing antibodies to bind (Abcam-IHC Protocols 2015).

For this, slides were heated using a microwave at 850 W for 5 min in sodium citrate buffer (10 mM sodium citrate, 0.05% Tween®-20, pH 6), allowed to cool at RT for 15 min and washed in PBS for 5 min.

III.13.3. Endogenous peroxidase blocking

Liver contains endogenous peroxidases, which would react with the chromogenic substrate solution, leading to high and non-specific background staining (false positives). To block this reaction, slides were incubated with peroxidase blocking solution (3% H_2O_2, 10% methanol, PBS) for 20 min at RT and washed twice in PBS-T for 5 min.

III.13.4. Immunohistochemical staining

All the incubations were carried out in a humidified chamber. In order to block non-specific binding sites, samples were incubated in PBS-T containing 6% BSA, 2% normal serum (from the species in which the secondary antibody was generated) and 0.1% Tween®-20 for 2 h. Slides were then incubated with the primary antibody prepared in diluted blocking solution (in PBS-T, 1:2) at 4º C overnight, and rinsed four times for 3 min before incubating with the secondary antibody in diluted blocking solution at RT for 1 h (Table III.8). A final washing step with PBS was performed (five times for 3 min).

PRIMARY ANTIBODY			
PROTEIN	**SOURCE/CLASS**	**DILUTION**	**COMPANY**
CD206	Rabbit polyclonal	1:100	Santa Cruz Biotechnology
F4/80	Rat monoclonal	1:150	AbD Serotec
SECONDARY ANTIBODY			
ANTIBODY	**LABELING**	**DILUTION**	**COMPANY**
Universal (Anti-Rabbit IgG/Mouse IgG) Antibody	Biotinylated	1:100	Vector Laboratories
Goat Anti-Rat IgG (H+L) Antibody	HRP	1:100	Thermo Fisher Scientific

Table III.8. Primary and secondary antibodies employed in IHC.

To achieve a stronger signal with biotinylated secondary antibody during the IHC, we used the Vectastain® Universal *Elite*® *ABC* Kit (Vector Laboratories, Burlingame, CA, USA). This method is based on the formation of avidin-biotinylated peroxidase complexes (*ABC*), which bind to the biotinylated secondary antibody through the unoccupied binding sites on avidin (Hsu et al. 1981). Following the manufacturer's instructions, slides were incubated in *ABC* solution for 45 min, and washed four times with PBS for 5 min.

The chromogenic substrate 3,3'-diaminobenzidine tetrahydrochloride (DAB Enhanced Liquid Substrate System, supplied by Sigma-Aldrich Chemicals) was employed to immunodetect target antigens. DAB is a precipitating substrate, which produces an intense brown stain by peroxidase action (enzyme present in secondary antibody and *ABC* complexes) (Figure III.5). DAB was prepared following the manufacturer's protocol, and then was added on the sample for 4-10 min (depend on the antibody) checking constantly the appearance of the brown stain. Once tissue is properly stained, the reaction was stopped immersing slides in water for 2 min, and washing three times with PBS for 10 min. The specificity of the immunostaining was verified by the absence of staining in analogous tissue sections in which the primary or secondary antibodies were excluded.

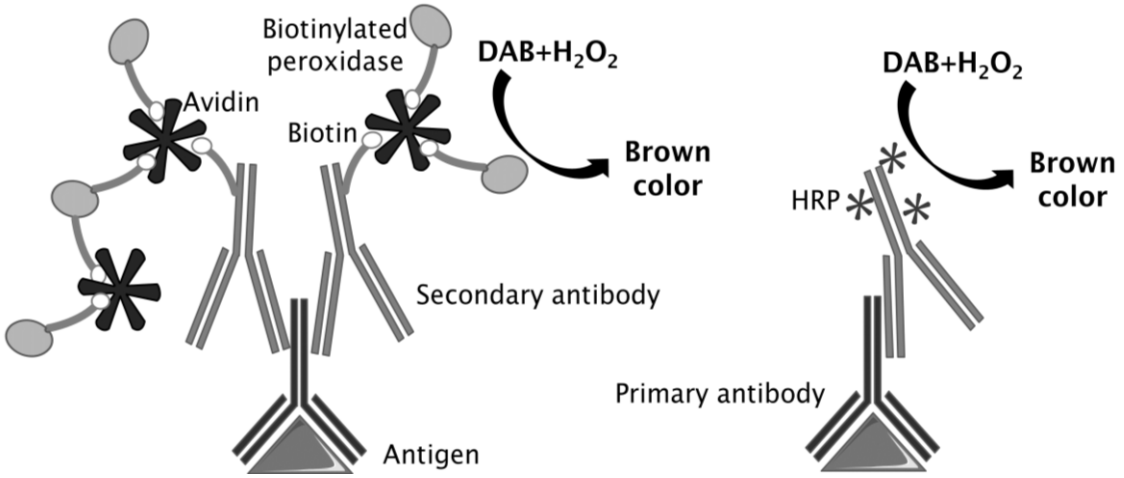

Figure III.5. Schematic illustration of the immunohistochemical staining reaction using biotin or HRP labeled secondary antibodies.

All tissue sections were counterstained with hematoxylin (Hematoxylin solution, Gill No. 3; Sigma-Aldrich Chemicals) for 30 sec. Next, tissues were rinsed with water for 10 sec and, sequentially, slides were immersed in 0.5% Ethanol-HCl for 10 sec, in $NaHCO_3$ for 1 min and in distilled water for 5 min.

III.13.5. Mounting and image acquisition

Tissue sections were dehydrated again (in graded alcohols and xylene), and then allowed to dry. Finally, coverslips were placed onto the slides just after applying the mounting medium on them (DPX® Mountant for histology, Sigma Aldrich Chemicals).

IHC images were acquired using a digital light microscope (Leica DMD 108, Leica Microsystems) at 10X, 20X and 40X magnification.

III.14. PRESENTATION OF DATA AND STATISTICAL ANALYSIS

All values are expressed as mean ± standard error of the mean (SEM). The number of independent experiments (n) for each parameter is indicated in the figure legends; all measurements were repeated 2-8 times. Data are represented as percentage of control (untreated cells considered 100%), unless otherwise stated.

Data were analyzed using GraphPad Prism® V6.01 (GraphPad Prism® Software Inc., La Jolla, CA, USA) with an one-way ANOVA followed by a Newman-Keuls

multiple comparison test (statistical significance versus vehicle: $*p < 0.05$, $**p < 0.01$ and $***p < 0.001$). Comparisons between two groups or with respect to control conditions were independently performed by Student *t*-test (statistical significance versus DMSO or untreated cells: $\#p < 0.05$, $\#\#p < 0.01$ and $\#\#\#p < 0.001$). Mitochondrial and cytosolic fractions were analyzed by two-way ANOVA multiple comparison test followed by a Sidak's test ($+p < 0.05$, $++p < 0.01$, $+++p < 0.001$).

Chapter IV. RESULTS

SECTION I: CHARACTERIZATION OF THE INFLAMMATORY RESPONSE INDUCED BY EFAVIRENZ IN HEPATOCYTES

IV.1. ACTIVATION OF NF-κB SIGNALING PATHWAY

IV.1.1. Determination of the NF-κB activation

The activation of the transcription factor NF-κB was studied by analysis of the protein expression of its inhibitor, IκB-α, which is phosphorylated by the IKK complex and subsequently degraded, allowing the translocation of NF-κB to the nucleus to activate target genes. WB assays revealed that Hep3B cells treated with EFV showed a concentration-dependent decrease in IκB-α expression (Figure IV.1).

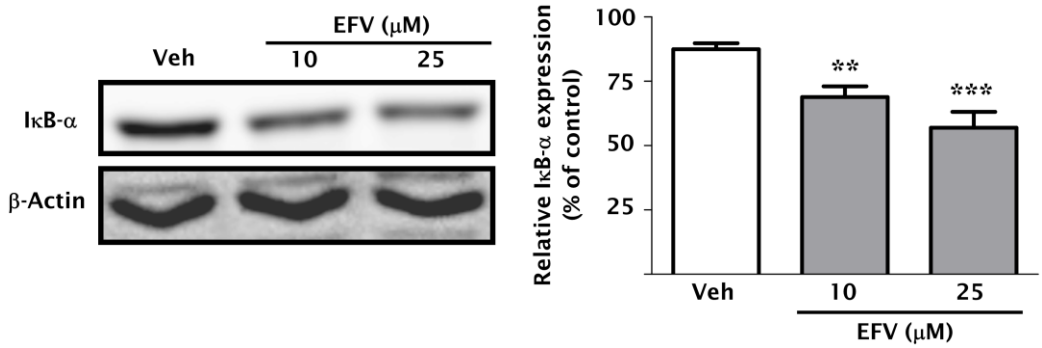

Figure IV.1. Analysis of IκB-α expression in EFV-treated Hep3B cells. Representative WB image of IκB-α and summary of densitometry data. Data (men±SEM, n=8) were calculated as percentage of control (untreated cells) and analyzed by one-way ANOVA multiple comparison test followed by a Newman-Keuls test (p<0.01, ***p<0.001 versus vehicle).**

Next, we determined the nuclear translocation of NF-κB by assessing the protein expression of the p65 subunit of this transcription factor in nuclear extracts by WB. Cells treated with EFV (10, 15 and 25 μM) showed a concentration-dependent increase in the levels of p65 subunit in nuclear extracts (Figure IV.2), indicating an increase of its translocation to the nucleus.

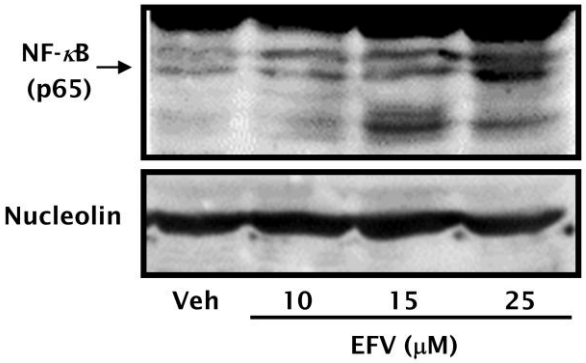

Figure IV.2. Evaluation of the nuclear translocation of NF-κB (p65) in EFV-treated Hep3B cells. Representative WB image of NF-κB (p65 subunit) and nucleolin (loading control) in nuclear extracts.

IV.1.2. Analysis of NF-κB target genes

When NF-κB is translocated to the nucleus, it binds to the *κB* sites to regulate the expression of many genes involved in inflammation, stress responses or immunity. We studied the expression of inflammation-related genes associated with NF-κB, specifically *IL6, TNF* and *SERPINE1* by qRT-PCR. Treatment with EFV upregulated the expression of these genes in Hep3B cells (Figure IV.3).

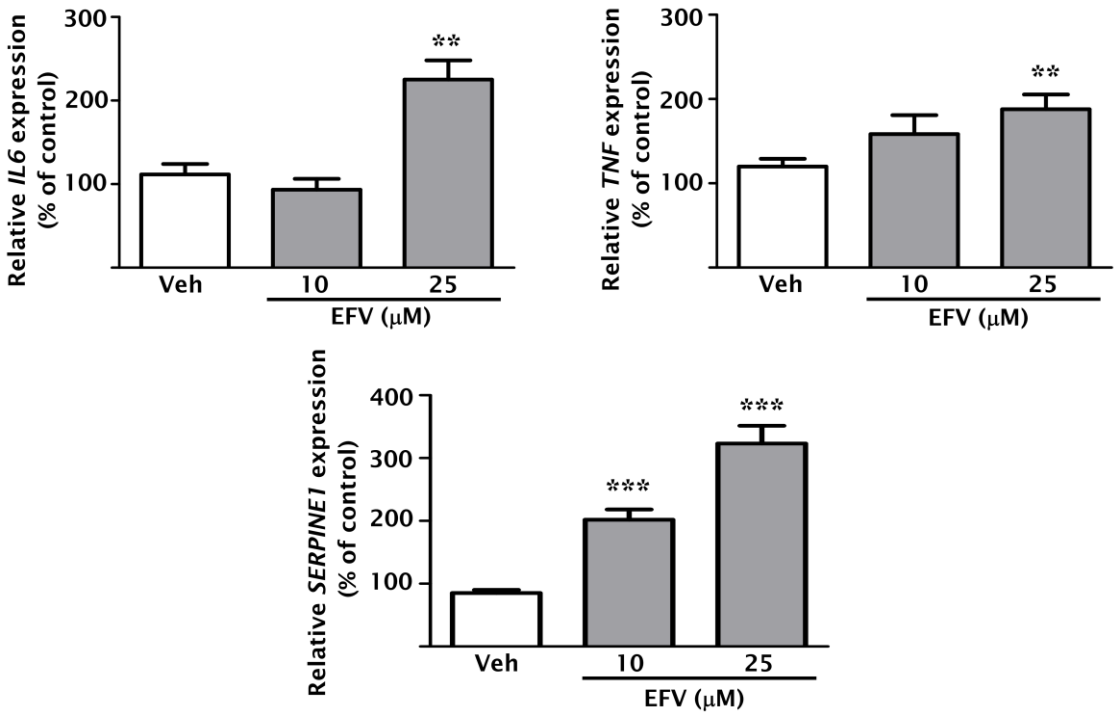

Figure IV.3. Analysis of the expression of inflammation-related genes known to be targets of NF-κB transactivation. Relative mRNA expression levels of the pro-inflammatory cytokines *IL6* and *TNF*, and the serine protease inhibitor *SERPINE1*, analyzed by qRT-PCR. Data (men±SEM, n=5) were normalized versus the expression of the housekeeping gene *ACTB,* calculated as percentage of control (untreated cells) and analyzed by one-way ANOVA multiple comparison test followed by a Newman-Keuls test (p<0.01, ***p<0.001 versus vehicle).**

IV.2. EVALUATION OF NLRP3 INFLAMMASOME ACTIVATION

IV.2.1. Expression of the NLRP3 inflammasome components

NF-κB plays an essential role in the inflammasome priming. For this reason, we decided to study the NLRP3 inflammasome and its downstream effectors in the hepatocytes. The transcription of two important NLRP3 inflammasome components, NLRP3 and caspase-1, and its downstream effector IL-1β were significantly enhanced by EFV in Hep3B cells, whereas the expression of the effector IL-18 did not increase, and in fact it decreased with the lowest concentration evaluated (10 μM) (Figure IV.4 A). In addition, confocal fluorescence microscopy revealed an increased protein expression of NLRP3 in EFV-treated Hep3B cells (Figure IV.4 B).

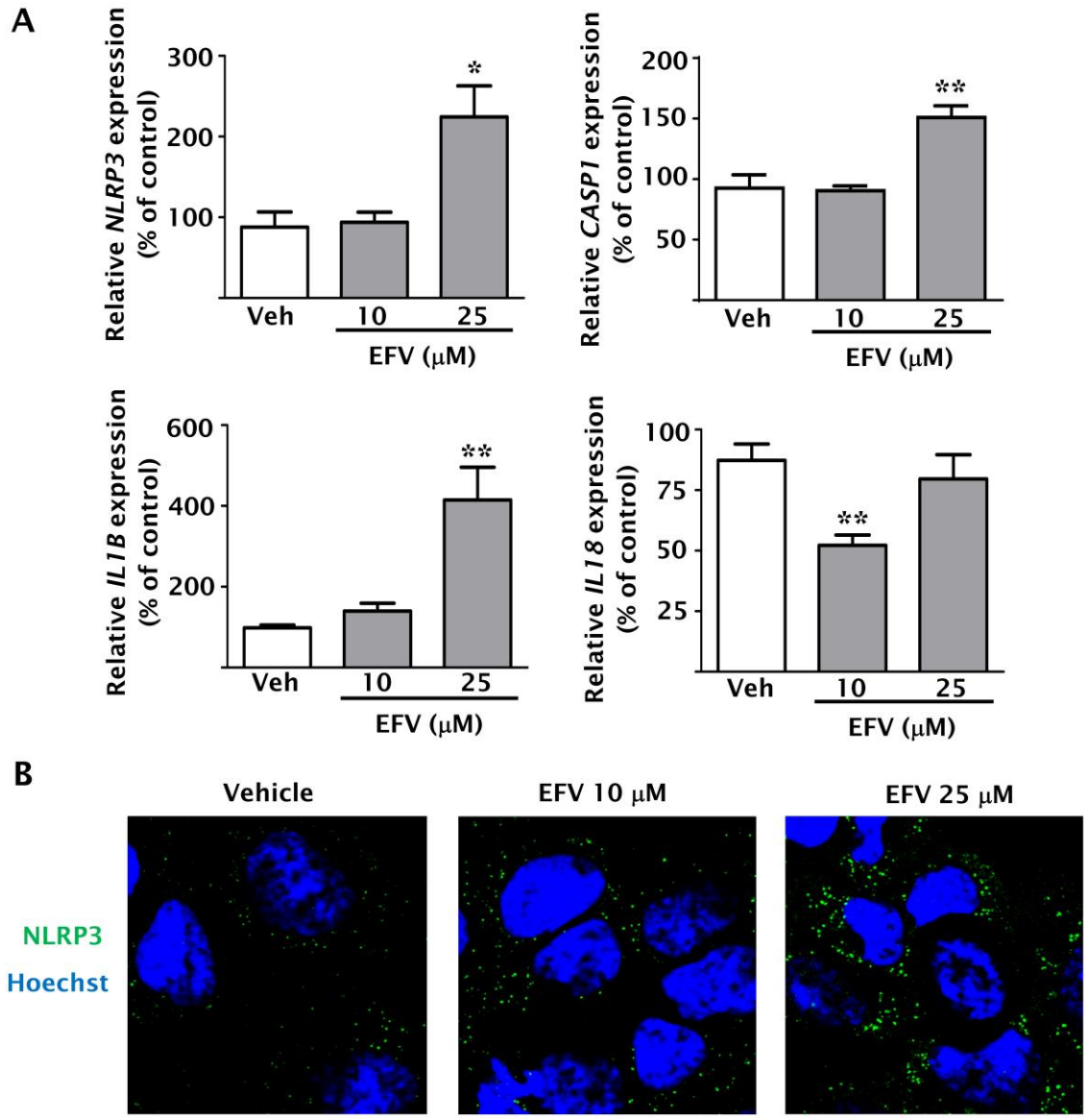

Figure IV.4. Characterization of the effects of EFV on NLRP3 Inflammasome components and effectors in Hep3B cells. (A) Relative mRNA expression levels of NLRP3 inflammasome-associated genes *NLRP3*, *CASP1*, *IL1B* and *IL18* in Hep3B cells, analyzed by qRT-PCR. Data (men±SEM, n=4-6) were normalized versus the expression of the housekeeping gene *ACTB*, calculated as percentage of control (untreated cells) and analyzed by one-way ANOVA multiple comparison test followed by a Newman-Keuls test (*p<0.0.5; **p<0.0.1 versus vehicle). (B) Representative images of confocal microscopy: Hoechst 33342 (blue) and NLRP3 antibody (green). Magnification 40x (n=3).

IV.2.2. Analysis of caspase-1 activation

In order to corroborate NRLP3 inflammasome activation in EFV-treated Hep3B cells, protein expression and activity of caspase-1 were assessed. Following incubation with this drug, cells exhibited a strong decrease of pro-caspase-1 expression, similar to that provoked by Rot, suggesting a cleavage of this enzyme to generate the smaller and active form. Importantly, such effect was not generated by TG (Figure IV.5 A). Additionally, a colorimetric assay of the activity of caspase-1 following EFV treatment demonstrated a significant increase of this parameter, comparable to that induced by LPSc (Figure IV.5 B).

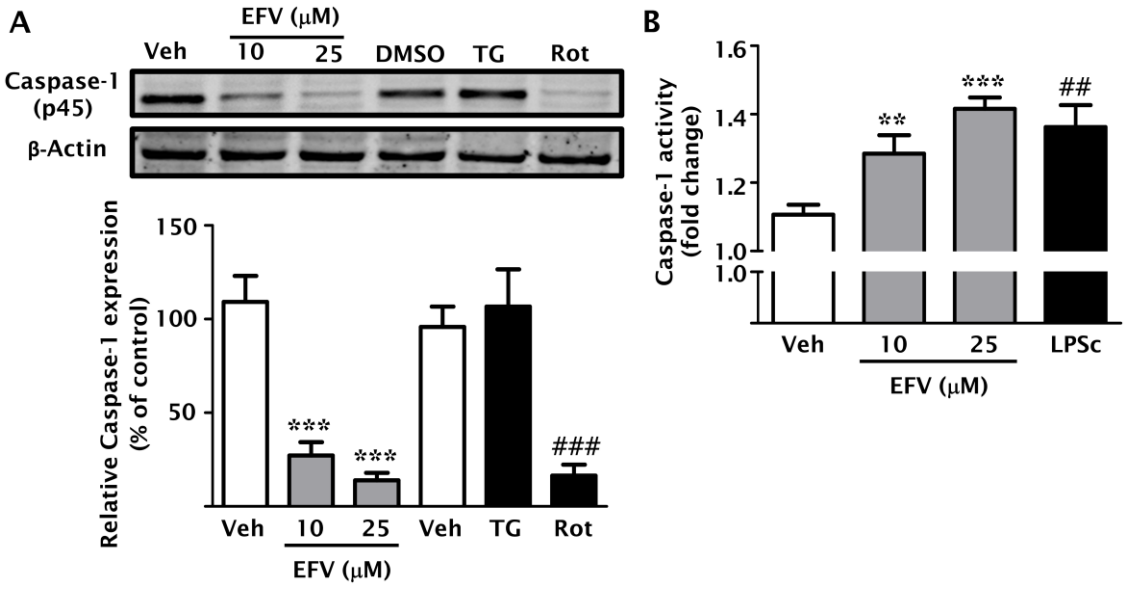

Figure IV.5. Determination of caspase-1 activation in EFV-treated Hep3B cells. (A) Representative WB image of pro-caspase-1 (45 kDa, inactive form) and summary of densitometry data (n=5). (B) Caspase-1 activity analyzed by a colorimetric assay (n=6). Data (men±SEM) were calculated as percentage of control (untreated cells) and analyzed by one-way ANOVA multiple comparison test followed by a Newman-Keuls test (***p*<0.01; ******p*<0.001 versus vehicle). Positive controls (TG, Rot and LPSc) were independently analyzed by a Student's *t*-test (\#\#*p*<0.01; \#\#****p*<0.001 versus control).**

IV.2.3. Involvement of oxidative stress in NLRP3 inflammasome activation

TXNIP is a negative regulator of the reduced TRX, whose primary function is to modulate the cellular redox state. In the presence of high concentrations of ROS, TXNIP is dissociated from TRX, allowing its binding to NLRP3 and

triggering NRLP3 inflammasome activation (Zhou et al. 2010). As EFV triggers oxidative stress in hepatocytes, we hypothesized that TXNIP can play a key role in the activation of inflammasome in our model. However, EFV did not induce a significant increase in *TNXIP* mRNA levels, and its expression even decreased with the lowest concentration studied (10 μM). On the other hand, Rot significantly enhanced the transcription of *TXNIP* (Figure IV.6).

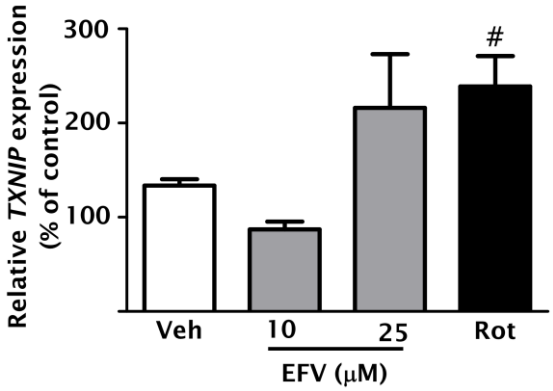

Figure IV.6. Analysis of *TXNIP* expression in Hep3B cells treated with EFV. Relative mRNA expression levels of *TXNIP* analyzed by qRT-PCR. Data (mean±SEM, n=6) were normalized versus the expression of the housekeeping gene *ACTB,* calculated as percentage of control (untreated cells) and analyzed by one-way ANOVA multiple comparison test followed by a Newman-Keuls test. Rot was independently analyzed by a Student's *t*-test (#*p*<0.05 versus control).

IV.3. CONFIRMATORY EXPERIMENTS IN PRIMARY HUMAN HEPATOCYTES

The results obtained in primary human hepatocytes were in line with those shown in the human hepatoma cell line Hep3B: EFV induced a significant upregulation of the inflammatory markers previously evaluated (NLRP3, caspase-1, IL-1β, TNF-α, and IL-6) (Figure IV.7).

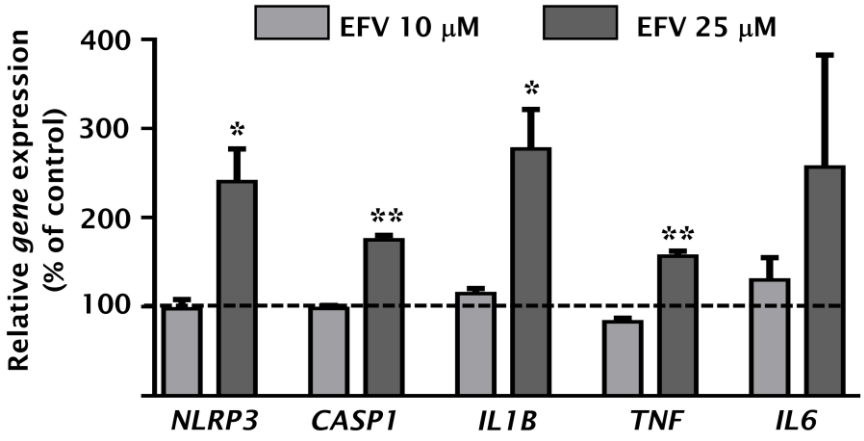

Figure IV.7. Evaluation of the effects of EFV on inflammatory mediators in primary human hepatocytes. qRT-PCR analysis of NLRP3 inflammasome-associated markers (NLRP3, caspase-1 and IL-1β) and pro-inflammatory cytokines (TNF-α and IL-6). Data (mean±SEM, n=2) were normalized versus the housekeeping gene *ACTB*, calculated as percentage of control (untreated cells) and analyzed by one-way ANOVA multiple comparison test followed by a Newman-Keuls test (*p<0.05, **p<0.01 versus vehicle).

IV.4. EFFECTS OF OTHER ANTIRETROVIRAL DRUGS ON CELLULAR VIABILITY

IV.4.1. Determination of cellular viability in hepatocytes

Our group has previously reported that EFV reduces the viability of cultured hepatocytes due to its mitochondrial toxicity (Apostolova et al. 2010; Blas-García et al. 2010). Currently, the use of EFV in first-line cART has been challenged by novel anti-HIV drugs with a safer toxicological profile compared to EFV, such as the PI DRV, the NNRTI RPV and the II RAL. With the goal of exploring the safety of these newer drugs, we analyzed cellular viability using the MTT assay in Hep3B cells after 48 h of treatment, and the results showed that clinically relevant concentrations of DRV, RPV and RAL provoked a slight but non-significant decrease in this parameter, whereas EFV produced a cytotoxic effect in these cells (Figure IV.8 A). Furthermore, NRTIs drugs, such as ABC and ddI, are crucial in several combinations of the cART and have been shown to produce severe hepatic side effects (Núñez 2010). Therefore, we decided to evaluate the effect on cellular viability of these two NRTIs in both Hep3B cells and differentiated HepaRG™ cells, hepatocyte-like cells that are a reliable model for their similarity to primary hepatocytes. MTT assays showed

that clinical concentrations of ABC and ddI did not provoke a decrease in the cellular viability after 48 h of treatment, whereas, as expected, EFV induced a significant reduction (Figure IV.8 B and C).

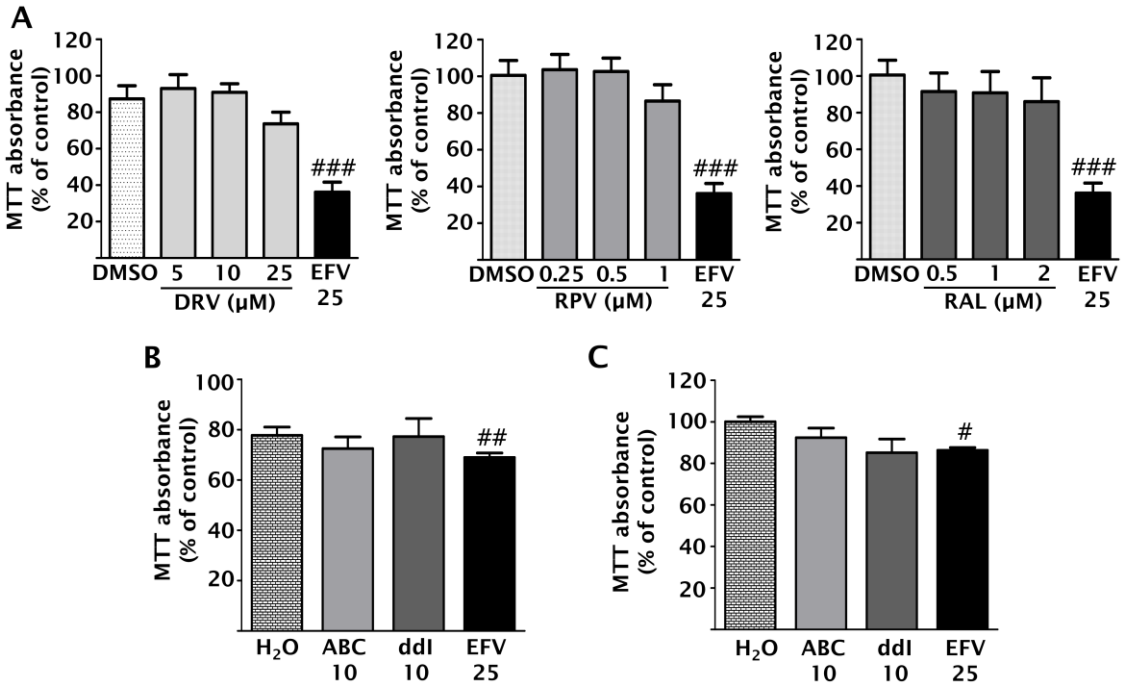

Figure IV.8. Analysis of cellular viability in human hepatocyte cell lines after 48 h of treatment. MTT assay of exponentially growing cells after treatment with (A) DRV, RPV, RAL and EFV in Hep3B cells; (B) ABC, ddI and EFV in HepaRG™ cells and (C) ABC, ddI and EFV in Hep3B cells. Data (mean±SEM, n=3-6) were calculated as percentage of control (untreated cells) and analyzed by one-way ANOVA multiple comparison test followed by a Newman-Keuls test. Data for ABC, ddI and EFV were independently analyzed by a Student's *t*-test (#p<0.05, ##p<0.01, ###p<0.001 versus the respective solvent; data of EFV-vehicle are not shown).

IV.4.2. Determination of the cellular viability in neurons

Recently, our group has shown that EFV alters mitochondrial respiration, inhibits mitochondrial complex I and enhances ROS generation in neurons from rat cerebral cortex (Funes et al. 2014; Apostolova et al. 2015a), decreasing their cellular viability, as shown in Figure IV.9 A. Although the mechanisms responsible for EFV-induced neurotoxicity are unclear, these findings may explain the mechanisms involved in the CNS-related side effects exhibited by EFV-treated patients, which include impaired concentration, sleep disturbances, depression, psychosis and neurocognitive disorders (Ciccarelli et al. 2011; Apostolova et al. 2015b). Similarly, to the experiments performed in

hepatocytes, we analyzed the effects in cellular viability of the new anti-HIV drugs DRV, RPV and RAL and compared them with those induced by EFV in neurons. MTT assays revealed that clinically relevant concentrations of DRV, RPV and RAL did not decrease the neuronal viability, whereas EFV reduced it significantly (Figure IV.9 B).

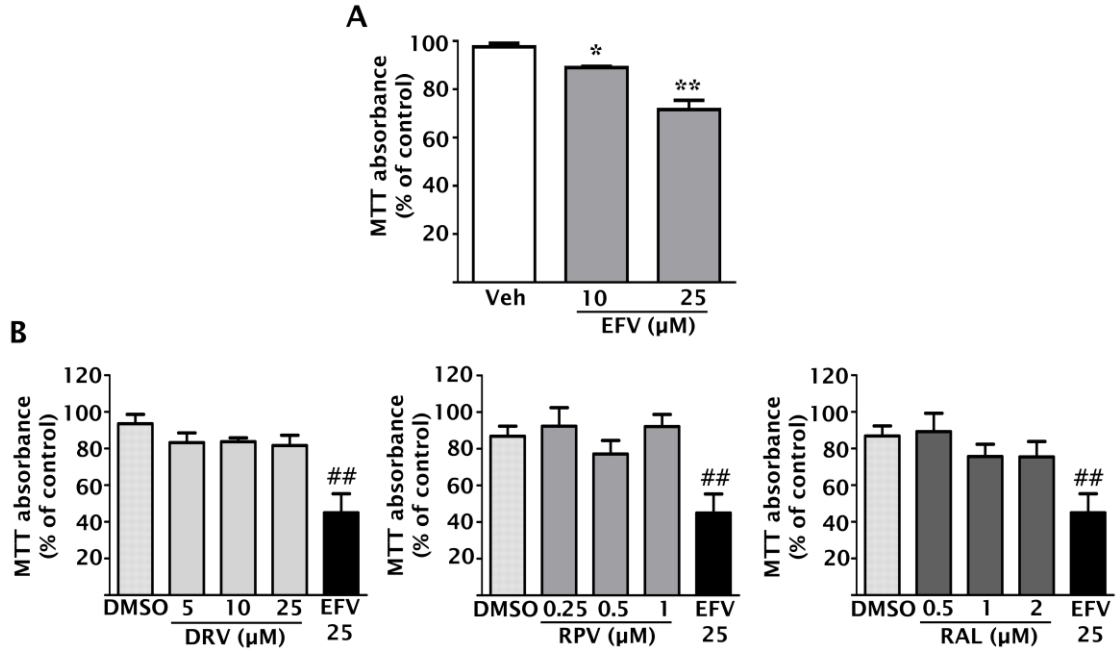

Figure IV.9. Analysis of the cellular viability in primary rat neurons. MTT assay of primary rat neurons of culture in presence of (A) EFV and (B) DRV, RPV, RAL and EFV (25 μM). Data (mean±SEM, n=3-5) were calculated as percentage of control (untreated cells) and analyzed by one-way ANOVA multiple comparison test followed by a Newman-Keuls test (*p<0.05; **p<0.01 versus the respective solvent). EFV in (B) was independently analyzed with a Student's t-test (##p<0.01versus its vehicle; data not shown).

SECTION II: CHARACTERIZATION OF THE INFLAMMATORY AND FIBROGENIC RESPONSES PRODUCED BY EFAVIRENZ IN HEPATIC STELLATE CELLS

IV.5. EVALUATION OF CELLULAR FUNCTIONS

IV.5.1. Analysis of mitochondrial function

To characterize the effects of EFV on mitochondrial function in HSCs, we evaluated $\Delta\Psi_m$, mitochondrial superoxide production and mitochondrial mass in the human immortalized line LX-2, using the fluorescence probes TMRM, MitoSOX™ and NAO, respectively.

Incubation with EFV enhanced the production of mitochondrial superoxide (Figure IV.10 A and B) and decreased $\Delta\Psi_m$ (Figure IV.10 A and C) in a concentration-dependent fashion. EFV-treated cells also showed a significant increase of NAO fluorescence (Figure IV.10 A and D), indicating augmented mitochondrial mass, which was statistically significant only with the highest concentration assessed (50 μM). These results supported EFV-induced mitochondrial dysfunction in LX-2 cells.

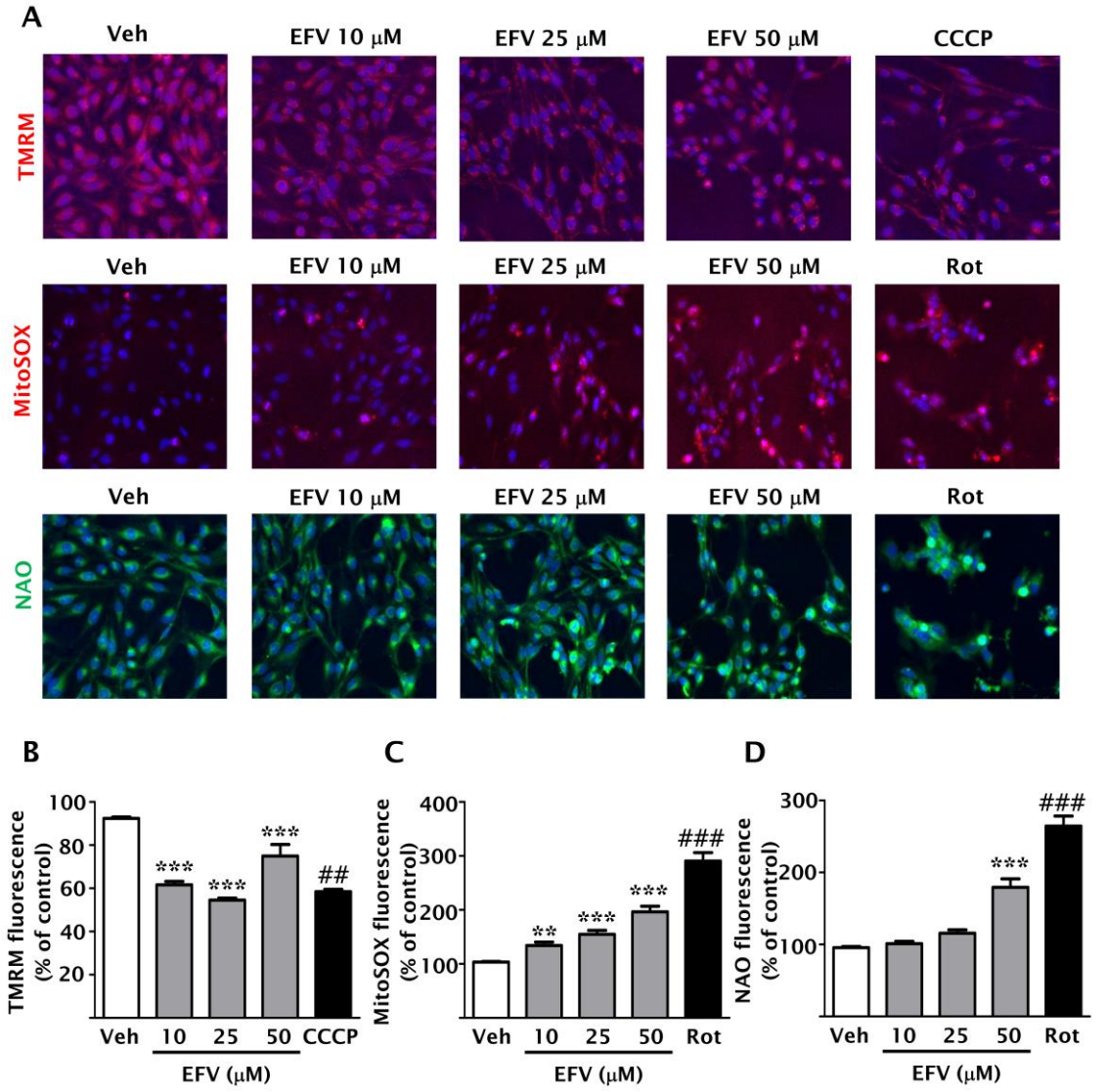

Figure IV.10. Analysis of mitochondrial parameters in EFV-treated LX-2 cells. (A) Representative fluorescence microscopy images (x10) of LX-2 cells treated with EFV, stained with TMRM (red; top row), MitoSOX (red; middle row) or NAO (green; bottom row). Nuclei were stained with Hoechst 33342 (blue). The graphs show quantitative analysis of (B) TMRM fluorescence, (C) MitoSOX fluorescence, and (D) NAO fluorescence. Data (mean±SEM, n=4) were calculated as percentage of control (untreated cells) and analyzed by one-way ANOVA multiple comparison test followed by a Newman-Keuls test (p<0.01; ***p<0.001 versus vehicle). Positive controls (Rot and CCCP) were independently analyzed by a Student´s t-test (##p<0.01, ###p<0.001 versus control).**

IV.5.2. Effects of efavirenz on endoplasmic reticulum function

To determine whether EFV affected the function of ER in LX-2 cells, several important mediators of UPR and ER stress were evaluated. Both protein (Figure IV.11 A) and mRNA expression levels (Figure IV.11 B) of CHOP and GRP78 were significantly increased in a concentration-dependent manner. LPSc and Rot also altered expression of parameters involved in ER stress in LX-2 cells. In addition, the transcription of another important ER stress marker, XBP1, was also significantly augmented by EFV, an effect that was reproduced by LPSc and Rot (Figure IV.11 B). Nonetheless, only the cells treated with 50 μM EFV exhibited an increase in ER Tracker Red fluorescence, a parameter indicative of alterations in ER morphology (Figure IV.11 C). Unexpectedly, TG did not induce a significant increase in this parameter. These results reveal that EFV induces ER stress in LX-2 cells, which is a relevant cellular condition in the activation of HSCs (Hernández-Gea et al. 2013).

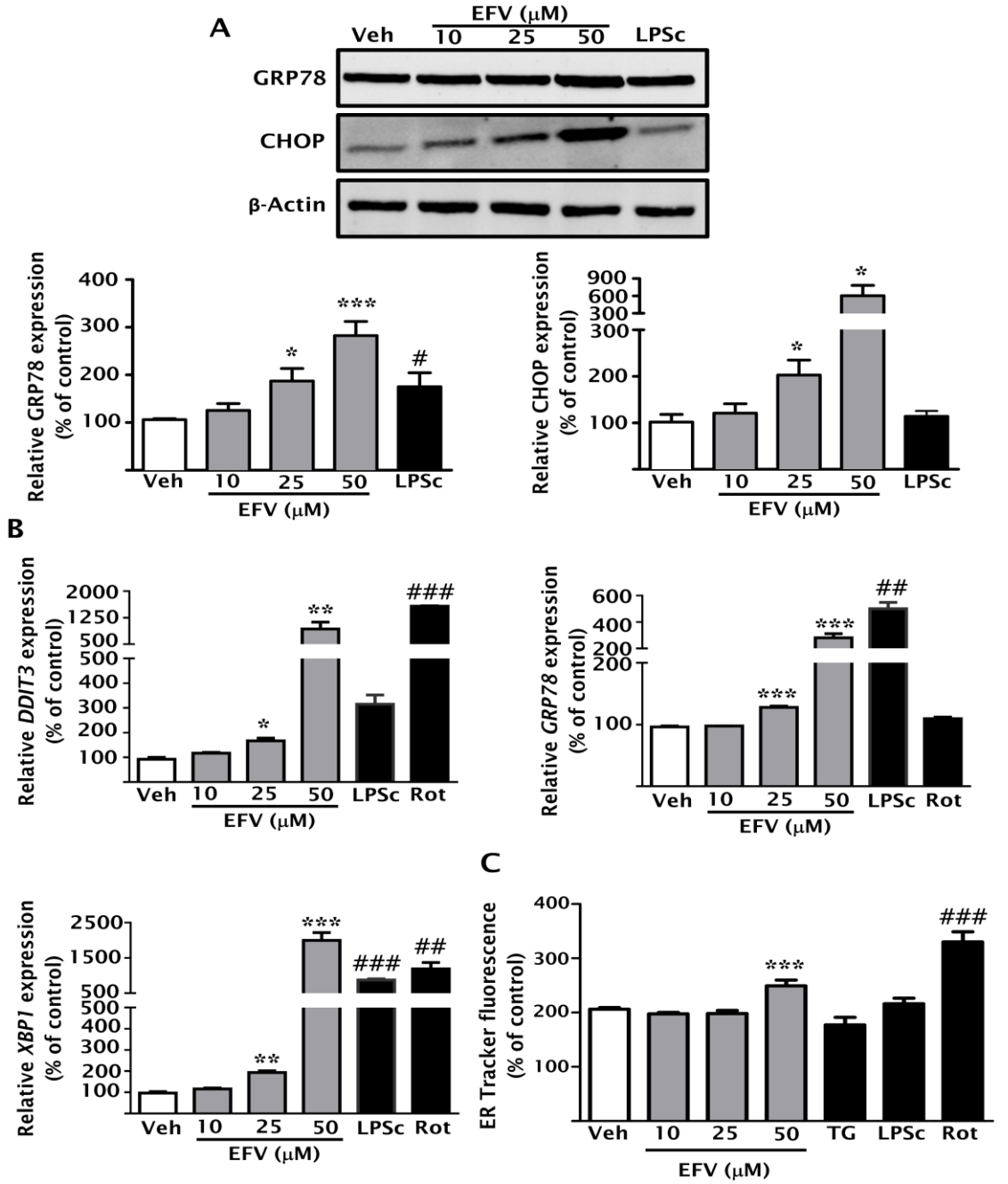

Figure IV.11. Evaluation of ER stress markers in EFV-treated LX-2 cells. (A) Representative WB images of the ER stress markers, GRP78 and CHOP, and summary of densitometry data. (B) Relative mRNA expression levels of ER stress-related genes *DDIT3* (which codes CHOP protein), *GRP78* and *XBP1* analyzed by qRT-PCR. Data were normalized versus the expression of the housekeeping gene *ACTB*. (C) Quantitative analysis of the ER signal (ER Tracker Red fluorescence). Data (mean±SEM, n=4-6) were calculated as percentage of control (untreated cells) and analyzed by one-way ANOVA multiple comparison test followed by a Newman-Keuls test (*p<0.05, **p<0.01, ***p<0.001 versus vehicle). Positive controls (Rot, TG and LPSc) were independently analyzed by a Student's *t*-test (#p<0.05; ##p<0.01; ###p<0.001 versus control).

IV.5.3. Evaluation of cellular proliferation/survival

We carried out a cell count using static cytometry in order to define whether the mitochondrial dysfunction and ER stress affected the survival/proliferation of LX-2 cells. This assay showed that only the highest concentration of EFV (50 μM) provoked a significant decrease in cell number (Figure IV.12 A). EFV induced a significant and concentration-dependent increase in Hoechst 33342 fluorescence, which is indicative of changes in nuclear morphology and size, features commonly involved in nuclear condensation in response to cellular stress (Figure IV.12 B). Similarly, both TG and Rot, but not LPSc, exerted deleterious effects on the number and nuclear morphology of these cells.

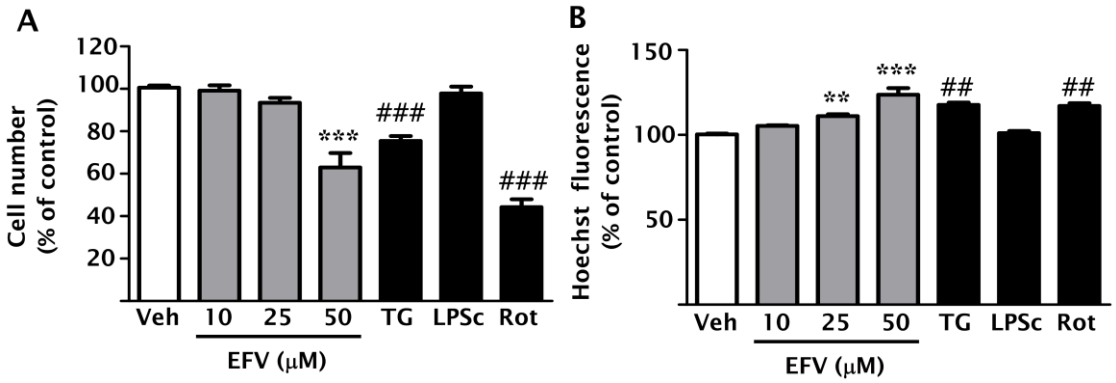

Figure IV.12. Assessment of cellular proliferation/survival in LX-2 cells. Quantitative analysis of (A) cell number and (B) nuclear fluorescence intensity by fluorescence microscopy. Nuclei were stained with the fluorescent dye Hoechst 33342. Data (mean±SEM, n=6) were calculated as percentage of control (untreated cells) and analyzed by one-way ANOVA multiple comparison test followed by a Newman-Keuls test (p<0.01, ***p<0.001 versus vehicle). Positive controls (TG, Rot and LPSc) were independently analyzed by a Student's t-test (##p<0.01, ###p<0.001 versus control).**

Considered together, the results shown in this section suggest that EFV induces a profile of cellular stress in LX-2 cells similar to that previously reported in hepatocytes (Apostolova et al. 2010, 2013; Blas-García et al. 2010), but LX-2 cells seem to be slightly more resistant to EFV-induced perturbations.

IV.6. ANALYSIS OF LIPOPHAGY

IV.6.1. Assessment of intracellular lipid droplets levels

The degradation of intracellular lipid droplets by autophagy is essential to provide energy to support HSCs activation. For this reason, we analyzed whether EFV influenced HSCs activation through autophagy.

We studied the effect of EFV on intracellular lipid accumulation in LX-2 cells employing the fluorescent dye Nile Red. This drug produced a differential response depending on the concentrations, with 10 and 25 μM decreasing the intensity of Nile Red signal and 50 μM slightly increasing it. Importantly, co-treatment with EFV 25 μM and the autophagic inhibitor 3MA reversed the reduction observed in the Nile Red signal, pointing to a role of autophagy in the effect induced by this NNRTI (Figure IV.13).

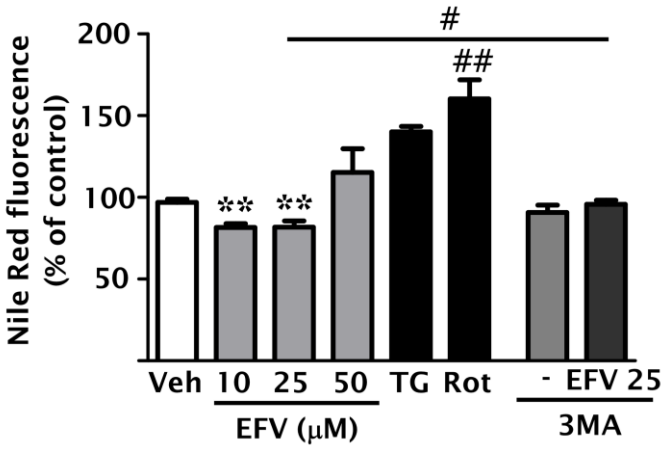

Figure IV.13. Measurement of intracellular lipid droplets in EFV-treated LX-2 cells. Quantitative analysis of intracellular lipid accumulation evaluated by Nile Red fluorescence and static cytometry. Data (mean±SEM, n=6) were calculated as percentage of control (untreated cells) and analyzed by one-way ANOVA multiple comparison test followed by a Newman-Keuls test (p<0.01 versus vehicle). Positive controls (TG, Rot and 3MA) and co-treatment with EFV and 3MA were independently analyzed by a Student's t-test (#p<0.05, ##p<0.01).**

IV.6.2. Evaluation of activation of autophagy

An augmented traffic of intracellular lysosomes is suggestive of an active autophagic flux. To study this parameter, EFV-treated LX-2 cells were incubated with the fluorescent dye Lysotracker® Red, and the analysis of its intensity of fluorescence by static cytometry revealed a significant increase only with EFV

50 µM. Positive controls TG and Rot, but not LPSc, showed the same effect (Figure IV.14 A). In addition, EFV enhanced protein expression of the classic autophagy marker LC3-II, pointing to an induction of autophagy (Figure IV.14 B), considering that the conversion of LC3-I to LC3-II is a common feature of autophagy.

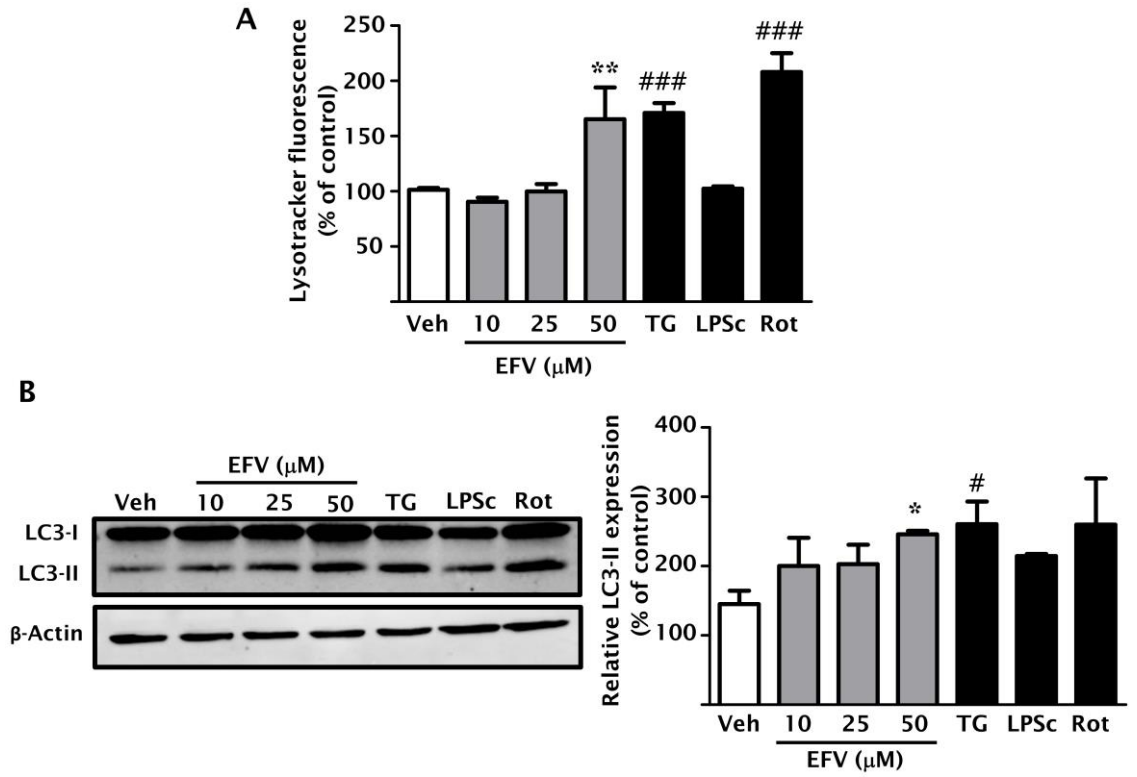

Figure IV.14. Analysis of autophagic markers in EFV-treated LX-2 cells. (A) Quantitative analysis of lysosome signal (Lysotracker Red fluorescence) by fluorescence microscopy (n=6). (B) Representative WB images of LC3-II and summary of densitometry (n=5). Data (mean±SEM) were calculated as percentage of control (untreated cells) and analyzed by one-way ANOVA multiple comparison test followed by a Newman-Keuls test (*p<0.05, **p<0.001 versus vehicle). Positive controls TG, Rot and LPSc were independently analyzed by a Student's t-test (#p<0.05, ###p<0.001 versus control).

IV.6.3. Analysis of the degradation of lipid droplets by autophagy

In order to determine if EFV activated the degradation of the intracellular lipid droplets by autophagy, also known as lipophagy, in LX-2 cells, we analyzed the correlation index between LC3 and Nile Red signals using confocal fluorescence microscopy. As expected, EFV favored the accumulation of LC3-II-characteristic punctae, particularly with the highest concentration. It also

induced a significant and concentration-dependent overlapping between LC3 and intracellular lipid droplets, thus suggesting the induction of lipophagy in LX-2 cells (Figure IV.15). Rot exerted similar effects to 50 μM EFV, whereas LPSc modified neither the individual levels of LC3 and Nile Red nor the co-localization of their signals.

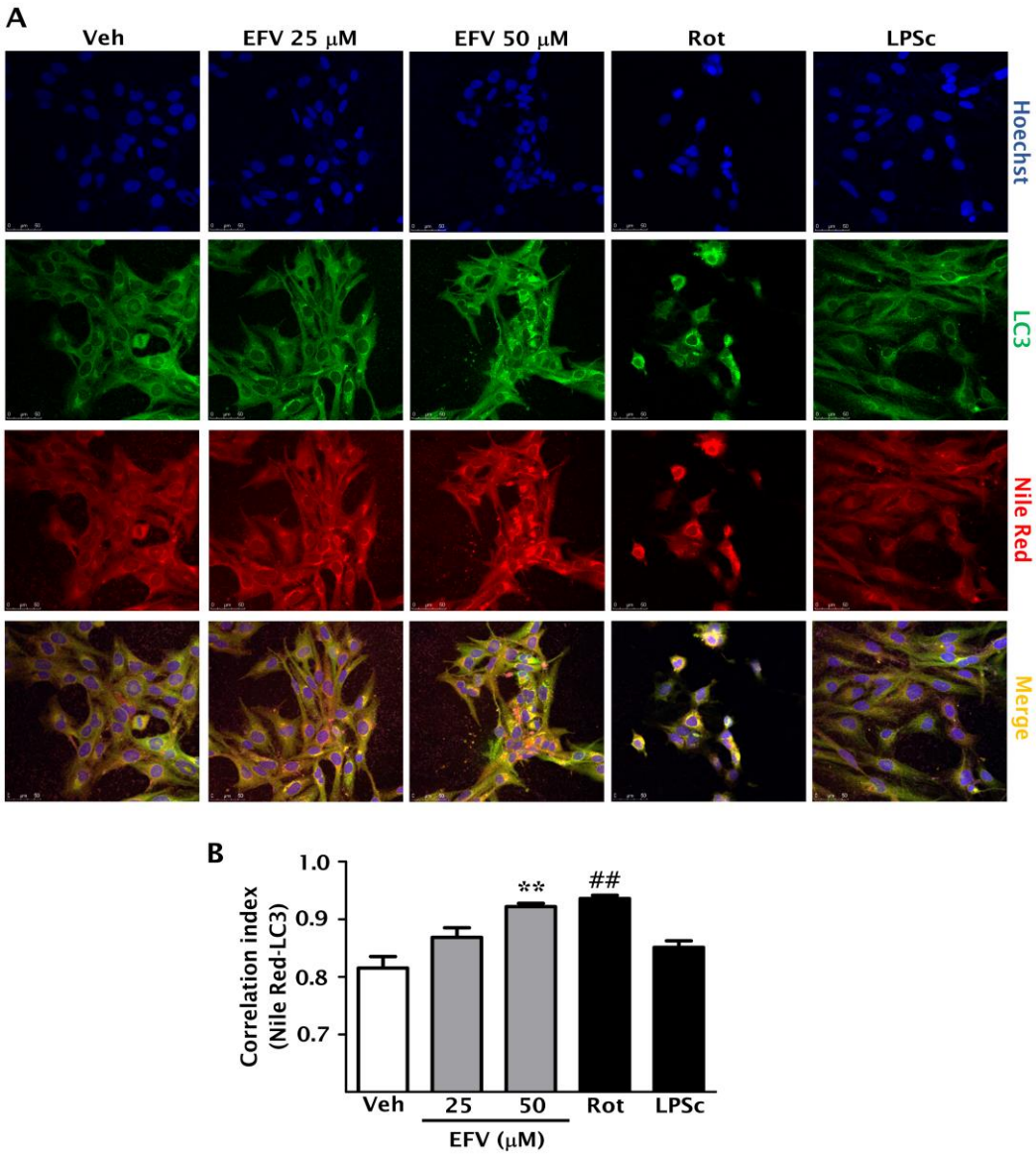

Figure IV.15. Evaluation of the induction of lipophagy in LX-2 cells by EFV. (A) Representative confocal fluorescence microscopy images of nuclei (Hoechst 33342), LC3 (LC3 antibody), intracellular lipid droplets (Nile Red) and merge. Magnification of 40X. (B) Correlation index between Nile Red and LC3 fluorescence signals, analyzed by the Colocalization Colormap script, a plugin in Fiji. Data (mean±SEM, n=3) were calculated as percentage of control (untreated cells) and analyzed by one-way ANOVA multiple comparison test followed by a Newman-Keuls test (p<0.01 versus vehicle). Positive controls (Rot and LPSc) were independently analyzed by a Student´s t-test (##p<0.01 versus control).**

IV.7. MODULATION OF THE INFLAMMATORY RESPONSE

Due to the capacity of EFV to induce mitochondrial dysfunction, ER stress and autophagy in the human hepatic stellate cell line LX-2, we assessed whether these actions could lead to NLRP3 activation and production of cytokines in HSCs, as occurs in hepatocytes, thus intensifying hepatic inflammatory response.

IV.7.1. Evaluation of the NLRP3 inflammasome pathway and pro-inflammatory cytokines.

qRT-PCR analysis revealed that EFV-treated LX-2 cells showed a concentration-dependent increase in the transcription of the NLRP3 inflammasome components, NLRP3 and caspase-1, and induced the expression of the pro-inflammatory cytokines IL-1β, TNF-α and IL-6; as in hepatocytes, no changes were observed in the expression of IL-18 (Figure IV.16 A). These results were confirmed and expanded by performing an array of genes associated with immunity, inflammasome function and cellular stress, in which EFV enhanced the expression of these and other genes, such as *PYCARD* (which encodes the NLRP3 inflammasome component, ASC), *IL33*, *PANX1* and *NAIP* (Figure IV.17). As expected, protein analysis by WB using whole-cell extracts revealed a significantly increased expression of NLRP3 in EFV-treated cells (Figure IV.16 B). The alterations induced by EFV in these genes were in line with those exhibited by LPSc, but less pronounced. Interestingly, in spite of showing a similar profile of effects to EFV in hepatocytes, Rot did not affect these inflammatory parameters in HSCs.

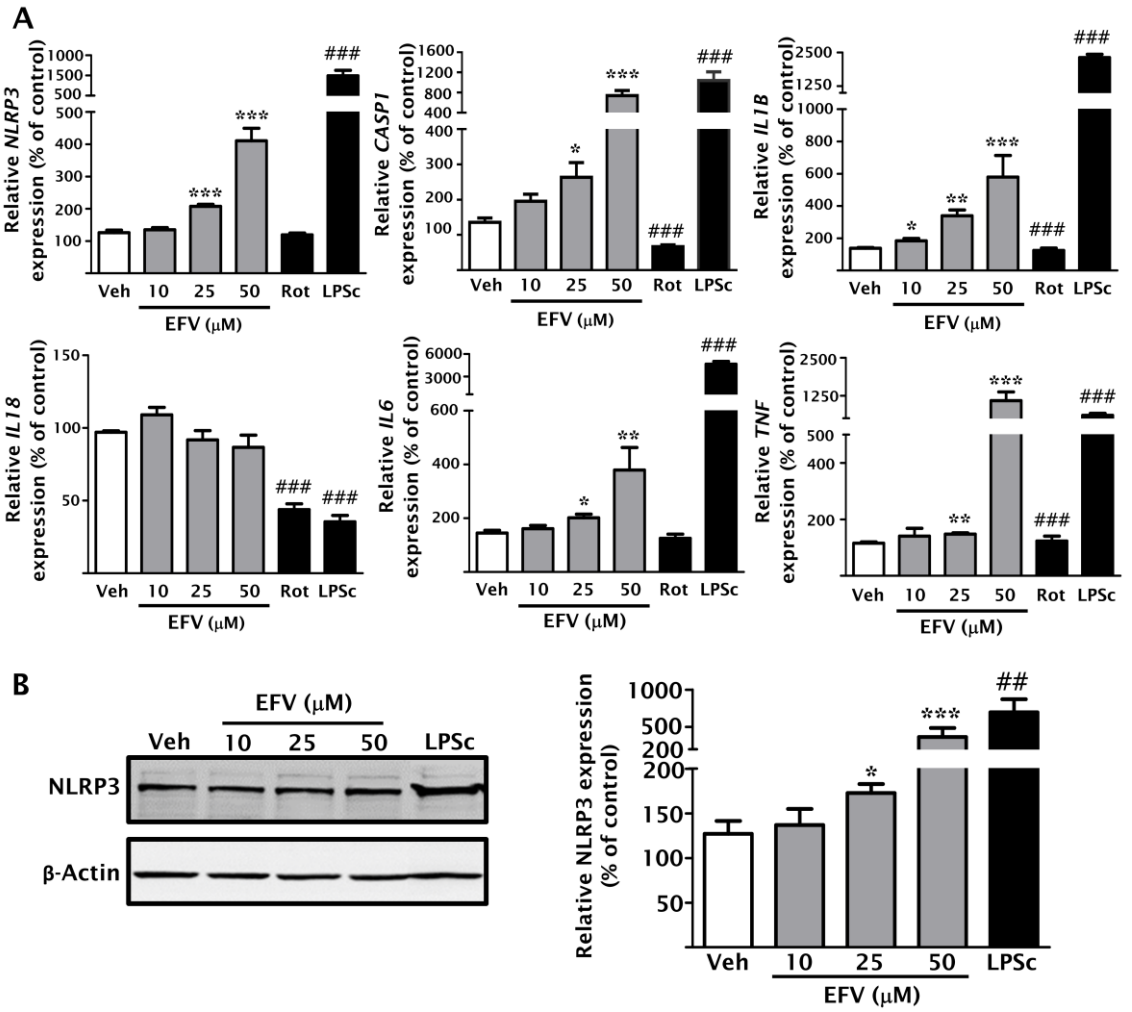

Figure IV.16. Analysis of the gene expression of NLRP3 inflammasome-associated markers and pro-inflammatory cytokines in EFV-treated LX-2 cells. (A) Relative mRNA expression levels of inflammasome-related genes and pro-inflammatory cytokines analyzed by qRT-PCR. Data were normalized versus the expression of the housekeeping gene *ACTB* (n=4-6). (B) Representative WB images of NLRP3 and summary of densitometry data (n=4). Data (mean±SEM) were calculated as percentage of control (untreated cells) and analyzed by one-way ANOVA multiple comparison test followed by a Newman-Keuls test (*p<0.05, **p<0.01, ***p<0.001 versus vehicle). Positive controls (Rot and LPSc) were independently analyzed by a Student's *t*-test (##p<0.01, ###p<0.001 versus control).

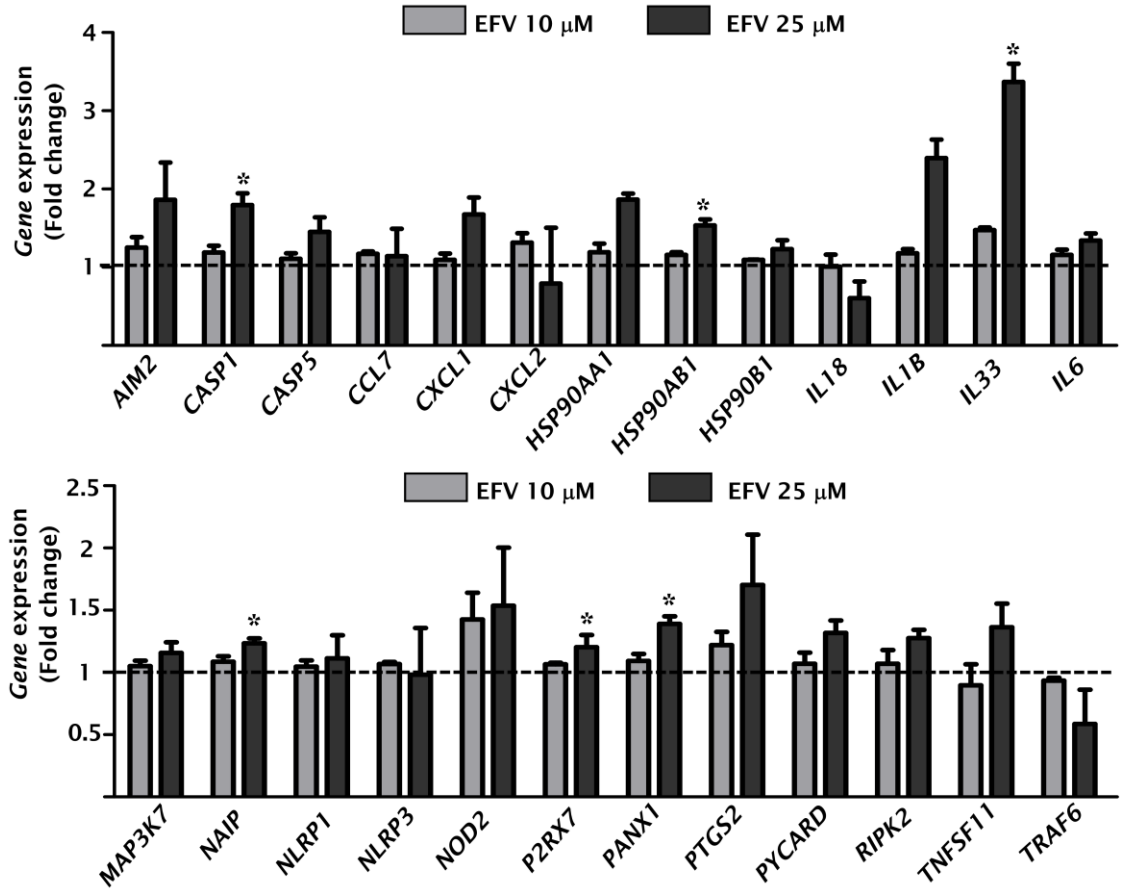

Figure IV.17. PCR array of inflammation and stress-related genes in LX-2 cells treated with EFV. The expression of each gene was normalized to the mean of mRNA expression of the housekeeping gene *GAPDH*. Gene expression is represented as fold change of expression with respect to that recorded in the vehicle-treated cells, which was considered 1. Data (mean±SEM, n=3) were analyzed by one-way ANOVA multiple comparison test followed by a Newman-Keuls test (*p<0.05 versus vehicle).

To confirm the activation of the NLRP3 inflammasome pathway, we assessed caspase-1 activity using protein extracts from treated cells. This assay showed a concentration-dependent increase in the activity of caspase-1 in EFV-treated cells (Figure IV.18 A). In addition, ELISA assay revealed an enhanced secretion of IL-1β after treatment with EFV (Figure IV.18 B). Once again, EFV-induced changes were similar but less intense than those elicited by LPSc.

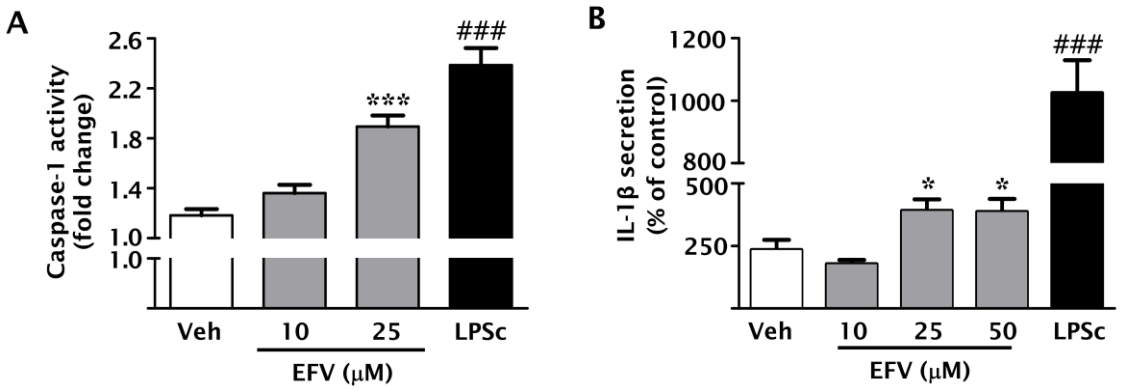

Figure IV.18. Analysis of the activation of caspase-1 in LX-2 cells treated with EFV. (A) Caspase-1 activity in protein extracts (n=7). Data are expressed as fold change of the activity with respect to control (untreated cells, considered 1). (B) Extracellular presence of IL-1β studied by ELISA (n=4). Data (mean±SEM) were calculated as percentage of untreated cells and analyzed by one-way ANOVA multiple comparison test followed by a Newman-Keuls test (*p<0.05, ***p<0.001 versus vehicle). LPSc was independently analyzed by Student´s t-test (###p<0.001 versus control).

IV.8. CHARACTERIZATION OF THE FIBROGENIC RESPONSE

As the main function of HSCs is the production and deposition of ECM in the liver, we studied the fibrogenic response of EFV, considering that EFV-induced changes described so far are compatible with HSCs activation and onset of the fibrogenic response.

qRT-PCR experiments of LX-2 cells treated with EFV revealed that this drug significantly and concentration-dependently upregulated several markers of activated HSC-related processes, such as fibrogenesis (TGF-β1) and altered ECM degradation (TIMP-1, MMP-2 and MMP-9), although no significant changes were found in the mRNA expression of collagen 1α1 (Figure IV.19 A). However, WB experiments revealed that the protein expression of α-SMA was not altered by EFV either (Figure IV.19 B). This response was mimicked by the positive control LPSc, while surprisingly the pro-oxidant stimulus induced by Rot provoked a downregulation of the markers TGF-β1, MMP-2, MMP-9 and collagen 1α1, and no changes in TIMP-1 expression.

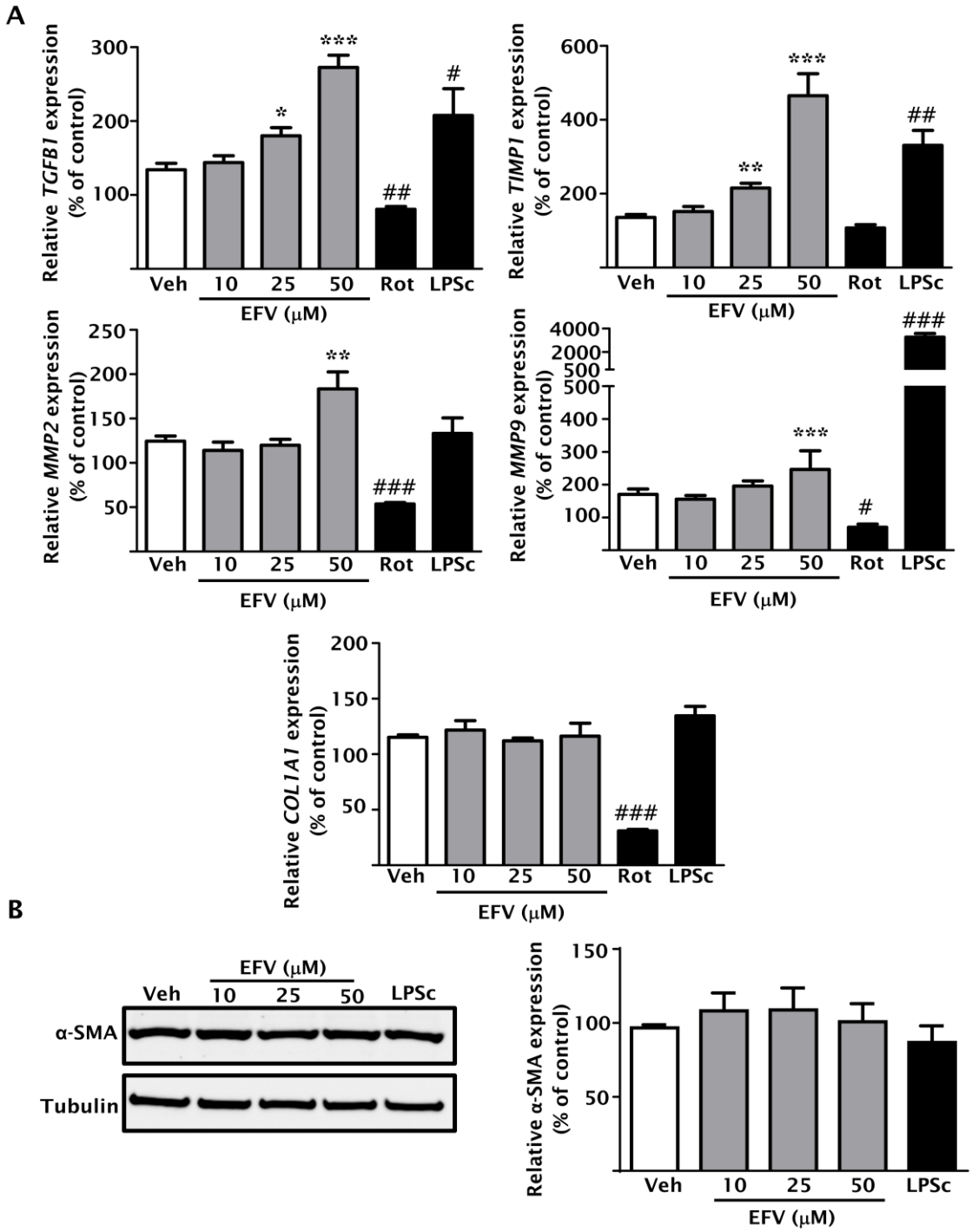

Figure IV.19. Analysis of fibrogenic pathways in EFV-treated LX-2 cells. (A) qRT-PCR analysis of fibrosis-related genes *TGFB1, MMP2, MMP9, TIMP1* and *COL1A1*. Data were normalized versus the housekeeping gene *ACTB* (n=6). (B) Representative WB image and densitometry of the myofibroblast marker α-SMA (n=3). Data (mean±SEM) were calculated as percentage of control (untreated cells) and analyzed by one-way ANOVA multiple comparison test followed by a Newman-Keuls test (*p<0.05, **p<0.01, ***p<0.001 versus vehicle). Positive controls (Rot and LPSc) were independently analyzed by Student's t-test (#p<0.05, ##p<0.01, ###p<0.001 versus control).

IV.9. ANALYSIS OF EFV-INDUCED EFFECTS IN PRIMARY HUMAN HEPATIC STELLATE CELLS

qRT-PCR analysis of key markers of the aforementioned pathways was performed in hHSCs, with the goal to assess the reproducibility of the results obtained in the human cell line LX-2. Importantly, the same pattern of gene expression was observed in human primary cells treated with EFV (10 and 25 μM). In contrast to the results obtained in LX-2 cells, the transcription of the downstream inflammasome effector IL-18 and the ECM component collagen 1α1 were upregulated (Figure IV.20). Furthermore, these alterations were more intense in primary hHSCs than in the cell line employed.

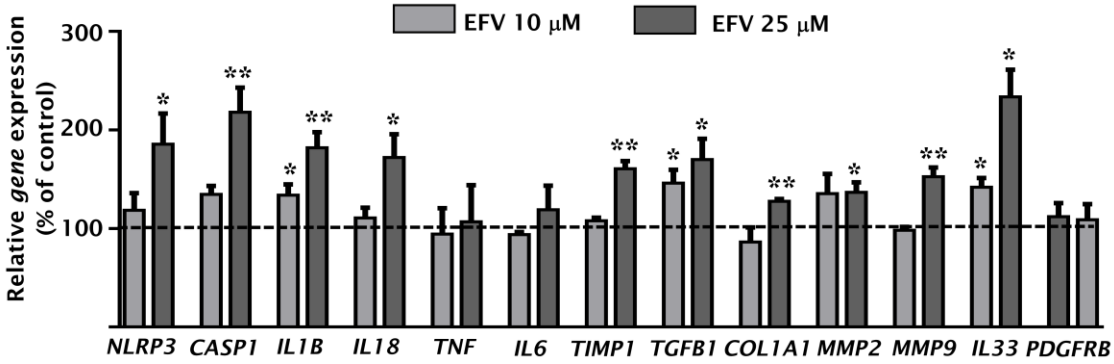

Figure IV.20. Effects of EFV on inflammatory and fibrogenic markers in primary hHSCs. Relative mRNA expression levels of NLRP3 inflammasome-associated markers (NLRP3, caspase-1, IL-1β and IL-18), pro-inflammatory cytokines (TNF-α, IL-6 and IL-33) and fibrosis-related mediators (TIMP-1, TGF-β1, collagen 1α1, MMP-2, MMP-9 and PDGFRB). Data (mean±SEM, n=3) were normalized versus the expression of the housekeeping gene *ACTB*, calculated as percentage of control (untreated cells) and analyzed by one-way ANOVA multiple comparison test followed by a Newman-Keuls test (*p<0.0.5; **p<0.0.1 versus vehicle).

SECTION III: CHARACTERIZATION OF THE EFFECTS OF EFAVIRENZ ON THE FUNCTION AND PHENOTYPE OF MACROPHAGES

IV.10. EVALUATION OF INFLAMMATORY PATHWAYS

An array of genes related to immunity, inflammasome function and cellular stress was performed in U937-derived macrophages treated with EFV, in a similar way as previously done in LX-2 cells. The results obtained showed a reduction in the gene expression of NLRP3 and caspase-1, while ASC (*PYCARD)*, IL-1β and IL-18 were slightly overexpressed. Regarding P2RX7 signaling, we observed an enhanced expression of this purinergic receptor, although mRNA levels of PANX1 were similar to those in vehicle-treated cells. This antiretroviral drug also upregulated two kinases, IRAK1 and RIPK2, which have been traditionally involved in pro-inflammatory responses, and which exert relevant functions in M2 (anti-inflammatory) macrophages. In addition, EFV induced a significant and concentration-dependent overexpression of the anti-inflammatory inflammasome NLRP12 and downregulation of the pro-inflammatory cytokine TNFSF4 (Figure IV.21).

Protein analysis performed by WB showed that EFV did not induce significant changes in the expression of NLRP3 and caspase-1 (p45) in U937-derived macrophages, corroborating the results obtained in the array (Figure IV.22 A). As expected, LPSc (employed to polarize macrophages towards the pro-inflammatory phenotype M1) produced a significant increase in the expression of both proteins, and IL-4 treatment (employed to polarize macrophages towards the anti-inflammatory phenotype M2) did not induce relevant alterations. However, Rot treatment produced a significant decrease in NLRP3 protein levels, but no changes in caspase-1 levels. Due to this potential anti-inflammatory phenotype of EFV-treated macrophages, we decided to analyze the protein expression of the well-known anti-inflammatory transcription factor PPAR-γ. WB experiments revealed a significant and concentration-dependent augmentation of the expression of this protein following incubation with EFV (Figure IV.22 B). As expected, treatment with IL-4 produced a relevant increase of its expression, whereas no changes were induced by LPSc.

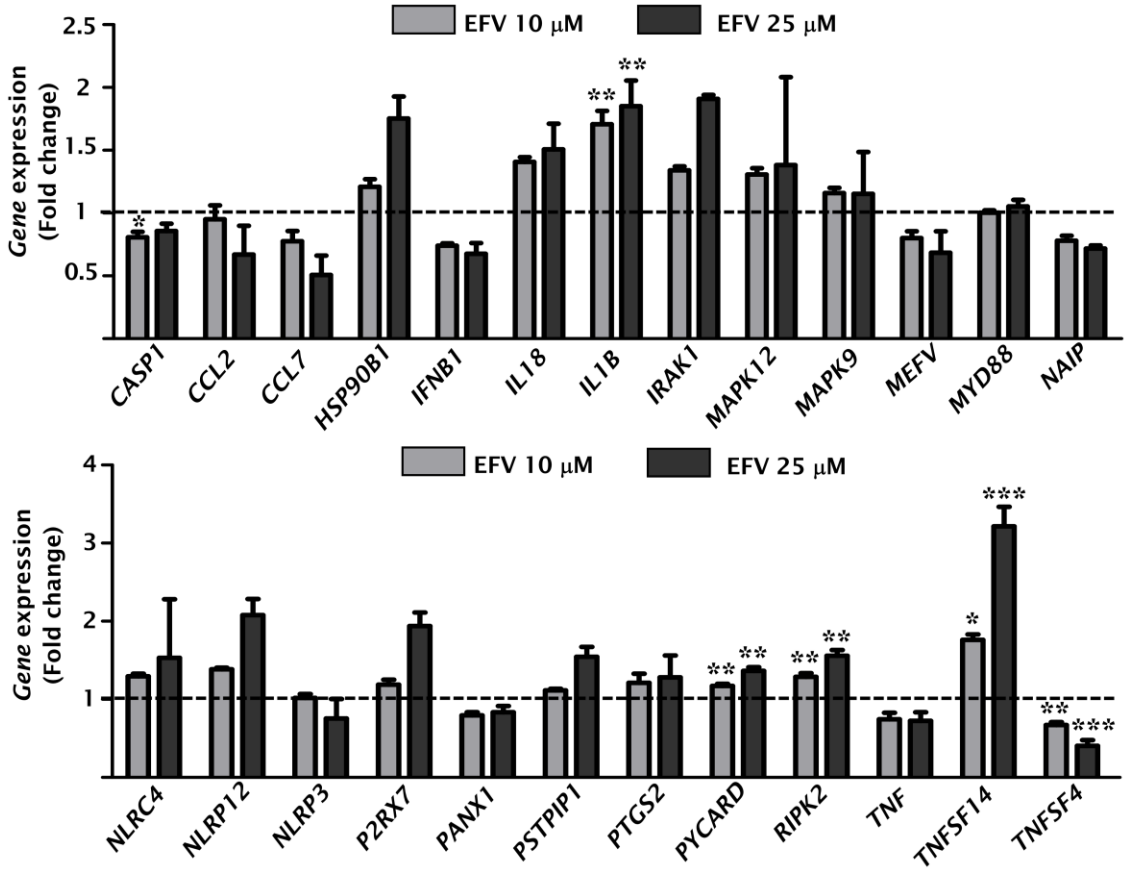

Figure IV.21. PCR array of inflammation and stress-related genes in U937-derived macrophages treated with EFV. The expression of each gene was normalized to the mean of the mRNA of the housekeeping gene *HPRT1*. Data are represented as fold change of the expression with respect to that recorded in the vehicle-treated cells, which was considered 1. Data (mean±SEM, n=3) were analyzed by one-way ANOVA multiple comparison test followed by a Newman-Keuls test (*p<0.05, **p<0.01, ***p<0.001 versus vehicle).

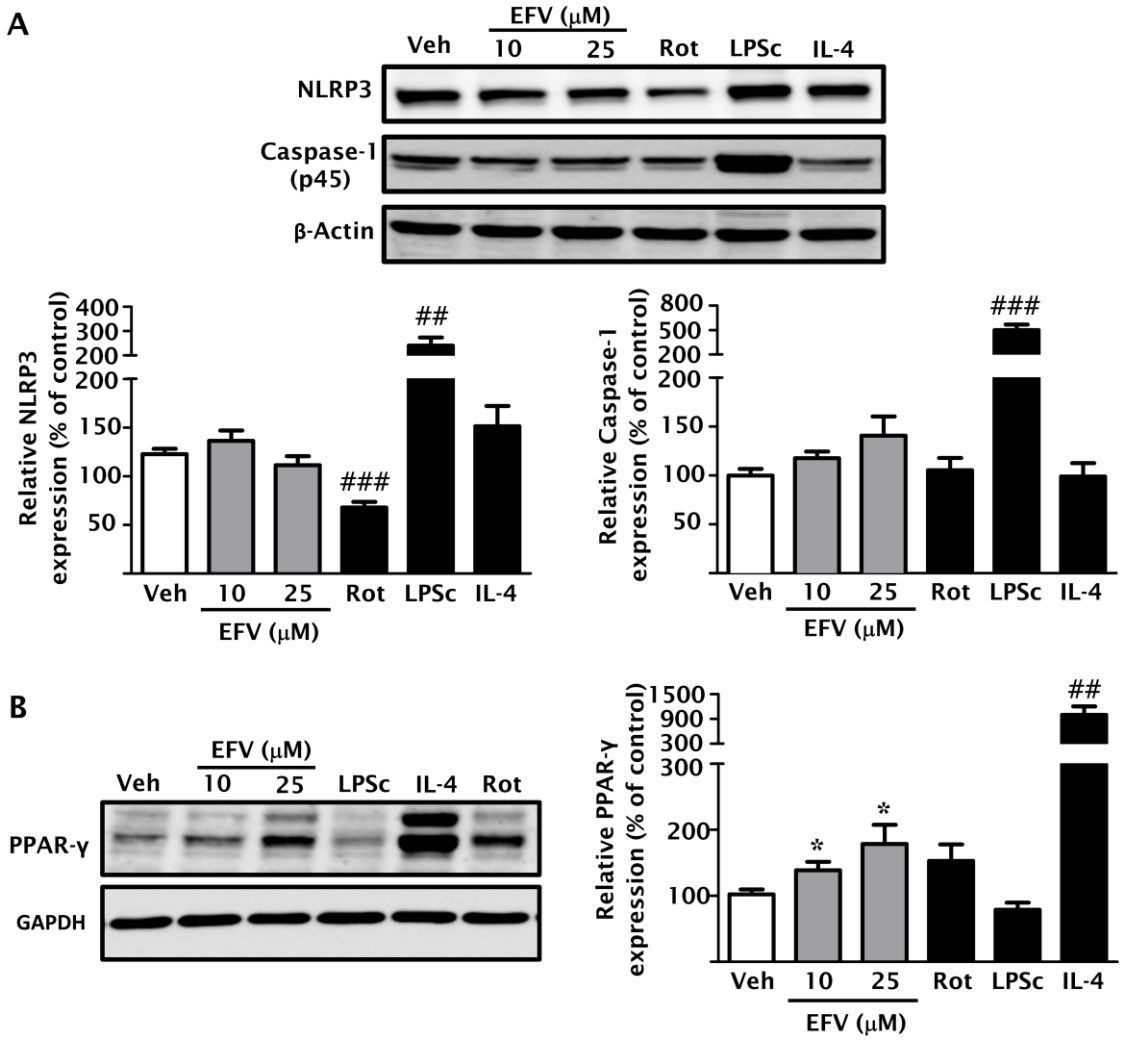

Figure IV.22. Analysis of the expression of inflammation-related proteins in EFV-treated macrophages by WB. Representative images of (A) NLRP3 and caspase-1 (p45, inactive form) and (B) PPAR-γ, and summary of densitometry data. Data (mean±SEM, n=4-8) were calculated as percentage of control (untreated cells) and analyzed by one-way ANOVA multiple comparison test followed by a Newman-Keuls test (*p<0.05 versus vehicle). Positive controls (Rot, LPSc and IL-4) were independently analyzed by Student's t-test (##p<0.01, ###p<0.001 versus control).

IV.11. MACROPHAGE POLARIZATION BY EFAVIRENZ

We analyzed the expression of specific markers of M1 and M2 subtypes in order to determine the influence of EFV in the polarization of U937-derived macrophages. EFV upregulated the transcription of both M1 (*NOS2*, *CD86*, *IL1B*) and M2 (*ARG1*, *MRC1* and *TGFB1*) markers. However, EFV slightly downregulated the gene expression of the cytokine IL-10, which is related to M2 macrophages, and no changes were observed in IL-6 (M1 macrophages)

(Figure IV.23). Overall, these actions in U937-macrophages are suggestive of an anti-inflammatory profile induced by EFV, which may promote the resolution of the initial inflammatory response.

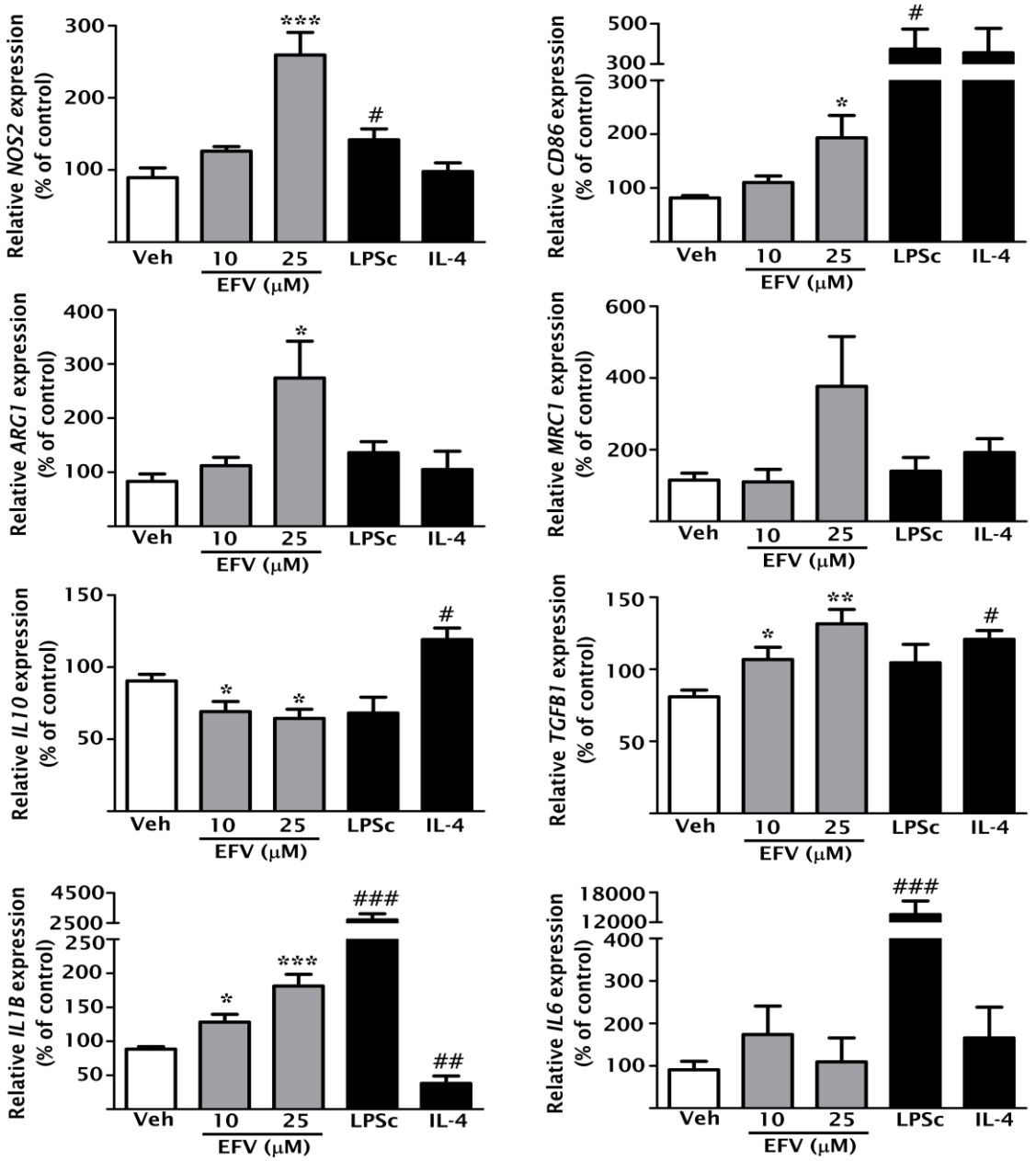

Figure IV.23. Characterization of M1 and M2 markers in U937-derived macrophages treated with EFV. Relative mRNA expression levels of M1 (*INOS/NOS2, CD86, IL1B* and *IL6*) and M2 (*ARG1, MRC1/CD206, IL10* and *TGFB1*) markers analyzed by qRT-PCR. Data (mean±SEM, n=4-6) were normalized versus the expression of the housekeeping gene *ACTB*, calculated as percentage of control (untreated cells) and analyzed by one-way ANOVA multiple comparison test followed by a Newman-Keuls test (*p<0.05, **p<0.01, ***p<0.001 versus vehicle). Positive controls (LPSc and IL-4) were independently analyzed by a Student's *t*-test (#p<0.05, ##p<0.01, ###p<0.001 versus control).

IV.12. EVALUATION OF THE EFFECTS INDUCED BY EFAVIRENZ IN PRIMARY HUMAN KUPFFER CELLS

We analyzed several relevant markers in hKCs in order to assess the reproducibility of the results observed in U937-derived macrophages. qRT-PCR analysis confirmed EFV-induced polarization towards the M2 phenotype as shown by the increase in the expression of M2 markers, such as *CD206/MRC1*, *ARG1* and *IL10*, and the decrease of M1 markers (*NOS2* or *CD86*). In contrast to the results obtained in U937-derived macrophages, EFV significantly upregulated gene expression of *NLRP3*, *TNF* and *IL6*, but did not induce relevant changes in *IL1B* and *TGFB1* (Figure IV.24).

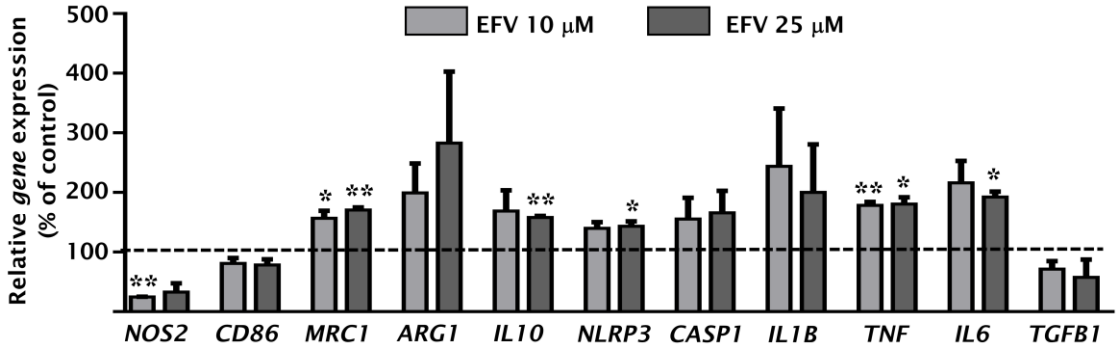

Figure IV.24. Evaluation of EFV-induced effects on macrophage polarization and inflammatory and fibrogenic markers in primary hKCs. Relative mRNA expression levels of markers of polarization and fibrogenesis/inflammation-related genes analyzed by qRT-PCR. Data (mean±SEM, n=2) were normalized versus the expression of the housekeeping gene *ACTB,* calculated as percentage of control (untreated cells) and analyzed by one-way ANOVA multiple comparison test followed by a Newman-Keuls test (*p<0.05; **p<0.01 versus vehicle).

SECTION IV: CHARACTERIZATION OF EFAVIRENZ-INDUCED LIVER INJURY IN A MURINE MODEL

The results obtained *in vitro* in the three cellular populations (hepatocytes, HSC and macrophages) suggested that EFV exerts a dual role in the progression of liver injury. Consequently, we analyzed liver samples of mice administered EFV (24h) to elucidate its effects in an *in vivo* model.

IV.13. ASSESSMENT OF EFAVIRENZ-INDUCED RESPONSE IN THE LIVER

Expression of genes involved in inflammation (*Nlrp3, Casp1, Il1b* and *Tnf*) and fibrosis (*Timp1, Col1a1, Mmp2* and *Tgfb1*) was assessed in whole liver tissue from mice treated with EFV at dosages in accordance with clinically relevant plasmatic concentrations found in humans -10, 25 and 50 μM- (see *III.3.2. In vivo treatments*). Interestingly, the results differed from those obtained in Hep3B and LX-2 cells. Unexpectedly, none of the genes analyzed (except *Tnf*) was significantly upregulated in the liver; many of them were not modified with the lowest dose or even downregulated with the two higher doses (Figure IV.26 A-B). However, EFV did provoke a significant and concentration-dependent increase in liver MPO activity, suggesting an enhanced neutrophil infiltration and inflammatory response (Figure IV.25).

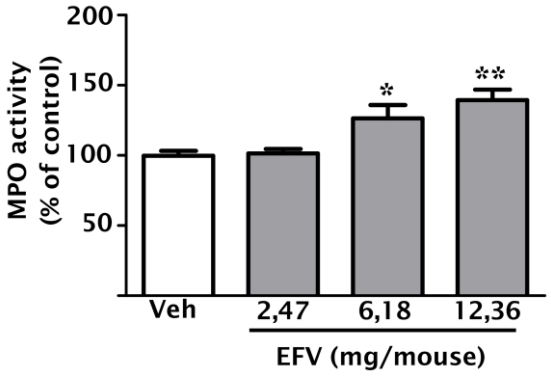

Figure IV.25. Measurement of liver MPO activity in EFV-treated mice. Data (mean±SEM, n=5) were calculated as percentage of untreated mice (considered 100%) and analyzed by one-way ANOVA multiple comparison test followed by a Newman-Keuls test (*p<0.05, **p<0.01 versus vehicle).

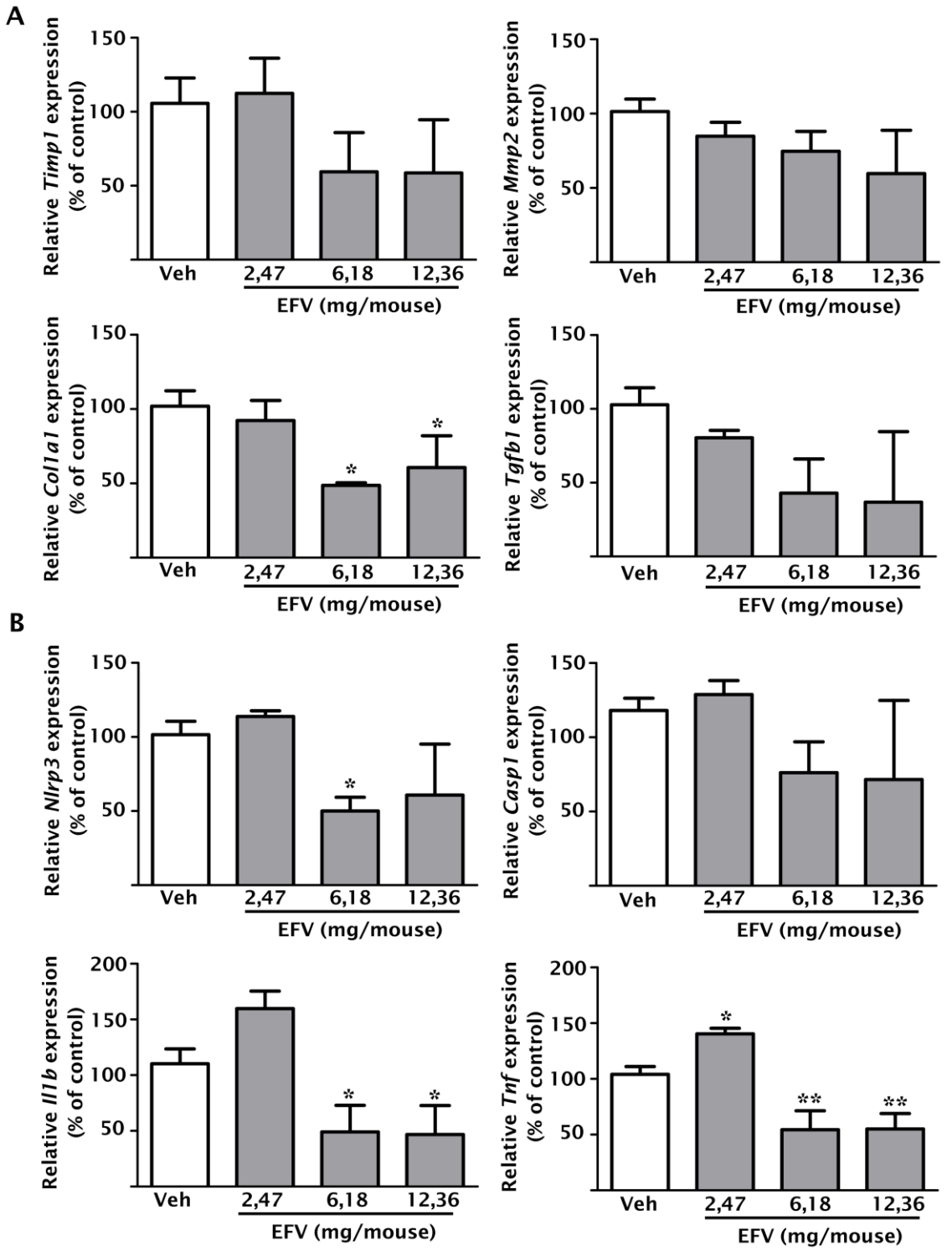

Figure IV.26. Analysis of inflammation- and fibrogenesis-related genes in whole liver tissue from an acute murine model of EFV treatment. qRT-PCR analysis of (A) fibrosis- and (B) inflammation-related genes. Data (mean±SEM, n=4) were normalized versus the expression of the housekeeping gene *Actb*, calculated as percentage of untreated mice (considered 100%) and analyzed by one-way ANOVA multiple comparison test followed by a Newman-Keuls test (*p<0.05, **p<0.01versus vehicle).

IV.14. RELEVANCE OF MACROPHAGES IN THE EFFECTS PRODUCED BY EFAVIRENZ *IN VIVO*

Given that the data obtained *in vivo* were unexpected and contradictory to those shown *in vitro*, we evaluated if this discrepancy was due to a differential effect induced by EFV on hepatocytes, HSCs and macrophages and, specifically, the role of liver macrophages in the response observed *in vivo*.

IV.14.1. Depletion of liver macrophages in a murine model

To evaluate the role played by liver macrophages in the response to EFV *in vivo*, these cells were transiently depleted by intravenous administration of $GdCl_3$, performed 24 h before EFV treatment. The efficiency of the depletion induced by this compound was demonstrated by the reduction of F4/80 expression in the liver, which was assessed by qRT-PCR, IHC and WB (Figure IV.27 A-C).

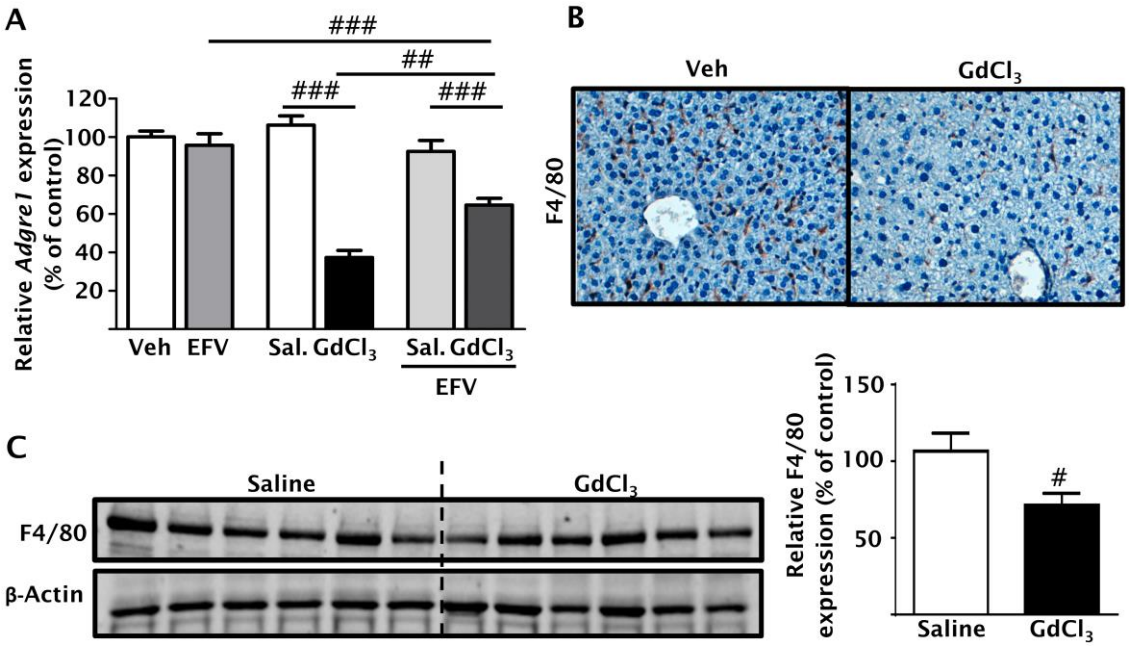

Figure IV.27. Confirmation of macrophage depletion in mice treated with $GdCl_3$. (A) Relative mRNA expression levels of the macrophage marker *Adgre1* (*F4/80*) analyzed by qRT-PCR (n=6). Data were normalized versus those of the housekeeping gene *Actb*. (B) Immunohistochemical analysis of F4/80 in murine liver tissue. Magnification of 20x. (C) Representative WB image of F4/80 with densitometry data (n=5). Data (mean±SEM) were calculated as percentage of untreated mice (considered 100%) and analyzed by a Student's *t*-test (#*p*<0.05, ##*p*<0.01, ###*p*<0.001 versus the respective solvent or treatment).

No significant alterations in F4/80 mRNA levels were induced by EFV treatment (2,47 mg/mouse, dose equivalent to 10 μM); however, this drug significantly increased F4/80 expression when it was administered to mice in which liver macrophages had been depleted (Figure IV.27 A).

IV.14.2. Analysis of macrophage polarization markers *in vivo*

The assessment of M1 (CD86) and M2 (arginase-1, CD206 and CD163) macrophage markers by qRT-PCR in total liver extracts showed a general decrease of their expression, except for arginase-1, in GdCl3-treated mice. The lack of reduction in arginase-1 expression by GdCl3 could be because this protein is also synthetized in hepatocytes as a component of the urea cycle (Nissim et al. 2005; Peters et al. 2008). EFV did not induce significant changes in CD86 and CD163 expression in mice with fully functional macrophages, but it downregulated CD206 and arginase-1 expression. Finally, co-administration of EFV and GdCl3 did not produce significant alterations in the expression of these markers with respect to EFV treatment, although interestingly CD206 and arginase-1 expression were slightly increased, whereas CD86 expression was reduced (Figure IV.28 A). Immunohistochemical analysis of CD206 in murine liver tissue corroborated this analysis, with the difference that EFV seemed to augment this macrophage marker (Figure IV.28 B).

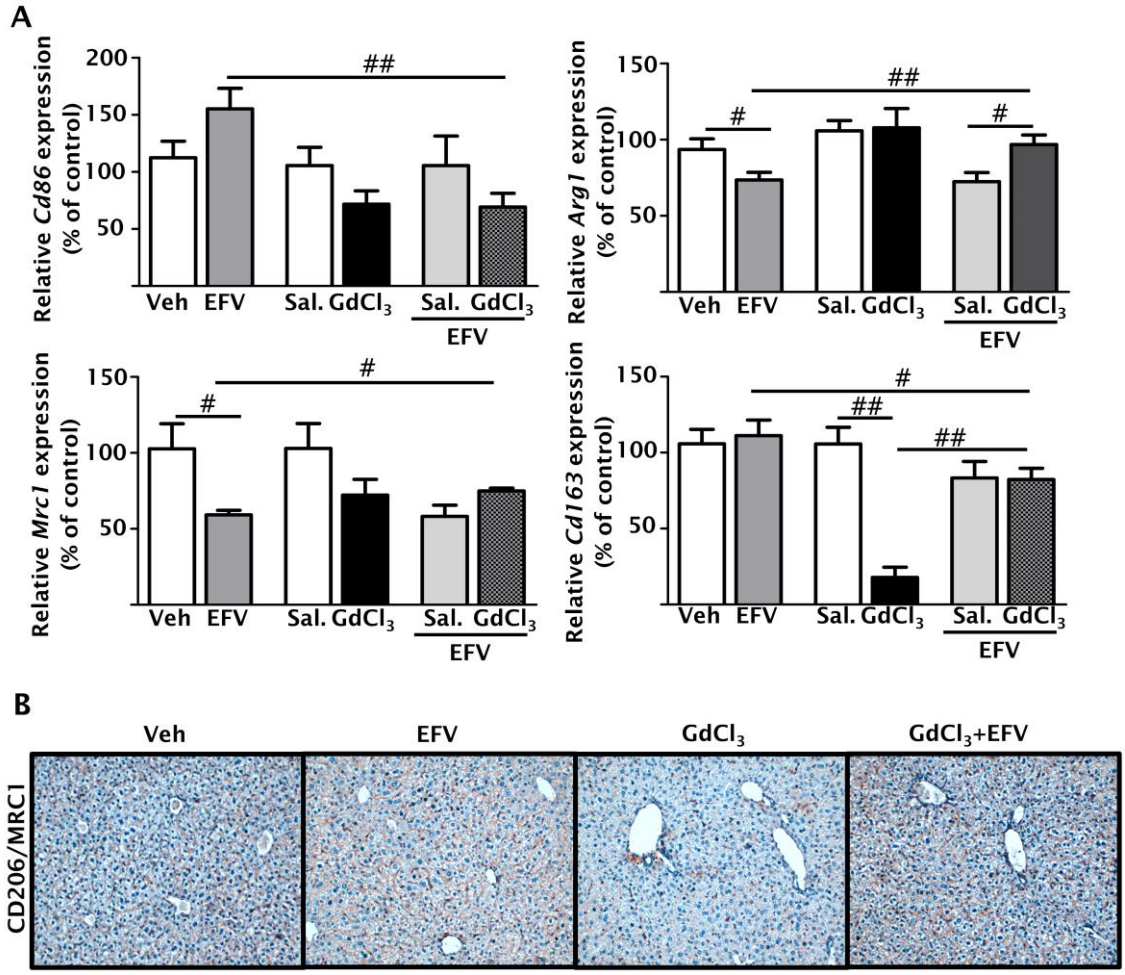

Figure IV.28. Evaluation of macrophage polarization markers *in vivo*. (A) Relative mRNA expression levels of M1 (CD86) and M2 (arginase 1, CD206/MRC1 and CD163) markers in mice co-administered with EFV and $GdCl_3$. Data (mean±SEM, n=3-4) were normalized versus the expression of the housekeeping gene *Actb*, calculated as percentage of untreated mice (considered 100%) and analyzed by a Student's *t*-test (#*p*<0.05, ##p<0.01 versus vehicle or treatment). (B) Representative images of CD206/MRC1 immunostaining in murine liver tissue. Magnification 20x.

IV.14.3. Characterization of efavirenz-induced inflammatory and fibrogenic responses in livers from macrophage-depleted mice

We administered the lowest EFV dose, which did not induce significant changes in any of the parameters previously analyzed (see Figure IV.26), to mice previously administered $GdCl_3$ in order to assess how EFV modulated hepatic inflammatory and fibrogenic pathways in this model. qRT-PCR analysis in whole liver tissue from mice with macrophage depletion revealed that EFV-induced actions on inflammatory and fibrogenic responses were similar to those obtained in hepatocytes and HSCs *in vitro*. Regarding fibrogenesis, co-administered mice exhibited a significant upregulation of several genes compared to EFV-treated mice, such as *Col1a1, Acta2, Vim, Timp1* and *Mmp2,* but *Tgfb1* expression was not enhanced (Figure IV.29). Importantly, mRNA expression levels of all these fibrosis-related markers were significantly increased in $GdCl_3$-administered mice. This enhanced expression could be related to the fact that macrophages play an important function in favoring an anti-inflammatory and anti-fibrogenic microenvironment during liver homeostasis (e.g. phagocytizing apoptotic hepatocytes or secreting anti-inflammatory cytokines as IL-10), even in physiological conditions (Wynn and Barron 2010; Sica et al. 2014). Thus, depletion of this population and associated beneficial actions is likely to induce some injury in this tissue. EFV also provoked a significant increase in the expression of pro-inflammatory cytokines, such as TNF-α, and IL-33, and iNOS in the liver of macrophage-depleted mice. However, no relevant modifications were observed in the expression of NLRP3 inflammasome. Furthermore, expression of the anti-inflammatory cytokine IL-10 was significantly downregulated by EFV only in the animals treated with $GdCl_3$, while the transcription factor PPAR-γ, involved in anti-inflammatory responses, was upregulated (Figure IV.30).

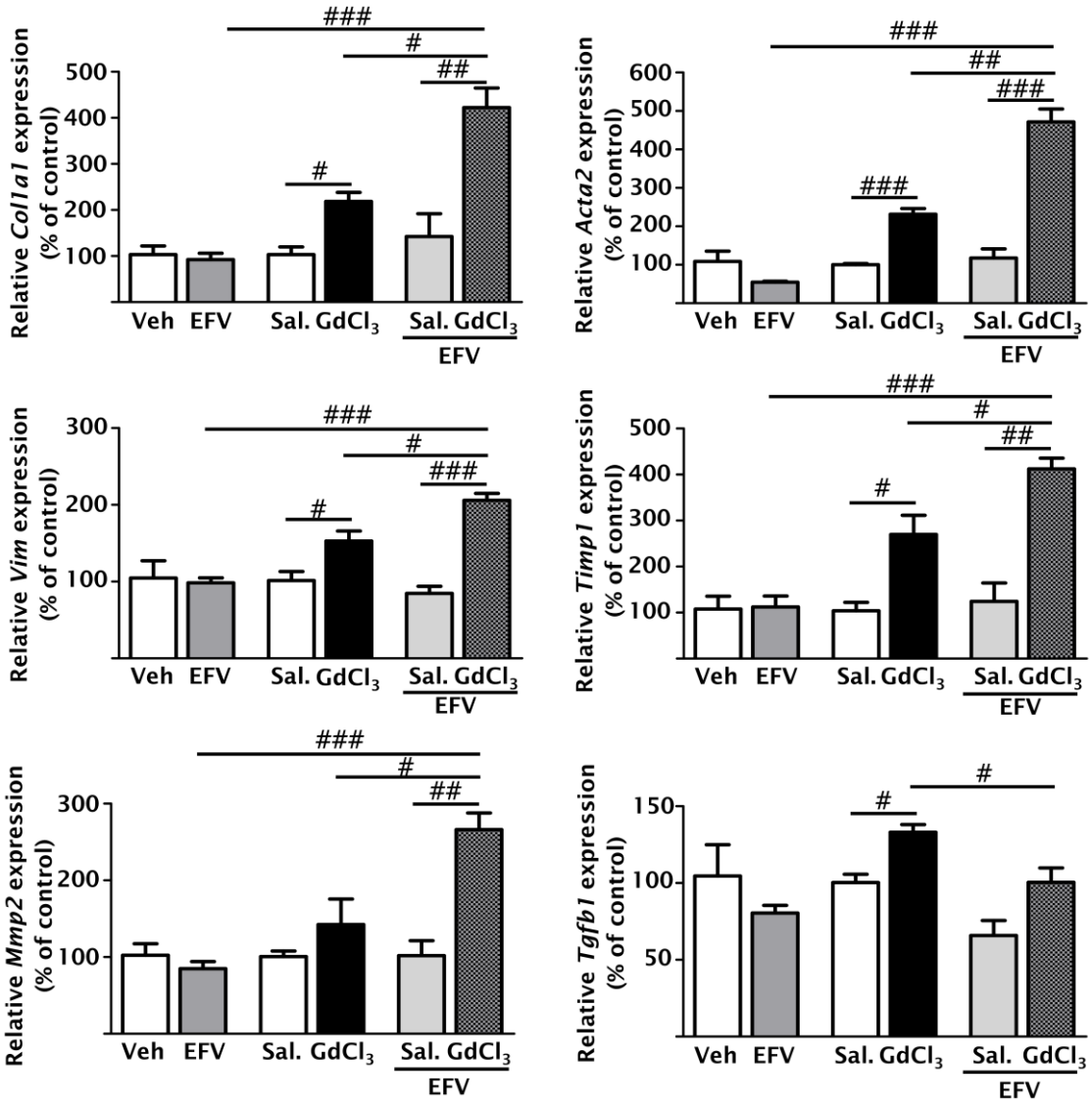

Figure IV.29. Analysis of the expression of fibrogenic markers in mice administered $GdCl_3$ and/or EFV. qRT-PCR analysis of fibrosis-related markers (collagen 1α1, α-SMA, vimentin, TIMP-1, MMP-2 and TGF-β1). Data (mean±SEM, n=4-5) were normalized versus the housekeeping gene *Actb,* calculated as percentage of untreated mice (considered 100%) and analyzed by a Student's *t*-test (#*p*<0.05, ##*p*<0.01, ###*p*<0.001 versus the respective solvent or treatment).

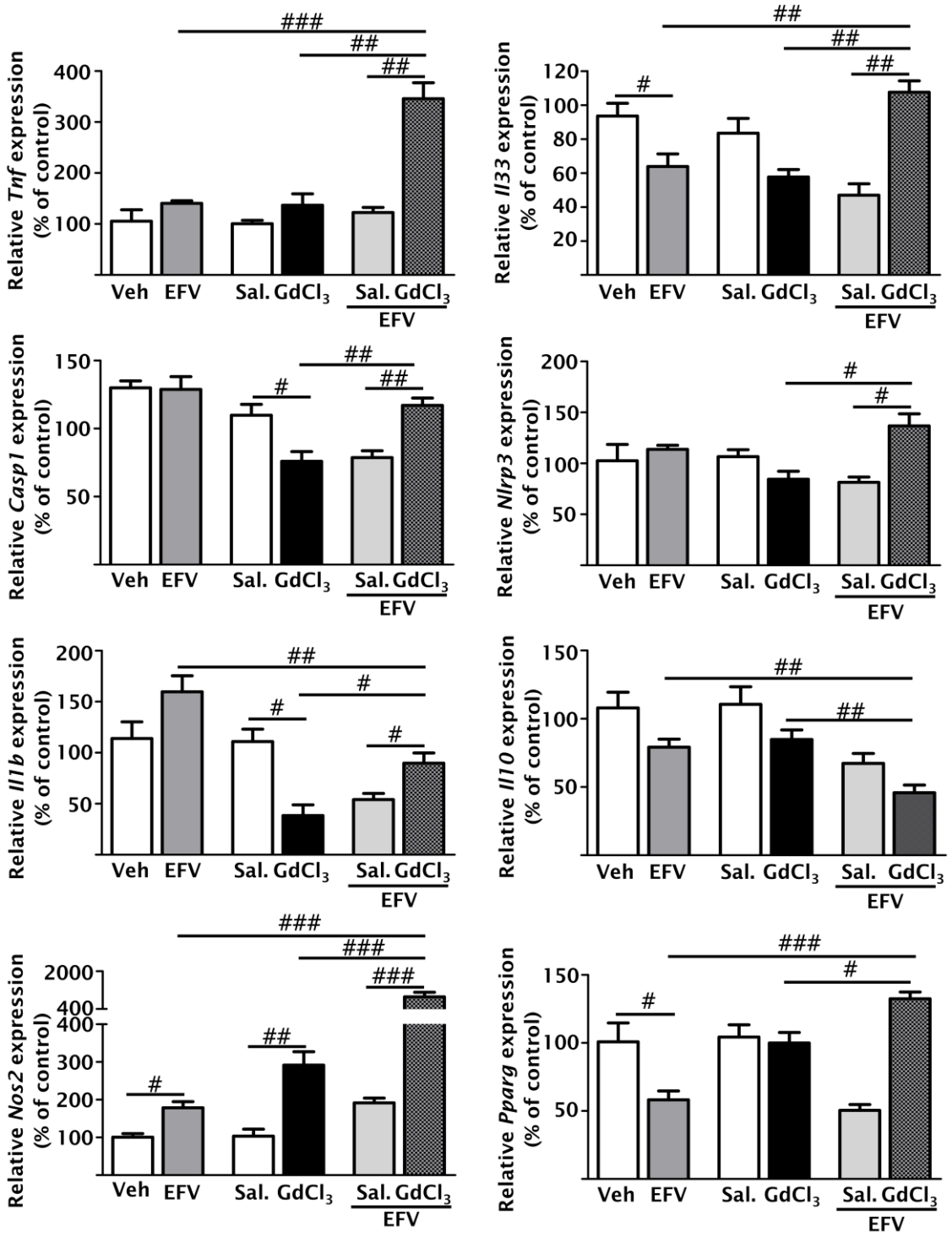

Figure IV.30. Analysis of the expression of markers linked to inflammation in EFV-treated mice with macrophage depletion. qRT-PCR analysis of inflammation-related markers (TNF-α, IL-33, caspase-1, NLRP3, IL-1β, IL-10, iNOS and PPAR-γ). Data (mean±SEM, n=4-5) were normalized versus the housekeeping gene *Actb*, calculated as percentage of untreated mice (considered 100%) and analyzed by a Student's *t*-test (#p<0.05, ##p<0.01, ###p<0.001 versus the respective solvent or treatment).

In addition, MPO activity assay confirmed an enhanced inflammatory response in mice treated with $GdCl_3$ and EFV (Figure IV.31). Taken together, the data obtained in the murine model with depletion of macrophages strengthen the hypothesis that liver macrophages play a key role in the resolution of the EFV-induced damage, counteracting the inflammatory and fibrogenic pathways activated in hepatocytes and HSCs.

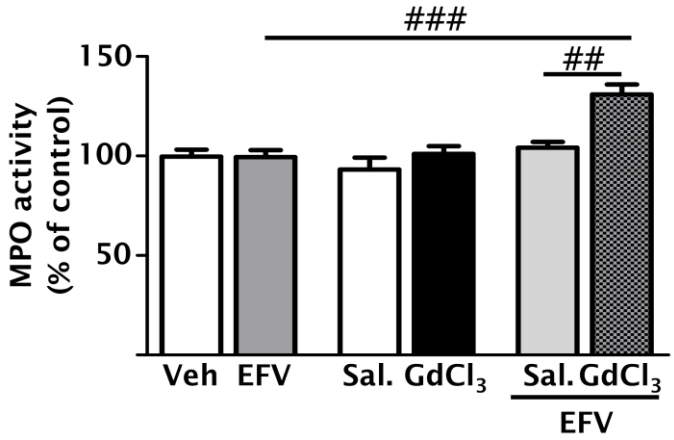

Figure IV.31. Measurement of liver MPO activity in EFV- and $GdCl_3$-treated mice. Data (mean±SEM, n=5) was calculated as percentage of untreated mice (considered 100%) and analyzed by a Student's *t*-test (##*p*<0.01, ###*p*<0.001 versus the respective solvent or treatment).

Finally, in order to prove whether cytokines released from M2 macrophages could alleviate the inflammatory response in hepatocytes, we decided to employ conditioned medium from M2 U937-derived macrophages to treat Hep3B cells incubated with EFV (25 μM). The analysis of inflammation-related genes by qRT-PCR, specifically *NLRP3*, *CASP1*, *IL1B* and *IL6*, showed a reduction after 24 h of treatment with EFV in M2 conditioned medium when compared to the M0 (resting macrophages) conditioned medium; however, *TNF* was slightly overexpressed (Figure IV.32).

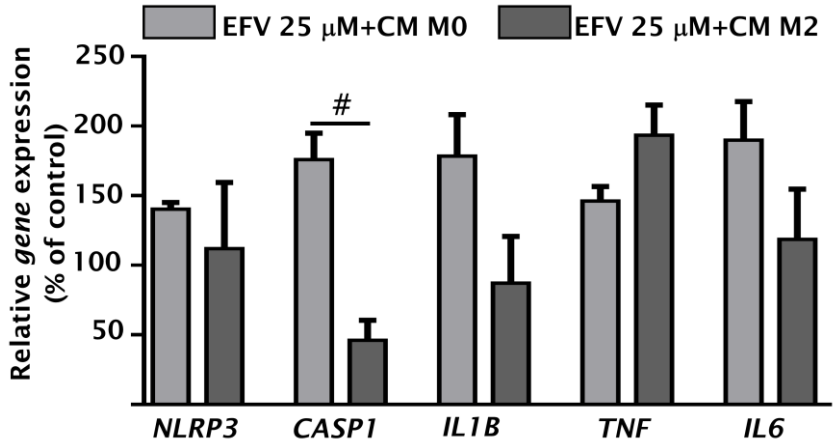

Figure IV.32. Evaluation of the expression of inflammatory genes in Hep3B cells treated with EFV in the presence of conditioned medium from M2 macrophages. Relative mRNA expression levels of inflammatory markers (NLRP3, caspase-1, IL-1β, TNF-α and IL-6) analyzed by qRT-PCT. Data (mean±SEM, n=3) were normalized versus the expression of the housekeeping gene *ACTB*, calculated as percentage of control (untreated cells) and analyzed by a Student's *t*-test (#*p*<0.05 versus the comparable treatment).

SECTION V: ROLE OF p62 IN THE RESPONSE TO CELLULAR STRESS INDUCED BY EFAVIRENZ IN HEPATOCYTES

p62 is a multifunctional protein involved in redox homeostasis, autophagic clearance and regulation of inflammatory response. As previously stated, EFV treatment induces mitochondrial dysfunction and ER stress in human hepatic cells, an effect paralleled by enhanced autophagy. In addition, the data previously showed in this thesis have revealed an induction of the inflammatory response in hepatocytes. Therefore, we decided to explore the role of p62 in the cellular response to stress induced by this NNRTI in hepatocytes.

IV.15. EVALUATION OF p62 EXPRESSION

IV.15.1. Analysis of p62 protein levels in hepatocytes

WB analysis of p62 in whole-cell extracts from Hep3B cells treated with EFV, and with several mitochondrial (Rot and CCCP) and ER (TG) stressors, showed that this antiretroviral drug promoted a significant and concentration-dependent increase p62. Both Rot and TG, but not CCCP, enhanced p62 protein levels (Figure IV.33 A). These results were confirmed by immunocytochemical analysis of this protein in EFV-treated Hep3B cells (Figure IV.33 B). In order to elucidate the timing of this effect, we performed a time course (4, 8, 24 and 48 h) of p62 protein expression in EFV-exposed Hep3B cells. The results obtained by WB showed that p62 content was already increased following 4 h of treatment, peaked at 24 h and continued enhanced after 48 h, although in the latter time point p62 expression was lower compared to that detected at 24 h (Figure IV.33 C).

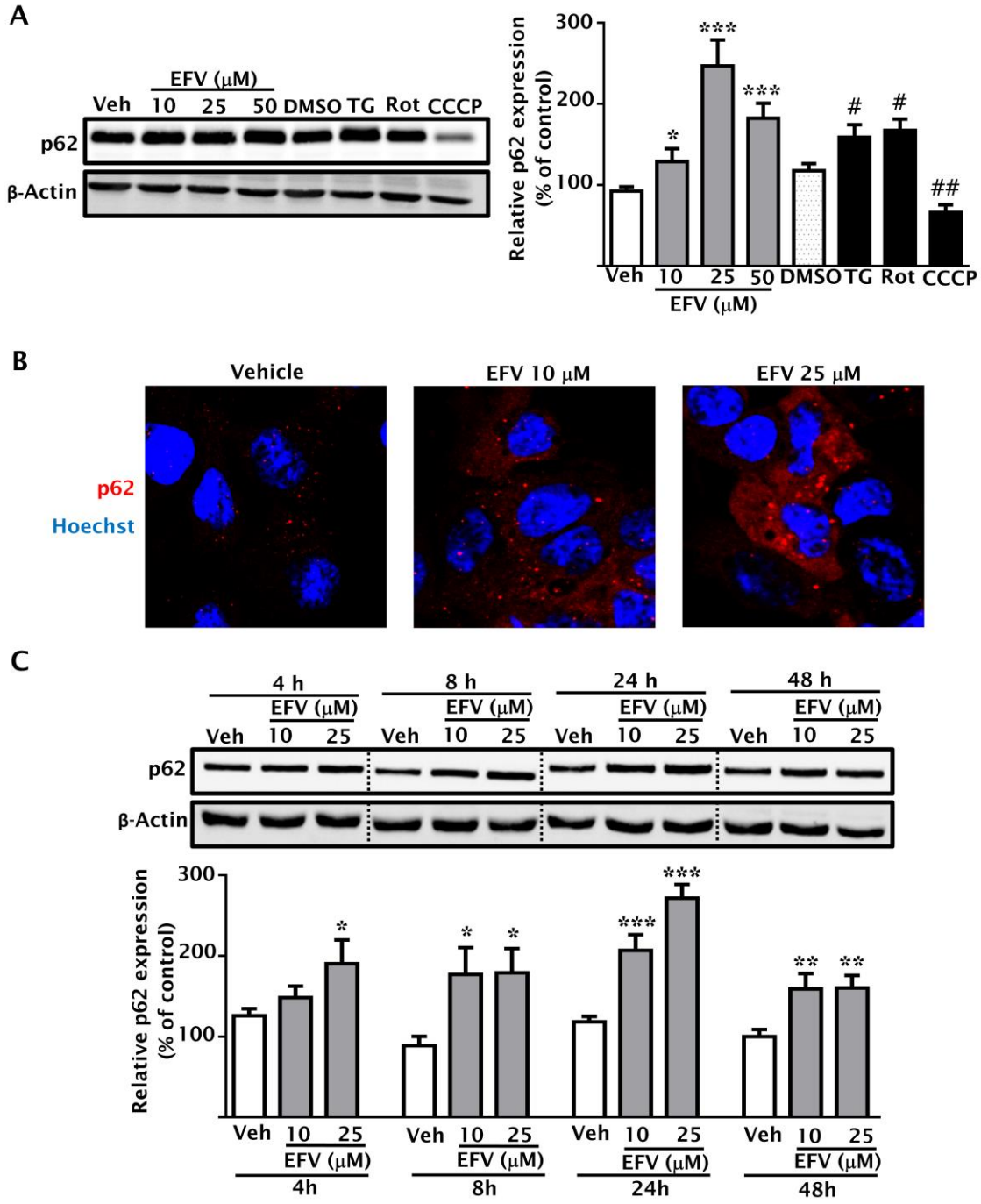

Figure IV.33. Analysis of p62 protein expression in EFV-treated Hep3B cells. (A) Representative WB image of p62 and densitometry data following (n=6). (B) Representative images of confocal microscopy: Hoechst 33342 (blue) and p62 antibody (red). Magnification 40x (n=3). (C) Representative WB image of p62 (time course of expression) with densitometry (n=6). Data (mean±SEM) were calculated as percentage of the control (untreated cells) and analyzed by one-way ANOVA multiple comparison test followed by a Newman-Keuls test (*p<0.05, **p<0.01, ***p<0.001 versus the respective vehicle). Positive controls (Rot, TG and CCCP) were independently analyzed by a Student's t-test (#p<0.05, ##p<0.01 versus their solvent-DMSO-).

IV.15.2. Characterization of p62 expression in rho^o cells

Growing evidence has shown that p62 is localized in mitochondria under physiological conditions where it performs critical roles in mitochondrial dynamics, bioenergetics and genome integrity (Du et al. 2009a, 2009b; Seibenhener et al. 2013). Taking this into account and considering EFV-induced mitochondrial toxicity, we thought that this organelle may be involved in p62 upregulation. In order to prove this hypothesis, we generated Hep3B ρ^o cells, which are characterized by the presence of not fully functional mitochondria. The ρ^o phenotype was confirmed by O_2 consumption analysis in cells employing a Clark-type O_2 electrode, which showed a severe drop in the mitochondrial respiration of Hep3B ρ^o cells, maintaining 15% of the basal rate recorded in wild-type Hep3B cells (Figure IV.34 A). Additionally, analysis of mitochondrial proteins in total cellular extracts by WB demonstrated an important reduction on the subunit II of the mitochondrial complex IV and a reduction in the expression of ND1 (a complex I subunit), both mitochondrial DNA-encoded proteins, whereas no alterations were found in the expression of CV-β and porin, both encoded by nuclear genes (Figure IV.34 B). Protein analysis in whole cell extracts from this cellular model revealed that the increase in p62 expression induced by EFV and TG was substantially reduced, and completely abolished in Rot-treated cells, thus suggesting mitochondrial involvement in the upregulation of p62 (Figure IV.35).

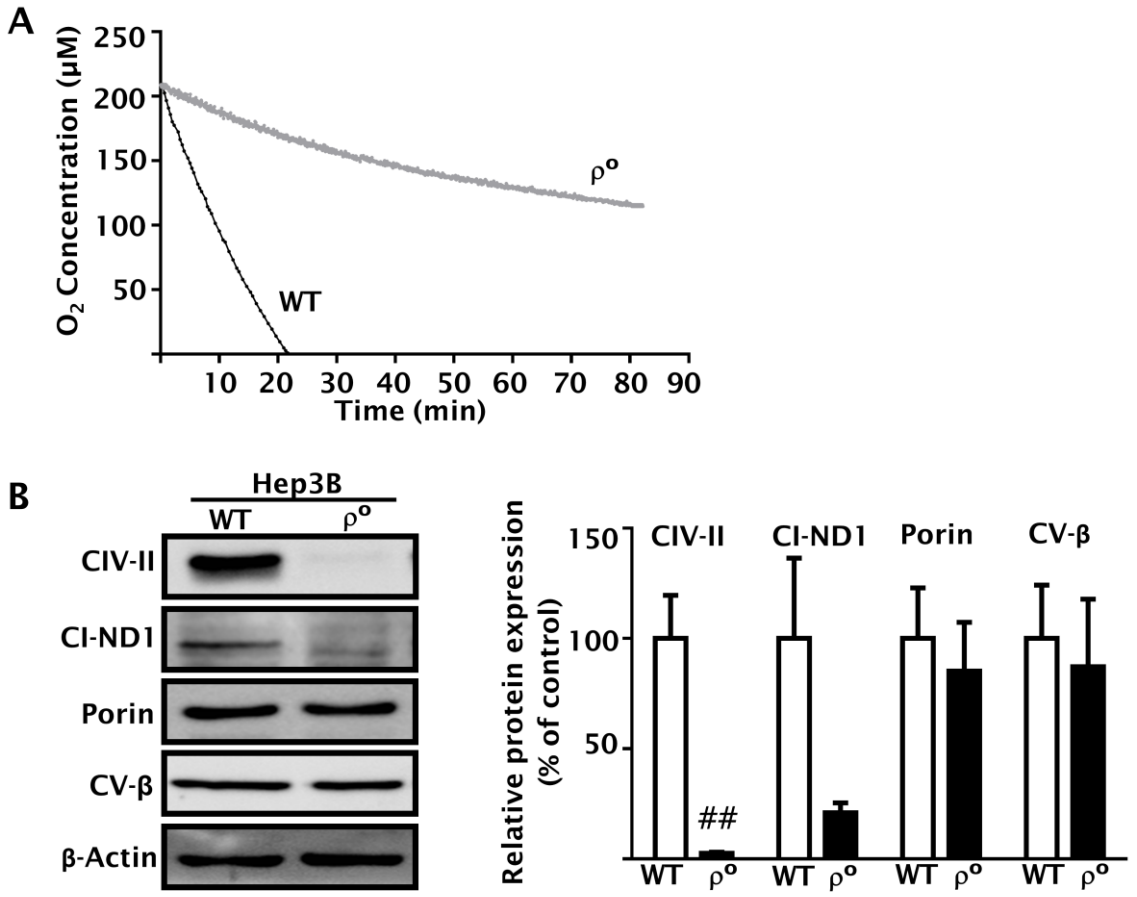

Figure IV.34. Characterization of Hep3B ρº phenotype. (A) Electrochemical measurement of O_2 consumption. Representative trace showing O_2 consumption in wild-type and ρº cells detected in cells using Clark-type O_2 electrode (4 million cells were employed in each experiment). (B) Representative WB images and densitometry data of mitochondrial proteins (complex IV subunit II, complex I subunit ND1, complex V subunit β and porin) in total cell extracts of wild-type and ρº cells. Data (mean±SEM, n=4) were analyzed by a Student's *t*-test (##*p*<0.01 versus WT cells).

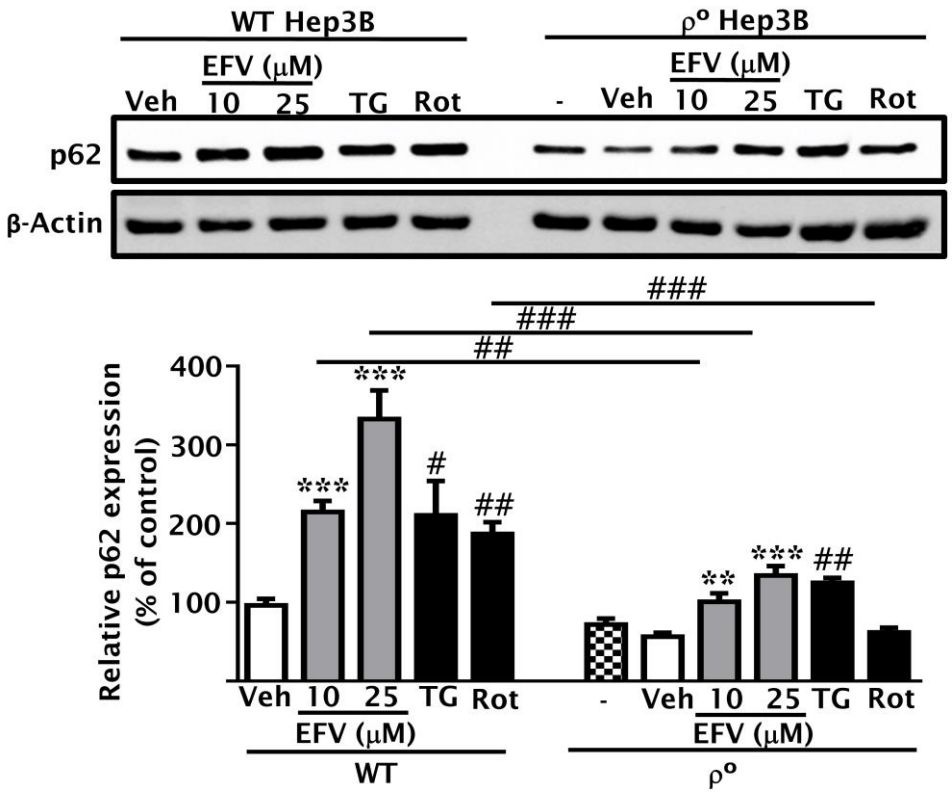

Figure IV.35. Evaluation of p62 protein in Hep3b ρº cells. Immunoblot analysis of p62 showing representative images and summary of densitometry data in wild-type and ρº cells treated with EFV or several cellular stressors. Data (mean±SEM, n=4) were calculated as a percentage of untreated wild-type cells (considered 100%) and analyzed by a one-way ANOVA multiple comparison test followed by a Newman-Keuls test (***p*<0.01 ******p*<0.001 versus vehicle). Comparison between wild-type and ρº cells, and positive controls (TG and Rot) were independently analyzed by a Student's *t*-test (#*p*<0.05 ##*p*<0.01, ###*p*<0.001 versus ρº cells or untreated cells).**

IV.15.3. Evaluation of *SQSTM1* gene expression and its connection with p62 protein levels in hepatocytes

qRT-PCR analysis revealed that EFV and TG induced a significant increase in mRNA levels of p62. Of note, CCCP did not produce changes in the gene expression of p62, which is in accordance with its lack of effect on protein levels (Figure IV.36 A). Experiments performed in primary human hepatocytes showed a similar EFV-induced increase of p62 mRNA levels (Figure IV.36 B). Furthermore, WB analysis of Hep3B cells co-treated with EFV and ActD, an inhibitor of gene transcription, did not display an enhanced p62 protein

expression, indicating that the induction of p62 is regulated at the transcriptional level (Figure IV.36 C).

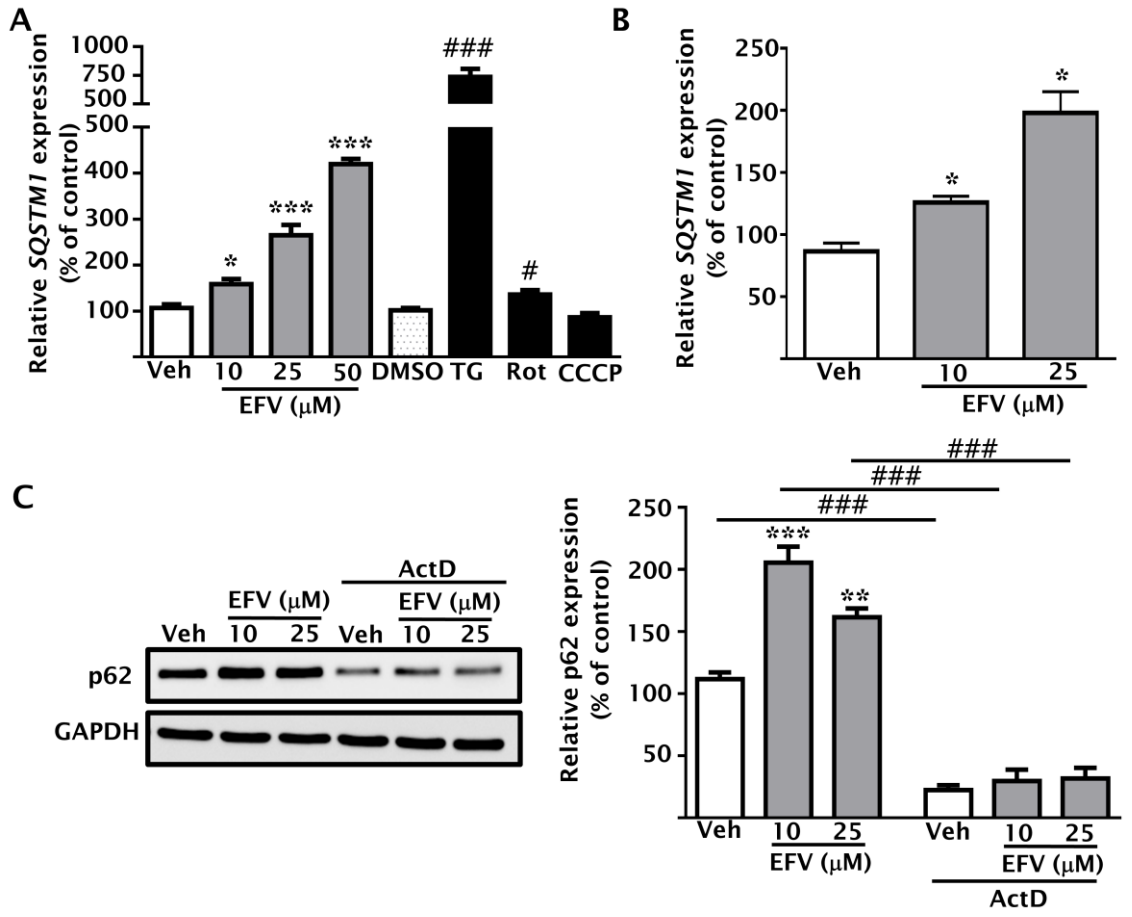

Figure IV.36. Analysis of *SQSTM1* expression and its connection with p62 protein levels. Relative mRNA expression levels of *SQSTM1* in (A) Hep3B cells and (B) primary human hepatocytes analyzed by qRT-PCR. Data were normalized versus those obtained with the housekeeping gene *ACTB* (n=2-4). (C) Representative WB image of p62 and summary of densitometry data in Hep3B cells co-treated with EFV and ActD (n=4). Data (mean±SEM) were calculated as percentage of control (untreated cells) and analyzed by one-way ANOVA multiple comparison test followed by a Newman-Keuls test (*p<0.05, **p<0.01, ***p<0.001 versus the vehicle). Comparison between absence and presence of ActD and the analysis of the positive controls (TG, Rot, and CCCP) were performed independently by a Student's *t*-test (#p<0.05; ###p<0.001 versus ActD or solvent –DMSO-).

IV.15.4. Characterization of p62 expression in other cell types

Although the study of p62 has been focused on hepatocytes, preliminary experiments were also performed to evaluate the actions of EFV in other cell types employed in previous studies with this NNRTI, such as LX-2 cells and U937-derived macrophages. WB and qRT-PCR experiments confirmed that this drug also induced both mRNA and protein levels of p62 in LX-2 cells (Figure IV.37). Additionally, analysis of p62 protein expression in EFV-treated U937-derived macrophages revealed similar effects to those obtained in hepatocytes and LX-2 cells (Figure IV.38). These results suggest that EFV-induced p62 overexpression is a general mechanism in hepatic cells.

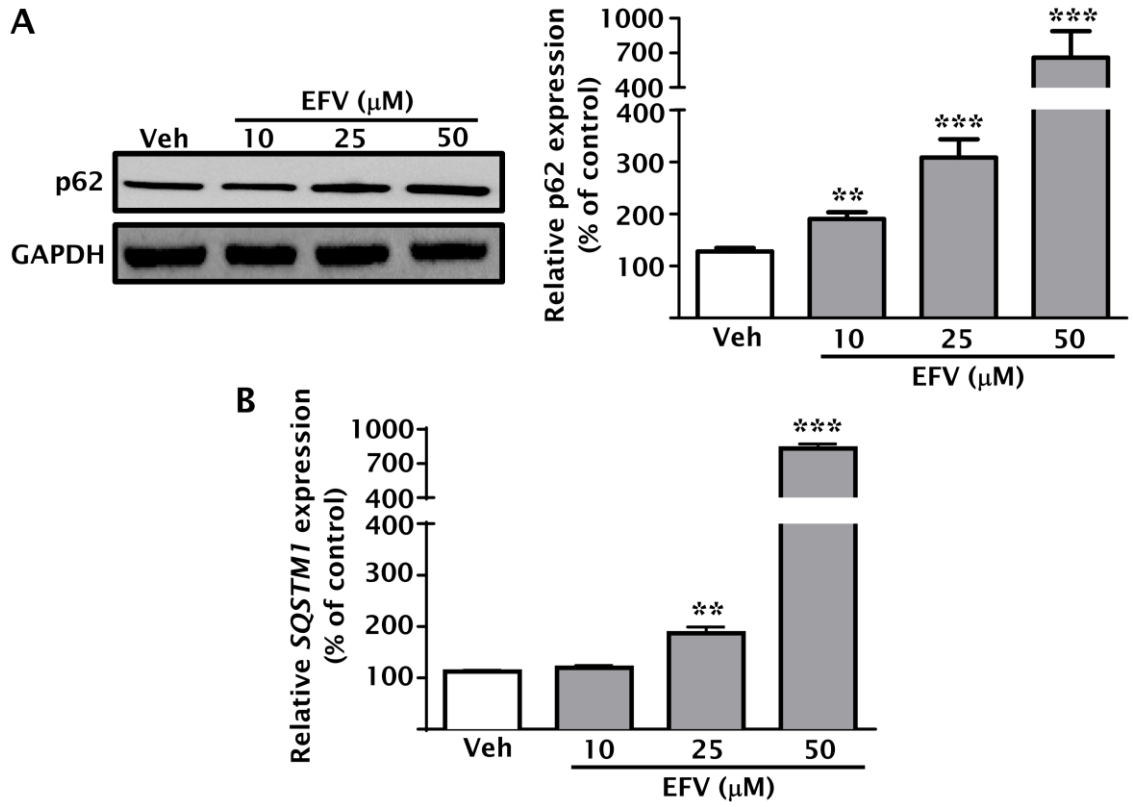

Figure IV.37. Evaluation of p62 expression in EFV-treated LX-2 cells. (A) Representative image of p62 and summary of densitometry data (n=5). (B) Relative mRNA expression levels of *SQSTM1* analyzed by qRT-PCR (n=3) and normalized versus the expression of the housekeeping gene *ACTB*. Data (mean±SEM) were calculated as percentage of control (untreated cells) and analyzed by one-way ANOVA multiple comparison test followed by a Newman-Keuls test (p<0.01, ***p<0.001 versus vehicle).**

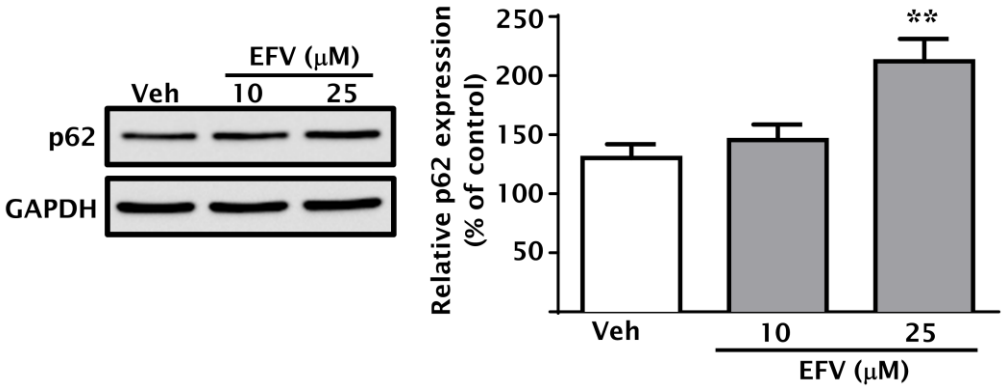

Figure IV.38. Analysis of p62 expression in EFV-treated U937-derived macrophages. Representative WB image of p62 and summary of densitometry. Data (mean±SEM, n=7) were calculated as percentage of control (untreated cells) and analyzed by one-way ANOVA multiple comparison test followed by a Newman-Keuls test (p<0.01 versus vehicle).**

IV.16. EVALUATION OF ANOTHER AUTOPHAGIC CARGO RECEPTOR: NBR1

Our next aim was to analyze whether the changes found in the p62 expression could be also detected in other proteins related to p62 function, such as NBR1. As p62, it is a selective autophagy substrate and cargo receptor for degradation of ubiquitinated proteins by autophagy (Johansen and Lamark 2011; Lippai and Low 2014), and displays similar domains (Xu et al. 2015). In order to explore the effect of EFV on NBR1 expression, we treated Hep3B cells with this drug and the cellular stressors TG, Rot and CCCP. WB (Figure IV.39 A) and qRT-PCR (Figure IV.39 B) analysis revealed that EFV also induced a significant and concentration-dependent increase in NBR1 expression, although less severe than that recorded with p62. Regarding the control cell stressors, TG enhanced NBR1 expression in the same manner as p62; however, Rot and CCCP did not produce significant changes. EFV-induced effects in the gene expression of NBR1 were corroborated in primary human hepatocytes (Figure IV.39 C).

Although EFV induced similar alterations in NBR1 expression to those observed with p62, for following experiments we decided to focus on p62 due to its pivotal functions in mitochondria physiology, ER stress response and regulation of inflammation.

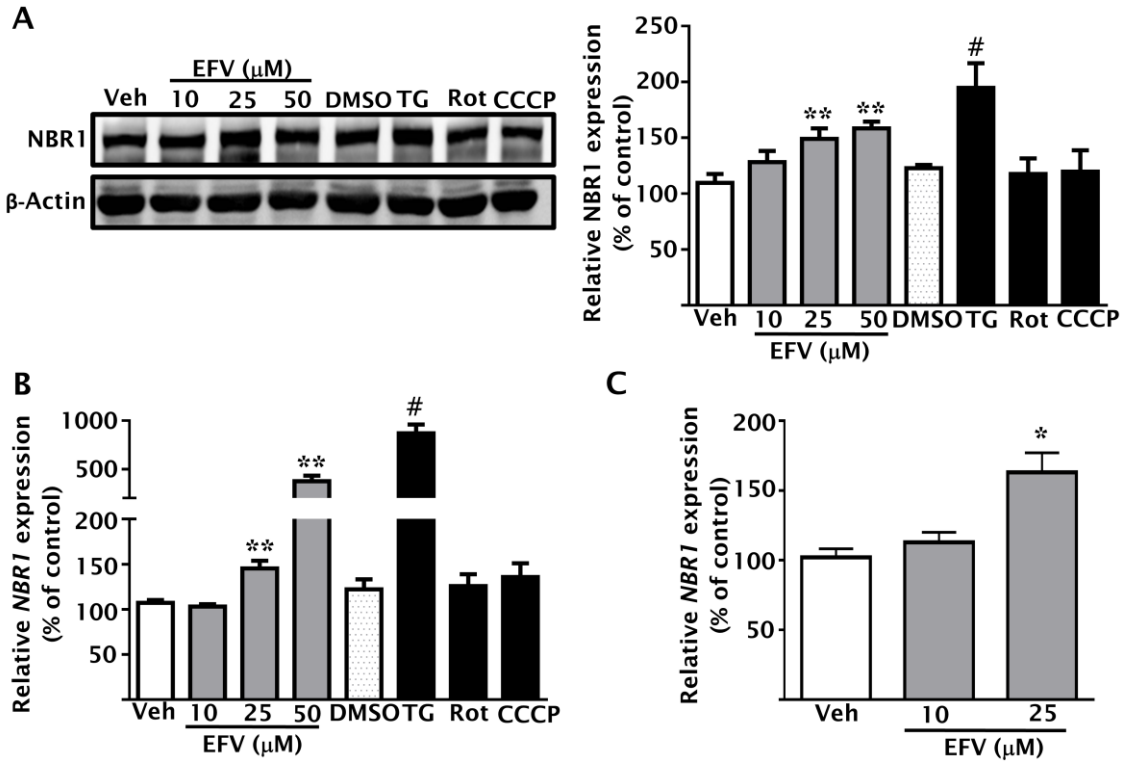

Figure IV.39. Analysis of NBR1 expression in EFV-treated hepatic cells. (A) Representative WB image of NBR1 and summary of densitometry data (n=8) in Hep3B cells. (B, C) Relative mRNA expression levels of NBR1 in (B) Hep3B cells (n=5) and (C) primary human hepatocytes (n=2) analyzed by qRT-PCR and normalized versus the gene housekeeping *ACTB*. Data (mean±SEM) were calculated as percentage of control (untreated cells) and analyzed by one-way ANOVA multiple comparison test followed by a Newman-Keuls test (*p<0.05, **p<0.01 versus vehicle). Positive controls (TG, Rot and CCCP) were independently analyzed by a Student's *t*-test (#p<0.05 versus the respective solvent –DMSO-).

IV.17. CELLULAR LOCALIZATION OF p62 UPON TREATMENT WITH EFAVIRENZ

Having demonstrated that p62 levels were modified by EFV in whole-cell extracts and in order to confirm the important function of mitochondria in the p62 expression in our model, we explored the levels of this protein in mitochondria-enriched fractions, comparing them to those in cytosolic fractions from Hep3B cells. The purity of these fractions was assessed by analyzing protein expression of porin (a mitochondrial outer membrane protein) and β-actin (a cytoskeletal protein). Interestingly, EFV induced an increase of p62 protein expression in both extracts, although this increase was

greater in the mitochondrial fraction when compared to the cytosolic. Regarding the other cellular stressors, Rot only increased the levels of p62 in the mitochondrial fraction, whereas TG did not induce relevant changes in the expression of this protein in neither extract. As suggested by qRT-PCT analysis, CCCP did not lead to an increase in p62 levels; in fact, a significant reduction was found both in mitochondria-enriched and cytosolic fractions (Figure IV.40).

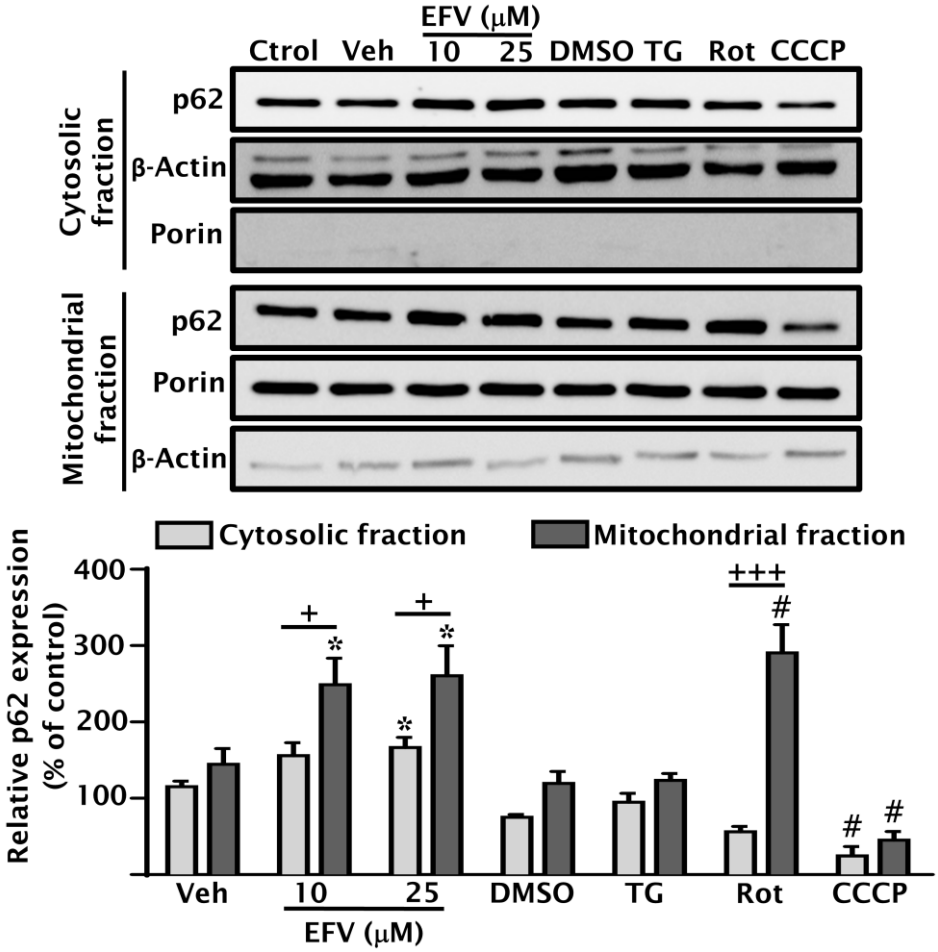

Figure IV.40. Determination of the subcellular localization of p62 protein. Representative WB images of p62 and summary of densitometry data in mitochondria-enriched and cytosolic fractions obtained from Hep3B cells treated with EFV, TG, Rot and CCCP. β-Actin and porin were employed as housekeeping proteins for mitochondria-enriched and cytosolic extracts, respectively. Data (mean±SEM, n=4) were calculated a percentage of untreated cells (considered 100% in both fractions) and analyzed by one-way ANOVA multiple comparison test followed by a Newman-Keuls test (*p<0.05 versus the vehicle). TG, Rot and CCCP were independently analyzed by a Student's t-test (#p<0.05 versus DMSO). Data of cytosolic versus mitochondrial fractions were analyzed by a two-way ANOVA with the post hoc Sidak's test multiple comparison test (+p<0.05, +++p<0.001).

IV.18. REGULATION OF p62 EXPRESSION IN HEPATOCYTES TREATED WITH EFAVIRENZ

IV.18.1. Role of Keap1-Nrf2 pathway in p62 expression

Nrf2, one of the major master regulators against antioxidant responses, is constantly degraded in non-stressed cells by the proteasome due to the function of its binding partner, Keap1, an adaptor ubiquitin ligase. Importantly, p62 is involved in the activation of the Keap1-Nrf2 pathway through the selective autophagy of Keap1, and *SQSTM1* is one of the gene targets of Nrf2, resulting in a regulatory positive-feedback loop (Inoue et al. 2015; Katsuragi et al. 2015). To determine whether EFV can activate this pathway in hepatocytes, we analyzed protein expression of Keap1 and Nrf2 in cytosolic and nuclear extracts from Hep3B cells treated with this antiretroviral drug. WB assays showed that EFV produced a significant and concentration-dependent decrease in Keap1 levels in the cytosolic fraction, whereas it did not induce the nuclear translocation of Nrf2 (Figure IV.41), suggesting that Keap1-Nrf2 pathway does not play a relevant role neither in the defense mechanism against EFV-induced oxidative stress nor in the regulation of p62 expression after 24 h of treatment.

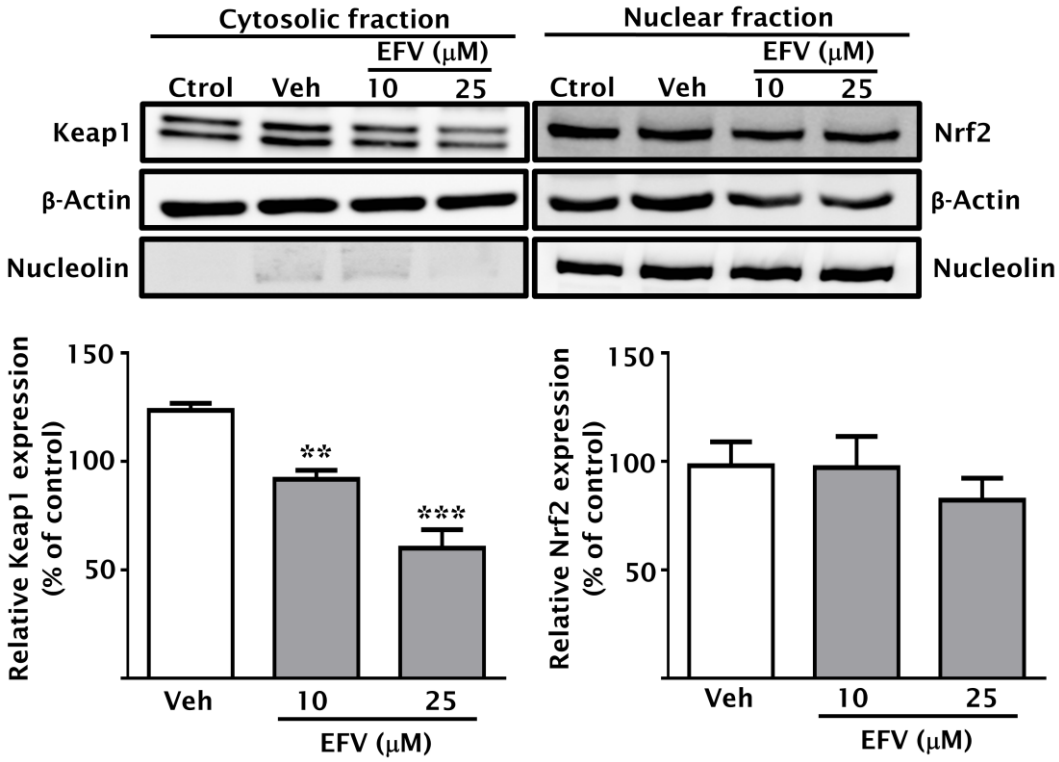

Figure IV.41. Analysis of Keap1-Nrf2 pathway in EFV-treated Hep3B cells. Representative WB images of Keap1 and Nrf2 analyzed in cytosolic and nuclear fraction, respectively, from cells treated with EFV, and summary of densitometry data. β-actin and nucleolin were employed as housekeeping proteins for cytosolic and nuclear fraction, respectively. Data (mean±SEM, n=4-8) were calculated as percentage of untreated cells (considered 100% for both extracts) and analyzed by one-way ANOVA multiple comparison test followed by a Newman-Keuls test (p<0.01, ***p<0.001 versus vehicle).**

IV.18.2. Implication of endoplasmic reticulum stress in p62 expression

As mentioned above, our team have demonstrated that EFV provokes ER stress in hepatocytes, as showed in Figure IV.42 A, paralleled to an increase in cytosolic Ca^{2+} concentration (Apostolova et al. 2013). We speculated that this Ca^{2+} increment could participate in p62 upregulation. In order to explore this hypothesis, Hep3B cells were treated with EFV, TG or Rot in absence or presence of Ca^{2+} chelator BAPTA. qRT-PCR (Figure IV.42 B) and WB (Figure IV.42 C) analysis showed that Ca^{2+} is involved in the enhancement of p62 expression triggered by EFV or TG, as indicated by the partial reversal of this increase in

presence of BAPTA. However, the upregulation of the *SQSTM1* expression induced by Rot was not reversed by BAPTA.

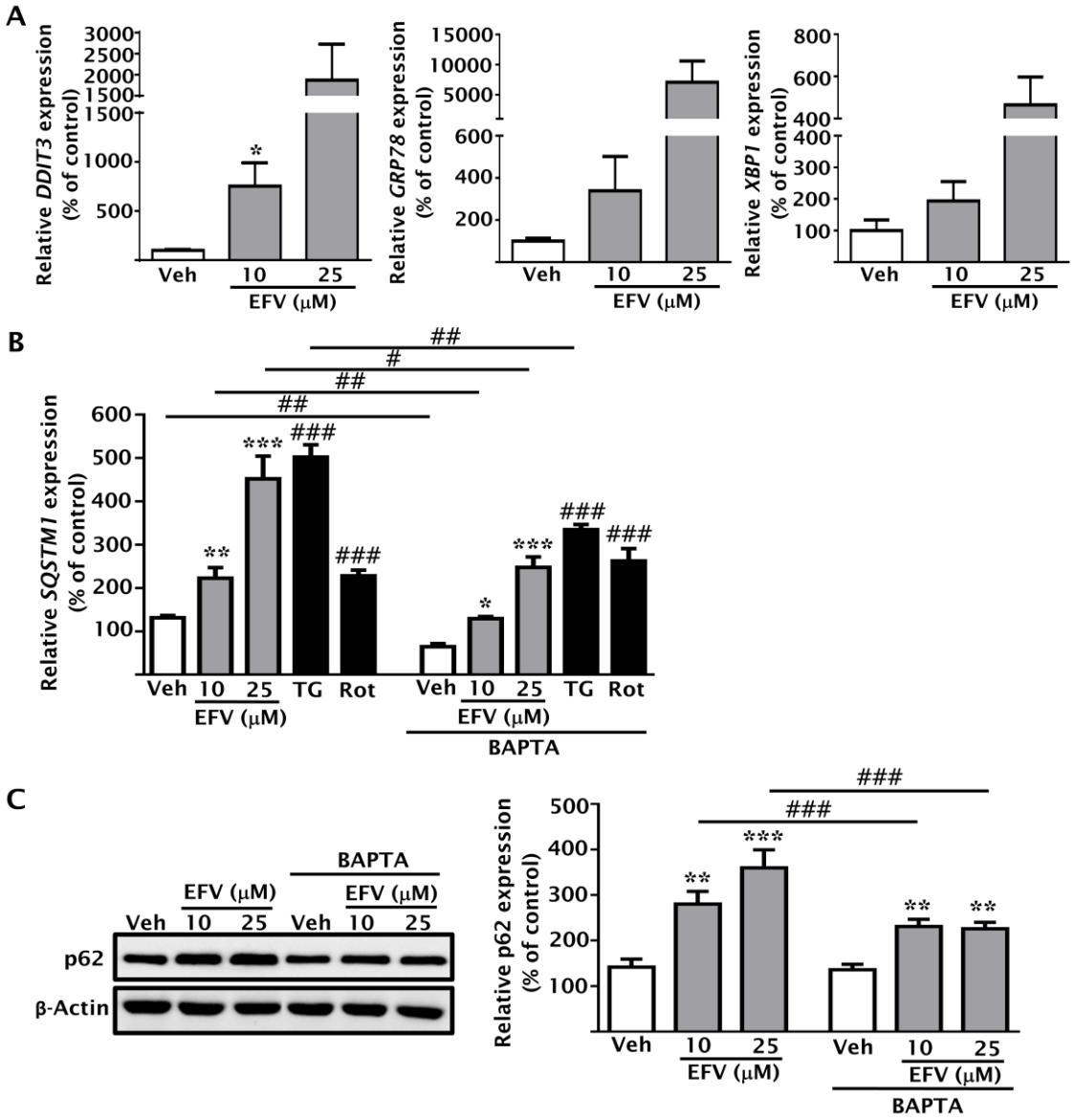

Figure IV.42. Evaluation of the participation of intracellular Ca^{2+} in the p62 expression in EFV-treated Hep3B cells. Relative mRNA expression levels of (A) ER stress markers (*DDIT3, GRP78, XBP1*), and (B) *SQSTM1* in Hep3B cells treated with EFV, TG or Rot in absence or presence of BAPTA (qRT-PCR). Data (A and B) were normalized versus the housekeeping gene *ACTB*. (C) Representative WB image of p62 and summary of densitometry data in EFV-treated cells in absence or presence of BAPTA. Data (mean±SEM, n=4-6) were calculated as percentage of control (untreated cells), and analyzed by one-way ANOVA multiple comparison test followed by a Newman-Keuls test (*p<0.05; **p<0.01; ***p<0.001 versus vehicle). Absence versus presence of BAPTA, and positive controls (TG and Rot) were independently analyzed by a Student's *t*-test (#p<0.05, ##p<0.01, ###p<0.001 versus control or BAPTA).

Next, we assessed whether enhanced p62 expression was related to the transcription factor CHOP, which is activated by both ER stress and oxidant stimuli, and p62 is one of its direct target genes (Han et al. 2013). *CHOP/DDIT3* was transiently silenced by means of siRNA in Hep3B cells and we studied the actions induced by EFV, TG and Rot. Importantly, the increment of p62 protein was considerably attenuated in Hep3B cells with silenced expression of *CHOP*, an effect observed with all the stimuli tested, pointing to a CHOP-mediated upregulation of p62 in our model (Figure IV. 43).

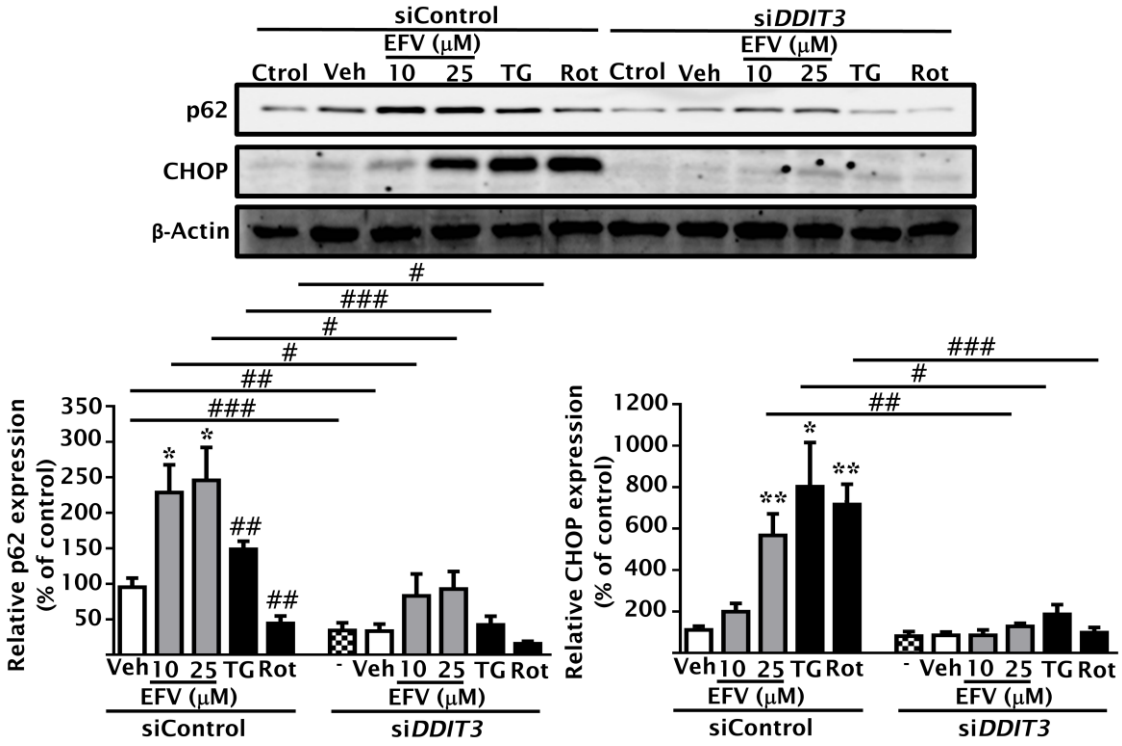

Figure IV.43. Characterization of the role of CHOP in the upregulation of p62 expression. Representative WB images of p62 and CHOP, and summary of densitometry data in Hep3B cells transiently transfected with siControl or si*DDIT3*. Data (mean±SEM, n=4) were expressed as a percentage of untreated siControl cells (considered 100%) and analyzed by one-way ANOVA multiple comparison test followed by a Newman-Keuls test (p*<0.05, ***p*<0.01 versus vehicle). Positive controls (TG and Rot), and siControl versus si*DDIT3* were independently analyzed by a Student's *t*-test (#*p*<0.05, ##*p*<0.01, ###*p*<0.001 versus control or si*DDIT3*).**

IV.18.3. Analysis of the *SQSTM1* promoter

Having assessed the effects induced by EFV on the transcription factors NF-κB (see Figure IV.1 and 2), Nrf2 and CHOP, we decided to perform a ChIP assay in

order to analyze whether these proteins interact with *SQSTM1* promoter after incubation with this drug in Hep3B cells. The results confirmed the implication of CHOP in the modulation of p62 transcription by this NNRTI, and ruled out a significant role of NF-κB and Nrf2, classical regulators of p62 (Figure IV.44).

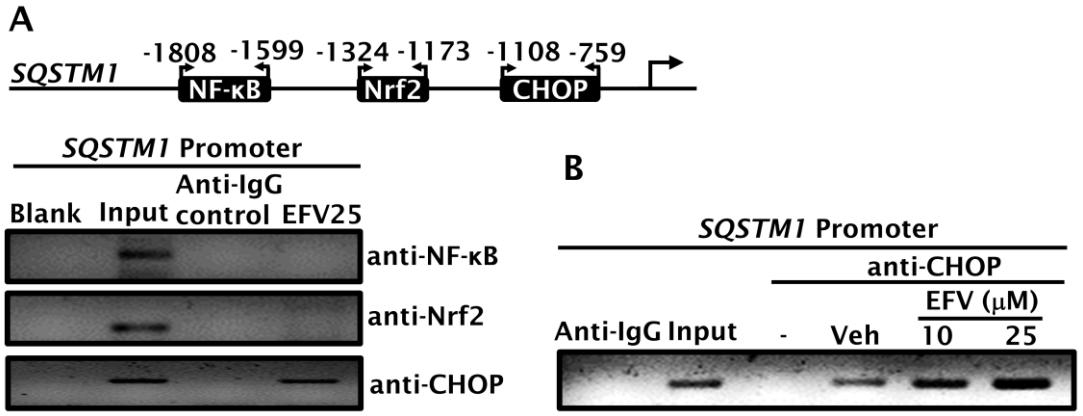

Figure IV.44. ChIP assay of *SQSTM1* promoter. (A) Representative image of semi-quantitative PCR after ChIP assay performed in EFV (25 μM)-treated Hep3B cells (lower panel). Chromatin was immunoprecipitated with anti-NF-κB, anti-Nrf2 or anti-CHOP antibodies, and PCR assay was performed to amplify the immunoprecipitated chromatin employing primers flanking the binding site of NF-κB, Nrf2 or CHOP on the *SQSTM1* promoter (upper panel). (B) Representative image showing the CHOP-*SQSTM1* promoter interaction in EFV-treated Hep3B cells. A non-related antibody anti-IgG and input control were used as a negative and a positive control, respectively.

IV.19. INVOLVEMENT OF AUTOPHAGY IN THE INCREASE OF p62 EXPRESSION

As previously stated, EFV (10 and 25 μM) induces autophagy in cultured hepatocytes (as shown in Figure IV.45 A and Apostolova et al. 2011). Given that p62 is selectively degraded by autophagy and traditionally employed as a marker of this mechanism (Moscat et al. 2007), we decided to explore the participation of p62 in the EFV-promoted autophagy. With this aim, we analyzed the levels of LC3 in Hep3B cells with transient silencing of *SQSTM1* by means of siRNA. We also employed TG as positive control, as it has exhibited similar effects to EFV in autophagy (Ogata et al. 2006; Grotemeier et al. 2010). WB analysis in whole-cell extracts showed that p62 silencing did not alter LC3 expression in EFV- or TG-treated Hep3B cells, and it did not affect basal levels of this autophagy marker (Figure IV.45 B). The lack of correlation between p62

expression and autophagy was also proved employing 3MA, as this inhibitor had no significant effects on the gene expression of p62 in EFV-treated Hep3B cells (Figure IV.45 C).

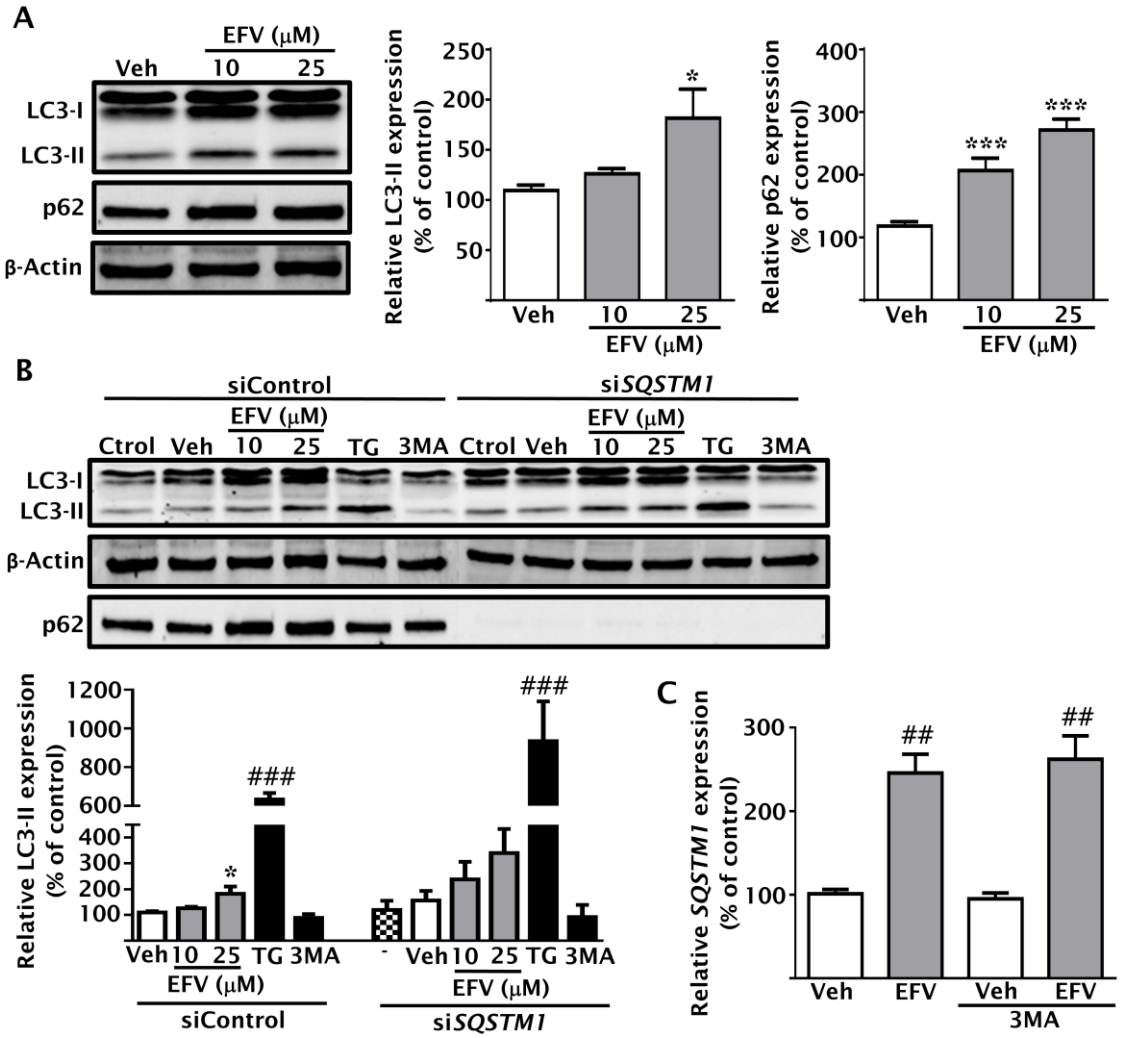

Figure IV.45. Analysis of the participation of autophagy in p62 upregulation in EFV-treated Hep3B cells. (A) Representative WB images of LC3 and p62, and summary of densitometry data. (B) Representative WB image of LC3 with densitometry data of LC3-II in cells transiently transfected with siControl or si*SQSTM1*. Untreated siControl cells were considered 100%. (C) Relative mRNA expression levels of *SQSMT1* were analyzed by qRT-PCR, in absence or presence of 3MA, and normalized versus the housekeeping gene *ACTB*. Data (mean±SEM, n=4) were calculated as percentage of control (untreated cells), and analyzed by on-way ANOVA multiple comparison test followed by a Newman-Keuls test (*p<0.05, ***p<0.001 versus the vehicle). TG and 3MA, siControl versus si*SQSTM1*, and absence or presence of 3MA were independently analyzed by a Student's *t*-test (##p<0.01, ###p<0.001 versus control, si*SQSTM1* or presence of 3MA).

IV.20. PARTICIPATION OF p62 IN ENDOPLASMIC RETICULUM AND MITOCHONDRIAL FUNCTION IN HEPATOCYTES

IV.20.1. Role of p62 in the endoplasmic reticulum stress induced by efavirenz

In order to further explore the role of p62 in the ER stress and UPR response induced by EFV in hepatocytes, we analyzed representative parameters of this cellular response in Hep3B cells with transiently silenced *SQSTM1.* Protein analysis by WB showed that p62 silencing did not significantly affect the upregulation of CHOP or GRP78, proteins that are enhanced by EFV treatment in a similar manner to the classic ER stressor, TG (Figure IV.46).

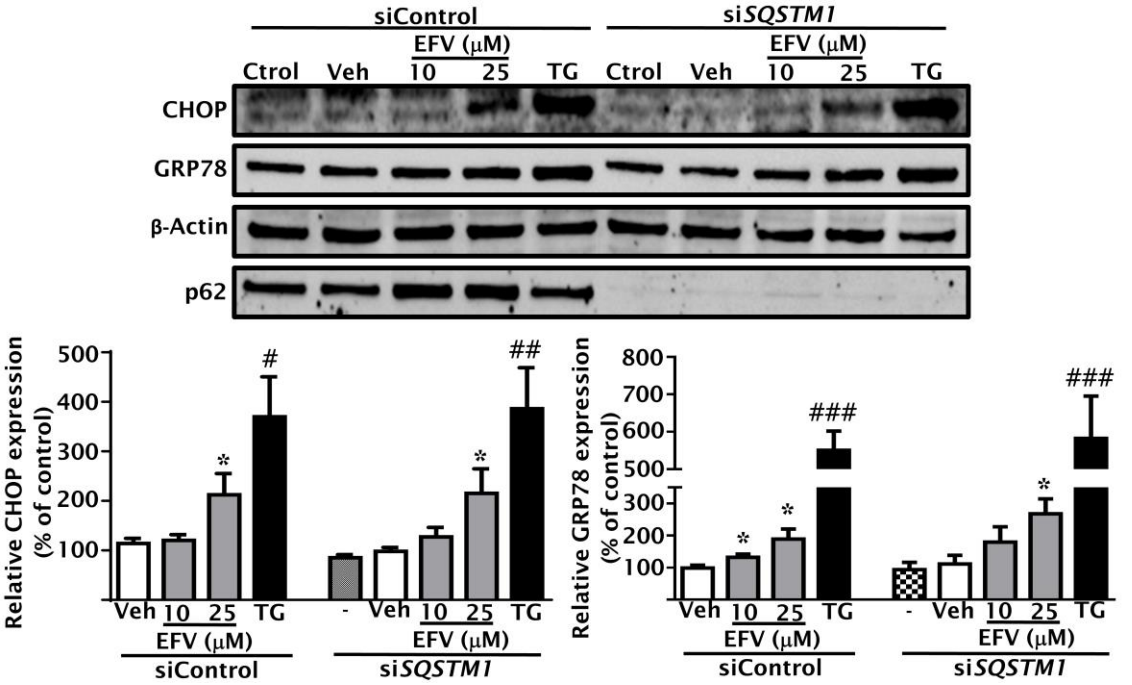

Figure IV.46. Determination of the effect of *SQSTM1* silencing on the UPR response induced by EFV. Representative WB images of ER stress markers (CHOP and GRP78) and summary of densitometry data in Hep3B cells transiently transfected with siControl or si*SQSTM1*. The absence of p62 protein confirmed the efficacy of *SQSTM1* silencing. Data (mean±SEM, n=4) were calculated as percentage of control (untreated siControl cells) and analyzed by a one-way ANOVA multiple comparison test followed by a Newman-Keuls test (p*<0.05 versus vehicle). TG, and siControl versus si*SQSTM1* were independently analyzed by a Student's *t*-test (#*p*<0.05, ##*p*<0.01, ###*p*<0.001 versus control or si*SQSTM1,* respectively).**

IV.20.2. Role of p62 in the preservation of the mitochondrial function

Having demonstrated that mitochondria is involved in the upregulation of p62 expression (see Figure IV.33 and 35) in our cellular model, we hypothesized that p62 could be playing a key role in the preservation of the mitochondrial function during EFV treatment. An evaluation of the mitochondrial function after EFV-treatment in cells with transiently silenced *SQSTM1*, revealed a greater increase in mitochondrial ROS, whereas the decline of $\Delta\Psi_m$ observed in absence of p62 was not exacerbated in comparison with siControl-transfected cells (Figure IV.47).

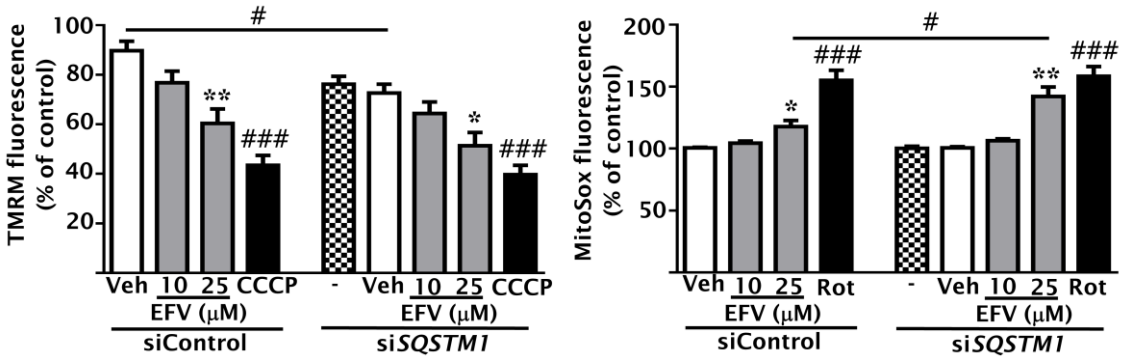

Figure IV.47. Analysis of mitochondrial parameters in Hep3B cells with transient silencing of *SQSTM1*. Quantitative analysis of $\Delta\Psi_m$ (TMRM fluorescence) and mitochondrial superoxide production (MitoSOX fluorescence) by fluorescence microscopy coupled to static cytometry. Data (mean±SEM, n=4-7) were calculated as percentage of control (untreated siControl cells, considered 100%), and analyzed by a one-way ANOVA multiple comparison test followed by a Newman-Keuls test (*p<0.01, **p<0.001 versus the vehicle). Positive controls (CCCP and Rot) and siControl versus si*SQSTM1* were independently analyzed by a Student's *t*-test (#p<0.05, ###p<0.001versus control or si*SQSTM1*).

IV.21. FUNCTION OF p62 ON THE INFLAMMATORY RESPONSE INDUCED BY EFAVIRENZ IN HEPATOCYTES

Mounting evidence has attributed p62 a crucial role in the control of inflammatory responses, including inflammasome activity (Shin et al. 2013; Valencia et al. 2014; Duran et al. 2016; Zhong et al. 2016). Considering this, we analyzed the effect of *SQSQTM1* silencing in gene expression of inflammasome-related markers (NLRP3 and IL-1β) and pro-inflammatory cytokines (IL-6 and TNF-α) in EFV-treated Hep3B cells. qRT-PCR assays revealed

that, when p62 was silenced, the upregulation of these markers by EFV was more pronounced (Figure IV.48), suggesting a protective function of p62 in the inflammatory response activation in this model.

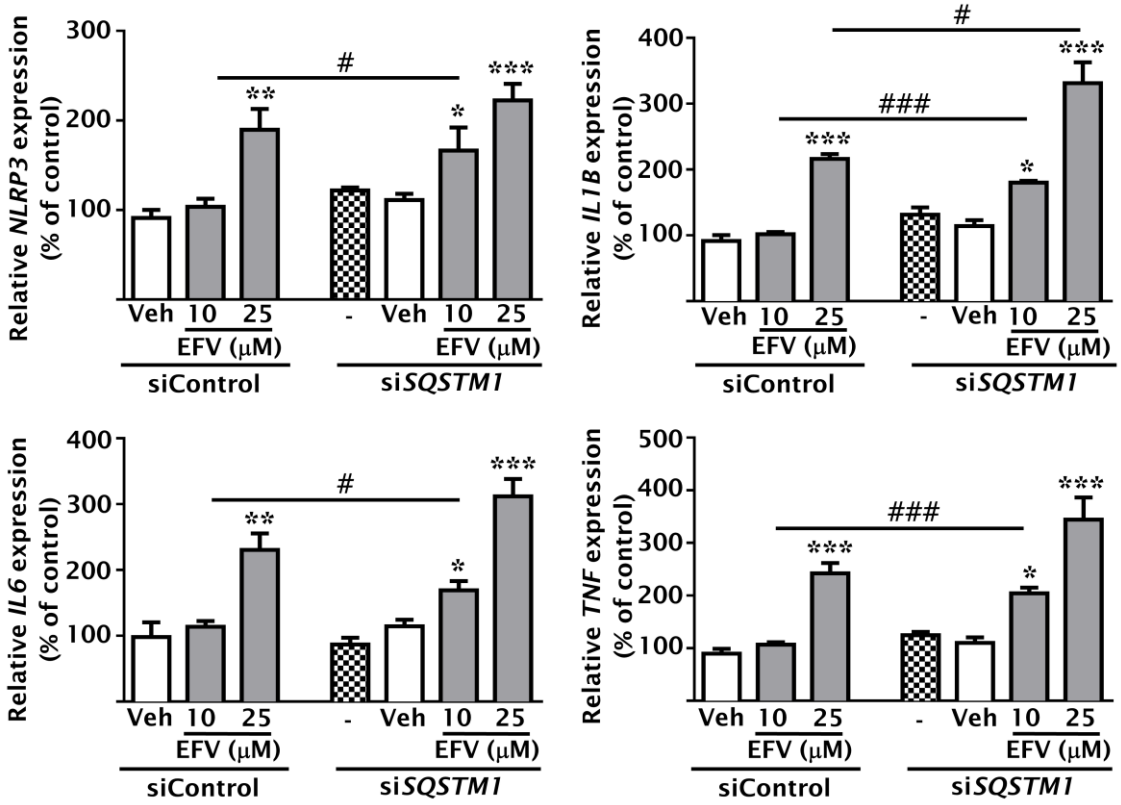

Figure IV.48. Analysis of the effects of *SQSTM1* silencing on several inflammatory markers. Relative mRNA expression levels of inflammasome-related markers (NLRP3 and IL-1β) and pro-inflammatory cytokines (IL-6 and TNF-α) in Hep3B cells transiently transfected with siControl or si*SQSTM1* treated with EFV (qRT-PCR). Data (mean±SEM, n=4) were normalized versus those obtained with the housekeeping gene *ACTB*, calculated as percentage of control (untreated siControl cells, considered 100%) and analyzed by one-way ANOVA multiple comparison test followed by a Newman-Keuls test (*p<0.05, **p<0.01, ***p<0.001 versus the vehicle). Cells transiently transfected with si*SQSTM1* versus siControl were independently analyzed by a Student's *t*-test (#*p*<0.05, ###*p*<0.001).

Chapter V. DISCUSSION

cART prescription has substantially prolonged the life expectancy in HIV-infected patients, converting AIDS from a fatal disease to a chronic manageable one (Broder 2010). Compared to previous pharmacological regimens, the current combined treatments are associated with an enhanced viral suppression, improved clinical results and lower discontinuation rates because of higher tolerability, safety and patient adherence (Luzuriaga 2016). However, characterization of the side effects associated with this therapy and the cellular and molecular mechanisms implicated in them have gained importance in the last years due to multiple factors, including (I) the lifelong administration of therapy due to its incapacity to eradicate HIV from the host organism, (II) a demographic aging shift among HIV-infected people, both newly infected and patients on long-term cART, and (III) the non-HIV related disorders clinicians have to confront, such as liver diseases, cardiovascular diseases and cancer, which may be aggravated by cART-related side effects (Carr 2003; Granich et al. 2010; Guaraldi et al. 2014).

In the present doctoral thesis, we have focused on EFV due to the fact that it has been the only evaluated drug that has affected cellular viability in our model, while clinically relevant concentration of DRV, RPV, RAL, ABC and ddI did not have a negative impact on this parameter. EFV is among the most widely used agents in cART. Although current guidelines, including GeSIDA and AIDSinfo (a part from US DHHS Panel), suggest to use EFV in alternative antiretroviral regimens, a recommendation followed by most of the clinicians in industrialized countries (AIDSinfo 2016; GeSIDA 2016; Günthard et al. 2016), this NNRTI forms part of first-line regimen in low and middle-income countries where, importantly, lives the majority of the HIV-infected population. The reasons for which EFV is broadly prescribed in these countries are its high efficacy, good tolerance in woman of childbearing potential and pregnancy, and the availability of a generic tablet formulation with a reduced cost since 2016 (WHO 2012; Ford et al. 2014; Sonderup et al. 2016; Thamrongwonglert et al. 2016; Chu et al. 2017). Although EFV is commonly considered safe, there is a concern about the side effects induced by EFV-containing regimens, such as rash, neuropsychiatric disorders, metabolic disturbances and DILI (Manosuthi et al. 2006; Loko et al. 2011; Decloedt et al. 2013; Patil et al. 2015). Regarding EFV-related liver injury, a positive correlation has been stablished between plasma concentration of this drug and hepatic adverse

effects, and up to 8% of HIV patients treated with EFV show severe liver injury with increased plasmatic concentrations of liver enzymes that may suppose therapy discontinuation (Abrescia et al. 2002, 2005; Kappelhoff et al. 2005; Mugusi et al. 2012; Sonderup et al. 2015).

In vitro studies have become an essential tool to understand the mechanisms underlying the side effects of anti-HIV drugs, given the difficulty to determine the specific adverse events associated with each antiretroviral drug, because they are administrated in combination, and taking into account the interindividual variability observed among patients. Although *in vitro* toxicity models cannot fully reflect the liver alterations provoked by these drugs in an *in vivo* model, experiments performed in cultured cells can reveal important information about specific drug-induced subcellular damage and responses, and become a cornerstone for *in vivo* approximations. The experimental conditions of this work, such as drug concentrations and cellular types employed, were chosen carefully in order to be as comparable as possible to the clinical and physiological conditions. The daily recommended dose of EFV in adults is 600 mg, which results in plasma levels of 5.6 μM – 12.9 μM (Starr et al. 1999; Staszewski et al. 1999), but the presence of other liver insults, such as co-infection with HBV and/or HCV, alcoholism, liver steatosis, and interindividual variations in drug metabolism can increase EFV plasma levels. In this line, many clinical studies have found higher plasma levels of EFV, specifically 30-50 μM, in up to 40% of HIV-infected patients (Marzolini et al. 2001; Burger et al. 2006; Stöhr et al. 2008; Leger et al. 2009; van Luin et al. 2009; Gounden et al. 2010), while in one study directed by EuroSIDA, the highest EFV concentration recorded was 80.75 μM and 14.1% of the patients exhibited supra-therapeutic plasma concentrations (van Luin et al. 2009). Additionally, the plasma concentration of EFV has been significantly enhanced in patients co-infected with HCV, specifically in those with severe liver fibrosis, reaching levels that double those observed in single infected HIV patients (Dominguez et al. 2010). The range of EFV concentrations employed in this study (10-50 μM) was chosen considering this significant interindividual variability in its plasma levels. Most of the alterations observed in this work were dependent on the concentration and exposure time, and were detected even at the lowest concentration evaluated, 10 μM. Hence, we can conclude that, although the effects induced by EFV in some parameters are moderate,

continuous exposure and high plasma levels could enhance the liver toxicity induced by this drug. On the other hand, the metabolism of this antiretroviral drug requires an active P450 system; for this reason, the human hepatoma cell line Hep3B, human HSC line LX-2 and U937 human monocyte cell line, were employed as cellular models of hepatocytes, HSC and macrophages, respectively (Nagai et al. 2002; Zhu et al. 2007; Friedman 2008; Rao and Kumar 2016). In some experiments, we used hepatocytes derived from HepaRG™ cells, as they display many characteristics of primary human hepatocytes. Several analysis were performed using primary rat neurons, a model in which our group has previously studied the effect of EFV (Apostolova et al. 2015; Funes et al. 2015), in order to compare the effects of EFV in different tissues. Additionally, key experiments were performed in primary human cells to confirm the results obtained in cell lines. EFV-induced effects in primary cells were similar to those detected in cell lines, and even more evident. In order to confirm the relevance of the *in vitro* results, we also performed some experiments in C57BL/6 mice, which were acutely administered clinically relevant concentrations of EFV.

The present study demonstrates cell-specific NLRP3 inflammasome activation in a pharmacological model of mitochondrial dysfunction and ER stress elicited by the antiretroviral drug EFV. This effect produced acute injury in both hepatocytes and HSCs, but not in macrophages. Our results also emphasize the crucial role of macrophages in the progression of liver injury, as shown by the fact that no evidence of inflammatory or fibrogenic damage was found in the liver of mice after acute exposure to EFV, whereas depletion of macrophages in this animal model permitted the *in vivo* manifestation of the deleterious effects detected in hepatocytes and HSCs. Furthermore, we also provide evidence of specific and autophagy-independent regulation of p62 in hepatocytes, where its induction was related to a condition of dual mitochondrial-ER stress and was mediated by the transcription factor CHOP but not by the classical regulators NF-κB or Nrf2. p62 upregulation induced by EFV is protective at mitochondrial oxidative state and exerts an anti-inflammatory action.

Upon exposure to hepatotoxic conditions, hepatocytes activate cellular stress responses, frequently orchestrated by the master regulator NF-κB resulting in moderate inflammatory response and anti-apoptotic activities, coupled with the

recruitment of immune cells, such as neutrophils and monocytes, thus contributing to the maintenance of liver homeostasis. However, sustained inflammation due to prolonged exposure to these stimuli or a failure to resolve it could become deleterious and lead to hepatocyte damage and cell death (Brenner et al. 2013; Woolbright and Jaeschke 2015). *In vitro* studies have shown that EFV exerts a pattern of stress-related actions in hepatocytes, including mitochondrial dysfunction, enhanced intracellular accumulation of lipid droplets, cell survival-promoting autophagy, apoptosis and ER stress (Apostolova et al. 2010, 2011, 2013; Blas-García et al. 2010), that are related to induction of inflammatory and fibrogenic responses in the liver (Seki and Schwabe 2015). In this study, EFV treatment in hepatocytes resulted in the activation of NF-κB and NLRP3-dependent pathways, which mediates the production of key mediators of inflammation and fibrogenesis. In fact, EFV enhanced the expression of the cytokines IL-6 and TNF-α, as well as inflammasome-related components and its effector IL-1β, a crucial feature of pathological conditions such as fibrosis, NAFLD and DILI (Czaja 2014; Guo et al. 2015; Blas-García et al. 2016); furthermore, it induced *SERPINE1* transcription, an effect associated with enhanced fibrogenesis in NAFLD (Sookoian et al. 2010). However, IL-18 mRNA levels, unlike IL-1β, were not increased following EFV exposure, which may be due to the fact that this interleukin is constitutively expressed in cells, and its expression may be enhanced only after sustained inflammasome activation (Lee et al. 2004; Latz et al. 2013). In addition, other studies have also reported a differential range of gene expression of these two inflammasome downstream effectors upon exposure to inflammasome inducers in monocytes and liver cells (Huang et al. 2004; Moschen et al. 2011; Stanton et al. 2011). Our study also demonstrates that NLRP3 inflammasome activation in hepatocytes by EFV does not seem to be associated with TXNIP, as the gene expression of this mediator involved in ROS-induced NLRP3 activation was not enhanced by EFV. There is however clear evidence that links TXNIP with activation of the NLRP3 inflammasome under stress conditions, such as oxidative and ER-stress (Zhou et al. 2010; Lerner et al. 2012; Mohamed et al. 2014; Abais et al. 2015). In line with our study, it has been also reported in macrophages that TXNIP deficiency did not affect NLRP3 inflammasome activation in response to several inflammasome activators, such as ROS, MSU or ATP (Masters et al. 2010).

HSC contribution to the progression of injury induced by noxious stimuli involves the regulation of NF-κB or NLRP3 inflammasome (Watanabe et al. 2009; Szabo and Csak 2012; Wree et al. 2014), and a direct role for NLRP3 and IL-1β in HSC activation has been suggested, for example, promoting its proliferation, actin reorganization and stellation, chemotaxis and secretion of fibrogenesis-related mediators, such as collagen 1α1 and TGF-β1 (Watanabe et al. 2009; Miura et al. 2010; Yaping et al. 2014; Cai et al. 2016). Our experiments demonstrate a clear induction of different molecular mechanisms involved in activation of HSCs following incubation with EFV; specifically, mitochondrial dysfunction coupled with overproduction of ROS and a drop of $\Delta\Psi_m$, presence of ER stress, induced autophagy of lipid droplets, and enhanced expression of pro-inflammatory mediators, including IL-6, TNF-α and NLRP3-related inflammasome components, resulting in an increased caspase-1 activity and secretion of IL-1β. Furthermore, EFV-treated HSCs exhibited upregulation of several fibrogenesis-related genes, including *TGFB1, TIMP1, MMP2, MMP9* and *COL1A1*, which points to an activation of the fibrogenic response (Hemmann et al. 2007; Puche et al. 2013). However, no changes were observed in the protein expression of the traditional marker of activated HSCs α-SMA in the cell line, a finding that can be explained by the fact that LX-2 cells are a myofibroblastic cell line, showing a partial activation, and thus express a high level of this intermediate filament protein (Xu et al. 2005; Castilho-Fernandes et al. 2011). Gene array experiments showed that EFV also upregulated the expression of other important mediators in HSCs, such as IL-33, a cytokine strongly associated with liver fibrosis in mice and humans and known to be produced mainly by HSCs under physiological and pro-inflammatory conditions. This cytokine also can be secreted by damaged hepatocyte, stimulating innate lymphoid cells to produce IL-13, that activates HSCs (Marvie et al. 2010; Mchedlidze et al. 2013; Weiskirchen and Tacke 2014). Additionally, *P2RX7* and *PANX1* upregulation in HSCs confirmed the ability of EFV to activate inflammatory responses in hepatic cells, which may occur either directly (by regulating mRNA expression) or indirectly (by increasing extracellular levels of ATP following mitochondrial dysfunction). The P2RX7/PANX1-mediated pathway has also been characterized as an inducer of the NRLP3 inflammasome, because the activation of this pathway promotes K^+ efflux (Ahmad 2007; Silverman et al. 2009; Iracheta-Vellve et al. 2015). Therefore, its activation may further contribute to the triggering of a NLRP3-dependent pro-

inflammatory response in cells exposed to EFV. This experiment also revealed an increased expression of several HSP90 isoforms induced by EFV. Besides their crucial roles in folding, assembly and transporting of proteins (Chen et al. 2005), these proteins also hold essential functions in inflammasome activation since they stabilize the mature NLRP3 allowing its subsequent oligomerization (Mayor et al. 2007), and serve as danger signals after being released from apoptotic/necrotic cells (Brenner et al. 2013).

As a clear example of the challenges met when extrapolating the effects of individual cell populations *in vitro* to a functional liver, the comprehensive inflammatory and fibrogenic response to EFV incubation exhibited by hepatocytes and HSCs was not reproduced in the murine model. However, livers of EFV-administered mice showed an increased and dose-dependent MPO activity, suggesting an incremented neutrophil infiltration. The progression and resolution of liver injury depend on a dynamic interaction between liver resident cells and infiltrating immune cells (Robinson et al. 2016); abundant evidence has shown that macrophages are essential determinants of the liver injury outcome (Possamai et al. 2014; Wynn and Vannella 2016). Thus, their polarization towards the different subtypes may directly modulate EFV-induced deleterious effects. Our data show that EFV-treated macrophages exhibit an increased expression of NLRP12, a damper of inflammatory responses in monocytes (Tuncer et al. 2014; Lukens et al. 2015; Shi et al. 2016) that undermines NF-κB activation by preventing IRAK1 phosphorylation (Jéru et al. 2008; Zaki et al. 2011; Allen et al. 2012), decreasing the production of many pro-inflammatory cytokines and chemokines dependent on this pathway. Moreover, the gene expression of the inflammasome components did not undergo any changes following the exposure to EFV, except for that of the adaptor ASC which was enhanced. The evaluation of the presence of macrophage subtypes suggested that EFV induces a polarization towards the M2 or anti-inflammatory/pro-resolving phenotype, an effect that could be associated with increased PPAR-γ expression. This transcription factor is implicated in anti-inflammatory responses and macrophage polarization towards the M2 phenotype, due to its ability to trans-repress NF-κB (Lawrence and Natoli 2011; Morán-Salvador et al. 2013; Zizzo and Cohen 2015). Although we have not evaluated in depth the specific subtype of the M2 macrophages detected in our model, enhanced expression of *MRC1, ARG1, IL10, IL1B, TNF*

and *IL6* suggests they may be M2b or M2c (Biswas and Mantovani 2010; Murray et al. 2014). However, our current data are not consistent enough to confirm this hypothesis, keeping in mind that it has been reported that macrophages can express both M1 and M2 markers simultaneously (Ramachandran et al. 2012; Tacke and Zimmermann 2014). Additionally, gene array experiments also showed an enhanced expression of *RIPK2* in macrophages. Besides mediating pro-inflammatory signaling from the sensors NOD1 and NOD2 (Canning et al. 2015), this kinase is highly expressed in alternatively (M2) activated macrophages by IL-4 and it is required for secretion of IL-10 (Scotton et al. 2005; Moreira et al. 2008; Woodward et al. 2012).

This macrophage polarization towards the M2 phenotype and the activation of the above-mentioned pro-resolving pathways could explain why while EFV induced pro-inflammatory and pro-fibrogenic effects in hepatocytes and HSCs *in vitro*, no evident liver injury was recorded *in vivo*. The relevance of macrophages in the control of the acute injury induced by EFV was pinpointed by the finding that liver samples from macrophage-depleted mice treated with EFV displayed enhanced inflammatory and fibrogenic responses, as shown by an upregulated expression of markers involved in these responses and augmented MPO activity. Additionally, experiments performed in Hep3B cells with conditioned M2 medium ratified the role of M2 macrophages in alleviating liver injury *in vivo,* since EFV effects were partially prevented with the addition of M2 supernatant, suggesting that cytokines and chemokines from this macrophage population prevent EFV-induced liver injury. In light of the reported variability regarding the role of macrophages in the onset of hepatic damage, further research is needed in order to clarify how these cells protect under other deleterious stimuli or inflammatory circumstances (Figure V.1).

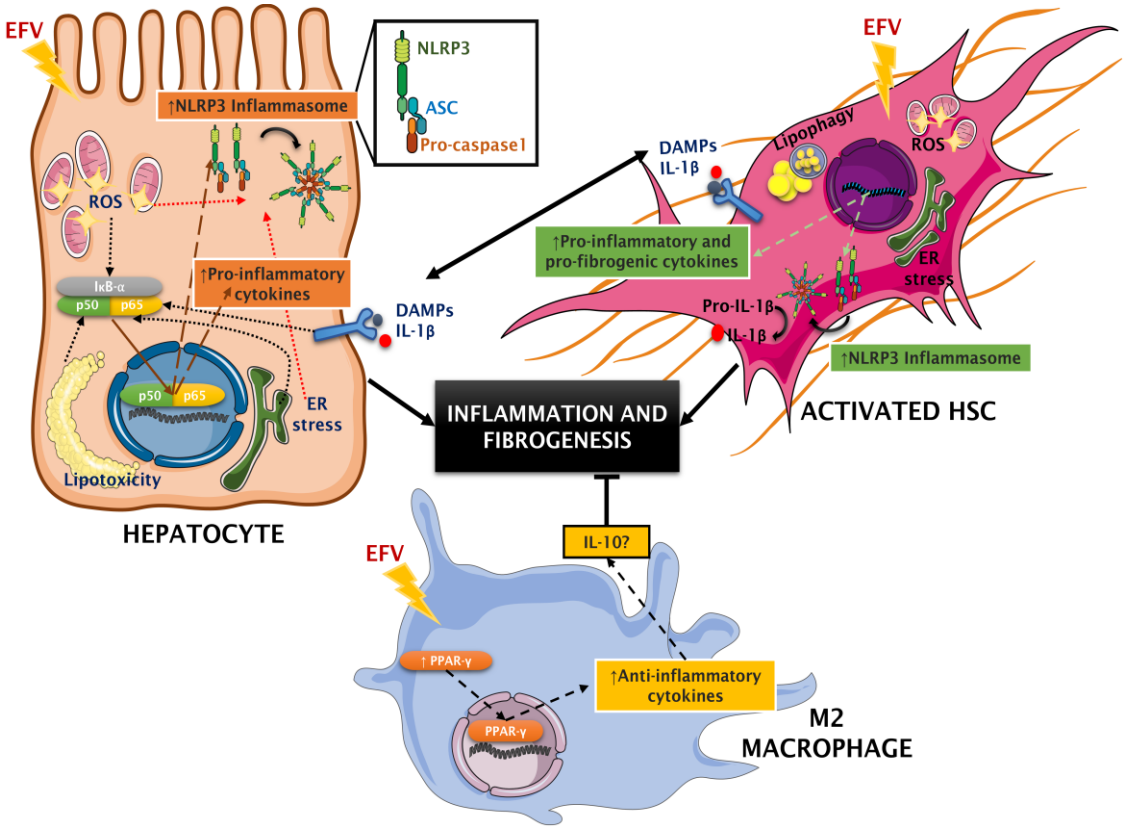

Figure V.1. Schematic representation of the potential interplay between hepatocytes, HSCs and macrophages in the liver following EFV treatment. In hepatocytes, EFV induces ER stress and mitochondrial dysfunction characterized by an increased ROS production and mitochondrial mass, and a decrease of $\Delta\Psi_m$ and ATP levels, which leads to an accumulation of intracellular lipids (Apostolova et al. 2010, 2013; Blas-García et al. 2010). These cellular events are associated with an enhanced nuclear translocation of NF-κB (p65/p50), a transcription factor that upregulates the expression of pro-inflammatory cytokines (IL-6, TNF-α, IL-1β) and inflammasome components, such as NLRP3 and caspase-1. On the other hand, EFV also activates HSCs, an effect associated with several EFV-induced actions in these cells such as enhanced oxidative stress and ER stress, and lipophagy. Moreover, EFV upregulates pro-inflammatory (such as IL-6, TNF-α, IL-1β, IL-18 and IL-33) and fibrogenic (such as TGF-β1, TIMP1, MMP-2 and MMP-9) mediators in HSCs. Importantly, in both hepatocytes and HSCs, EFV activates the NLRP3 inflammasome, which can lead to pyroptotic death cell and thereby release DAMPs, amplifying the inflammatory response. Conversely, EFV produces the macrophage polarization towards the anti-inflammatory/pro-resolving M2 phenotype, as shown by an increased expression of PPAR-γ and anti-inflammatory cytokines (such as IL-10), which alleviates the pro-inflammatory and pro-fibrogenic response in hepatocytes and HSCs.

Growing evidence is challenging the hepatic safety profile of EFV. Besides the EFV-induced deleterious actions observed in hepatocytes *in vitro* (Apostolova et al. 2010, 2011, 2013; Blas-García et al. 2010; Bumpus 2011; Gomez-Sucerquia et al. 2012; Imaizumi et al. 2015), there are recent clinical reports of hepatic toxicity related to this NNRTI, including transaminitis, mixed cholestasis-hepatitis, non-specific hepatitis, acute liver failure and submassive necrosis (Echenique and Rich 2013; Elsharkawy et al. 2013; Patil et al. 2015; Sonderup et al. 2015, 2016), and an association between cumulative exposure to EFV and hepatic steatosis progression has been reported (Macías et al. 2012). It is tempting to speculate that the balanced scenario usually observed in EFV-treated patients could be altered when yet-to-be-defined risk factors that promote the development of acute or chronic liver diseases in specific cases could tip the balance. These risk factors may include an additional activation of inflammasomes, as that observed in the pathophysiology of alcohol- and acetaminophen-liver injury (Imaeda et al. 2009; Petrasek et al. 2012; DeSantis et al. 2013; Peng et al. 2014), or in NAFLD/NASH, where saturated fatty acids induce upregulation of the NLRP3 inflammasome components, resulting in IL-1β and IL-18 secretion and release of danger signals to recruit immune cells (Miura et al. 2010, 2013; Csak et al. 2011; Farrell et al. 2012; Tilg et al. 2016). Importantly, these circumstances are not unusual among HIV-infected patients, since these patients have been reported to be particularly vulnerable to acetaminophen-induced hepatotoxicity and cART can lead to patterns of injury that include liver steatosis (Merriman 2006; Price and Thio 2011; Edelman et al. 2013; Hoffmann et al. 2015). Another possible factor underlying the variable toxicological profile of EFV drawn here is the link between HIV and liver fibrosis, as the virus itself infects HSCs promoting their activation and a subsequent fibrogenic response, as shown by an enhanced expression of collagen 1α1, TIMP-1, MMP-3, α-SMA and secretion of chemokines, such as MCP-1, in human HSCs (Tuyama et al. 2010; Lin et al. 2011); in fact, HIV matrix protein p17 has also been reported to activate HSCs (Renga et al. 2014). Moreover, HIV has been shown to regulate the progression of liver fibrosis through generation of ROS, and activation of NF-κB and SMAD3 signaling pathways in HSCs and hepatocytes; in addition, the co-infection with HCV accentuates the pro-fibrogenic response (Lin et al. 2011; Salloum et al. 2016). These factors may well be of transcendence in the context of current interest in the potential of this and other life-long administered antiretroviral drugs to

modulate inflammatory and fibrogenic complications, particularly as liver injury is a leading cause of death in HIV-infected patients. In this regard, HIV infection is characterized by a sustained systemic inflammatory status, even among patients with well controlled viral infection due to cell damage triggered by the virus and followed by the release of DAMPs and pro-inflammatory cytokines enhancing the innate immune response (Nasi et al. 2014; Shmagel et al. 2016). Moreover, mitochondrial toxicity, triggered by both cART and HIV, and the accelerated aging caused by HIV infection contribute to intrahepatic damage and mild levels of chronic inflammation, respectively (Chan et al. 2016; Debes et al. 2016).

As stated above, drug-induced toxicity is one of the main causes of morbidity and mortality among HIV-patients because of the complex clinical situations of this pathology, long-term treatments, presence or appearance of concomitant diseases that require additional therapies, and accelerated aging of HIV-infected patients (Meir-Shafrir and Pollack 2012; Smith et al. 2013; Margolis et al. 2014). Drug-induced toxicity can be triggered by different mechanisms that often involve mitochondrial uncoupling, altered levels of ATP and antioxidants, lipid and protein oxidation, and disturbance of Ca^{2+} homeostasis. These mechanisms result in the malfunction of specific subcellular compartments and organelles leading to pathological cellular events, such as mitochondrial dysfunction, plasma membrane blebs and ER stress (Grattagliano et al. 2009; Guengerich 2011; Yuan and Kaplowitz 2013). The latter cellular event is produced by the accumulation of misfolded proteins in the ER lumen, and to cope with ER stress, cells activate the UPR which is initiated by three stress sensors, PERK, IRE1α and ATF6 (Hetz et al. 2015; Senft and Ronai 2015). Both PERK (via ATF4) and ATF6 arms of the UPR can activate the transcription factor CHOP, which is known to induce growth arrest and inhibits expression of the gene encoding anti-apoptotic Bcl-2 resulting in cell death (Oyadomari and Mori 2004; Oakes and Papa 2014), but overall, CHOP-induced signaling is not well understood. A detailed molecular analysis revealed that CHOP is a master regulator of protein synthesis during ER stress and the gene that encodes multifunctional protein p62 is one of its direct targets (Han et al. 2013). Moreover, CHOP is also induced by mitochondrial stressors *in vitro*, including 6-OHDA (Oh et al. 2009), rotenone (Goswami et al. 2016), MPP^+ (Zhang et al.

2015) and the anti-HIV drugs EFV (Apostolova et al. 2013), LPV and RTV (Wu et al. 2010).

In the present work, EFV induced the upregulation of p62 protein and mRNA levels in hepatic cells in a process where autophagy seems not to be implicated. The virtual lack of p62 did not affect the autophagic process, which can be explained by the existence of other selective autophagy receptors such as NBR1 (whose expression is also increased in our model), NDP52, optineurin and TAX1BP1 (Katsuragi et al. 2015; Taniguchi et al. 2016). Unexpectedly, the increased transcription of *SQSTM1*, which hold an ARE element in its promoter, was not regulated by the transcription factor Nrf2, which is involved in antioxidant responses and whose nuclear translocation occurs in a p62-dependent process through degradation of the Nrf2 inhibitor Keap1 (Jain et al. 2010; Jaramillo and Zhang 2013). The absence of participation of Nrf2 in p62 upregulation may be due to the duration of the treatment (24 h) in our model. It has been demonstrated in experimental models of hepatotoxicity with 1,3-DCP (Lee et al. 2015) and Parkinson's-like disease in mice (Ahuja et al. 2016), that the peak of the nuclear presence of Nrf2 is at 6-12 h and then it is gradually decreased. Our results showed that the p62 induction occurs in a CHOP-dependent manner, suggesting that ER stress plays a pivotal role in this process. There is mounting evidence that points to the upregulation of p62 during ER stress. For instance, methotrexate (MTXR) treatment activates the pro-survival signaling in MTXR-resistant choriocarcinoma cells, which involves ROS-mediated JNK/p62 activation and downstream PERK-related autophagy activities (Shen et al. 2015). Importantly, in this model the IRE1α pathway was activated by MTXR but was not affected by ROS activation, indicating that ROS mediate PERK signaling without regulating IRE1α/JNK pathway. p62 depletion promoted CHOP expression in MTRX-treated cells, nevertheless in our model of Hep3B with transient silencing of *SQSTM1,* the expression of CHOP and GRP78 was not enhanced following EFV treatment. Similarly, the induction of ER stress by tunicamycin or brefeldin A in colon and breast cancer cell lines also results in the transcriptional upregulation of p62 and other autophagy receptors, specifically NRBBR11 and BNIP3L, in a PERK- and IRE1α-dependent manner (Deegan et al. 2015).

Another interesting finding of this doctoral thesis is the association of p62 with the NLRP3 inflammasome and pro-inflammatory cytokines, specifically

alleviating the inflammatory effect of EFV in hepatocytes. As previously indicated, human hepatic cells treated with this NNRTI display mitochondrial dysfunction with increased mitochondrial superoxide production (Apostolova et al. 2010; Blas-García et al. 2010), and our data show that the absence of p62 enhanced the mitochondrial superoxide generation, providing evidence of a protective role of p62 in this regard. Furthermore, the finding that EFV treatment augmented the mitochondrial presence of p62 and that cells lacking functional mitochondria (rho^0) display substantially lower increase in p62 expression compared to WT cells, are in line with the suggested specific role of p62 in mitochondrial normal function, dynamics, biogenesis and genome integrity (Seibenhener et al. 2013). As the major source and target of ROS in the cell, mitochondria are crucial players in the pro-inflammatory status, because they modulate innate immunity via redox-sensitive inflammatory pathways and promote the formation and activation of inflammasomes (Harijith et al. 2014; Gurung et al. 2015; van der Burgh and Boes 2015). Importantly, p62 deficiency enhanced the pro-inflammatory response induced by EFV in hepatocytes, as shown by a significantly increased transcription of *NLRP3, IL1B, TNF* and *IL6* (Figure V.2). Moreover, a key function of p62 in the regulation of inflammasome activation has been reported, which has mainly been connected with autophagy, as p62 restricts and prevent the inflammation through degradation of dysfunctional organelles and/or specific proteins, including inflammasome components (Chen et al. 2014; Katsuragi et al. 2015; Taniguchi et al. 2016; Zhong et al. 2016). Regarding this point, we report an autophagy-independent functional connection between p62 and NLRP3 upon EFV exposure. This result is in line with recently published evidence which has shown that p62 can inactivate NLRP3 inflammasomes by directly binding to NLR proteins (through its interaction with their NODs domains), thus preventing their self-oligomerization. Nevertheless, p62 does not bind to other inflammasome components, including ASC and caspase-1 (Ohtsuka et al. 2014). Our finding regarding the role of p62 beyond autophagy, may be of clinical relevance given that dysregulated inflammasome activity has been implicated in the pathogenesis of inflammatory disorders and neurodegenerative diseases, and has been shown to exacerbate symptoms of infectious diseases (Strowig et al. 2012; Guo et al. 2015). Moreover, these results may have a major relevance as p62 has been described as a potential receptor for the glycoproteins involved in the HIV-entry into the target cells,

specifically gp41 and gp36 (Chen et al. 2000; Yang et al. 2001), but also p62 has been reported to enhance TRIM5α protein, which potently inhibits HIV-1 infection (O'Connor et al. 2010).

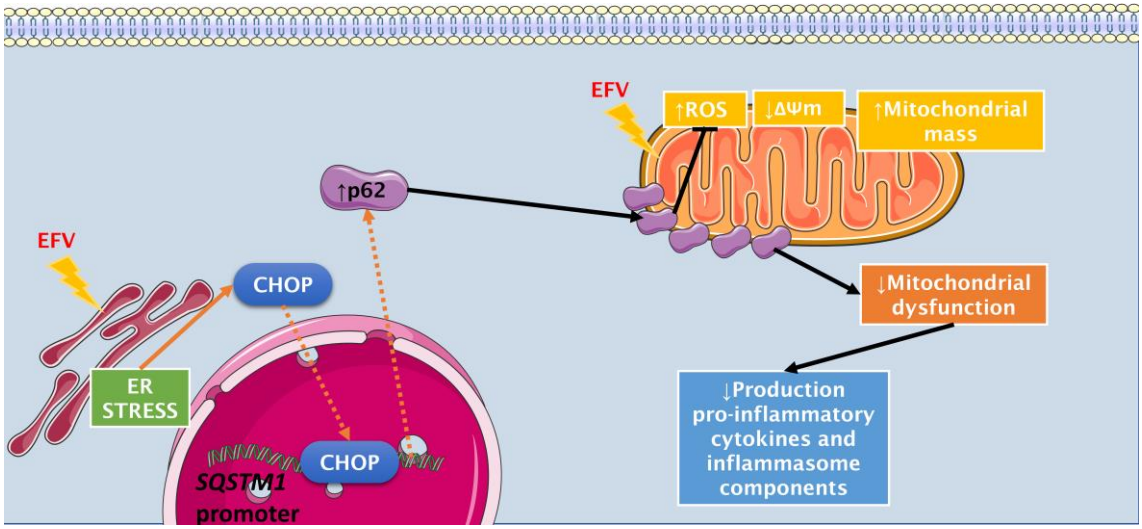

Figure V.2. Schematic representation of the EFV-induced effects on p62 expression and function. EFV induces p62 expression under conditions of dual mitochondrial-ER stress and the upregulation is mediated by the transcription factor CHOP, and not by the classical regulators Nrf2 or NF-κB. This increased p62 expression seems to be protective at the mitochondrial level, decreasing mitochondrial ROS production. Moreover, it also exerts an anti-inflammatory action, decreasing pro-inflammatory mediators such as cytokines (IL-1β, TNF-α, and IL-6) and inflammasome components (NLRP3).

In conclusion, the present study highlights a clear pro-inflammatory and pro-fibrogenic action of EFV in hepatocytes and HSCs that is triggered by NF-κB and NLRP3 inflammasome-dependent pathways. These pathways seem to be counteracted by macrophages and are likely to be modified by the diverse conditions that can occur in the clinical setting of HIV-infected patients. Importantly, the potential of this drug to promote macrophage polarization towards an anti-inflammatory phenotype is a novel and unexpected property with possible therapeutics applications in acute and chronic liver diseases. Furthermore, in hepatocytes, EFV enhanced the expression of p62 in a CHOP-dependent manner and without involvement of autophagy. Moreover, EFV-upregulated p62 results protective against mitochondrial ROS-generation and pro-inflammatory signaling induced by this NNRTI. This function of p62, as a negative regulator of inflammation, is of particular relevance in the case of HIV infection due to the chronic inflammatory status observed in these patients.

The complex response in this model of dual mitochondrial-ER stress underlines the dynamic interaction that takes place among the liver's cell populations, and surely deserves further characterization if we are to ascertain the molecular mechanisms that resolve inflammatory and fibrogenic responses in this organ.

Chapter VI. CONCLUSIONS

1. **The mitochondrial dysfunction and endoplasmic reticulum stress triggered by clinically relevant concentrations of efavirenz in hepatocytes are associated with the nuclear translocation of NF-κB, promoting the transcription of classic pro-inflammatory cytokines and components of the NLRP3 inflammasome. Moreover, NLRP3 inflammasome activity is enhanced, thereby increasing caspase-1 activity.**

2. **Efavirenz induces mitochondrial dysfunction, endoplasmic reticulum stress and autophagy of lipid droplets in hepatic stellate cells, which are crucial cellular events involved in the activation of hepatic stellate cells towards a myofibroblast-like phenotype.**

3. **Efavirenz promotes the expression of classic pro-fibrogenic and pro-inflammatory mediators in hepatic stellate cells; in addition, it induces the activation of the NLRP3 inflammasome and secretion of IL-1β.**

4. **In contrast to the efavirenz-induced pro-inflammatory and pro-fibrogenic effects found *in vitro* in hepatocytes and hepatic stellate cells, no liver injury was evident in a murine model of acute efavirenz exposure.**

5. **The *in vivo* findings may be related to the fact that efavirenz promotes macrophage polarization towards the anti-inflammatory M2 phenotype, an effect that may be mediated by the increased PPAR-γ expression. In addition, depletion of liver macrophages results in the *in vivo* manifestation of the inflammation-related deleterious effects detected in hepatocytes and hepatic stellate cells, emphasizing the pivotal role of macrophages in the mediation of efavirenz-induced liver injury.**

6. **p62 expression is upregulated in hepatocytes by efavirenz, and this occurs through the transcription factor CHOP, while other well-known regulators, such as Nrf2 and NF-κB are not involved.**

7. **These increased levels of p62 protect against efavirenz-induced mitochondrial reactive oxygen species generation, production of pro-inflammatory cytokines and NLRP3 inflammasome activation, a function which seems to be independent of autophagy.**

BIBLIOGRAPHY

Abais JM, Xia M, Zhang Y, Boini KM, Li PL. Redox regulation of NLRP3 inflammasomes: ROS as trigger or effector?. Antioxid Redox Signal 2015;22(13):1111–29.

Abcam-IHC Protocols. IHC-Paraffin Protocol General 2015. p.1–13. Available from: http://www.abcam.com/tag/ihc protocols.

Aberg JA. Lipid management in patients who have HIV and are receiving HIV therapy. Endocrinol Metab Clin North Am. 2009;38(1):207–22.

Abrescia N, D'Abbraccio M, Figoni M, Busto A, Butrico E, De Marco M, et al. Fulminant hepatic failure after the start of an efavirenz-based HAART regimen in a treatment-naive female AIDS patient without hepatitis virus co-infection. J Antimicrob Chemother. 2002;50(5):763–5.

Abrescia N, D'Abbraccio M, Figoni M, Busto A, Maddaloni A, De Marco M. Hepatotoxicity of antiretroviral drugs. Curr Pharm Des. 2005;11:3697–710.

Ahmad S. Pannexin-1: the missing link?. Nat Rev Microbiol. 2007;7(6):418–9.

Ahuja M, Ammal Kaidery N, Yang L, Calingasan N, Smirnova N, Gaisin A, et al. Distinct Nrf2 signaling mechanisms of fumaric acid esters and their role in neuroprotection against 1-methyl-4-phenyl-1,2,3,6-tetrahydropyridine-induced experimental Parkinson's-like disease. J Neurosci. 2016;36(23):6332–51.

AIDSinfo. Guidelines for the use of antiretroviral agents in HIV-1-Infected adults and adolescents. Department of Health and Human Services. Accessed (12/01/2017) [cited 2017 Jan 17]. Available from: http://aidsinfo.nih.gov/guidelines

Allen IC, Wilson JE, Schneider M, Lich JD, Roberts RA, Arthur JC, et al. NLRP12 suppresses colon inflammation and tumorigenesis through the negative regulation of noncanonical NF-κB signaling. Immunity. 2012;36(5):742–54.

Almeida A, Medina JM. Isolation and characterization of tightly coupled mitochondria from neurons and astrocytes in primary culture. Brain Res. 1997;764:167–72.

Amaral FA, Costa VV, Tavares LD, Sachs D, Coelho FM, Fagundes CT, et al. NLRP3 inflammasome-mediated neutrophil recruitment and hypernociception depend on leukotriene B(4) in a murine model of gout. Arthritis Rheum. 2012;64(2):474–84.

Anan A, Baskin-Bey ES, Bronk SF, Werneburg NW, Shah VH, Gores GJ. Proteasome inhibition induces hepatic stellate cell apoptosis. Hepatology. 2006;335–44.

Anthérieu S, Chesné C, Li R, Camus S, Lahoz A, Picazo L, et al. Stable expression, activity, and inducibility of cytochromes P450 in differentiated HepaRG cells. Drug Metab Dispos. 2010;38(3):516–25.

Antonucci L, Fagman JB, Kim JY, Todoric J, Gukovsky I, Mackey M, et al. Basal autophagy maintains pancreatic acinar cell homeostasis and protein synthesis and prevents ER stress. Proc Natl Acad Sci U S A. 2015;112(45):E6166–74.

Apostolova N, Blas-Garcia A, Esplugues JV. Mitochondria sentencing about cellular life and death: a matter of oxidative stress. Curr Pharm Des. 2011a;17(36):4047–60.

Apostolova N, Blas-Garcia A, Esplugues JV. Mitochondrial toxicity in HAART: an overview of in vitro evidence. Curr Pharm Des. 2011b;17(20):2130–44.

Apostolova N, Blas-García A, Esplugues JV. Mitochondrial interference by anti-HIV drugs: mechanisms beyond Pol-γ inhibition. Trends Pharmacol Sci. 2011c;32(12):715–25.

Apostolova N, Funes HA, Blas-Garcia A, Alegre F, Polo M, Esplugues JV. Involvement of nitric oxide in the mitochondrial action of efavirenz: a differential effect on neurons and glial cells. J Infect Dis. 2015a;211(12):1953–8.

Apostolova N, Funes HA, Blas-Garcia A, Galindo MJ, Alvarez A, Esplugues JV. Efavirenz and the CNS: What we already know and questions that need to be answered. J Antimicrob Chemother. 2015b;70(10):2693–708.

Apostolova N, Gomez-Sucerquia LJ, Alegre F, Funes HA, Victor VM, Barrachina MD, et al. ER stress in human hepatic cells treated with Efavirenz: Mitochondria again. J Hepatol. 2013;59(4):780–9.

Apostolova N, Gomez-Sucerquia LJ, Gortat A, Blas-Garcia A, Esplugues JV. Autophagy as a rescue mechanism in efavirenz-induced mitochondrial dysfunction: a lesson from hepatic cells. Autophagy. 2011d;7(11):1402–4.

Apostolova N, Gomez-Sucerquia LJ, Gortat A, Blas-Garcia A, Esplugues JV. Compromising mitochondrial function with the antiretroviral drug efavirenz induces cell survival-promoting autophagy. Hepatology. 2011e;54(3):1009–19.

Apostolova N, Gomez-Sucerquia LJ, Moran A, Alvarez A, Blas-Garcia A, Esplugues JV. Enhanced oxidative stress and increased mitochondrial mass during efavirenz-induced apoptosis in human hepatic cells. Br J Pharmacol. 2010;160(8):2069–84.

Arango-Duque G, Descoteaux A. Macrophage cytokines: Involvement in immunity and infectious diseases. Front Immunol. 2014;5:491.

Arend WP, Palmer G, Gabay C. IL-1, IL-18, and IL-33 families of cytokines. Immunol Rev. 2008;223:20–38.

Arrese M, Cabrera D, Kalergis AM, Feldstein AE. Innate Immunity and Inflammation in NAFLD/NASH. Dig Dis Sci. 2016; 61(5):1294-303.

Artlett CM, Thacker JD. Molecular activation of the NLRP3 Inflammasome in fibrosis: common threads linking divergent fibrogenic diseases. Antioxid Redox Signal. 2015;22(13):1162–75.

Arts EJ, Hazuda DJ. HIV-1 antiretroviral drug therapy. Cold Spring Harb Perspect Med. 2012;2(4):a007161.

Autran B, Carcelain G, Li TS, Blanc C, Mathez D, Tubiana R, et al. Positive effects of combined antiretroviral therapy on $CD4^+$ T cell homeostasis and function in advanced HIV disease. Science. 1997;277(5322):112–6.

Badowski ME, Pérez SE, Biagi M, Littler JA. New Antiretroviral treatment for HIV. Infect Dis Ther . 2016;5(3):329–52.

Baeck C, Tacke F. Balance of inflammatory pathways and interplay of immune cells in the liver during homeostasis and injury. EXCLI J. 2014;13:67–81.

Baroja-Mazo A, Martin-Sánchez F, Gomez AI, Martinez CM, Amores-Iniesta J, Compan V, et al. The NLRP3 inflammasome is released as a particulate danger signal that amplifies the inflammatory response. Nat Immunol. 2014;15(8):738–48.

Barré-Sinoussi F, Ross AL, Delfraissy JF. Past, present and future: 30 years of HIV research. Nat Rev Microbiol. 2013;11(12):877–83.

Barve S, Kapoor R, Moghe A, Ramirez JA, Eaton JW, Gobejishvili L, et al. Focus on the liver: alcohol use, highly active antiretroviral therapy, and liver disease in HIV-infected patients. Alcohol Res Heal. 2010;33(3):229–36.

Benoit M, Desnues B, Mege JL. Macrophage polarization in bacterial infections. J Immunol. 2008;181(6):3733–9.

Bensaude O. Inhibiting eukaryotic transcription: Which compound to choose? How to evaluate its activity?. Transcription. 2011;2(3):103–8.

Benyon RC, Arthur MJ. Extracellular matrix degradation and the role of hepatic stellate cells. Semin Liver Dis. 2001;21(3):373–84.

de Béthune MP. Non-nucleoside reverse transcriptase inhibitors (NNRTIs), their discovery, development, and use in the treatment of HIV-1 infection: a review of the last 20 years (1989–2009). Antiviral Res. 2010;85(1):75–90.

Bieghs V, Trautwein C. The innate immune response during liver inflammation and metabolic disease. Trends Immunol. 2013;34(9):446–52.

Biswas SK, Mantovani A. Macrophage plasticity and interaction with lymphocyte subsets : cancer as a paradigm. Nat Immunol. 2010;11(10):889–96.

Bjørkøy G, Lamark T, Pankiv S, Øvervatn A, Brech A, Johansen T. Chapter 12 Monitoring autophagic degradation of p62/SQSTM1. Methods Enzymol. Academic Press, 2009, Volume 452, Pages 181-197, ISBN 9780123745477.

Blas-Garcia A, Esplugues JV, Apostolova N. Twenty years of HIV-1 non-nucleoside reverse transcriptase inhibitors: time to reevaluate their toxicity. Curr Med Chem. 2011;18(14):2186–95.

Blas-García A, Apostolova N, Ballesteros D, Monleón D, Morales JM, Rocha M, et al. Inhibition of mitochondrial function by efavirenz increases lipid content in hepatic cells. Hepatology. 2010;52(1):115–25.

Blas-García A, Apostolova N, Valls-Bellés V, Esplugues JV. Endoplasmic reticulum and mitochondria: Independent roles and crosstalk in fatty liver diseases and hepatic inflammation. Current Pharm Des. 2016;22(18):2607-18.

Blas-García A, Polo M, Alegre F, Funes HA, Martínez E, Apostolova N, et al. Lack of mitochondrial toxicity of darunavir, raltegravir and rilpivirine in neurons and hepatocytes: a comparison with efavirenz. J Antimicrob Chemother. 2014;69(11):2995–3000.

Brempelis KJ, Crispe IN. Infiltrating monocytes in liver injury and repair. Clin Transl Immunology. 2016;5(11):e113.

Brenner C, Galluzzi L, Kepp O, Kroemer G. Decoding cell death signals in liver inflammation. J Hepatol. 2013;59(3):583–94.

Broder S. Twenty-five years of translational medicine in antiretroviral therapy: promises to keep. Sci Transl Med. 2010;2(39):39ps33.

Broderick L, Hoffman HM. cASCading specks. Nat Immunol. 2014;15(8):698–700.

Bryant C, Fitzgerald KA. Molecular mechanisms involved in inflammasome activation. Trends Cell Biol. 2009;19(9):455–64.

Brydges SD, Broderick L, Mcgeough MD, Pena CA, Mueller JL, Hoffman HM. Divergence of IL-1 , IL-18, and cell death in NLRP3 inflammasomopathies. J Clin Invest. 2013;123(11):4695–705.

Bumpus NN. Efavirenz and 8-hydroxyefavirenz induce cell death via a JNK- and BimEL-dependent mechanism in primary human hepatocytes. Toxicol Appl Pharmacol. 2011;257(2):227–34.

Burger D, van der Heiden I, La Porte C, van der Ende M, Groeneveld P, Richter C, et al. Interpatient variability in the pharmacokinetics of the HIV non-nucleoside reverse transcriptase inhibitor efavirenz: the effect of gender, race, and CYP2B6 polymorphism. Br J Clin Pharmacol. 2006;61(2):148–54.

van der Burgh R, Boes M. Mitochondria in autoinflammation: cause, mediator or bystander?. Trends Endocrinol Metab. 2015;26(5):263–71.

Cai SM, Yang RQ, Li Y, Ning ZW, Zhang LL, Zhou GS, et al. Angiotensin-(1-7) improves liver fibrosis by regulating the NLRP3 inflammasome via redox balance modulation. Antioxid Redox Signal. 2016;24(14):795-812.

Calmy A, Hirschel B, Cooper DA, Carr A. A new era of antiretroviral drug toxicity. Antivir Ther. 2009;14(2):165–79.

Canbay A, Feldstein AE, Higuchi H, Werneburg N, Grambihler A, Bronk SF, et al. Kupffer Cell engulfment of apoptotic bodies stimulates death ligand and cytokine expression. Hepatology. 2003a;38(5):1188–98.

Canbay A, Taimr P, Torok N, Higuchi H, Friedman S, Gores GJ. Apoptotic body engulfment by a human stellate cell line is profibrogenic. Lab Invest. 2003b;83(5):655–63.

Canning P, Ruan Q, Schwerd T, Hrdinka M, Maki JL, Saleh D, et al. Inflammatory signaling by NOD-RIPK2 is inhibited by clinically relevant type ii kinase inhibitors. Chem Biol. 2015;22(9):1174–84.

Carr A. Toxicity of antiretroviral therapy and implications for drug development. Nat Rev Drug Discov. 2003;2(8):624–34.

Carr DF, la Porte CJ, Pirmohamed M, Owen A, Cortes CP. Haplotype structure of CYP2B6 and association with plasma efavirenz concentrations in a Chilean HIV cohort. J Antimicrob Chemother. 2010;65(9):1889–93.

Casado JL. Liver toxicity in HIV-infected patients receiving novel second-generation nonnucleoside reverse transcriptase inhibitors etravirine and rilpivirine. AIDS Rev. 2013;15(3):139–45.

Castilho-Fernandes A, de Almeida DC, Fontes AM, Melo FUF, Picanço-Castro V, Freitas MC, et al. Human hepatic stellate cell line (LX-2) exhibits characteristics of bone marrow-derived mesenchymal stem cells. Exp Mol Pathol. 2011;91(3):664–72.

Center for Drug Evaluation and Research (CDER). Guidance for industry: estimating the maximum safe starting dose in initial clinical trials for therapeutics in adult healthy volunteers. Accessed (10/12/2016) [cited 2016 Dec 12]. Available from: http://www.fda.gov/downloads/drugs/guidance/

Chan AW, Patel YA, Choi S. Aging of the liver: what this means for patients with HIV. Curr HIV/AIDS Rep. 2016;13(6):309–17.

Chan DC, Fass D, Berger JM, Kim PS. Core structure of gp41 from the HIV envelope glycoprotein. Cell. 1997;89(2):263–73.

Chen B, Piel WH, Gui L, Bruford E, Monteiro A. The HSP90 family of genes in the human genome: Insights into their divergence and evolution. Genomics. 2005;86(6):627–37.

Chen CJ, Kono H, Golenbock D, Reed G, Akira S, Rock KL. Identification of a key pathway required for the sterile inflammatory response triggered by dying cells. Nat Med. 2007;13(7):851–6.

Chen C, Deng M, Sun Q, Loughran P, Billiar TR, Scott MJ. Lipopolysaccharide stimulates p62-dependent autophagy-like aggregate clearance in hepatocytes. Biomed Res Int. 2014;2014:267350.

Chen GY, Núñez G. Sterile inflammation: sensing and reacting to damage. Nat Rev Immunol. 2010;10(12):826–37.

Chen K, Zeng J, Xiao H, Huang C, Hu J, Yao W, et al. Regulation of glucose metabolism by p62/SQSTM1 through HIF1α. J Cell Sci. 2016;817–30.

Chen M, Suzuki A, Borlak J, Andrade RJ, Lucena MI. Drug-induced liver injury: Interactions between drug properties and host factors. J Hepatol. 2015;63(2):503–14.

Chen P, Chen BK, Mosoian A, Hays T, Ross MJ, Klotman PE, et al. Virological synapses allow HIV-1 uptake and gene expression in renal tubular epithelial cells. J Am Soc Nephrol. 2011;22(3):496–507.

Chen Y, Xiao YI, Wu W, Wang Q, Luo G, Dierich MP. HIV-2 transmembrane protein gp36 binds to the putative cellular receptor proteins P45 and P62. Immunobiology. 2000;201(3–4):317–22.

Choe JY, Jung HY, Park KY, Kim SK. Enhanced p62 expression through impaired proteasomal degradation is involved in caspase-1 activation in monosodium urate crystal-induced interleukin-1β expression. Rheumatol (Oxford). 2014;53(6):1043–53.

Chu KM, Manzi M, Zuniga I, Rasschaert F, Zachariah R, Biot M, et al. Nevirapine- and efavirenz-associated hepatotoxicity under programmatic conditions in Kenya and Mozambique. Int J STD AIDS. 2012;23(6)403–7.

Ciccarelli N, Fabbiani M, Di Giambenedetto S, Fanti I, Baldonero E, Bracciale L, et al. Efavirenz associated with cognitive disorders in otherwise asymptomatic HIV-infected patients. Neurology. 2011;76(16):1403–9.

Cihlar T, Fordyce M. Current status and prospects of HIV treatment. Curr Opin Virol. 2016;18:50–6.

Clark LC. J, Wolf R, Granger D, Taylor Z. Continuous recording of blood oxygen tensions by polarography. J Appl Physiol. 1953;6(3):189–93.

Clark SJ, Creighton S, Portmann B, Taylor C, Wendon JA, Cramp ME. Acute liver failure associated with antiretroviral treatment for HIV: A report of six cases. J Hepatol. 2002;36(2):295–301.

De Clercq E. The design of drugs for HIV and HCV. Nat Rev Drug Discov. 2007;6(12):1001–18.

De Clercq E. Anti-HIV drugs: 25 compounds approved within 25 years after the discovery of HIV. Int J Antimicrob Agents. 2009;33(4):307–20.

De Clercq E. Antiretroviral drugs. Curr Opin Pharmacol. 2010;10:507–15.

De Clercq E. The nucleoside reverse transcriptase inhibitors, nonnucleoside reverse transcriptase inhibitors, and protease inhibitors in the treatment of HIV infections (AIDS). Adv Pharmacol. 2013;67:317-58.

Cohen-Naftaly M, Friedman SL. Current status of novel antifibrotic therapies in patients with chronic liver disease. Therap Adv Gastroenterol. 2011;4(6):391–417.

Compan V, Baroja-Mazo A, López-Castejón G, Gomez AI, Martínez CM, Angosto D, et al. Cell volume regulation modulates NLRP3 inflammasome activation. Immunity. 2012;37(3):487–500.

Coons AH, Kaplan MH. Localization of antigen in tissue cells; improvements in a method for the detection of antigen by means of fluorescent antibody. J Exp Med. 1950;91(1):1-13.

Cosín-Roger J, Ortiz-Masiá D, Calatayud S, Hernández C, Álvarez A, Hinojosa J, et al. M2 Macrophages activate WNT signaling pathway in epithelial cells: relevance in ulcerative colitis. PLoS One. 2013;8(10):e78128.

Creagh EM. Caspase crosstalk: integration of apoptotic and innate immune signalling pathways. Trends Immunol. 2014;35(12):631–40.

Crispe IN. Hepatocytes as immunological agents. J Immunol. 2016;196(1):17–21.

Csak T, Ganz M, Pespisa J, Kodys K, Dolganiuc A, Szabo G. Fatty acid and endotoxin activate inflammasomes in mouse hepatocytes that release danger signals to stimulate immune cells. Hepatology. 2011;54(1):133–44.

Cuervo AM, Wong E. Chaperone-mediated autophagy: roles in disease and aging. Cell Res. 2014;24(1):92–104.

Cullen SP, Henry CM, Kearney CJ, Logue SE, Feoktistova M, Tynan GA, et al. Fas/CD95-induced chemokines can serve as "find-me" signals for apoptotic Cells. Mol Cell. 2013;49(6):1034–48.

Czaja AJ. Hepatic inflammation and progressive liver fibrosis in chronic liver disease. World J Gastroenterol. 2014;20(10):2515–32.

Czaja MJ, Ding WX, Donohue TM, Friedman SL, Kim JS, Komatsu M, et al. Functions of autophagy in normal and diseased liver. Autophagy. 2013;9(8):1131–58.

Davidovich P, Kearney CJ, Martin SJ. Inflammatory outcomes of apoptosis, necrosis and necroptosis. Biol Chem. 2014;395(10):1163–71.

Davies LC, Jenkins SJ, Allen JE, Taylor PR. Tissue-resident macrophages. Nat Immunol. 2013;14(10):986–95.

Debes JD, Bohjanen PR, Boonstra A. Mechanisms of accelerated liver fibrosis progression during HIV infection. J Clin Transl Hepatol. 2016;4:328–35.

Decloedt EH, Maartens G. Neuronal toxicity of efavirenz : a systematic review. Expert Opin Drug Saf. 2013;12(6):841–6.

Deegan S, Koryga I, Glynn SA, Gupta S, Gorman AM, Samali A. A close connection between the PERK and IRE arms of the UPR and the transcriptional regulation of autophagy. Biochem Biophys Res Commun. 2015;456(1):305–11.

Deeks SG, Lewin SR, Havlir DV. The end of AIDS: HIV infection as a chronic disease. Lancet. 2013;382(9903):1525–33.

Deeks SG, Overbaugh J, Phillips A, Buchbinder S. HIV infection. Dis Prim. 2015;1:15035.

Deeks SG, Smith M, Holodnly M, Kahn JO. HIV-1 protease inhibitors. A review for clinicians. JAMA. 1997;227(2):145–53.

DeSantis DA, Ko CW, Liu Y, Liu X, Hise AG, Nunez G, et al. Alcohol-induced liver injury is modulated by Nlrp3 and Nlrc4 inflammasomes in mice. Mediators Inflamm. 2013;2013:751374.

Dieter P, Fitzke E, Duyster J. BAPTA induces a decrease of intracellular free calcium and a translocation and inactivation of protein kinase C in macrophages. Biol Chem Hoppe Seyler. 1993;374:171–4.

Dinarello CA. Immunological and inflammatory functions of the interleukin-1 family. Annu Rev Immunol. 2009;27(1):519–50.

Dinarello CA, Novick D, Kim S, Kaplanski G. Interleukin-18 and IL-18 binding protein. Front Immunol. 2013;4:289.

Dixon LJ, Berk M, Thapaliya S, Papouchado BG, Feldstein AE. Caspase-1-mediated regulation of fibrogenesis in diet-induced steatohepatitis. Lab Invest. 2012;92(5):713–23.

Dixon LJ, Flask CA, Papouchado BG, Feldstein AE, Nagy LE. Caspase-1 as a central regulator of high fat diet-induced non-alcoholic steatohepatitis. PLoS One. 2013;8(2):e56100.

Domingo P, Lozano F. Management of antiretroviral drug toxicity. Enferm Infecc Microbiol Clin. 2011;29(7):535–44.

Dominguez S, Ghosn J, Peytavin G, Guiguet M, Tubiana R, Valantin MA, et al. Impact of hepatitis C and liver fibrosis on antiretroviral plasma drug concentrations in HIV-HCV co-infected patients: The HEPADOSE study. J Antimicrob Chemother. 2010;65(11):2445–9.

Du Y, Wooten MC, Gearing M, Wooten MW. Age-associated oxidative damage to the p62 promoter: implications for Alzheimer disease. Free Radic Biol Med. 2009a;46(4):492–501.

Du Y, Wooten MC, Wooten MW. Oxidative damage to the promoter region of SQSTM1/p62 is common to neurodegenerative disease. Neurobiol Dis. 2009b;35(2):302–10.

Duprez L, Takahashi N, Van Hauwermeiren F, Vandendriessche B, Goossens V, Vanden Berghe T, et al. RIP kinase-dependent necrosis drives lethal systemic inflammatory response syndrome. Immunity. 2011;35(6):908–18.

Duran A, Amanchy R, Linares JF, Joshi J, Abu-Baker S, Porollo A, et al. p62 is a key regulator of nutrient sensing in the mTORC1 pathway. Mol Cell. 2011;44(1):134–46.

Duran A, Hernandez ED, Reina-Campos M, Castilla EA, Subramaniam S, Raghunandan S, et al. p62/SQSTM1 by binding to vitamin D receptor inhibits hepatic stellate cell activity, fibrosis, and liver cancer. Cancer Cell. 2016;30(4):595–609.

Echenique IA, Rich JD. EFV/FTC/TDF-associated hepatotoxicity: a case report and review. AIDS Patient Care STDS. 2013;27(9):493–7.

Edelman EJ, Gordon KS, Lo Re V 3rd, Skanderson M, Fiellin DA, Justice AC, et al. Acetaminophen receipt among HIV-infected patients with advanced hepatic fibrosis. Pharmacoepidemiol Drug Saf. 2013;22(12):1352–6.

Elliott EI, Sutterwala FS. Initiation and perpetuation of NLRP3 inflammasome activation and assembly. Immunol Rev. 2015;265(1):35–52.

Elsharkawy AM, Oakley F, Mann DA. The role and regulation of hepatic stellate cell apoptosis in reversal of liver fibrosis. Apoptosis. 2005;10(4):927–39.

Elsharkawy AM, Schwab U, McCarron B, Burt AD, Daly AK, Hudson M, et al. Efavirenz induced acute liver failure requiring liver transplantation in a slow drug metaboliser. J Clin Virol. 2013;58(1):331–3.

Erhardt A, Tiegs G. IL-33-A cytokine which balances on a knife's edge?. J Hepatol. 2012;56(1):7–10.

Farrell GC, van Rooyen D, Gan L, Chitturi S. NASH is an inflammatory disorder: pathogenic, prognostic and therapeutic implications. Gut Liver. 2012;6(2):149–71.

Feldman N, Rotter-Maskowitz A, Okun E. DAMPs as mediators of sterile inflammation in aging-related pathologies. Ageing Res Rev. 2015;24:29–39.

Feng JY, Johnson AA, Johnson KA, Anderson KS. Insights into the molecular mechanism of mitochondrial toxicity by aids drugs. J Biol Chem. 2001;276(26):23832–7.

Feng Y, He D, Yao Z, Klionsky DJ. The machinery of macroautophagy. Cell Res. 2014;24(1):24–41.

Fernandez-Montero JV, Eugenia E, Barreiro P, Labarga P, Soriano V. Antiretroviral drug-related toxicities – clinical spectrum, prevention, and management. Expert Opin Drug Saf. 2013;12(5):697–707.

Filomeni G, Zio D De, Cecconi F. Oxidative stress and autophagy: the clash between damage and metabolic needs. Cell Death Differ. 2015;22(3):377–88.

Fink DL, Bloch E. Liver transplantation for acute liver failure due to efavirenz hepatotoxicity: the importance of routine monitoring. Int J STD AIDS. 2013;24(10):831–3.

Fischl MA, Richman DD, Grieco MH, Gottlieb MS, Volberding PA, Laskin OL, et al. The efficacy of azidothymidine (AZT) in the treatment of patients with AIDS and AIDS-related complex. A double-blind, placebo-controlled trial. N Engl J Med. 1987;317(4):185–91.

Fisher K, Vuppalanchi R, Saxena R. Drug-induced liver injury. Arch Pathol Lab Med. 2015;139(7):876-87.

Flexner C. HIV drug development: the next 25 years. Nat Rev Drug Discov. 2007;6(12):959–66.

Fontana RJ. Pathogenesis of idiosyncratic drug-induced liver injury and clinical perspectives. Gastroenterology. 2014;146(4):914–28.

Ford N, Mofenson L, Shubber Z, Calmy A, Andrieux-Meyer I, Vitoria M, et al. Safety of efavirenz in the first trimester of pregnancy: an updated systematic review and meta-analysis. AIDS. 2014;28 Suppl 2:S123-31.

Franchi L, Eigenbrod T, Muñoz-Planillo R, Nuñez G. The inflammasome: a caspase-1-activation platform that regulates immune responses and disease pathogenesis. Nat Immunol. 2009;10(3):241–7.

Franklin BS, Bossaller L, De Nardo D, Ratter JM, Stutz A, Engels G, et al. The adaptor ASC has extracellular and “prionoid” activities that propagate inflammation. Nat Immunol. 2014;15(8):727–37.

Freed EO. HIV-1 assembly, release and maturation. Nat Rev Microbiol. 2015;13(8):484–96.

Freshney R. Protocol 22.2.8 HepaRG human hepatocytes. In: Culture of animal cells: a manual of basic technique and specialized applications, Sixth Edition. Wiley-Blackwell. 2011. p.383–432, ISBN: 9780470528129.

Friedman SL. Hepatic Stellate cells : protean , multifunctional , and enigmatic cells of the liver. Physiol Rev. 2008;2454:125–72.

Friedman SL. Evolving challenges in hepatic fibrosis. Nat Rev Gastroenterol Hepatol. 2010;7(8):425–36.

Friedman SL. Liver fibrosis in 2012: convergent pathways that cause hepatic fibrosis in NASH. Nat Rev Gastroenterol Hepatol. 2013;10(2):71–2.

Friedman SL, Sheppard D, Duffield JS, Violette S. Therapy for fibrotic diseases: nearing the starting line. Sci Transl Med. 2013;5(167):167sr1.

Funes HA, Apostolova N, Alegre F, Blas-Garcia A, Alvarez A, Marti-Cabrera M, et al. Neuronal bioenergetics and acute mitochondrial dysfunction: A clue to understanding the central nervous system side effects of efavirenz. J Infect Dis. 2014;210(9):1385–95.

Funes HA, Blas-Garcia A, Esplugues JV, Apostolova N. Efavirenz alters mitochondrial respiratory function in cultured neuron and glial cell lines. J Antimicrob Chemother. 2015;70(8):2249–54.

Fung HB, Guo Y. Enfuvirtide: first fusion inhibitor for treatment of HIV infection. Clin Ther. 2004;26(3):352–78.

Galluzzi L, Kepp O, Kroemer G. Mitochondria: master regulators of danger signalling. Nat Rev Mol Cell Biol. 2012a;13(12):780–8.

Galluzzi L, Kepp O, Trojel-Hansen C, Kroemer G. Mitochondrial control of cellular life, stress, and death. Circ Res. 2012b;111(9):1198–207.

Gao B, Radaeva S, Park O. Liver natural killer and natural killer T cells: immunobiology and emerging roles in liver diseases. J Leukoc Biol. 2009;86(3):513–28.

Garg AD, Nowis D, Golab J, Vandenabeele P, Krysko DV, Agostinis P. Immunogenic cell death, DAMPs and anticancer therapeutics: an emerging amalgamation. Biochim Biophys Acta. 2010;1805(1):53–71.

GBD 2013 Mortality and Causes of Death Collaborators. Global, regional, and national age-sex specific all-cause and cause-specific mortality for 240 causes of death, 1990-2013: a systematic analysis for the Global Burden of Disease Study 2013. Lancet. 2015;385(385):117–71.

Geetha T, Vishwaprakash N, Sycheva M, Babu JR. Sequestosome 1/p62: across diseases. Biomarkers. 2012a;17(2):99–103.

Geetha T, Zheng C, Vishwaprakash N, Broderick TL, Babu JR. Sequestosome 1/p62, a scaffolding protein, is a newly identified partner of IRS-1 protein. J Biol Chem. 2012b;287(35):29672–8.

GeSIDA. Documento de consenso de Gesida/Plan Nacional sobre el Sida respecto al tratamiento antirretroviral en adultos infectados por el virus de la inmunodeficiencia humana (Actualización enero 2016). Accessed (13/01/2017) [cited 2017 Jan 17]. Available from: https://www.msssi.gob.es/ciudadanos/

Gharagozloo M, Mahvelati TM, Imbeault E, Gris P, Zerif E, Bobbala D, et al. The nod-like receptor, Nlrp12, plays an anti-inflammatory role in experimental autoimmune encephalomyelitis. J Neuroinflammation. 2015;12:198.

Ghosh S, May MJ, Kopp EB. NF-kappa B and Rel proteins: evolutionarily conserved mediators of immune responses. Annu Rev Immunol. 1998;16:225–60.

Gieling RG, Wallace K, Han YP. Interleukin-1 participates in the progression from liver injury to fibrosis. Am J Physiol Gastrointest Liver Physiol. 2009;296(6):G1324-31.

Glick D, Barth S, Macleod KF. Autophagy : cellular and molecular mechanisms. J Pathol. 2010;221(1):3–12.

Gomez-Sucerquia LJ, Blas-Garcia A, Marti-Cabrera M, Esplugues JV, Apostolova N. Profile of stress and toxicity gene expression in human hepatic cells treated with Efavirenz. Antiviral Res. 2012;94(3):232–41.

Goswami P, Gupta S, Biswas J, Joshi N, Swarnkar S, Nath C, et al. Endoplasmic reticulum stress plays a key role in rotenone-induced apoptotic death of neurons. Mol Neurobiol. 2016;53(1):285–98.

Gounden V, van Niekerk C, Snyman T, George JA. Presence of the CYP2B6 516G> T polymorphism, increased plasma Efavirenz concentrations and early neuropsychiatric side effects in South African HIV-infected patients. AIDS Res Ther. 2010;7:32.

Granich R, Crowley S, Vitoria M, Smyth C, Kahn JG, Bennett R, et al. Highly active antiretroviral treatment as prevention of HIV transmission: review of scientific evidence and update. Curr Opin HIV AIDS. 2010;5(4):298–304.

Grattagliano I, Bonfrate L, Diogo CV, Wang HH, Wang DQ, Portincasa P. Biochemical mechanisms in drug-induced liver injury: certainties and doubts. World J Gastroenterol. 2009;15(39):4865–76.

Gray MW, Burger G, Lang BF. Mitochondrial evolution. Science. 1999;283(5407):1476-81.

Greenspan P, Fowler SD. Spectrofluorometric studies of the lipid probe, nile red. J Lipid Res. 1985;26:781–9.

Gripon P, Rumin S, Urban S, Le Seyec J, Glaise D, Cannie I, et al. Infection of a human hepatoma cell line by hepatitis B virus. Proc Natl Acad Sci U S A. 2002;99(24):15655–60.

Grootjans J, Kaser A, Kaufman RJ, Blumberg RS. The unfolded protein response in immunity and inflammation. Nat Rev Immunol. 2016;16(8):469–84.

Grotemeier A, Alers S, Pfisterer SG, Paasch F, Daubrawa M, Dieterle A, et al. AMPK-independent induction of autophagy by cytosolic Ca2+ increase. Cell Signal. 2010;22(6):914–25.

Guaraldi G, Prakash M, Moecklinghoff C, Stellbrink HJ. Morbidity in older HIV-infected patients: Impact of long-term antiretroviral use. AIDS Rev. 2014a;16(2):75–89.

Guaraldi G, Silva AR, Stentarelli C. Multimorbidity and functional status assessment. Curr Opin HIV AIDS. 2014b;9(4):386–97.

Guengerich FP. Mechanisms of drug toxicity and relevance to pharmaceutical development. Drug Metab Pharmacokinet. 2011;26(1):3–14.

Günthard HF, Saag MS, Benson CA, del Rio C, Eron JJ, Gallant JE, et al. Antiretroviral drugs for treatment and prevention of HIV infection in adults. 2016 recommendations of the International Antiviral Society-USA Panel. JAMA. 2016;316(2):191-210.

Guo H, Callaway JB, Ting JP. Inflammasomes: mechanism of action, role in disease, and therapeutics. Nat Med. 2015;21(7):677–87.

Gurunathan S, Habib R El, Baglyos L, Meric C, Plotkin S, Dodet B, et al. Use of predictive markers of HIV disease progression in vaccine trials. Vaccine. 2009;27:1997–2015.

Gurung P, Lukens JR, Kanneganti TD. Mitochondria: diversity in the regulation of the NLRP3 inflammasome. Trends Mol Med. 2015;21(3):193–201.

Gutiérrez F, Navarro A, Padilla S, Antón R, Masia M, Borrás J, et al. Prediction of neuropsychiatric adverse events associated with long-term efavirenz therapy, using plasma drug level monitoring. Clin Infect Dis. 2005;41:1648–53.

Haas DW, Ribaudo HJ, Kim RB, Tierney C, Wilkinson GR, Gulick RM, et al. Pharmacogenetics of efavirenz and central nervous system side effects: an adult AIDS clinical trials group study. AIDS. 2004;18(18):2391–400.

Hammer SM, Katzenstein DA, Hughes MD, Gundacker H, Schooley RT, Haubrich RH, et al. A trial comparing nucleoside monotherapy with combination therapy in hiv-infected adults with CD4 cell counts from 200 to 500 per cubic millimeter. N Engl J Med. 1996;335(15):1081–90.

Han D, Ybanez MD, Ahmadi S, Yeh K, Kaplowitz N. Redox regulation of tumor necrosis factor signaling. Antioxid Redox Signal. 2009;11(9):2245–63.

Han J, Back SH, Hur J, Lin YH, Gildersleeve R, Shan J, et al. ER-stress-induced transcriptional regulation increases protein synthesis leading to cell death. Nat Cell Biol. 2013;15(5):481–90.

Hardy H, Skolnik PR. Enfuvirtide, a new fusion inhibitor for therapy of human immunodeficiency virus infection. Pharmacotherapy. 2004;24(2):198–211.

Harijith A, Ebenezer DL, Natarajan V. Reactive oxygen species at the crossroads of inflammasome and inflammation. Front Physiol. 2014;5:352.

Harper JW, Schulman BA. Structural complexity in ubiquitin recognition. Cell. 2006;124(6):1133–6.

Hart GJ, Orr DC, Penn CR, Figueiredo HT, Gray NM, Boehme RE, et al. Effects of (-)-2'-deoxy-3'-thiacytidine (3TC) 5'-triphosphate on human immunodeficiency virus reverse transcriptase and mammalian DNA polymerases. Antimicrob Agents Chemother. 1992;36(8):1688–94.

Hashiguchi K, Zhang-Akiyama QM. Establishment of human cell lines lacking mitochondrial DNA. In: Mitochondrial DNA, Methods and Protocols. 2009;554:383–91.

Hasse B, Gunthard HF, Bleiber G, Krause M. Efavirenz intoxication due to slow hepatic metabolism. Clin Infect Dis. 2005;40(3):e22-3.

Hayes JD, McMahon M. Nrf2 and Keap1 mutations: permanent activation of an adaptive response in cancer. Trends Biochem Sci. 2009;34(4):176–88.

He W, Wang B, Yang J, Zhuang Y, Wang L, Huang X, et al. Chloroquine improved carbon tetrachloride-induced liver fibrosis through its inhibition of the activation of hepatic stellate cells: role of autophagy. Biol Pharm Bull. 2014;37(9):1505–9.

He Y, Hara H, Núñez G. Mechanism and regulation of NLRP3 inflammasome activation. Trends Biochem Sci. 2016;41(12):1012–21.

Hedbrant A, Erlandsson A, Delbro D, Wijkander J. Conditioned media from human macrophages of M1 phenotype attenuate the cytotoxic effect of 5-fluorouracil on the HT-29 colon cancer cell line. Int J Oncol. 2015;46(1):37–46.

Hellerbrand C, Jobin C, Licato LL, Sartor RB, Brenner DA. Cytokines induce NF-kappaB in activated but not in quiescent rat hepatic stellate cells. Am J Physiol. 1998;275(2 Pt 1):G269-78.

Hemmann S, Graf J, Roderfeld M, Roeb E. Expression of MMPs and TIMPs in liver fibrosis - a systematic review with special emphasis on anti-fibrotic strategies. J Hepatol. 2007;46(5):955–75.

Henao-Mejia J, Elinav E, Strowig T, Flavell RA. Inflammasomes: far beyond inflammation. Nat Immunol. 2012;13(4):321–4.

Hernández-Gea V, Friedman SL. Pathogenesis of liver fibrosis. Annu Rev Pathol. 2011;6:425–56.

Hernández-Gea V, Ghiassinejad Z, Rozenfeld R, Gordon R, Fiel MI, Yue Z, et al. Autophagy releases lipid that promotes fibrogenesis by activated hepatic stellate cells in mice and in human tissues. Gastroenterology. 2012;142(4):938–46.

Hernández-Gea V, Hilscher M, Rozenfeld R, Lim MP, Nieto N, Werner S, et al. Endoplasmic reticulum stress induces fibrogenic activity in hepatic stellate cells through autophagy. J Hepatol. 2013;59(1):98–104.

Hernandez LV, Gilson I, Jacobson J, Affi A, Puetz TR, Dindzans VJ. Antiretroviral hepatotoxicity in human immunodeficiency virus-infected patients. Aliment Pharmacol Ther. 2001;15(10):1627–32.

Hetz C. The unfolded protein response: controlling cell fate decisions under ER stress and beyond. Nat Rev Mol Cell Biol. 2012;13(2):89–102.

Hetz C, Chevet E, Oakes SA. Proteostasis control by the unfolded protein response. Nat Cell Biol. 2015;17(7):829–38.

Heymann F, Tacke F. Immunology in the liver - from homeostasis to disease. Nat Rev Gastroenterol Hepatol. 2016;13(2):88–110.

Ho DD, Neumann AU, Perelson AS, Chen W, Leonard JM, Markowitz M. Rapid turnover of plasma virions and CD4 lymphocytes in HIV-1 infection. Nature. 1995;373(6510)123-6.

Hoffmann CJ, Charalambous S, Thio CL, Martin DJ, Pemba L, Fielding KL, et al. Hepatotoxicity in an African antiretroviral therapy cohort : the effect of tuberculosis and hepatitis B. AIDS. 2007;21(10)1301-8.

Hoffmann CJ, Hoffmann JD, Kensler C, van der Watt M, Omar T, Chaisson RE, et al. Tuberculosis and hepatic steatosis are prevalent liver pathology findings among HIV-infected patients in South Africa. PLoS One. 2015;10(2):e0117813.

Hofman P, Nelson AM. The pathology induced by highly active antiretroviral therapy against human immunodeficiency virus: an update. Curr Med Chem. 2006;13(26):3121–32.

Hoque R, Farooq A, Mehal WZ. Sterile inflammation in the liver and pancreas. J Gastroenterol Hepatol. 2013;28(Suppl 1):61–7.

Hoque R, Sohail MA, Salhanick S, Malik AF, Ghani A, Robson SC, et al. P2X7 receptor-mediated purinergic signaling promotes liver injury in acetaminophen hepatotoxicity in mice. Am J Physiol Gastrointest Liver Physiol. 2012;302(10):G1171-9.

Hsu SM, Raine L, Fanger H. Use of avidin-biotin-peroxidase complex (ABC) in immunoperoxidase techniques: a comparison between ABC and unlabeled antibody (PAP) procedures. J Histochem Cytochem. 1981;29(4):577–80.

Hu J, Han H, Lau MY, Lee H, Macveigh-Aloni M, Ji C. Effects of combined alcohol and anti-HIV drugs on cellular stress responses in primary hepatocytes and hepatic stellate and Kupffer cells. Alcohol Clin Exp Res. 2015;39(1):11–20.

Huang W, Metlakunta A, Dedousis N, Zhang P, Sipula I, Dube JJ, et al. Depletion of liver Kupffer cells prevents the development of diet-induced hepatic steatosis and insulin resistance. Diabetes. 2010;59(2):347–57.

Huang WX, Huang P, Hillert J. Increased expression of caspase-1 and interleukin-18 in peripheral blood mononuclear cells in patients with multiple sclerosis. Mult Scler. 2004;10(5):482–7.

Huang Y, Luo F, Li H, Jiang T, Zhang N. Conditioned medium from alternatively activated macrophages induce mesangial cell apoptosis via the effect of Fas. Exp Cell Res. 2013;319(19)3051-7.

Huff JR, Anderson PS, Olsen DB, Carroll SS, Young SD, Britcher SF, et al. L-743, 726 (DMP-266): a novel, highly potent nonnucleoside inhibitor of the human immunodeficiency virus type 1 reverse transcriptase. Antimicrob Agents Chemother. 1995;39(12):2602–5.

Hughes PJ, Cretton-Scott E, Teague A, Wensel TM. Protease Inhibitors for patients with HIV- 1 infection a comparative overview. Pharm Ther. 2011;36(6):332–45.

Ichimura Y, Kumanomidou T, Sou YS, Mizushima T, Ezaki J, Ueno T, et al. Structural basis for sorting mechanism of p62 in selective autophagy. J Biol Chem. 2008;283(33):22847–57.

Ichimura Y, Waguri S, Sou YS, Kageyama S, Hasegawa J, Ishimura R, et al. Phosphorylation of p62 activates the Keap1-Nrf2 pathway during selective autophagy. Mol Cell. 2013;51(5):618–31.

Imaeda AB, Watanabe A, Sohail MA, Mahmood S, Mohamadnejad M, Sutterwala FS, et al. Acetaminophen-induced hepatotoxicity in mice is dependent on TLR9 and the Nalp3 inflammasome. J Clin Invest. 2009;119(2):305–14.

Imaizumi N, Kwang Lee K, Zhang C, Boelsterli UA. Mechanisms of cell death pathway activation following drug-induced inhibition of mitochondrial complex I. Redox Biol. 2015;4:279–88.

Inami Y, Waguri S, Sakamoto A, Kouno T, Nakada K, Hino O, et al. Persistent activation of Nrf2 through p62 in hepatocellular carcinoma cells. J Cell Biol. 2011;193(2):275–84.

Inoue H, Kobayashi K, Ndong M, Yamamoto Y, Katsumata S, Suzuki K, et al. Activation of Nrf2/Keap1 signaling and autophagy induction against oxidative stress in heart in iron deficiency. Biosci Biotechnol Biochem. 2015;79(8):1366–8.

Ioannou GN, Van Rooyen DM, Savard C, Haigh WG, Yeh MM, Teoh NC, et al. Cholesterol-lowering drugs cause dissolution of cholesterol crystals and disperse Kupffer cell crown-like structures during resolution of NASH. J Lipid Res. 2015;56(2):277–85.

Iracheta-Vellve A, Petrasek J, Satishchandran A, Gyongyosi B, Saha B, Kodys K, et al. Inhibition of sterile danger signals, uric acid and ATP, prevents inflammasome activation and protects from alcoholic steatohepatitis in mice. J Hepatol. 2015;63(5):1147–55.

Iredale JP, Thompson A, Henderson NC. Extracellular matrix degradation in liver fibrosis: biochemistry and regulation. Biochim Biophys Acta. 2013;1832(7):876–83.

Iser DM, Lewin SR. The pathogenesis of liver disease in the setting of HIV – hepatitis B virus coinfection. Antivir Ther. 2009;6535:155–64.

Ishiguro H, Yasuda K, Ishii N, Ihara K, Ohkubo T, Hiyoshi M, et al. Enhancement of oxidative damage to cultured cells and Caenorhabditis elegans by mitochondrial electron transport inhibitors. IUBMB Life. 2001;51(4):263–8.

Ishii T, Warabi E, Siow RC, Mann GE. Sequestosome1/p62: A regulator of redox-sensitive voltage-activated potassium channels, arterial remodeling, inflammation, and neurite outgrowth. Free Radic Biol Med. 2013;65:102–16.

Ishii T, Yanagawa T, Kawane T, Yuki K, Seita J, Yoshida H, et al. Murine peritoneal macrophages induce a novel 60-kDa protein with structural similarity to a tyrosine kinase p56lck-associated protein in response to oxidative stress. Biochem Biophys Res Commun.1996;460:456–60.

Jaeschke H. Reactive oxygen and mechanisms of inflammatory liver injury: Present concepts. J Gastroenterol Hepatol. 2011;26(Suppl. 1):173–9.

Jain A, Lamark T, Sjøttem E, Larsen KB, Awuh JA, Øvervatn A, et al. p62/SQSTM1 is a target gene for transcription factor Nrf2 and creates a positive feedback loop by inducing antioxidant response element-driven gene transcription. J Biol Chem. 2010;285(29):22576–91.

Jaramillo M, Zhang D. The emerging role of the Nrf2–Keap1 signaling pathway in cancer. Genes Dev. 2013;27:2179–91.

Jéru I, Duquesnoy P, Fernandes-Alnemri T, Cochet E, Yu JW, Lackmy-Port-Lis M, et al. Mutations in NALP12 cause hereditary periodic fever syndromes. Proc Natl Acad Sci U S A. 2008;105(5):1614–9.

Jiang P, Mizushima N. LC3- and p62-based biochemical methods for the analysis of autophagy progression in mammalian cells. Methods. 2015;75:13–8.

Jiang T, Harder B, Rojo de la Vega M, Wong PK, Chapman E, Zhang DD. p62 links autophagy and Nrf2 signaling. Free Radic Biol Med. 2015;88:199–204.

Jin W, Chang M, Paul EM, Babu G, Lee AJ, Reiley W, et al. Deubiquitinating enzyme CYLD negatively regulates RANK signaling and osteoclastogenesis in mice. J Clin Invest. 2008;118(5):1858–66.

Jo EK, Kim JK, Shin DM, Sasakawa C. Molecular mechanisms regulating NLRP3 inflammasome activation. Cell Mol Immunol. 2016;13(2):148–59.

Johansen T, Lamark T. Selective autophagy mediated by autophagic adapter proteins. Autophagy. 2011;7(3):279–96.

Jones M, Núñez M. Liver toxicity of antiretroviral drugs. Semin Liver Dis. 2012;32(2):167–76.

Ju C, Tacke F. Hepatic macrophages in homeostasis and liver diseases: from pathogenesis to novel therapeutic strategies. Cell Mol Immunol. 2016;13:316-27.

Kalapila AG, Marrazzo J. Antiretroviral therapy for prevention of human immunodeficiency virus infection. Med Clin North Am. 2016;100(4):927–50.

Kamari Y, Shaish A, Vax E, Shemesh S, Kandel-Kfir M, Arbel Y, et al. Lack of interleukin-1alpha or interleukin-1beta inhibits transformation of steatosis to steatohepatitis and liver fibrosis in hypercholesterolemic mice. J Hepatol 2011;55(5):1086–94.

Kanayama M, Inoue M, Danzaki K, Hammer G, He Y, Shinohara ML. Autophagy enhances NFkB activity in specific tissue macrophages by sequestering A20 to boost antifungal immunity. Nat Commun. 2015;6:1–14.

Kansanen E, Kuosmanen SM, Leinonen H, Levonenn AL. The Keap1-Nrf2 pathway: mechanisms of activation and dysregulation in cancer. Redox Biol. 2013;1(1):45–9.

Kanters S, Vitoria M, Doherty M, Socias ME, Ford N, Forrest JI, et al. Comparative efficacy and safety of first-line antiretroviral therapy for the treatment of HIV infection: a systematic review and network meta-analysis. Lancet HIV. 2016;3(11):e510–20.

Kappelhoff BS, Huitema AD, Yalvaç Z, Prins JM, Mulder JW, Meenhorst PL, et al. Population pharmacokinetics of efavirenz in an unselected cohort of HIV-1-infected individuals. Clin Pharmacokinet. 2005;44(8):849–61.

Katsuragi Y, Ichimura Y, Komatsu M. p62/SQSTM1 functions as a signaling hub and an autophagy adaptor. FEBS J. 2015;282(24):4672–8.

Kaur J, Debnath J. Autophagy at the crossroads of catabolism and anabolism. Nat Rev Mol Cell Biol. 2015;16(8):461–72.

Kearney CJ, Sheridan C, Cullen SP, Tynan GA, Logue SE, Afonina IS, et al. Inhibitor of apoptosis proteins (IAPs) and their antagonists regulate spontaneous and tumor necrosis factor (TNF)-induced proinflammatory cytokine and chemokine production. J Biol Chem. 2013;288(7):4878–90.

Kim HY, Kim SJ, Lee SM. Activation of NLRP3 and AIM2 inflammasomes in Kupffer cells in hepatic ischemia/reperfusion. FEBS J. 2015;282:259-70.

Kim JY, Ozato K. p62 attenuates cytokine gene expression in activated macrophages by inhibiting IFN regulatory factor 8 and TNF receptor-associated factor 6/NF-kappaB activity. J Immunol. 2009;182(4):2131–40.

Koelsch KK, Cooper DA. Integrase inhibitors in salvage therapy regimens for HIV-1 infection. Curr Opin HIV AIDS. 2009;4(6):518–23.

Kojima S, Hayashi S, Shimokado K, Suzuki Y, Shimada J, Crippa MP, et al. Transcriptional activation of urokinase by the Krüppel-like factor Zf9/COPEB activates latent TGF-β1 in vascular endothelial cells. Blood. 2000 Feb 15;95(4):1309–16.

Komatsu M, Kageyama S, Ichimura Y. p62/SQSTM1/A170: physiology and pathology. Pharmacol Res. 2012;66(6):457–62.

Koo JH, Lee HJ, Kim W, Kim SG. Endoplasmic reticulum stress in hepatic stellate cells promotes liver fibrosis via PERK-mediated degradation of HNRNPA1 and up-regulation of SMAD2. Gastroenterology. 2016;150(1):181–193.e8.

Kovari H, Weber R. Influence of antiretroviral therapy on liver disease. Curr Opin HIV AIDS. 2011;6(4):272–7.

Kroemer G, Galluzzi L, Brenner C. Mitochondrial membrane permeabilization in cell death. Physiol Reveiw. 2007;99–163.

Krysko DV, Agostinis P, Krysko O, Garg AD, Bachert C, Lambrecht BN, et al. Emerging role of damage-associated molecular patterns derived from mitochondria in inflammation. Trends Immunol. 2011;32(4):157–64.

Kryst J, Kawalec P, Pilc A. Efavirenz-based regimens in antiretroviral-naive HIV-infected patients: a systematic review and meta-analysis of randomized controlled trials. PLoS One. 2015;10(5):1–23.

Kubes P, Mehal WZ. Sterile inflammation in the liver. Gastroenterology. 2012;143(5):1158–72.

Kuusisto E, Suuronen T, Salminen A. Ubiquitin-binding protein p62 expression is induced during apoptosis and proteasomal inhibition in neuronal cells. Biochem Biophys Res Commun. 2001;280(1):223–8.

Kwara A, Lartey M, Sagoe KW, Rzek NL, Court MH. CYP2B6 (c.516G-->T) and CYP2A6 (*9B and/or *17) polymorphisms are independent predictors of efavirenz plasma concentrations in HIV-infected patients. Br J Clin Pharmacol. 2009;67(4):427–36.

Kwon J, Han E, Bui CB, Shin W, Lee J, Lee S, et al. Assurance of mitochondrial integrity and mammalian longevity by the p62-Keap1-Nrf2-Nqo1 cascade. EMBO Rep. 2012;13(2):150–6.

Lamkanfi M, Dixit VM. Mechanisms and functions of inflammasomes. Cell. 2014/05/27. 2014;157(5):1013–22.

Lamkanfi M, Van de Walle L, Kanneganti TD. Deregulated inflammasome signaling in disease. Immunol Rev. 2011;243(1):163–73.

Lane T, Flam B, Lockey R, Kolliputi N. TXNIP shuttling : missing link between oxidative stress and inflammasome activation. 2013;4:50.

Larder BA, Darby G, Richman DD. HIV with reduced sensitivity to zidovudine (AZT) isolated during prolonged therapy. Science. 1989;243(4889):1731-4.

Laskey SB, Siliciano RF. A mechanistic theory to explain the efficacy of antiretroviral therapy. Nat Rev Micro. 2014;12(11):772–80.

Latz E. The inflammasomes: mechanisms of activation and function. Curr Opin Immunol. 2010;22(1):28–33.

Latz E, Xiao TS, Stutz A. Activation and regulation of the inflammasomes. Nat Rev Immunol. 2013;13(6):397–411.

Laurin N, Brown JP, Morissette J, Raymond V, Aksentijevich I, Galon J, et al. Recurrent mutation of the gene encoding sequestosome 1 (SQSTM1/p62) in Paget disease of bone. Am J Hum Genet. 2002;70(6):1582–8.

Lawrence T. The nuclear factor NF-kB pathway in inflammation. Cold Spring Harb Perspect Med. 2009;1(6):a001651.

Lawrence T, Natoli G. Transcriptional regulation of macrophage polarization: enabling diversity with identity. Nat Rev Immunol. 2011;11(11):750–61.

Lederman MM, Connick E, Landay A, Kuritzkes DR, Spritzler J, St Clair M, et al. Immunologic responses associated with 12 weeks of combination antiretroviral therapy consisting of zidovudine, lamivudine, and ritonavir: results of AIDS Clinical Trials Group Protocol 315. J Infect Dis. 1998;178(1):70–9.

Lee G, Subramanian N, Kim AI, Aksentijevich I, Goldbach-Mansky R, Sacks DB, et al. The calcium-sensing receptor regulates the NLRP3 inflammasome through Ca2+ and cAMP. Nature. 2012;492(7427):123–7.

Lee HM, Shin DM, Yuk JM, Shi G, Choi DK, Lee SH, et al. Autophagy negatively regulates keratinocyte inflammatory responses via scaffolding protein p62/SQSTM1. J Immunol. 2011;186(2):1248–58.

Lee IC, Ko JW, Lee SM, Kim SH, Shin IS, Moon OS, et al. Time-course and molecular mechanism of hepatotoxicity induced by 1,3-dichloro-2-propanol in rats. Environ Toxicol Pharmacol. 2015a;40(1):191–8.

Lee JK, Kim SH, Lewis EC, Azam T, Reznikov LL, Dinarello CA. Differences in signaling pathways by IL-1beta and IL-18. Proc Natl Acad Sci U S A. 2004;101(23):8815–20.

Lee SJ, Pfluger PT, Kim JY, Nogueiras R, Duran A, Pagès G, et al. A functional role for the p62-ERK1 axis in the control of energy homeostasis and adipogenesis. EMBO Rep. 2010;11(3):226–32.

Lee YA, Wallace MC, Friedman SL. Pathobiology of liver fibrosis: a translational success story. Gut. 2015;64(5):830–41.

Lee YH, Ko J, Joung I, Kim JH, Shin J. Immediate early response of the p62 gene encoding a non-proteasomal multiubiquitin chain binding protein. FEBS Lett. 1998;438(3):297–300.

Leger P, Dillingham R, Beauharnais CA, Kashuba AD, Rezk NL, Fitzgerald DW, et al. CYP2B6 variants and plasma efavirenz concentrations during antiretroviral therapy in Port-au-Prince, Haiti. J Infect Dis. 2009a;200(6):955–64.

Leise MD, Poterucha JJ, Talwalkar JA. Drug-induced liver injury. Mayo Clin Proc. 2014;89(1):95–106.

Lerner AG, Upton JP, Praveen PVK, Ghosh R, Nakagawa Y, Igbaria A, et al. IRE1α induces thioredoxin-interacting protein to activate the NLRP3 inflammasome and promote programmed cell death under irremediable ER stress. Cell Metab. 2012;16(2):250–64.

Li WW, Li J, Bao JK. Microautophagy: lesser-known self-eating. Cell Mol Life Sci. 2012;69(7):1125–36.

Li X, Wang Y, Wang H, Huang C, Huang Y, Li J. Endoplasmic reticulum stress is the crossroads of autophagy, inflammation, and apoptosis signaling pathways and participates in liver fibrosis. Inflamm Res. 2015;64(1):1–7.

Liedtke C, Trautwein C. The role of TNF and Fas dependent signaling in animal models of inflammatory liver injury and liver cancer. Eur J Cell Biol. 2012;91(6):582–9.

Lin J, Schyschka L, Mühl-Benninghaus R, Neumann J, Hao L, Nussler N, et al. Comparative analysis of phase i and II enzyme activities in 5 hepatic cell lines identifies Huh-7 and HCC-T cells with the highest potential to study drug metabolism. Arch Toxicol. 2012;86(1):87–95.

Lin W, Wu G, Li S, Weinberg EM, Kumthip K, Peng LF, et al. HIV and HCV cooperatively promote hepatic fibrogenesis via induction of reactive oxygen species and NF-κB. J Biol Chem. 2011;286(4):2665–74.

Lippai M, Low P. The role of the selective adaptor p62 and ubiquitin-like proteins in autophagy. Biomed Res Int. 2014;2014.

Liu XD, Ko S, Xu Y, Fattah EA, Xiang Q, Jagannath C, et al. Transient aggregation of ubiquitinated proteins is a cytosolic unfolded protein response to inflammation and endoplasmic reticulum stress. J Biol Chem. 2012;287(23):19687–98.

Liu X, Zhang Z, Ruan J, Pan Y, Magupalli VG, Wu H, et al. Inflammasome-activated gasdermin D causes pyroptosis by forming membrane pores. Nature. 2016;535(7610):153–8.

Liu Y, Liu H, Kim BO, Gattone VH, Li J, Nath A, et al. CD4-independent infection of astrocytes by human immunodeficiency virus type 1: requirement for the human mannose receptor. J Virol. 2004;78(8):4120–33.

Loken MR. Simultaneous quantitation of hoechst 33342 and immunofluorescence on viable cells using a fluorescence activated cell sorter. Cytometry. 1980;1(2):136–42.

Loko MA, Bani-Sadr F, Winnock M, Lacombe K, Carrieri P, Neau D, et al. Impact of HAART exposure and associated lipodystrophy on advanced liver fibrosis in HIV/HCV-coinfected patients. J Viral Hepat. 2011;18(7).

Lopez-Castejon G, Brough D. Understanding the mechanism of IL-1β secretion. Cytokine Growth Factor Rev. 2011;22(4):189–95.

Lou PH, Hansen BS, Olsen PH, Tullin S, Murphy MP, Brand MD. Mitochondrial uncouplers with an extraordinary dynamic range. Biochem J. 2007;407(1):129–40.

Lowenhaupt EA, Matson K, Qureishi B, Saitoh A, Pugatch D. Psychosis in a 12-year-old HIV- positive girl with an increased serum concentration of efavirenz. Clin Infect Dis. 2007;45:2004–6.

Lu A, Magupalli VG, Ruan J, Yin Q, Atianand MK, Vos MR, et al. Unified polymerization mechanism for the assembly of ASC-dependent inflammasomes. Cell. 2014;156(6):1193–206.

Luedde T, Kaplowitz N, Schwabe RF. Cell death and cell death responses in liver disease: mechanisms and clinical relevance. Gastroenterology. 2014;147(4):765–783.e4.

Luedde T, Schwabe RF. NF-κB in the liver-linking injury, fibrosis and hepatocellular carcinoma. Nat Rev Gastroenterol Hepatol. 2011;8(2):108–18.

Luheshi NM, Giles JA, Lopez-Castejon G, Brough D. Sphingosine regulates the NLRP3-inflammasome and IL-1beta release from macrophages. Eur J Immunol. 2012;42(3):716–25.

van Luin M, Bannister WP, Mocroft A, Reiss P, Di Perri G, Peytavin G, et al. Absence of a relation between efavirenz plasma concentrations and toxicity-driven evafirenz discontinuations in the EuroSIDA study. Antivir Ther. 2009;14(1):75–83.

Lukens JR, Gurung P, Shaw PJ, Barr MJ, Zaki MH, Brown SA, et al. The NLRP12 sensor negatively regulates autoinflammatory disease by modulating interleukin-4 production in T cells. Immunity. 2015;42(4):654–64.

Luzuriaga K. Early combination antiretroviral therapy limits HIV-1 persistence in children. Annu Rev Med. 2016;67(1):201–13.

Ma Q, Okusanya OO, Smith PF, Dicenzo R, Slish JC, Catanzaro LM, et al. Pharmacokinetic drug interactions with non-nucleoside reverse transcriptase inhibitors. Expert Opin Drug Metab Toxicol. 2005;1(3):473-85.

Maartens G, Celum C, Lewin SR. HIV infection: epidemiology, pathogenesis, treatment, and prevention. Lancet. 2014;384(9939):258–71.

Macías J, Berenguer J, Japón MA, Girón-González JA, Rivero A, López-Cortés LF, et al. Hepatic steatosis and steatohepatitis in human immunodeficiency virus/hepatitis C virus-coinfected patients. Hepatology. 2012a;56:1261-70.

Macías J, Neukam K, Mallolas J, López-Cortés LF, Cartón JA, Domingo P, et al. Liver toxicity of initial antiretroviral drug regimens including two nucleoside analogs plus one non-nucleoside analog or one ritonavir-boosted protease inhibitor in HIV/HCV-coinfected patients. HIV Clin Trials. 2012b;13(2):61-9.

Maftah A, Petit JM, Ratinaud MH, Julien R. 10-N-Nonyl-Acridine Orange: a fluorescent probe which stains mitochondria independently of their energetic state. Biochem Biophys Res Commun. 1989;164:185-90.

Maggiolo F. Efavirenz: a decade of clinical experience in the treatment of HIV. J Antimicrob Chemother. 2009;64(5):910-28.

Malhi H, Kaufman RJ. Endoplasmic reticulum stress in liver disease. J Hepatol. 2011;54(4):795-809.

Manfredi R, Calza L, Chiodo F. Efavirenz versus nevirapine in current clinical practice : a prospective, open-label observational study. J Acquir Immune Defic Syndr. 2004;35(5):492-502.

Manley S, Williams JA, Ding WX. Role of p62/SQSTM1 in liver physiology and pathogenesis. Exp Biol Med (Maywood). 2013;238(5):525-38.

Mann J, Mann DA. Transcriptional regulation of hepatic stellate cells. Vol. 61, Adv Drug Deliv Rev. 2009;61(7-8)497-512.

Manosuthi W, Thongyen S, Chumpathat N, Muangchana K, Sungkanuparph S. Incidence and risk factors of rash associated with efavirenz in HIV-infected patients with preceding nevirapine-associated rash. HIV Med. 2006;7(6):378-82.

Margolis AM, Heverling H, Pham PA, Stolbach A. A review of the toxicity of hiv medications. J Med Toxicol. 2014;10(1):26-39.

Mariathasan S, Weiss DS, Newton K, McBride J, O'Rourke K, Roose-Girma M, et al. Cryopyrin activates the inflammasome in response to toxins and ATP. Nature. 2006;440(7081):228-32.

Martín-Carbonero L, Núñez M, González-Lahoz J, Soriano V. Incidence of liver injury after beginning antiretroviral therapy with efavirenz or nevirapine. HIV Clin Trials. 2003;4(2):115-20.

Martinez FO, Gordon S. The M1 and M2 paradigm of macrophage activation: time for reassessment. F1000Prime Rep. 2014;6:13.

Martinez FO, Helming L, Gordon S. Alternative activation of macrophages: an immunologic functional perspective. Annu Rev Immunol. 2009;27(1):451–83.

Martinon F, Mayor A, Tschopp J. The inflammasomes: guardians of the body. Annu Rev Immunol. 2009;27:229–65.

Marvie P, Lisbonne M, L'helgoualc'h A, Rauch M, Turlin B, Preisser L, et al. Interleukin-33 overexpression is associated with liver fibrosis in mice and humans. J Cell Mol Med. 2010;14(6B):1726–39.

Marzolini C, Telenti A, Decosterd LA, Greub G, Biollaz J, Buclin T. Efavirenz plasma levels can predict treatment failure and central nervous system side effects in HIV-1-infected patients. AIDS. 2001;15(1):71–5.

Masters SL, Dunne A, Subramanian SL, Hull RL, Tannahill GM, Sharp F A, et al. Activation of the NLRP3 inflammasome by islet amyloid polypeptide provides a mechanism for enhanced IL-1β in type 2 diabetes. Nat Immunol. 2010;11(10):897–904.

Mathew R, Karp CM, Beaudoin B, Vuong N, Chen G, Chen HY, et al. Autophagy suppresses tumorigenesis through elimination of p62. Cell. 2009;137(6):1062–75.

Mathiesen S, Justesen US, von Lüttichau HR, Hansen AB. Genotyping of CYP2B6 and therapeutic drug monitoring in an HIV-infected patient with high efavirenz plasma concentrations and severe CNS. Scand J Infect Dis. 2009;38(8):733–5.

Matusiak M, van Opdenbosch N, Lamkanfi M. CARD- and pyrin-only proteins regulating inflammasome activation and immunity. Immunol Rev. 2015;265(1):217–30.

Mayor A, Martinon F, De Smedt T, Petrilli V, Tschopp J. A crucial function of SGT1 and HSP90 in inflammasome activity links mammalian and plant innate immune responses. Nat Immunol. 2007;8(5):497–503.

McDonald B, Kubes P. Innate immune cell trafficking and function during sterile inflammation of the liver. Gastroenterology. 2016;151(6):1087–95.

Mchedlidze T, Waldner M, Zopf S, Walker J, Rankin AL, Schuchmann M, et al. Interleukin-33-dependent innate lymphoid cells mediate hepatic fibrosis. Immunity. 2013;39(2):357–71.

Medina-Caliz I, Robles-Diaz M, Garcia-Muñoz B, Stephens C, Ortega-Alonso A, Garcia-Cortes M, et al. Definition and risk factors for chronicity following acute idiosyncratic drug-induced liver injury. J Hepatol. 2016;65(3):532–42.

Medzhitov R, Horng T. Transcriptional control of the inflammatory response. Nat Rev Immunol. 2009;9(10):692–703.

Mehal WZ. The inflammasome in liver injury and non-alcoholic fatty liver disease. Dig Dis. 2014;32(5):507–15.

Meir-Shafrir K, Pollack S. Accelerated aging in HIV patients. Rambam Maimonides Med J. 2012;3(4):e0025.

Merriman RB. Nonalcoholic Fatty Liver Disease and HIV Infection. Curr HIV/AIDS Rep. 2006;3:113-7.

Miura K, Kodama Y, Inokuchi S, Schnabl B, Aoyama T, Ohnishi H, et al. Toll-like receptor 9 promotes steatohepatitis by induction of interleukin-1beta in mice. Gastroenterology. 2010;139(1):323–34.

Miura K, Yang L, van Rooijen N, Brenner DA, Ohnishi H, Seki E. Toll-like receptor 2 and palmitic acid cooperatively contribute to the development of nonalcoholic steatohepatitis through inflammasome activation in mice. Hepatology 2013;57:577–89.

Mizushima N, Komatsu M. Autophagy: renovation of cells and tissues. Cell. 2011;147(4):728–41.

Mohamed IN, Hafez SS, Fairaq A, Ergul A, Imig JD, El-Remessy AB. Thioredoxin-interacting protein is required for endothelial NLRP3 inflammasome activation and cell death in a rat model of high-fat diet. Diabetologia. 2014;57(2):413–23.

Moir S, Chun TW, Fauci AS. Pathogenic mechanisms of HIV disease. Annu Rev Pathol Mech Dis. 2011;6:223–48.

Morán-Salvador E, Titos E, Rius B, González-Périz A, García-Alonso V, López-Vicario C, et al. Cell-specific PPARγ deficiency establishes anti-inflammatory and anti-fibrogenic properties for this nuclear receptor in non-parenchymal liver cells. J Hepatol. 2013;59(5):1045–53.

Moreira LO, El Kasmi KC, Smith AM, Finkelstein D, Fillon S, Kim YG, et al. The TLR2-MyD88-NOD2-RIPK2 signalling axis regulates a balanced pro-inflammatory and IL-10-mediated anti-inflammatory cytokine response to Gram-positive cell walls. Cell Microbiol. 2008;10(10):2067–77.

Morel E, Mehrpour M, Botti J, Dupont N, Hama A, Nascimbeni AC, et al. Autophagy: A Druggable Process. Ann Rev Pharmacol. 2017;57:375-398.

Moscat J, Diaz-Meco MT. Feedback on fat: p62-mTORC1-autophagy connections. Cell. 2011;147(4):724–7.

Moscat J, Diaz-Meco MT. p62: a versatile multitasker takes on cancer. Trends Biochem Sci. 2012;37(6):230–6.

Moscat J, Diaz-Meco MT, Wooten MW. Signal integration and diversification through the p62 scaffold protein. Trends Biochem Sci. 2007;32(2):95–100.

Moscat J, Karin M, Diaz-Meco MT. p62 in Cancer: Signaling Adaptor Beyond Autophagy. Cell. 2016;167(3):606–9.

Moschen A, Molnar C, Enrich BA, Geiger S, Ebenbichler CF, Tilg H. Adipose and liver expression of interleukin (IL)-1 family members in morbid obesity and effects of weight loss. Mol Med. 2011;17(7–8):840–5.

Mosmann T. Rapid colorimetric assay for cellular growth and survival : application to proliferation and cytotoxicity assays. J Immunol Methods. 1983;65:55–63.

Mugusi S, Ngaimisi E, Janabi M, Minzi O, Bakari M, Riedel KD, et al. Liver enzyme abnormalities and associated risk factors in HIV patients on efavirenz-based HAART with or without tuberculosis co-infection in Tanzania. PLoS One. 2012;7(7):1–9.

Murakami T, Ockinger J, Yu J, Byles V, Mccoll A, Hofer AM. Critical role for calcium mobilization in activation of the NLRP3 inflammasome. Proc Natl Acad Sci U S A. 2012;109(28):11282-7.

Muriel P. NF-kappaB in liver diseases: a target for drug therapy. J Appl Toxicol. 2009;29(2):91–100.

Murray PJ, Allen JE, Biswas SK, Fisher EA, Gilroy DW, Goerdt S, et al. Macrophage activation and polarization: nomenclature and experimental guidelines. Immunity. 2014;41(1):14–20.

Murray PJ, Wynn TA. Protective and pathogenic functions of macrophage subsets. Nat Rev Immunol. 2011;11(11):723–37.

Nagai F, Hiyoshi Y, Sugimachi K, Tamura HO. Cytochrome P450 (CYP) expression in human myeloblastic and lymphoid cell lines. Biol Pharm Bull. 2002;25(3):383–5.

Naif HM. Pathogenesis of HIV infection. Infect Dis Rep. 2013;5:s1e6.

Naito M, Hasegawa G, Takahashi K. Development, differentiation, and maturation of Kupffer cells. Microsc Res Tech. 1997;39(4):350–64.

Napetschnig J, Wu H. Molecular basis of NF-κB signaling. Annu Rev Biophys. 2013;42:443–68.

Nasi M, Pinti M, Mussini C, Cossarizza A. Persistent inflammation in HIV infection: established concepts, new perspectives. Immunol Lett. 2014;161(2):184–8.

Navad M, Gharavi N, Watson AD. Inflammation and metabolic disorders. Curr Opin Clin Nutr Metab Care. 2008;11:459–64.

Negash AA, Ramos HJ, Crochet N, Lau DT, Doehle B, Papic N, et al. IL-1beta production through the NLRP3 inflammasome by hepatic macrophages links hepatitis C virus infection with liver inflammation and disease. PLoS Pathog. 2013;9(4):e1003330.

Netea MG, van der Veerdonk FL, van der Meer JW, Dinarello CA, Joosten LA. Inflammasome-independent regulation of IL-1-family cytokines. Annu Rev Immunol. 2015;33:49–77.

Neukam K, Mira JA, Collado A, Rivero-Juárez A, Monje-Agudo P, Ruiz-Morales J, et al. Liver toxicity of current antiretroviral regimens in HIV-infected patients with chronic viral hepatitis in a real-life setting: The HEPAVIR SEG-HEP Cohort. PLoS One. 2016;11(2):1–12.

Neukam K, Mira JA, Ruiz-Morales J, Rivero A, Collado A, Torres-Cornejo A, et al. Liver toxicity associated with antiretroviral therapy including efavirenz or ritonavir-boosted protease inhibitors in a cohort of HIV/hepatitis C virus co-infected patients. J Antimicrob Chemother. 2011;66(11):2605–14.

Nezis IP, Stenmark H. p62 at the interface of autophagy, oxidative stress signaling, and cancer. Antioxid Redox Signal. 2012;17(5):786–93.

Nguyen T, Nioi P, Pickett CB. The Nrf2-antioxidant response element signaling pathway and its activation by oxidative stress. J Biol Chem. 2009;284(20):13291–5.

Ni HM, Boggess N, McGill MR, Lebofsky M, Borude P, Apte U, et al. Liver-specific loss of Atg5 causes persistent activation of Nrf2 and protects against acetaminophen-induced liver injury. Toxicol Sci. 2012;127(2):438–50.

Nieto N, Friedman SL, Cederbaum AL. Cytochrome P450 2E1-derived reactive oxygen species mediate paracrine stimulation of collagen i protein synthesis by hepatic stellate cells. J Biol Chem. 2002;277(12):9853–64.

Nissim I, Luhovyy B, Horyn O, Daikhin Y, Nissim I, Yudkoff M. The role of mitochondrially bound arginase in the regulation of urea synthesis: Studies with [U-15N4]arginine, isolated mitochondria, and perfused rat liver. J Biol Chem. 2005;280(18):17715–24.

Novo E, Cannito S, Paternostro C, Bocca C, Miglietta A, Parola M. Cellular and molecular mechanisms in liver fibrogenesis. Arch Biochem Biophys. 2014;548:20–37.

Novobrantseva TI, Majeau GR, Amatucci A, Kogan S, Brenner I, Casola S, et al. Attenuated liver fibrosis in the absece of B cells. J Clin Invest. 2005;115(11):3072–82.

Núñez M. Clinical syndromes and consequences of antiretroviral-related hepatotoxicity. Hepatology. 2010;52(3):1143–55.

Nurutdinova D, Overton ET. A review of nucleoside reverse transcriptase inhibitor use to prevent perinatal transmission of HIV. Expert Opin Drug Saf. 2009;8(6):683–94.

O'Connor C, Pertel T, Gray S, Robia SL, Bakowska JC, Luban J, et al. p62/sequestosome-1 associates with and sustains the expression of retroviral restriction factor TRIM5alpha. J Virol. 2010;84(12):5997–6006.

Oakes SA, Papa FR. The role of endoplasmic reticulum stress in human pathology. Annu Rev Pathol. 2015;10:173–94.

Ogata M, Hino SI, Saito A, Morikawa K, Kondo S, Kanemoto S, et al. Autophagy is activated for cell survival after endoplasmic reticulum stress. Mol Cell Biol. 2006;26(24):9220–31.

Ogura Y, Sutterwala FS, Flavell RA. The inflammasome: first line of the immune response to cell stress. Cell. 2006;126(4):659–62.

Oh YM, Jang EH, Ko JH, Kang JH, Park CS, Han SB, et al. Inhibition of 6-hydroxydopamine-induced endoplasmic reticulum stress by l-carnosine in SH-SY5Y cells. Neurosci Lett. 2009;459(1):7–10.

Ohtsuka S, Ishii Y, Matsuyama M, Ano S, Morishima Y, Yanagawa T, et al. SQSTM1 regulates the severity of Legionella pneumophila pneumonia by modulating inflammasome activity. Eur J Immunol. 2014;44(4):1084–92.

Oyadomari S, Mori M. Roles of CHOP/GADD153 in endoplasmic reticulum stress. Cell Death Differ. 2004;11(4):381–9.

Pahl HL. Activators and target genes of Rel/NF-kappaB transcription factors. Oncogene. 1999;18(49):6853–66.

Paik YH, Lee KS, Lee HJ, Yang KM, Lee SJ, Lee DK, et al. Hepatic stellate cells primed with cytokines upregulate inflammation in response to peptidoglycan or lipoteichoic acid. Lab Invest. 2006;86(7):676–86.

Paik YH, Schwabe RF, Bataller R, Russo MP, Jobin C, Brenner DA. Toll-like receptor 4 mediates inflammatory signaling by bacterial lipopolysaccharide in human hepatic stellate cells. Hepatology. 2003;37(5):1043–55.

Palella FJ, Delaney K, Moorman AC, Loveless MO, Fuhrer J, Satten GA, et al. Declining Morbidity and mortality among patients with advanced human immunodeficiency virus infection. N Engl J Med. 1998;338(13):853–60.

Pankiv S, Lamark T, Bruun JA, Øvervatn A, Bjørkøy G, Johansen T. Nucleocytoplasmic shuttling of p62/SQSTM1 and its role in recruitment of nuclear polyubiquitinated proteins to promyelocytic leukemia bodies. J Biol Chem. 2010;285(8):5941–53.

Pantaleo G, Graziosi C, Fauci AS. The immunopathogenesis of human immunodeficiency virus infection. N Engl J Med. 1993;328(5):327–35.

Park S, Ha SD, Coleman M, Meshkibaf S, Kim SO. p62/SQSTM1 enhances NOD2-mediated signaling and cytokine production through stabilizing NOD2 oligomerization. PLoS One. 2013;8(2):e57138.

Patel MN, Carroll RG, Galván-Peña S, Mills EL, Olden R, Triantafilou M, et al. Inflammasome Priming in Sterile Inflammatory Disease. Trends Mol Med. 2017;23(2)165-180.

Patil R, Ona MA, Papafragkakis H, Carey J, Moshenyat Y, Alhaddad A, et al. Acute Liver Toxicity due to Efavirenz/Emtricitabine/Tenofovir. Case Reports Hepatol. 2015;2015:1–2.

Pedraza-Alva G, Pérez-Martinez L, Valdez-Hernández L, Meza-Sosa KF, Ando-Kuri M. Negative regulation of the inflammasome: keeping inflammation under control. Immunol Rev. 2015;265(1):231–57.

Pellicoro A, Aucott RL, Ramachandran P, Robson AJ, Fallowfield JA, Snowdon VK, et al. Elastin accumulation is regulated at the level of degradation by macrophage metalloelastase (MMP-12) during experimental liver fibrosis. Hepatology. 2012;55(6):1965–75.

Pellicoro A, Ramachandran P, Iredale JP, Fallowfield JA. Liver fibrosis and repair: immune regulation of wound healing in a solid organ. Nat Rev Immunol. 2014;14(3):181–94.

Peng Y, French BA, Tillman B, Morgan TR, French SW. The inflammasome in alcoholic hepatitis: Its relationship with Mallory-Denk body formation. Exp Mol Pathol. 2014;97(2):305–13.

Pessayre D, Fromenty B, Berson A, Robin MA, Lettéron P, Moreau R, et al. Central role of mitochondria in drug-induced liver injury. Drug Metab Rev. 2012;44(1):34–87.

Peters SJ, Haagsman HP, van Norren K. Arginase release by primary hepatocytes and liver slices results in rapid conversion of arginine to urea in cell culture media. Toxicol In Vitro. 2008;22(4):1094–8.

Petrasek J, Bala S, Csak T, Lippai D, Kodys K, Menashy V, et al. IL-1 receptor antagonist ameliorates inflammasome-dependent alcoholic steatohepatitis in mice. J Clin Invest. 2012;122(10):3476–89.

Polo M, Alegre F, Funes HA, Blas-Garcia A, Victor VM, Esplugues JV, et al. Mitochondrial (dys)function - a factor underlying the variability of efavirenz-induced hepatotoxicity?. Br J Pharmacol. 2015;172(7):1713–27.

Possamai LA, Thursz MR, Wendon JA, Antoniades CG. Modulation of monocyte/macrophage function: a therapeutic strategy in the treatment of acute liver failure. J Hepatol. 2014;61(2):439–45.

Pradere JP, Kluwe J, De Minicis S, Jiao JJ, Gwak GY, Dapito DH, et al. Hepatic macrophages but not dendritic cells contribute to liver fibrosis by promoting the survival of activated hepatic stellate cells in mice. Hepatology. 2013;58(4):1461–73.

Price JC, Thio CL. Liver Disease in the HIV-infected individual. Clin Gastroenterol Hepatol. 2011;8(12):1002–12.

Puche JE, Saiman Y, Friedman SL. Hepatic stellate cells and liver fibrosis. Compr Physiol. 2013;3(4):1473–92.

Puissant A, Auberger P. AMPK- and p62/SQSTM1-dependent autophagy mediate resveratrol-induced cell death in chronic myelogenous leukemia. Autophagy. 2010;6(5):655–7.

Puissant A, Fenouille N, Auberger P. When autophagy meets cancer through p62/SQSTM1. Am J Cancer Res. 2012;2(4):397–413.

Pulli B, Ali M, Forghani R, Schob S, Hsieh KL, Wojtkiewicz G, et al. Measuring myeloperoxidase activity in biological samples. PLoS One. 2013;8(7):e67976.

Purnell PR, Fox HS. Efavirenz induces neuronal autophagy and mitochondrial alterations. J Pharmacol Exp Ther. 2014;351(2):250–8.

Ramachandran G, Ramesh K, Kumar AK, Jagan I, Vasantha M, Padmapriyadarsini C, et al. Association of high T allele frequency of CYP2B6 G516T polymorphism among ethnic south Indian HIV-infected patients with elevated plasma efavirenz and nevirapine. J Antimicrob Chemother. 2009;63(4):841–3.

Ramachandran P, Iredale JP. Macrophages: central regulators of hepatic fibrogenesis and fibrosis resolution. J Hepatol. 2012;56(6):1417–9.

Ramachandran P, Pellicoro A, Vernon MA, Boulter L, Aucott RL, Ali A, et al. Differential Ly-6C expression identifies the recruited macrophage phenotype, which orchestrates the regression of murine liver fibrosis. Proc Natl Acad Sci U S A. 2012;109(46):E3186–95.

Rao PS, Kumar S. Chronic effects of ethanol and/or darunavir/ritonavir on U937 monocytic cells: regulation of cytochrome P450 and antioxidant enzymes, oxidative stress, and cytotoxicity. Alcohol Clin Exp Res. 2016;40(1):73–82.

Rathinam VA, Vanaja SK, Fitzgerald KA. Regulation of inflammasome signaling. Nat Immunol. 2012;13(4):333–42.

Rauch I, Müller M, Decker T. The regulation of inflammation by interferons and their STATs. JAK-STAT. 2013;2(1):e23820.

Rea SL, Majcher V, Searle MS, Layfield R. SQSTM1 mutations - Bridging Paget disease of bone and ALS/FTLD. Exp Cell Res. 2014;325(1):27–37.

Reagan-Shaw S, Nihal M, Ahmad N. Dose translation from animal to human studies revisited. FASEB J. 2007;22:659–61.

Reiter FP, Wimmer R, Wottke L, Artmann R, Nagel JM, Carranza MO, et al. Role of interleukin-1 and its antagonism of hepatic stellate cell proliferation and liver fibrosis in the Abcb4(-/-) mouse model. World J Hepatol. 2016;8(8):401–10.

Renga B, Francisci D, Schiaroli E, Carino A, Cipriani S, D'Amore C, et al. The HIV matrix protein p17 promotes the activation of human hepatic stellate cells through interactions with CXCR2 and Syndecan-2. PLoS One. 2014;9(4).

Rippe RA, Schrum LW, Stefanovic B, Solís-Herruzo JA, Brenner DA. NF-κB inhibits expression of the alpha1(I) collagen gene. DNA Cell Biol. 1999;18(10):751–61.

Robinson MW, Harmon C, O'Farrelly C. Liver immunology and its role in inflammation and homeostasis. Cell Mol Immunol. 2016;13(10):267–76.

Rodríguez-Nóvoa S, Barreiro P, Jiménez-Nácher I, Soriano V. Overview of the pharmacogenetics of HIV therapy. Pharmacogenomics J. 2006;6(4):234–45.

Rodriguez A, Durán A, Selloum M, Champy MF, Diez-Guerra FJ, Flores JM, et al. Mature-onset obesity and insulin resistance in mice deficient in the signaling adapter p62. Cell Metab. 2006;3(3):211–22.

Rogov V, Dötsch V, Johansen T, Kirkin V. Interactions between autophagy receptors and ubiquitin-like proteins form the molecular basis for selective autophagy. Mol Cell. 2014;53(2):167–78.

Rossol M, Pierer M, Raulien N, Quandt D, Meusch U, Rothe K, et al. Extracellular Ca2+ is a danger signal activating the NLRP3 inflammasome through G protein-coupled calcium sensing receptors. Nat Commun. 2012;3:1329.

Rőszer T. Understanding the mysterious M2 macrophage through activation markers and effector mechanisms. Mediators Inflamm. 2015;2015:1–16.

Rubinsztein DC, Shpilka T, Elazar Z. Mechanisms of autophagosome biogenesis. Curr Biol. 2012;22(1):R29–34.

Van der Ryst E. Maraviroc - A CCR5 antagonist for the treatment of HIV-1 infection. Front Immunol. 2015;6:277.

Salguero Palacios R, Roderfeld M, Hemmann S, Rath T, Atanasova S, Tschuschner A, et al. Activation of hepatic stellate cells is associated with cytokine expression in thioacetamide-induced hepatic fibrosis in mice. Lab Invest. 2008;88(11):1192–203.

Salloum S, Holmes JA, Jindal R, Bale SS, Brisac C, Alatrakchi N, et al. HIV/HCV in hepatic and stellate cell lines reveals cooperative profibrotic transcriptional activation between viruses and cell types. Hepatology. 2016;64:1951-1968.

Sander LE, Blander JM. Inflammasome and toll-like receptor 9: Partners in crime in toxic liver injury. Hepatology. 2009;49(6):2119–21.

Sanz L, Sanchez P, Lallena M, Diaz-Meco MT, Moscat J, Baeuerle P, et al. The interaction of p62 with RIP links the atypical PKCs to NF-kappa B activation. EMBO J. 1999;18(11):3044–53.

Schindelin J, Arganda-Carreras I, Frise E, Kaynig V, Longair M, Pietzsch T, et al. Fiji: an open-source platform for biological-image analysis. Nat Methods. 2012;9(7):676–82.

Schmittgen TD, Lee EJ, Jiang J, Sarkar A, Yang L, Elton TS, et al. Real-time PCR quantification of precursor and mature microRNA. Methods. 2008;44(1):31–8.

Schroder K, Tschopp J. The inflammasomes. Cell. 2010;140(6):821–32.

Schuppan D, Kim YO. Evolving therapies for liver fibrosis. J Clin Invest. 2013;123(5):1887–901.

Schuppan D, Krebs A, Bauer M, Hahn EG. Hepatitis C and liver fibrosis. Cell Death Differ. 2003;10:S59–67.

Schwabe RF, Bataller R, Brenner DA. Human hepatic stellate cells express CCR5 and RANTES to induce proliferation and migration. Am J Physiol Gastrointest Liver Physiol. 2003;285(5):G949-58.

Scotton CJ, Martinez FO, Smelt MJ, Sironi M, Locati M, Mantovani A, et al. Transcriptional profiling reveals complex regulation of the monocyte IL-1 beta system by IL-13. J Immunol. 2005;174:834–45.

Seglen PO, Gordon PB. 3-Methyladenine: specific inhibitor of autophagic/lysosomal protein degradation in isolated rat hepatocytes. PNAS. 1982;79:1889–92.

Seibenhener M, Babu J. Sequestosome 1/p62 is a polyubiquitin chain binding protein involved in ubiquitin proteasome degradation. Mol Cell Biol. 2004;24(18):8055–68.

Seibenhener ML, Du Y, Diaz-Meco MT, Moscat J, Wooten MC, Wooten MW. A role for sequestosome 1/p62 in mitochondrial dynamics, Import and genome integrity. Biochim Biophys Acta. 2013;1833(3):452–9.

Seibenhener ML, Geetha T, Wooten MW. Sequestosome 1/p62 - more than just a scaffold. FEBS Lett. 2007;581(2):175–9.

Seki E, Brenner DA, Karin M. A liver full of JNK: signaling in regulation of cell function and disease pathogenesis, and clinical approaches. Gastroenterology. 2012;143(2):307–20.

Seki E, Schwabe RF. Hepatic inflammation and fibrosis: functional links and key pathways. Hepatology. 2015;61(3):1066–79.

Senft D, Ronai ZA. UPR, autophagy, and mitochondria crosstalk underlies the ER stress response. Trends Biochem Sci. 2015;40(3):141–8.

Shaid S, Brandts CH, Serve H, Dikic I. Ubiquitination and selective autophagy. Cell Death Differ. 2012;20(1):21–30.

Shen Y, Yang J, Zhao J, Xiao C, Xu C, Xiang Y. The switch from ER stress-induced apoptosis to autophagy via ROS-mediated JNK/p62 signals: a survival mechanism in methotrexate-resistant choriocarcinoma cells. Exp Cell Res. 2015;334(2):207–18.

Shi F, Yang Y, Kouadir M, Xu W, Hu S. Inflammasome-independent role of NLRP12 in suppressing colonic inflammation regulated by Blimp-1. Oncotarget. 2016;7(21):30575-84.

Shin JN, Fattah EA, Bhattacharya A, Ko S, Eissa NT. Inflammasome activation by altered proteostasis. J Biol Chem. 2013;288(50):35886–95.

Shmagel K V, Saidakova EV, Shmagel NG, Korolevskaya LB, Chereshnev VA, Robinson J, et al. Systemic inflammation and liver damage in HIV/hepatitis C virus coinfection. HIV Med. 2016;17(8):581–9.

Sica A, Invernizzi P, Mantovani A. Macrophage plasticity and polarization in liver homeostasis and pathology. Hepatology. 2014;59(5):2034–42.

Sica A, Mantovani A. Macrophage plasticity and polarization: *in vivo* veritas. J Clin Invest. 2012;122(3):787–95.

Silverman WR, de Rivero Vaccari JP, Locovei S, Qiu F, Carlsson SK, Scemes E, et al. The pannexin 1 channel activates the inflammasome in neurons and astrocytes. J Biol Chem. 2009;284(27):18143–51.

Slim J, Saling CF. A Review of management of inflammation in the HIV population. Biomed Res Int. 2016;2016.

Smedsrød B, Le Couteur D, Ikejima K, Jaeschke H, Kawada N, Naito M, et al. Hepatic sinusoidal cells in health and disease: Update from the 14th International Symposium. Liver Int. 2009;29(4):490–501.

Smith PK, Krohn RI, Hermanson GT, Mallia AK, Gartner FH, Provenzano MD, et al. Measurement of protein using bicinchoninic acid. Anal Biochem. 1985;150(1):76–85.

Smith RL, de Boer R, Brul S, Budovskaya Y, van der Spek H. Premature and accelerated aging: HIV or HAART? Front Genet. 2013;3:328.

Sollberger G, Strittmatter GE, Garstkiewicz M, Sand J, Beer H. Caspase-1 : the inflammasome and beyond. Innate Immun. 2014; 20(2):115-25.

Son G, Iimuro Y, Seki E, Hirano T, Kaneda Y, Fujimoto J. Selective inactivation of NF-κB in the liver using NF-κB decoy suppresses CCl4-induced liver injury and fibrosis. Am J Physiol Gastrointest Liver Physiol. 2007;293:G631–9.

Sonderup MW, Maughan D, Gogela N, Setshedi M, Wainwright H, Meintjes G, et al. Identification of a novel and severe pattern of efavirenz drug-induced liver injury in South Africa. AIDS. 2016;30(9):1483–5.

Sonderup MW, Wainwright H, Hall P, Hairwadzi H, Spearman CW. A clinicopathological cohort study of liver pathology in 301 patients with human immunodeficiency virus/acquired immune deficiency syndrome. Hepatology. 2015;61(5):1721–9.

Sookoian S, Castaño GO, Burgueño AL, Rosselli MS, Gianotti TF, Mallardi P, et al. Circulating levels and hepatic expression of molecular mediators of atherosclerosis in nonalcoholic fatty liver disease. Atherosclerosis. 2010;209(2):585–91.

Soriano V, Puoti M, Garcia-Gascó P, Rockstroh JK, Benhamou Y, Barreiro P, et al. Antiretroviral drugs and liver injury. AIDS. 2008;22(1):1-13.

Souza DG, Cassali GD, Poole S, Teixeira MM. Effects of inhibition of PDE4 and TNF-α on local and remote injuries following ischaemia and reperfusion injury. Br J Pharmacol. 2001;134(5):985–94.

Spengler U, Lichterfeld M, Rockstroh JK. Antiretroviral drug toxicity - A challenge for the hepatologist?. J Hepatol. 2002;36(2):283–94.

Stanton MC, Chen SC, Jackson JV, Rojas-Triana A, Kinsley D, Cui L, et al. Inflammatory Signals shift from adipose to liver during high fat feeding and influence the development of steatohepatitis in mice. J Inflamm (Lond). 2011;8(1):8–22.

Starr SE, Fletcher CV, Spector SA, Yong FH, Fenton T, Brundage RC, et al. Combination therapy with efavirenz, nelfinavir, and nucleoside reverse-transcriptase inhibitors in children infected with human immunodeficiency virus type 1. N Engl J Med. 1999;341:1874–81.

Staszewski S, Moreales-Ramirex J, Tashima KT, Rachils A. Indinavir, and indinavir plus zidovudine and lamivudine in the treatment of hiv-1 infection in adults. N Engl J Med. 1999;341(25):1865–73.

Stevenson M. HIV-1 pathogenesis. Nat Med. 2003;9(7):853–60.

Stöhr W, Back D, Dunn D, Sabin C, Winston A, Gilson R, et al. Factors influencing efavirenz and nevirapine plasma concentration: effect of ethnicity, weight and co-medication. Antivir Ther. 2008;13(5):675–85.

Strowig T, Henao-Mejia J, Elinav E, Flavell R. Inflammasomes in health and disease. Nature. 2012;481(7381):278–86.

Stutz A, Golenbock DT, Latz E. Inflammasomes: too big to miss. J Clin Invest. 2009;119(12):3502–11.

Subramanian N, Natarajan K, Clatworthy MR, Wang Z, Germain RN. The adaptor MAVS promotes NLRP3 mitochondrial localization and inflammasome activation. Cell. 2013;153(2):348–61.

Sulkowski MS, Thomas DL, Mehta SH, Chaisson RE, Moore RD. Hepatotoxicity associated with nevirapine or efavirenz-containing antiretroviral therapy: Role of hepatitis C and B infections. Hepatology. 2002;35(1):182–9.

Sutterwala FS, Haasken S, Cassel SL. Mechanism of NLRP3 inflammasome activation. Ann N Y Acad Sci. 2014;1319:82–95.

Suzuki K, Ota H, Sasagawa S, Sakatani T, Fujikura T. Assay method for myeloperoxidase in human polymorphonuclear leukocytes. Anal Biochem. 1983;132(2):345-52.

Szabo G, Csak T. Inflammasomes in liver diseases. J Hepatol. 2012;57(3):642–54.

Szabo G, Iracheta-Vellve A. Inflammasome activation in the liver: Focus on alcoholic and non-alcoholic steatohepatitis. Clin Res Hepatol Gastroenterol. 2015;39:S18-23.

Szabo G, Petrasek J. Inflammasome activation and function in liver disease. Nat Rev Gastroenterol Hepatol. 2015;12(7):387–400.

Szabo G, Petrasek J, Bala S. Innate immunity and alcoholic liver disease. Dig Dis. 2012;30 Suppl 1:55–60.

Tacke F, Zimmermann HW. Macrophage heterogeneity in liver injury and fibrosis. J Hepatol. 2014;60(5):1090–6.

Taguchi K, Motohashi H, Yamamoto M. Molecular mechanisms of the Keap1-Nrf2 pathway in stress response and cancer evolution. Genes to Cells. 2011;16(2):123–40.

Tang N, Zhang YP, Ying W, Yao XX. Interleukin-1beta upregulates matrix metalloproteinase-13 gene expression via c-Jun N-terminal kinase and p38 MAPK pathways in rat hepatic stellate cells. Mol Med Rep. 2013;8(6):1861–5.

Taniguchi K, Yamachika S, He F, Karin M. p62/SQSTM1- Dr. Jekyll and Mr. Hyde that prevents oxidative stress but promotes liver cancer. FEBS Lett. 2016;590:2375–97.

Tanjore H, Lawson WE, Blackwell TS. Endoplasmic reticulum stress as a pro-fibrotic stimulus. Biochim Biophys Acta. 2013;1832(7):940–7.

Tashima KT, Bausserman L, Alt EN, Aznar E, Flanigan TP. Lipid changes in patients initiating efavirenz- and indinavir-based antiretroviral regimens. HIV Clin Trials. 2003;4(1):29–36.

Taylor S, Reynolds H, Sabin CA, Drake SM, White DJ, Back DJ, et al. Penetration of efavirenz into the male genital tract: drug concentrations and antiviral activity in semen and blood of HIV-1-infected men. AIDS. 2001;15(15):2051–3.

Thamrongwonglert P, Chetchotisakd P, Anunnatsiri S, Mootsikapun P. Improvement of lipid profiles when switching from efavirenz to rilpivirine in HIV-infected patients with dyslipidemia. HIV Clin Trials. 2016;17(1):12–6.

Thastrup O, Cullen PJ, Drøbak BK, Hanley MR, Dawson AP. Thapsigargin, a tumor promoter, discharges intracellular Ca2+ stores by specific inhibition of the endoplasmic reticulum Ca2(+)-ATPase. Proc Natl Acad Sci U S A. 1990;87(7):2466–70.

Thomas JA, Pope C, Wojtacha D, Robson AJ, Gordon-Walker TT, Hartland S, et al. Macrophage therapy for murine liver fibrosis recruits host effector cells improving fibrosis, regeneration, and function. Hepatology. 2011;53(6):2003–15.

Thompson MA, Aberg JA, Hoy JF, Telenti A, Benson C, Cahn P, et al. Antiretroviral Treatment of Adult HIV Infection. JAMA. 2012;308(4):493–505.

Tilg H, Moschen AR, Szabo G. Interleukin-1 and inflammasomes in ALD/AAH and NAFLD/NASH. Hepatology. 2016;64:955-65.

Trautwein C, Friedman SL, Schuppan D, Pinzani M. Hepatic fibrosis: Concept to treatment. J Hepatol. 2015;62:S15-24.

Tsung A, Sahai R, Tanaka H, Nakao A, Fink MP, Lotze MT, et al. The nuclear factor HMGB1 mediates hepatic injury after murine liver ischemia-reperfusion. J Exp Med. 2005;201(7):1135–43.

Tsutsui H, Cai X, Hayashi S. Interleukin-1 Family Cytokines in Liver Diseases. Mediat Inflamm. 2015;2015:630265.

Tu T, Calabro SR, Lee A, Maczurek AE, Budzinska MA, Warner FJ, et al. Hepatocytes in liver injury: Victim, bystander, or accomplice in progressive fibrosis?. J Gastroenterol Hepatol. 2015;30(12):1696–704.

Tuncer S, Fiorillo MT, Sorrentino R. The multifaceted nature of NLRP12. J Leukoc Biol. 2014;96(6):991–1000.

Tuyama AC, Hong F, Saiman Y, Wang C, Ozkok D, Mosoian A, et al. Human Immunodeficiency Virus (HIV)-1 infects human hepatic stellate cells and promotes collagen I and monocyte chemoattractant protein-1 expression: Implications for the pathogenesis of HIV/hepatitis C virus-induced liver fibrosis. Hepatology. 2010;52(2):612–22.

Umemura A, He F, Taniguchi K, Nakagawa H, Yamachika S, Font-Burgada J, et al. p62, Upregulated during preneoplasia, induces hepatocellular carcinogenesis by maintaining survival of stressed HCC-initiating cells. Cancer Cell. 2016;29(6):935–48.

UNAIDS. Global AIDS Update 2016. World Heal Organ. 2016a. Accessed (20/01/2017) [cited 2017 Jan 21] Available from: http://www.unaids.org/

UNAIDS. UNAIDS Fact Sheet 2016. Global statistics-2015. 2016b. Accessed (20/01/2017) [cited 2017 Jan 21] Available from: http://www.unaids.org/

Urtasun R, Lopategi A, George J, Leung TM, Lu Y, Wang X, et al. Osteopontin, an oxidant stress sensitive cytokine, up-regulates collagen-I via integrin $\alpha(V)\beta(3)$ engagement and PI3K/pAkt/NFκB signaling. Hepatology. 2012;55(2):594–608.

Usach I, Melis V, Peris JE. Non-nucleoside reverse transcriptase inhibitors: A review on pharmacokinetics, pharmacodynamics, safety and tolerability. J Int AIDS Soc. 2013;16:1-14.

Vadlamudi RK, Shin J. Genomic structure and promoter analysis of the p62 gene encoding a non-proteasomal multiubiquitin chain binding protein. FEBS Lett. 1998;435(2–3):138–42.

Valasek MA, Repa JJ. The power of real-time PCR. AJP Adv Physiol Educ. 2005;29(3):151–9.

Valencia T, Kim JY, Abu-Baker S, Moscat-Pardos J, Ahn CS, Reina-Campos M, et al. Metabolic reprogramming of stromal fibroblasts through p62-mTORC1 signaling promotes inflammation and tumorigenesis. Cancer Cell. 2014;26(1):121–35.

Vanaja SK, Rathinam VA, Fitzgerald KA. Mechanisms of inflammasome activation: recent advances and novel insights. Trends Cell Biol. 2015;25(5):308–15.

Vaughn BP, Robson SC, Longhi MS. Purinergic signaling in liver disease. Dig Dis. 2014;32(5):516–24.

Viñas O, Bataller R, Sancho-Bru P, Ginès P, Berenguer C, Enrich C, et al. Human hepatic stellate cells show features of antigen-presenting cells and stimulate lymphocyte proliferation. Hepatology. 2003;38(4):919–29.

Walker UA, Setzer B, Venhoff N. Increased long-term mitochondrial toxicity in combinations of nucleoside analogue reverse-transcriptase inhibitors. AIDS. 2002;16(16):2165–73.

Wallace MC, Friedman SL, Mann DA. Emerging and disease-specific mechanisms of hepatic stellate cell activation. Semin Liver Dis. 2015; 35:107-18.

Ward BA, Gorski JC, Jones DR, Hall SD, Flockhart DA, Desta Z. The cytochrome P450 2B6 (CYP2B6) is the main catalyst of efavirenz primary and secondary metabolism: implication for HIV/AIDS therapy and utility of efavirenz as a substrate marker of CYP2B6 catalytic activity. J Pharmacol Exp Ther. 2003;306(1):287–300.

Watanabe A, Sohail MA, Gomes DA, Hashmi A, Nagata J, Sutterwala FS, et al. Inflammasome-mediated regulation of hepatic stellate cells. Am J Physiol Gastrointest Liver Physiol. 2009;296(6):G1248-57.

Waters L, John L, Nelson M. Non-nucleoside reverse transcriptase inhibitors: a review. Int J Clin Pract. 2007;61(1):105–18.

Wei X, Ghosh SK, Taylor ME, Johnson VA, Emini EA, Deutsch P, et al. Viral dynamics in human immunodeficiency virus type 1 infection. Nature. 1995;373(6510):117-22.

Weiskirchen R, Tacke F. Cellular and molecular functions of hepatic stellate cells in inflammatory responses and liver immunology. Hepatobiliary Surg Nutr. 2014;3(6):344–63.

Wen H, Miao EA, Ting JP. Mechanisms of NOD-like receptor-associated inflammasome activation. Immunity. 2013;39(3):432–41.

Whitehead TP, Kricka LJ, Carter TJ, Thorpe GH. Analytical luminescence: its potential in the clinical laboratory. Clin Chem. 1979;25(9).

WHO. Use of efavirenz during pregnancy : a public health perspective. Technical update on treatment. 2012;(June):8–9. ISBN: 978924150379.2

Wilkin TJ, Gulick RM. CCR5 antagonism in HIV infection: current concepts and future opportunities. Annu Rev Med. 2012;63(1):81–93.

Williams JA, Thomas AM, Li G, Kong B, Zhan L, Inaba Y, et al. Tissue specific induction of p62/sqstm1 by farnesoid X receptor. PLoS One. 2012;7(8):1–8.

Willy J, Yong S, Stevens J, Masouka H, Wek R. CHOP links endoplasmic reticulum stress to NF-κB activation in the pathogenesis of nonalcoholic steatohepatitis. Mol Biol Cell. 2015;26(12):2190–204.

Won M, Sun H, Kyeong B, Park A, Min G. Post-translational control of NF-κB signaling by ubiquitination. Arch Pharm Res. 2016;39(8):1075-84.

Wong E, Trustman N, Yalong A. HIV pharmacotherapy: A review of integrase inhibitors. J Am Acad Physician Assist. 2016;29(2):36–40.

Woodward EA, Kolesnik TB, Nicholson SE, Prêle CM, Hart PH. The anti-inflammatory actions of IL-4 in human monocytes are not mediated by IL-10, RP105 or the kinase activity of RIPK2. Cytokine. 2012;58(3):415–23.

Woolbright BL, Jaeschke H. Sterile inflammation in acute liver injury: myth or mystery?. Expert Rev Gastroenterol Hepatol. 2015;9(8):1027–9.

Woolbright BL, Jaeschke H. Role of the inflammasome in acetaminophen-induced liver injury and acute liver failure. J Hepatol. 2016;S0168-82178.

Wooten MW, Geetha T, Seibenhener ML, Babu JR, Diaz-Meco MT, Moscat J. The p62 scaffold regulates nerve growth factor-induced NF-??B activation by influencing TRAF6 polyubiquitination. J Biol Chem. 2005;280(42):35625–9.

Wree A, Eguchi A, McGeough MD, Pena CA, Johnson CD, Canbay A, et al. NLRP3 inflammasome activation results in hepatocyte pyroptosis, liver inflammation, and fibrosis in mice. Hepatology. 2014a;59(3):898–910.

Wree A, McGeough MD, Pena CA, Schlattjan M, Li H, Inzaugarat ME, et al. NLRP3 inflammasome activation is required for fibrosis development in NAFLD. J Mol Med. 2014b;92(10):1069–82.

Wree A, Mehal WZ, Feldstein AE. Targeting cell death and sterile inflammation loop for the treatment of nonalcoholic steatohepatitis. Semin Liver Dis. 2016;36(1):27–36.

Wu X, Sun L, Zha W, Studer E, Gurley E, Chen L, et al. HIV protease inhibitors induce endoplasmic reticulum stress and disrupt barrier integrity in intestinal epithelial cells. Gastroenterology. 2010;138(1):197–209.

Wyen C, Hendra H, Siccardi M, Platten M, Jaeger H, Harrer T, et al. Cytochrome P450 2B6 (CYP2B6) and constitutive androstane receptor (CAR) polymorphisms are associated with early discontinuation of efavirenz-containing regimens. J Antimicrob Chemother. 2011;66(9):2092–8.

Wynn TA, Barron L. Macrophages: master regulators of inflammation and fibrosis. Semin Liver Dis. 2010;30(3):245–57.

Wynn TA, Vannella KM. Macrophages in tissue repair, regeneration, and fibrosis. Immunity. 2016;44(3):450–62.

Xu L, Hui AY, Albanis E, Arthur MJ, O'Byrne SM, Blaner WS, et al. Human hepatic stellate cell lines, LX-1 and LX-2: new tools for analysis of hepatic fibrosis. Gut. 2005;54(1):142–51.

Xu Z, Yang L, Xu S, Zhang Z, Cao Y. The receptor proteins: Pivotal roles in selective autophagy. Acta Biochim Biophys Sin (Shanghai). 2015;47(8):571–80.

Yan C, Zhou L, Han YP. Contribution of hepatic stellate cells and matrix metalloproteinase 9 in acute liver failure. Liver Int. 2008;28(7):959–71.

Yang H, Xiao Y, Lu Y, Chen YH. Characterization of interaction between C-domain on HIV-1 gp41 and the putative receptor protein p62. Immunobiology. 2001;203(5):778–85.

Yaping Z, Ying W, Luqin D, Ning T, Xuemei A, Xixian Y. Mechanism of interleukin-1beta-induced proliferation in rat hepatic stellate cells from different levels of signal transduction. APMIS. 2014;122(5):392–8.

Yoshimura K. Current status of HIV/AIDS in the ART era. J Infect Chemother. 2017;23(1):12–6.

Young FE. The role of the FDA in the effort against AIDS. Public Health Rep. 1988;103(2):242–5.

Young LM, Kheifets JB, Ballaron SJ, Young JM. Edema and cell infiltration in the phorbol ester-treated mouse ear are temporally separate and can be differentially modulated by pharmacologic agents. Agents Actions. 1989;26(3–4):335–41.

Yuan L, Kaplowitz N. Mechanisms of drug-induced liver injury. Clin Liver Dis. 2013;17(4):507–5148.

Zaki H. The Emerging Role of NOD-like Receptors in Colorectal Cancer. J Neopl. 2016;21:20–6.

Zaki MH, Vogel P, Malireddi RK, Body-Malapel M, Anand PK, Bertin J, et al. The NOD-like receptor NLRP12 attenuates colon inflammation and tumorigenesis. Cancer Cell. 2011;20(5):649–60.

Zatloukal K, French SW, Stumptner C, Strnad P, Harada M, Toivola DM, et al. From Mallory to Mallory-Denk bodies: What, how and why? Exp Cell Res. 2007;313(10):2033–49.

Zatloukal K, Stumptner C, Fuchsbichler A, Heid H, Schnoelzer M, Kenner L, et al. p62 Is a common component of cytoplasmic inclusions in protein aggregation diseases. Am J Pathol. 2002;160(1):255–63.

Zelová H, Hošek J. TNF-α signalling and inflammation: Interactions between old acquaintances. Inflamm Res. 2013;62:641–51.

Zhan SS, Jiang JX, Wu J, Halsted C, Friedman SL, Zern MA, et al. Phagocytosis of apoptotic bodies by hepatic stellate cells induces NADPH oxidase and is associated with liver fibrosis in vivo. Hepatology. 2006;43(3):435–43.

Zhang GF, Zhang Y, Zhao G. Crocin protects PC12 cells against MPP(+)-induced injury through inhibition of mitochondrial dysfunction and ER stress. Neurochem Int. 2015a;89:101–10.

Zhang H, Davies KJA, Forman HJ. Oxidative stress response and Nrf2 signaling in aging. Free Radic Biol Med. 2015b;88:314–36.

Zhengtong L, Chu Y, Wang Y. HIV protease inhibitors: a review of molecular selectivity and toxicity. HIV/AIDS (Auckl). 2015;7:95–104.

Zhong Z, Umemura A, Sanchez-Lopez E, Liang S, Shalapour S, Wong J, et al. NF-κB restricts inflammasome activation via elimination of damaged mitochondria. Cell. 2016;164(5):896–910.

Zhou R, Tardivel A, Thorens B, Choi I, Tschopp J. Thioredoxin-interacting protein links oxidative stress to inflammasome activation. Nat Immunol. 2010;11(2):136–40.

Zhou R, Yazdi AS, Menu P, Tschopp J. A role for mitochondria in NLRP3 inflammasome activation. Nature. 2011;469(7329):221–5.

Zhou Z, Xu MJ, Gao B. Hepatocytes: a key cell type for innate immunity. Cell Mol Immunol. 2015;13:301–15.

Zhu XH, Wang CH, Tong YW. Cytotoxicity of formaldehyde on human osteoblastic cells is related to intracellular glutathione levels. J Biomed Mater Res Part B Appl Biomater. 2007;83(2):340-4.

Zimmermann HW, Trautwein C, Tacke F. Functional role of monocytes and macrophages for the inflammatory response in acute liver injury. Front Physiol. 2012;3:56.

Zitvogel L, Kepp O, Kroemer G. Decoding cell death signals in inflammation and immunity. Cell. 2010;140(6):798–804.

Zizzo G, Cohen PL. The PPAR-γ antagonist GW9662 elicits differentiation of M2c-like cells and upregulation of the MerTK/Gas6 axis: a key role for PPAR-γ in human macrophage polarization. J Inflamm (Lond). 2015;12(1):36.

ANNEXES

ANNEX I: GENE SYMBOLS AND THEIR RESPECTIVE FULL NAMES

SYMBOL	FULL NAME/DESCRIPTION
ACTA2	Actin, alpha 2, smooth muscle, aorta
ACTB	Actin, beta
Adgre1	Adhesion G protein-coupled receptor E1 (F4/80)
ARG1	Arginase 1
CASP1	Caspase 1, apoptosis-related cysteine peptidase
CASP5	Caspase 5, apoptosis-related cysteine peptidase
CCL2	Chemokine (C-C motif) ligand 2
CCL7	Chemokine (C-C motif) ligand 7
CD163	CD163 molecule
CD86	CD86 molecule
COL1A1	Collagen tyoe I alpha chain
CXCL1	Chemokine (C-X-C motif) ligand 1
CXCL2	Chemokine (C-X-C motif) ligand 2
DDIT3	DNA damage inducible transcript 3 (CHOP)
GAPDH	Glyceraldehyde-3-phosphate dehydrogenase
GRP78	78 kDa glucose-regulated protein
HPRT1	Hypoxanthine phosphoribosyltransferase 1
HSP90AA1	Heat shock protein 90kDa alpha (cytosolic), class A member 1
HSP90AB1	Heat shock protein 90kDa alpha (cytosolic), class B member 1
HSP90B1	Heat shock protein 90kDa beta (Grp94), member 1
IFNB1	Interferon, beta 1, fibroblast
IL10	Interleukin 10
IL10RB	Interleukin 10 receptor subunit beta
IL18	Interleukin 18 (interferon-gamma-inducing factor)
IL1B	Interleukin 1, beta
IL33	Interleukin 33
IL6	Interleukin 6 (interferon, beta 2)
IRAK1	Interleukin-1 receptor-associated kinase 1
MAP3K7	Mitogen-activated protein kinase kinase kinase 7
MAPK12	Mitogen-activated protein kinase 12
MAPK9	Mitogen-activated protein kinase 9
MEFV	Mediterranean fever, pyrin innate immunity regulator
MMP2	Matrix metallopeptidase 2
MMP9	Matrix metallopeptidase 9
MRC1	Mannose receptor C-type 1
MYD88	Myeloid differentiation primary response gene (88)
NAIP	NLR family, apoptosis inhibitory protein
NBR1	NBR1, autophagy cargo receptor
NLRC4	NLR family, CARD domain containing 4
NLRP1	NLR family, pyrin domain containing 1
NLRP12	NLR family, pyrin domain containing 12
NLRP3	NLR family, pyrin domain containing 3
NOS2	Nitric oxide synthase 2, inducible
P2RX7	Purinergic receptor P2X, ligand-gated ion channel, 7
PANX1	Pannexin 1

SYMBOL	FULL NAME/DESCRIPTION
PDGFRB	Platelet derived growth factor receptor beta
PPARG	Peroxisome proliferator activated receptor gamma
PSTPIP1	Proline-serine-threonine phosphatase interacting protein 1
PTGS2	Prostaglandin-endoperoxide synthase 2 (prostaglandin G/H synthase and cyclooxygenase)
PYCARD	PYD and CARD domain containing
RIPK2	Receptor-interacting serine-threonine kinase 2
SERPINE1	Serpin family E member 1
SQSTM1	Sequestosome 1
TGFB1	Transforming growth factor, beta 1
TIMP1	Tissue inhibitor of metalloproteinase 1
TNF	Tumor necrosis factor
TNFSF11	Tumor necrosis factor (ligand) superfamily, member 11
TNFSF14	Tumor necrosis factor (ligand) superfamily, member 14
TNFSF4	Tumor necrosis factor (ligand) superfamily, member 4
TRAF6	TNF receptor-associated factor 6
TXNIP	Thioredoxin interacting protein
Vim	Vimentin
XBP1	X-box binding protein 1

ANNEX II: BIBLIOGRAPHIC PRODUCTION RELATED TO THIS THESIS

- **Alegre F**, Martí-Rodrigo A, Polo M, Ortiz-masia D, Pinti M, Apostolova N, Esplugues JV, Blas-Garcia A. Modulation by macrophages of hepatic injury involving NLRP3 inflammasome activation: the example of Efavirenz. *Gut*. [Under review]
- **Alegre F**, Polo M, Martí-Rodrigo A, Esplugues JV, Blas-Garcia A, Apostolova N. Role of p62/SQSTM1 beyond autophagy: a lesson learned from drug-induced toxicity. *British Journal of Pharmacology*. [Under review]
- Polo M, **Alegre F**, Gibellini L, Martí-Rodrigo A, Blas-Garcia A, Esplugues JV, Apostolova N. Lon protease: a novel function in the interconnection between mitochondrial dysfunction and ER stress. *British Journal of Pharmacology*. [Under review]
- **Alegre F**, Pelegrín P, Feldstein AE. Inflammasomes in liver fibrosis. *Seminars in liver diseases* 2017. *In press*
- Blas-García A, Martí-Rodrigo A, Victor VM, Polo M, **Alegre F**, Funes HA, Apostolova N., Esplugues jV. The purine analogues abacavir and didanosine increase acetaminophen-induced hepatotoxicity by enhancing mitochondrial dysfunction. *Journal of Antimicrobial Chemotherapy* 2016; 71(4):916-26.
- Apostolova N, Funes HA, Blas-García A, **Alegre F**, Polo M, Esplugues JV. Involvement of nitric oxide in the mitochondrial action of efavirenz: a differential effect on neurons and glia. *Journal of Infectious Diseases* 2015; 211(12):1953-8.
- Polo M, **Alegre F**, Funes HA, Blas-García A, Víctor VM, Esplugues JV, Apostolova N. Mitochondrial (dys)function – a factor underlying the variability of efavirenz-induced hepatotoxicity?. *British Journal of Pharmacology* 2015; 172(7):1713-27.
- Blas-García A, Polo M, **Alegre F**, Funes HA, Martínez E, Apostolova N, Esplugues JV. Lack of mitocondrial toxicity of darunavir, raltegravir and rilpivirine in neurons and hepatocytes: a comparison with efavirenz. *Journal of Antimicrobial Chemotherapy* 2014; 69(11): 2995-3000.
- Funes HA, Apostolova N, **Alegre F**, Blas-García A, Alvarez A, Martí-Cabrera M, Esplugues JV. Neuronal bioenergetics and mitochondrial dysfunction: a clue to understanding the CNS side effects of the anti-HIV drug Efavirenz. *Journal of Infectious Diseases* 2014; 210(9): 1385-1395.
- Apostolova N, Gómez-Sucerquia LJ, **Alegre F**, Funes HA, Víctor VM, Barrachina MD, Blas-García A, Esplugues JV. ER-stress in human hepatic cells treated with Efavirenz: mitochondria again. *Journal of Hepatology* 2013; 59(4):780-7.